STUDIES IN STELLAR STRUCTURE AND EVOLUTION

C. Simon Jeffery

A Thesis Submitted for the Degree of PhD
at the
University of St Andrews

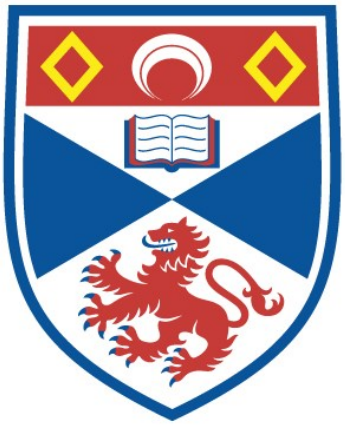

1983

STUDIES IN STELLAR STRUCTURE AND EVOLUTION

by

C. SIMON JEFFERY

A Thesis presented for the Degree of Doctor of Philosophy in the University of St Andrews

November 1982

ProQuest LLC.
789 East Eisenhower Parkway
P.O. Box 1346
Ann Arbor, MI 48106 – 1346

To my wife

ANGELA

And above all these put on love,
which binds everything together
in perfect harmony.

Paul, Colossians, Ch.2, v.14.

I, Christopher Simon Jeffery, hereby certify that this thesis, which is approximately 30,000 words in length, has been written by me, and that it has not been submitted in any previous application for a higher degree.

I was admitted as a research student under Ordinance No.12 on the 1st October 1979 and as a candidate for the degree of Ph.D. on the 1st October 1980; the higher study for which this is a record was carried out in the University of St Andrews between 1979 and 1982.

12: November: 1982

C. S. JEFFERY

In submitting this thesis to the University of St Andrews I understand that I am giving permission for it to be made available for use in accordance with the regulations of the University Library for the time being in force, subject to any copyright vested in the work not being affected thereby. I also understand that the title and abstract will be published, and that a copy of the work may be made and supplied to any bona fide library or research worker.

I hereby certify that the candidate has fulfilled the conditions of the Resolution and Regulations appropriate to the degree of Ph.D. of the University of St Andrews and that he is qualified to submit this thesis in application for that degree.

T. R. CARSON
Supervisor

ACKNOWLEDGEMENTS

I would like to express my thanks to the following :
Dr T.R. Carson, my supervisor, for his interest and the valuable advice and guidance which was given throughout the period of the project, and also for making his opacity data available to me. Professor D.W.N. Stibbs, Director of the University Observatory, for the facilities made available to me, which have helped the project run smoothly. The Science and Engineering Research Council for the award of a postgraduate research studentship.

I also wish to thank Dr R. Stothers and Dr R.W. Hilditch for suggesting the studies of horizontal branch stars and the apsidal motion constant, respectively, and for many other helpful comments. Messrs. A. Bridger and J.K. Worrell made invaluable contributions in providing tests for some of the computer programmes, and in developing the computer graphics package GIPSY (used to develop many diagrams in this thesis).

Thanks are also due to the staff and research students (past and present) of the University Observatory for many helpful discussions and continuous support and encouragement, to the staff at the St Andrews and Aberdeen University Computer Centres for their assistance in running lengthy programmes, to Mrs. L. Cuthbert for typing this dissertation and to my wife and family for their faith in me, which was usually stronger than mine.

ABSTRACT

We investigate stellar models for main-sequence and horizontal-branch stars constructed using the Carson opacities and make comparisons with models based on the Cox-Stewart opacities. A Henyey code based on the prescription of Kippenhahn et al (1967) is used for most of the calculations of stellar structure amd evolution. In the equation of state we treat ionisation equilibrium and non-relativistic degeneracy for separate temperature-density regimes. The opacity is obtained by 4-dimensional linear interpolation in the Carson opacity tables. Nuclear energy generation rates are taken from Fowler et al (1975) and neutrino losses from the approximation due to Beaudet et al (1967). Electron-screening factors are from Reeves (1965). The standard local mixing-length theory of Böhm-Vitense (1958) is used to treat non-adiabatic convection, although some models are calculated with modifications due to Deupree et al (1979, 1980). We neglect semiconvection.

The Carson opacities have only a small effect on the position of ZAHB models, but this may be metallicity dependent. The drop in the hydrogen-shell luminosity due to the helium-core expansion during HB evolution is greater than that obtained with the Cox-Stewart opacities. Allowing for the inclusion of semiconvection and convective overshooting, we find that adoption of the Carson opacities leads to a reduction of approximately 25% in the HB lifetimes. For a given range of values for the masses and envelope helium abundances of stars on a synthetic HB, the width in effective temperature is increased, and in luminosity the width is decreased. The dependence of the core luminosity on the falling core helium abundance is increased by approximately 16%.

Studies of main-sequence stars lead to agreement with Stothers' (1974a, 1974b, 1976) results for homogeneous models constructed with the Carson opacities. The evolution of main-sequence stars of intermediate mass is unaffected by the change in the opacity. Two evolutionary sequences

(for 1 $M_\odot$ stars) suggest that the main-sequence lifetimes of low mass stars may be reduced by as much as 30%. Combined with a shift in the ZAMS position this will move isochrones for low mass stars towards lower effective temperatures and densities. If studies of red-giant evolution indicate little change in the luminosity level of the horizontal branch, globular cluster ages determined from the position of the main-sequence turnoff point may be substantially reduced (possibly by as much as 50%). This could save a conflict between observed values for globular cluster ages and a value for the Hubble constant of 90.

Studies of the apsidal motion constant, k_2, for evolved MS stars shows that the discrepancy between observed values of k_2 for eclipsing binary systems and theoretical values obtained from homogeneous stellar models may be resolved by considering the evolution of the binary components. CO Lac is an exception to this result, but analysis of the observations suggests that a redetermination of the orbital semi-amplitudes may resolve the conflict.

CONTENTS

TABLES

FIGURES

1 A BRIEF INTRODUCTION TO STELLAR EVOLUTION

Theoretical studies of stellar evolution are essential to the interpretation of observations of the sun and stars and to provide clues to the nature of stellar interiors. The only intrinsic properties of stars available to observation are, in general, their luminosities, surface temperatures and surface compositions. If we plot stellar luminosities against their surface (effective) temperatures we obtain what is known as a Hertzsprung-Russell (HR) diagram[1]. Figure 1.1 is one such diagram in which the locations of various groups of observed stars are shown. Most stars, including the Sun, lie on the main-sequence. They may be roughly divided into two main groups. Population I stars represent young and metal-rich stars typical of stars in the disk of the Galaxy. Population II stars represent old and metal-poor stars typical of stars in the outer regions, or halo, of the Galaxy. Many stars are found in clusters. It is generally believed that the stars within any given cluster were formed at roughly the same time and from the same material, differing only in their initial masses Consequently star clusters provide a very powerful tool for studies of stellar evolution. HR diagrams for some typical galactic (pop.I) and globular (pop.II) clusters are shown in figures 1.2 and 1.3.

In this thesis we are concerned only with pop.I stars on the main-sequence and pop.II stars. The main features of HR diagrams for globular clusters are labelled in fig.1.3. In this introduction we describe briefly the historical development of the theory of stellar evolution, and outline the major phases of stellar evolution.

[1] In fact observations do not lead directly to this form of the HR diagram which is generally known as the theoretical HR diagram. Observations of visual magnitude are usually plotted against colour or spectral type. These have to be converted to bolometric magnitudes and effective temperatures by relations which have been obtained empirically.

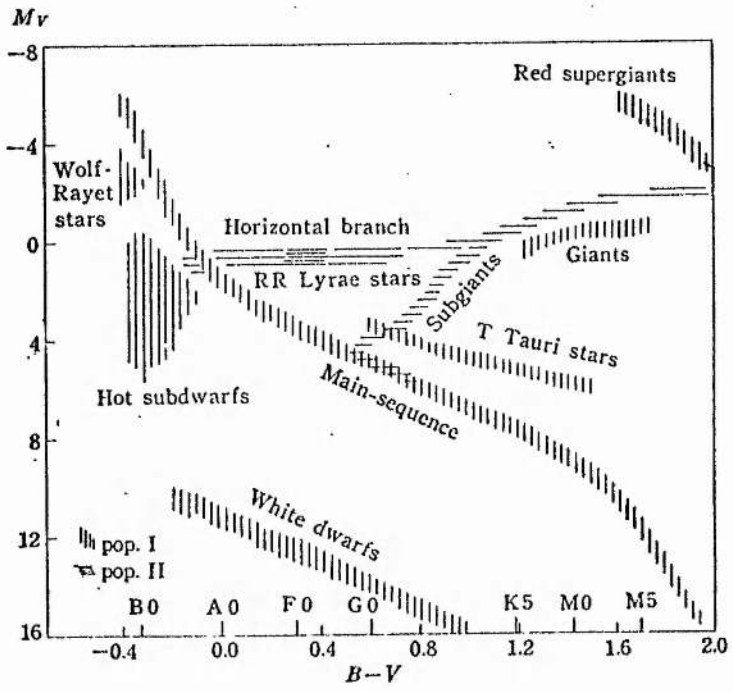

Figure 1.1 Schematic HR diagram of stars, showing the locations of various sequences. The spectral types are for the main-sequence stars. M_V, the visual magnitude, is related to the luminosity by

$$M_V = 4.63 - 2.5 \log L/L_\odot - B.C.,$$

where B.C., the bolometric correction, and B-V, the colour, are empirically (and to some extent theoretically) known functions of the effective temperature. This figure is from Hayashi et al (1962).

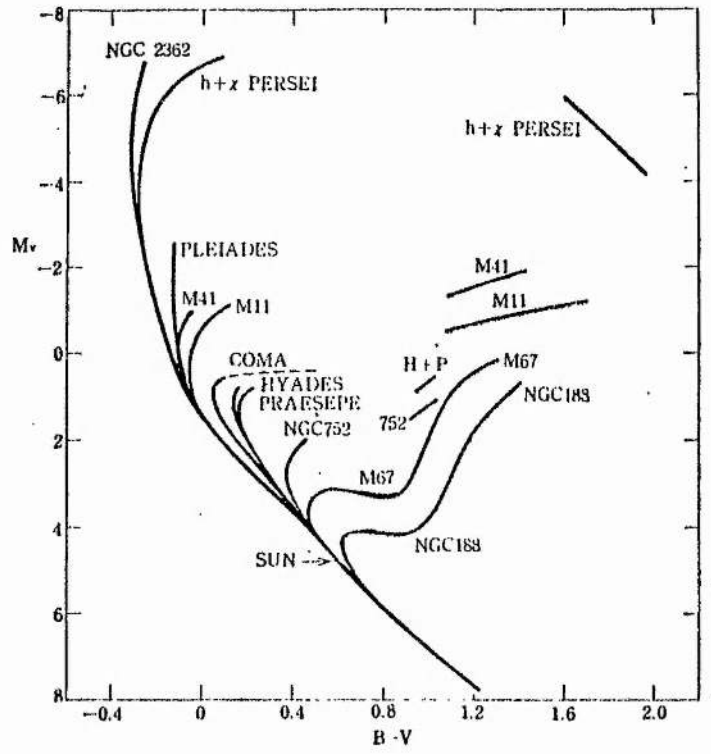

Figure 1.2 HR diagrams of galactic clusters, from

Sandage, A.R., 1957. Astrophys. J., 125, 435.

Sandage, A.R., 1962. Astrophys. J., 135, 333.

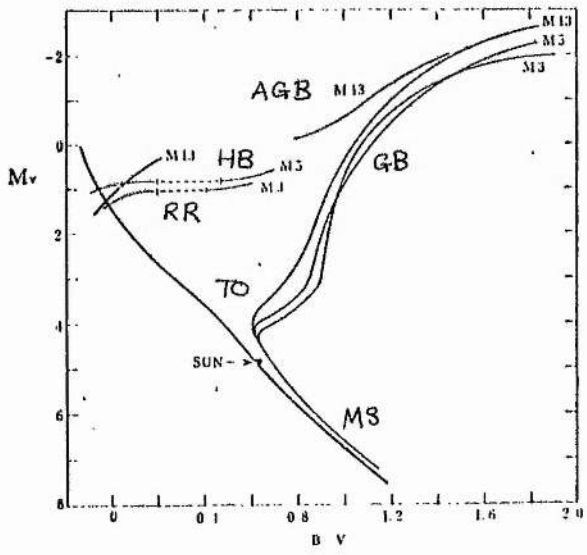

MS Main-sequence

TO Turn-off

GB Giant branch

AGB Asymptotic GB

HB Horizontal branch

RR RR Lyraes

Figure 1.3 HR diagrams of globular clusters, from

Sandage, (1962, cit.).

Early studies of stellar interiors attempted to construct gaseous spheres in hydrostatic equilibrium by assuming a particular form for the equation of state (Emden, 1907). At this stage the energy source that makes stars shine was unknown. Mechanical, chemical and radio-active sources fail to provide enough energy to keep the sun shining with its present strength for at least 4,000 million years. In 1920 J. Perrin and A.S. Eddington (Eddington, 1926) suggested that the nuclear energy released by the combination of four hydrogen nuclei to form one helium nucleus could provide the energy required. As the neutron was not discovered until 1932, Perrin and Eddington did not know whether the process was possible, but suggested that stellar interiors were the most likely locations for the formation of helium. Without knowing the rate of sub-atomic energy release, Eddington (1926) was able to set down the basic theory of stellar structure by combining classical thermodynamics, the theory of radiative equilibrium and the Bohr theory of atomic structure. In order to obtain the stellar opacity, Eddington adopted Kramers' (1923) opacity based on classical electromagnetic theory. His achievement was to establish a theoretical basis for the observed relationship between the masses and luminosities of main-sequence stars.

Progress to 1939 is summarised by Chandrasekhar (1939). He adopts appropriate approximations to most of the physical processes occurring in stars, which by this time had been guessed at, but not precisely determined. Many extensions of previous work are established principally as solutions to a number of simplified mathematical statements of the problem of stellar structure. One of these was a detailed theory of white dwarfs. At the same time progress in atomic and nuclear physics enabled Strömgren (1932) and Morse (1940) to obtain opacities from quantum-mechanical methods and Bethe (1939) to establish the nuclear origin of stellar energy.

In response to the increasingly complex ensemble of physical processes found to be occurring in stellar interiors it became clear that approximate analytic solutions to the stellar structure equations are no longer realistic

The advent of electronic computers in the early 1950s enabled Schwarzschild (1958) and others to calculate more sophisticated models of stellar interiors. Largely through this work and that of Baade (1944), the relationship between the Hertzsprung-Russell diagram and stellar evolution was first established.

Schwarzschild's method for solving the differential equations of stellar structure was to perform a large number of numerical integrations simultaneously from the surface and the centre of the star, improving his estimates of the boundary values until the two sets of integrations were consistent. Henyey et al. (1959) developed a method whereby the differential equations are replaced by difference equations. The solution of a large number of simultaneous linear equations is required to obtain corrections to an approximate stellar model. Both of these methods have been used in this study. The particular forms in which they are treated are described in chapter 2 of this thesis, where a mathematical statement of the problem of stellar structure may also be found.

Following Schwarzschild's (1958) study, work by Hayashi, Hōshi and Sugimoto (1962) established the major phases of stellar evolution and nucleo-synthesis. In a series of papers summarised by Iben (1967) the evolution of several stars is described in some detail.

It had already been realised that stars on the main-sequence were burning hydrogen in their cores to form helium. In low-mass stars the dominant reaction network is the p - p chain which takes place in a radiative core. In higher mass stars, higher central temperatures enable the CN(O) cycle to take place. The high temperature sensitivity of this reaction causes the core to be convective. As hydrogen is converted into helium the mean atomic weight, and hence the density, rises in the core. At the same time the luminosity rises and the star expands. When the hydrogen abundance in the core has dropped to about 5% of the total chemical composition, the increasing density cannot compensate the nuclear reactio-

rate for the loss of available nuclear fuel. As the nuclear energy production drops the core begins to contract, releasing gravitational energy, which results in the star maintaining its overall size and luminosity. When the hydrogen in the core has all been converted into helium, the core continues to contract. The hydrogen-rich material outside the core follows this contraction, increasing in temperature and density until nuclear reactions start to burn the hydrogen in a shell just outside the helium-rich core. At this point the star leaves the main-sequence. It is evident that stellar evolution depends critically on the initial mass of the star. The time spent by a star on the main-sequence varies inversely with the initial mass. Subsequent evolution only broadly follows the outline described below.

As hydrogen burns in a thin shell outside a contracting helium-core, the star moves on to and up the red-giant branch. In the helium-core temperatures and densities continue to rise. At these densities electrons become degenerate and highly conductive. The core therefore becomes nearly isothermal. When the core has reached a temperature high enough for helium reactions (via the 3-α process) to occur, the helium core is "ignited" (the "helium flash"). In high mass stars the helium reactions begin before the core becomes degenerate. These stars may correspond to the supergiants of fig.1.1.

After the core-helium flash, the core density falls and the electron degeneracy is lifted. In pop.II stars, the helium core burning phase is associated with the horizontal branch in the HR diagram for globular clusters. This phase is described in greater detail in chapter 4.

After the exhaustion of helium in the core, the star returns to the giant branch where it contains a degenerate carbon/oxygen core, a helium-burning shell and a hydrogen-burning shell. If the star is massive enough the central temperature may become sufficiently high for carbon and more massive elements to "burn". If the mass is less than the Chandrasekhar

mass limit (~1.4 solar masses), the exhaustion of available nuclear fuel will be followed by gravitational collapse until the star becomes a white dwarf. The advanced evolutionary stages of more massive stars are not well understood, but appear to depend on whether the star is a member of a binary system or not. They are suggested to be the progenitors of neutron stars and black holes and the participants in supernovae explosions and cataclysmic variable systems. As such, these objects do not occupy well determined regions in the HR diagram.

Hence theoretical studies of stellar evolution have successfully associated models for stellar interiors with many of the observed positions of stars in the HR diagram. Some exceptions (e.g. the Wolf-Rayet stars, the Helium stars, the Blue Stragglers, etc.) and many quantitative problems (e.g. mass loss in red-giant stars, the solar neutrino flux etc.) remain.

The detailed evolution of stars is not only sensitive to the initial mass and chemical composition. The precise nature of the physical processes within the star (e.g. the nuclear reaction rates, the convective mixing processes) and the interaction of the star with its environment (e.g. binary systems) both have important consequences. It is the aim of stellar evolution studies to identify these processes and, ultimately perhaps, to be able to determine the history of all observed stars. It is not possible in this introduction to review the work carried out by many authors over the past fifteen years.

In this thesis we examine a number of aspects of stellar evolution. In particular we investigate the effect of using opacities calculated by Carson rather than those calculated by Cox, Stewart and others which have been adopted in most other studies. The methods used in constructing stellar models and evolutionary sequences are described in chapter 2. The physics used is described in chapter 3, where a more extensive discussion of the opacity may be found in addition to the treatments for

the equation of state, the nuclear energy generation processes and convection. The structure and evolution of horizontal branch stars with the Carson opacities is examined in chapter 4, while some aspects of main-sequence stars are studied in chapter 5. Some suggestions arising from these results are made in chapter 6.

The nature of our investigation is largely exploratory. Instead of setting out to solve a particular problem, we start by asking "What happens to our picture of stellar evolution if the Carson opacities are adopted?" The subsequent question "Does this new picture fit the observations better?" is more difficult to answer, as we attempt to make clear.

2 METHODS FOR CONSTRUCTING STELLAR MODELS AND EVOLUTIONARY SEQUENCES

2.1 THE EQUATIONS OF STELLAR STRUCTURE AND EVOLUTION

The classical problem of stellar structure is by now well known (e.g. Schwarzschild, 1958). The assumption of spherical symmetry reduces the problem to one dimension. We choose the Lagrangian variable M_r, the mass within a sphere of radius r around the centre, as our independent variable. All unknown functions describing the structure of the star may be considered dependent only upon M_r and t, the time. The problem of stellar evolution is the determination of these functions.

We write P for the total pressure, T for the temperature, L_r for the energy leaving a sphere of radius r per second and Xi for the relative abundance by mass of the chemical element i.

From the definition of M_r, the conditions of hydrostatic equilibrium and energy balance, and from the transport equation, we have

$$\frac{\partial r}{\partial M_r} = \frac{1}{4\pi r^2 \rho} \tag{2-1}$$

$$\frac{\partial L_r}{\partial M_r} = \varepsilon - T\frac{\partial S}{\partial t} \tag{2-2}$$

$$\frac{\partial P}{\partial M_r} = \frac{-GM_r}{4\pi r^4} \tag{2-3}$$

$$\frac{\partial T}{\partial M_r} = \frac{-GM_r T}{4\pi r^4 P}\cdot\nabla \tag{2-4}$$

Here the density, ρ, the nuclear energy generation, ε, the entropy, S, and the temperature gradient ∇ are considered to be functions of P, T and the chemical composition. If the total nuclear energy generation rate is written as

$$\varepsilon = \sum_k \varepsilon_k$$

where for any element i reactions k' destroy i and k'' produce i, then

$$\frac{\partial X_i}{\partial t} = -\sum_{k'}\frac{\varepsilon_{k'}}{Q_{ik'}} + \sum_{k''}\frac{\varepsilon_{k''}}{Q_{ik''}} \tag{2-5}$$

where Q represents the energy gain per gram of element i processed.

If we have a convective region with instantaneous mixing which possesses nuclear energy sources and/or a boundary moving at rate $\frac{dM_{conv}}{dt}$ into a region of mean composition Xi', then the change in composition Xi within the convective region is given by

$$\frac{dX_i}{dt} = \frac{\int_{conv}\left(-\sum_{k'}\varepsilon_{k'}/Q_{ik'} + \sum_{k''}\varepsilon_{k''}/Q_{ik''}\right)dM_r + (X_i' - X_i)\frac{dM_{conv}}{dt}}{\int_{conv} dM_r} \qquad (2\text{-}6)$$

where the integrals are taken over the whole convective region.

Providing the functions ρ, ε, S and ∇ are continuous and differentiable, their special forms have no influence on the method described in this chapter. The forms used are discussed in chapter 3.

To complete the mathematical statement of the problem of stellar structure, boundary conditions for equations (2-1) to (2-4) are given by

$$r = 0, \quad L_r = 0, \qquad \text{at} \quad M_r = 0, \qquad (2\text{-}7)$$

$$P_g = 0, \quad T = T(L, R, \tau), \qquad \text{at} \quad M_r = M_*, \qquad (2\text{-}8)$$

where P_g is the gas pressure, τ is optical depth and M_*, L, R are the stellar mass, luminosity and radius respectively.

In general analytic solutions to (2-1) to (2-4) are not available and since boundary conditions appear at both ends of the domain of M_r, some form of numerical iteration is required.

A number of methods have been proposed. Haselgrove and Hoyle (1956) and Schwarzschild (1958) developed a procedure for fitting inward and outward integrations at a fitting point. This method had the advantages of not requiring an existing solution and could be used with a high-order numerical integration algorithm. It has been used in this study to construct some initial models. Henyey, Wilets, Böhm, LeLevier and Levee (1959) developed a procedure where the first order differential equations are replaced by a system of difference equations. This method has been widely adopted, although extensively modified (e.g. Henyey, Forbes and Gould, 1964). Its major advantage over the integration procedure is that it is computationally faster. It has been adopted for most of the current study, where our method closely follows the description given by Kippenhahn,

Weigert and Hofmeister (1967) and will be described later in this chapter.

A number of other methods have been proposed, of which we note the following. One disadvantage of the Lagrangian grid is that regions where quantities (e.g. Pressure) vary rapidly with mass (e.g. the surface layers) have to be treated separately. Eggleton (1971) adopts a non-Lagrangian mesh which enables the entire star to be treated in a consistent manner, although increasing the number of difference equations. Reiz and Petersen[1] and Wilson (1981) independently developed a generalisation of the Henyey and integration methods by adopting a number of fitting points (typically $3 < n < 12$). Trial values serve both as starting values for integrations to the next fitting point, and in forming differences with integrations from the preceding point, in order to iterate to render discontinuities equal to zero.

1 Unpublished, but see Hejlesen (1980), Wilson (1981) for details.

2.2 THE CALCULATION OF INITIAL MODELS

Beginning with the boundary conditions (2-7) and (2-8), we choose suitable estimates for

$$L_r = L_* \ , \quad T = T_{eff} \qquad \text{at} \quad M_r = M_* \ ,$$

$$P = P_c \ , \quad T = T_c \qquad \text{at} \quad M_r = 0 \ ,$$

where L_* is the total stellar luminosity, T_{eff} the effective temperature, and where subscript c denotes central values. Mass in the stellar atmosphere, i.e. in regions outside the layer in which $T = T_{eff}$, is assumed to be negligible in calculations for stellar interiors. We now have four boundary values at each end of the domain $\{M_* \geq M_r \geq 0\}$ Equations (2-1) to (2-4) may be integrated from each boundary to some fitting point M_f, to obtain fitting values, $\{r_{if}, L_{if}, P_{if}, T_{if}, r_{ef}, L_{ef}, P_{ef}, T_{ef}\}$ where subscripts $_{if}$ and $_{ef}$ refer to values at the fitting point from the interior and exterior, or outward and inward, integrations respectively. If the conditions

$$r_{if} = r_{ef} \ , \quad L_{if} = L_{ef} \ , \quad P_{if} = P_{ef} \ , \quad T_{if} = T_{ef} \qquad (2\text{-}9)$$

are satisfied. we have obtained a solution.

In practice, the exterior integration is started from some point M_s, $M_s < M_*$, where the starting values r_s, L_s, P_s and T_s are obtained as functions of L_* and T_{eff} from a separate integration of the surface layers, using Pressure as the independent variable. The treatment of the surface integration will be discussed further in a later section.

Similarly the interior integration is not begun at $M_r = 0$. The inner boundary condition (2-7) may be rewritten to provide starting values r_0, L_0, P_0, T_0 at some point M_0, $\{ 0 < M_0/M_* << 1 \}$ as functions of P_c and T_c. Applying a Maclaurin's series expansion to equations (2-1) - (2-4) and neglecting higher orders of M_r, we obtain

$$r_0 = \left(3/4\pi\rho\right)_c^{1/3} M_r^{1/3}$$

$$L_0 = \left(\varepsilon - T\frac{\partial S}{\partial t}\right)_c M_r$$

$$P_0 = P_c - \frac{1}{2}(4\pi/3)^{1/3} G \rho_c^{4/3} M_r^{2/3}$$

$$T_0 = T_c - \frac{1}{2}(4\pi/3)^{1/3} G (\rho_c^{4/3}/P_c) \nabla_c T_c M_r^{2/3}$$

Since all variables range over several orders of magnitude in the stellar interior, it is convenient to make a suitable transformation. For all the interior integrations (i.e. excluding the integration of the surface layers mentioned above) we have adopted those suggested by Kippenhahn et al (1967). Thus the independent variable becomes

$$\xi = \log\left(1 - M_r/(1+\eta)M_*\right) \qquad (2\text{-}14)$$

which provides high resolution in M_r near the surface for equal increments in ξ. For the unknown quantities, logarithmic variables are used,

$$x = \log r, \qquad l = \log\left(1 + L_r/L'\right),$$

$$p = \log P, \qquad t = \log T,$$

where the positive constant L' allows for a negative L so long as $L_r > -L'$

The estimated boundary conditions are now written

$$\lambda = \log (L_*/L_\odot), \qquad \tau = \log T_{eff},$$
$$p_c = \log P_c, \qquad t_c = \log T_c, \tag{2-16}$$

and their second forms become

$$x_s(\lambda,\tau),\ l_s(\lambda,\tau),\ p_s(\lambda,\tau),\ t_s(\lambda,\tau) \text{ at } \xi(M_s); \tag{2-17}$$

$$x_o(p_c,t_c),\ l_o(p_c,t_c),\ p_o(p_c,t_c),\ t_o(p_c,t_c) \text{ at } \xi(M_o). \tag{2-18}$$

Equations (2-1) to (2-4), appropriately transformed, are integrated from each of these sets of boundary values using a fourth-order Runge-Kutta algorithm with self-adjusting step-size. At a point $\xi_f = \xi(M_f)$ each integration yields values for $\{x_{ef}, l_{ef}, p_{ef}, t_{ef}\}$ and $\{x_{if}, l_{if}, p_{if}, t_{if}\}$. We have obtained a solution for the structure of the stellar interior when condition (2-9), which may be rewritten as

$$\delta x_f = x_{ef} - x_{if} = 0, \qquad \delta l_f = l_{ef} - l_{if} = 0,$$
$$\delta p_f = p_{ef} - p_{if} = 0, \qquad \delta t_f = t_{ef} - t_{if} = 0, \tag{2-19}$$

is satisfied. In order to satisfy this condition, a Newton-Raphson iteration scheme similar to those described by Faulkner (1966) and Ezer and Cameron (1962) is used.

If initial estimates for the boundary conditions λ, τ, p_c and t_c are good enough, and are denoted by $A = \{b_i^{k=0}\ ; i = 1,4\}$, and if the fitting values are denoted by $\{v_{ef}^j\ ; j=1,4\}$ and $\{v_{if}^j\ ; j=1,4\}$ such that

$$\Delta v_f^j = v_{ef}^j - v_{if}^j \ ; \ j = 1,4$$

then by performing two additional pairs of integrations with boundary conditions $B = \{b_1^k + \delta b_1, b_2^k, b_3^k + \delta b_3, b_4^k\}$ and $C = \{b_1^k, b_2^k + \delta b_2, b_3^k, b_4^k + \delta b_4\}$ we obtain corrections $\Delta b_i\ ; i = 1,4$ from the system

$$\begin{pmatrix} \frac{\partial v_{ef}^1}{\partial b_1} & \frac{\partial v_{ef}^1}{\partial b_2} & -\frac{\partial v_{if}^1}{\partial b_3} & -\frac{\partial v_{if}^1}{\partial b_4} \\ \frac{\partial v_{ef}^2}{\partial b_1} & \frac{\partial v_{ef}^2}{\partial b_2} & -\frac{\partial v_{if}^2}{\partial b_3} & -\frac{\partial v_{if}^2}{\partial b_4} \\ \frac{\partial v_{ef}^3}{\partial b_1} & \frac{\partial v_{ef}^3}{\partial b_2} & -\frac{\partial v_{if}^3}{\partial b_3} & -\frac{\partial v_{if}^3}{\partial b_4} \\ \frac{\partial v_{ef}^4}{\partial b_1} & \frac{\partial v_{ef}^4}{\partial b_2} & -\frac{\partial v_{if}^4}{\partial b_3} & -\frac{\partial v_{if}^4}{\partial b_4} \end{pmatrix} \cdot \begin{pmatrix} \Delta b_1 \\ \Delta b_2 \\ \Delta b_3 \\ \Delta b_4 \end{pmatrix} = - \begin{pmatrix} \Delta v_f^1 \\ \Delta v_f^2 \\ \Delta v_f^3 \\ \Delta v_f^4 \end{pmatrix} \qquad (2\text{-}20)$$

Then setting

$$b_i^k = b_i^{k-1} + \Delta b_i \quad ; \quad i = 1,4 \qquad (2\text{-}21)$$

the procedure may be repeated until we obtain

$$\Delta v_f^j < \eta v_f^j \quad ; \quad j = 1,4 \quad ; \quad \eta \ll 1 \qquad (2\text{-}22)$$

where η represents the required convergence limit.

To obtain convergence, it is necessary that the initial estimates λ, τ, p_c, t_c are close enough to those satisfying (2-19). In order to obtain these estimates we use a procedure based on one described by Ezer and Cameron (1962) which uses the homology invariants

$$U = \frac{\partial \ln M_r}{\partial \ln r} \quad , \quad W = \frac{\partial \ln L_r}{\partial \ln r} \quad , \quad V = \frac{\partial \ln P}{\partial \ln T} \quad . \qquad (2\text{-}23)$$

Trial inward integrations from points on a sparse grid in (λ, τ) are carried out. If the trial integration becomes unstable, the integration is halted. Instability is said to have occurred if U or W very much exceed 3, if U decreases, if V increases or if V becomes smaller than 0. The values (λ, τ) for which the trial integration reaches deepest into the star, in terms of M_r, are then used as starting values for a Newton-Raphson iteration to obtain corrections from the scheme

$$\begin{pmatrix} \frac{\partial U_c}{\partial \lambda} & \frac{\partial U_c}{\partial \tau} \\ \frac{\partial V_c}{\partial \lambda} & \frac{\partial V_c}{\partial \tau} \end{pmatrix} \cdot \begin{pmatrix} \Delta\lambda \\ \Delta\tau \end{pmatrix} = \begin{pmatrix} 3 - U_c \\ -V_c \end{pmatrix} \qquad (2\text{-}24)$$

in order to satisfy the conditions

$$|3 - U_c| < \eta, \quad |V_c| < \eta \qquad (2\text{-}25)$$

where η again represents the required convergence limit.

These integrations now provide $\{\lambda, \tau, p_c, t_c\} \equiv \{b_i^k, i = \ , 4\}$.

2.3 TREATMENT OF THE SURFACE LAYERS

In the outermost regions of a star, we find that while $M_r \simeq M_*$ the pressure, P, may vary over several orders of magnitude. It is therefore no longer appropriate to use an independent Lagrangian variable to solve the structure equations in these regions. Some authors (e.g. Eggleton, 1971) therefore prefer to use a non-Lagrangian variable (e.g. $f = f(P, L_r, M_r)$ as independent variable for the entire star. The approach adopted here is to treat the region of the star above a point $M_r = M_f$ separately, using pressure as the independent variable. Since surface layer integrations are time consuming, (they pass through the hydrogen and helium ionisation zones and convection is non-adiabatic) a scheme to keep the number of such integrations to a minimum is required. That adopted is described in full by Kippenhahn, Weigert and Hofmeister (1967). The object is to obtain boundary conditions in the form of (2-17).

In the stellar atmosphere we have to a good approximation

$$M_r = M_*, \quad L_r = L_*, \qquad (2\text{-}26)$$

where R is the stellar radius. Given the stellar luminosity, L_*, and effective temperature, T_{eff}, the radius R is obtained for the layer of the star at which $T = T_{eff}$ as derived from the Stefan-Boltzmann radiation law.

The black body flux

$$B(\tau) = \sigma T^4 \tag{2-27}$$

is integrated over the sphere to obtain

$$L_* = 4\pi R^2 \sigma T_{eff}^4 \tag{2-28}$$

where σ is the radiation constant.

Above this layer equation (2-4) no longer holds, but may be replaced by a suitable function

$$T = T(L_*, T_{eff}, \tau) \tag{2-29}$$

obtained from the study of stellar atmospheres (Mihalas, 1978), where, in reference to stellar atmospheres, τ is the optical depth defined by the relation

$$\frac{\partial \tau}{\partial r} = -\kappa \rho \quad ; \quad \tau(\rho = 0) = 0 . \tag{2-30}$$

For a grey atmosphere in local thermodynamic equilibrium (LTE) and radiative equilibrium, this has the form

$$T^4(\tau) = 3/4\, T_{eff}^4 (\tau + q(\tau)) \tag{2-31}$$

where in the Eddington approximation the Hopf function $q(\tau) \equiv 2/3$. The influence of other approximations for $T(L, T_{eff}, \tau)$ on stellar structure calculations is examined by Henyey, Vardya and Bodenheimer (1965). More recent approximations have been derived, e.g. by Krishna-Swamy (1966) and by Gingerich et al. (1971), from observations. Demarque, King and Diaz (1982) have constructed an analytic fit to the nongrey model atmospheres for red giants due to Bell et al. (1976). Since all approximations have limited validity, we currently use the Eddington approximation in all models. Combining the definition of optical depth (2-20) with the equation of hydrostatic equilibrium provides the second atmospheric equation

$$\frac{\partial P}{\partial \tau} = \frac{g}{\kappa} \quad ; \quad P_g(\tau = 0) = 0 \tag{2-32}$$

where the surface gravity g is given by

$$g = G M_* / R^2 \tag{2-33}$$

A starting value for integrating (2-32) is obtained by solving

$$P = \tau g / \kappa(P,T) + P_r(\tau) \qquad (2\text{-}34)$$

for P at $\tau = \tau_0 = \tau_1/n$, where τ_1 is the value of τ for which $T(\tau) = T_{eff}$ and n is the number of steps used in integrating (2-32), (2-34) is solved using a Newton-Raphson iteration. If an error condition arises during the iteration, i.e. if $P < P_r(\tau)$ or convergence fails, (2-34) is replaced by Iben's (1971a) condition

$$P(\tau_0) = 4\, P_r(\tau_0) \qquad (2\text{-}34a)$$

With the starting value $P(\tau_0)$, (2-32) is integrated using a fourth order Runge-Kutta algorithm from $\tau = \tau_0$ to $\tau = \tau_1$. The number of steps n is usually 25. Varying n from 10 to 50 has little effect on $P(\tau_1)$. Given T_{eff} and L_*, we have obtained values for R and P at $M_r = M_*$, giving starting conditions for the integration of equations (2-1) to (2-4).

The structure of the outermost layers beneath the atmosphere is obtained by integrating equations (2-1), (2-3) and (2-4) from $M_r = M_*$ to $M_r = M_s$. The assumption that $L_r = L_*$ in these layers holds to a high degree, since nuclear processes make a negligible contribution for $T < 10^6$ K. Logarithmic variables are used throughout with a fourth-order Runge-Kutta integration with self-adjusting step-width, and with log P as the independent variable. The transformed differential equations used in the integration become

$$\frac{\partial \log M_r}{\partial \log P} = \frac{4\pi P_r^4}{G M_r^2} \qquad (2\text{-}35)$$

$$\frac{\partial \log r}{\partial \log P} = \frac{P_r}{G M_r \rho} \qquad (2\text{-}36)$$

$$\frac{\partial \log T}{\partial \log P} = \nabla \qquad (2\text{-}37)$$

The integration is halted when $M_r < M_s$. Values for X_s, L_s, ρ_s and t_s (see condition : 2-17) are then interpolated in M_r at $M_r = M_s$

M_s is determined in such a way that providing

$$10^{-6} \leq (1 - M_s / M_*) \leq 10^{-2} \tag{2-38}$$

then the temperature at M_s is required to fulfil the condition

$$4.5 \leq (t_s = \log_{10} T_s) \leq 5.0 \tag{2-39}$$

This condition is designed to place the time-consuming treatment of the H and He ionisation zones within the surface integration scheme (cf. Sweigart and Gross, 1974). In the current programme, changes to M_s during evolutionary sequences are restricted in the interest of computational speed. In addition, most sequences studied with the current programme are restricte to one phase of evolution, where changes in t_s are slow.

In order to reduce the number of times the surface layers are integrated, a scheme is used which avoids repeating the integration procedure each time surface conditions for new values of $\lambda = \log L_*$ and $\tau = \log T_{eff}$ are require Linearised relations between $\lambda, \tau, X_s, l_s, p_s$ and t_s are obtained using the scheme described in detail by Kippenhahn, Weigert and Hofmeister (1967) (§ IV.A). The following is a summary of its main features.

Assuming that the (λ, τ) plane is covered by a net of congruent right triangles, outer layer integrations are carried out for the three corners $(\lambda_i, \tau_i;\ i = 1,3)$ of the triangle in which the (λ, τ) point for a given model lies. From these integrations we can obtain linearised conditions of the form

$$\begin{aligned} X_s &= \alpha(\tau, \lambda) = \alpha_0 + \alpha_1 \tau + \alpha_2 \lambda , \\ l_s &= \beta(\tau, \lambda) , \quad p_s = \gamma(\tau, \lambda) , \quad t_s = \delta(\tau, \lambda) \end{aligned} \tag{2-40}$$

and

$$\begin{aligned} \lambda &= \varepsilon(p_s, t_s) = \varepsilon_0 + \varepsilon_1 p_s + \varepsilon_2 t_s , \\ \tau &= \zeta(p_s, t_s), \quad X_s = \eta(p_s, t_s) , \quad l_s = \nu(p_s, t_s) \end{aligned} \tag{2-41}$$

where the coefficients $\alpha_j;\ j = 0,2$, etc., are obtained as solutions to systems of the form

$$\begin{pmatrix} 1 & \tau_1 & \lambda_1 \\ 1 & \tau_2 & \lambda_2 \\ 1 & \tau_3 & \lambda_3 \end{pmatrix} \cdot \begin{pmatrix} \alpha_0 \\ \alpha_1 \\ \alpha_2 \end{pmatrix} = \begin{pmatrix} X_{s1} \\ X_{s2} \\ X_{s3} \end{pmatrix} \tag{2-42}$$

While the (λ,τ) point for a given model remains within this triangle, the surface conditions do not need to be recomputed. When the evolutionary track in the (λ,τ) plane moves to another triangle new conditions must be derived, but if the new triangle has one or two corners in common with the old triangle, these do not need to be reintegrated.

In the current study we have used triangles with sides $\Delta\lambda = 0.1$ and $\Delta\tau = 0.02$, as in Kippenhahn et al (1967). No substantial difference in the zero-age models was found using a reduced grid-size with $\Delta\lambda = 0.03$ $\Delta\tau = 0.01$ (e.g. Sweigart and Gross, 1974), although while constructing zero-age horizontal branch models, the smaller grid-size gave rise to a solution which oscillated between adjacent triangles in the (λ,τ) plane. This was immediately resolved on using the larger grid-size. The consequent reduction in the number of surface integrations required during an evolutionary sequence justified using the larger grid-size during the current study.

The linearised conditions (2-40) are used in the code for calculating initial models (section 2.2). The conditions (2-41) determine the surface conditions from a relaxed interior solution, and provide the outer boundary conditions for the interior solution as required by the Henyey code to be described in the next section.

2.4 THE HENYEY CODE

INTRODUCTION

The Henyey code for calculating stellar structure operates on the following principle. Given an initial estimate for the numerical solution of a differential equation, the differential equation may be replaced by a difference equation, and a first order solution obtained by setting up and solving a system of linear equations. We have followed the prescription given by Kippenhahn, Weigert and Hofmeister (1967). Given an initial estimate for the stellar model consisting of values for

$$\xi_j, x_j, l_j, p_j, t_j, (X_{ij}; i=1,k) : j=1,m \qquad (2\text{-}43)$$

where $\xi_1 = \xi_s$, $\xi_{m-1} = \xi_o$, $\xi_m = \xi_c$ and ξ, x, l, p, t are defined by some transformation (e.g. 2-14 and 2-15) of the form

$$\xi = \xi(M_r), x = x(r), l = l(L_r), p = p(P), t = t(T) \qquad (2\text{-}44)$$

a system of linear equations is formed and solved for the corrections

$$\delta x_j, \delta l_j, \delta p_j, \delta t_j ; j=1,m$$

When applied, a new estimate for the stellar model is obtained, and the process is repeated until the corrections become small enough to satisfy some convergence criterion. This solves the stellar structure equations. A separate procedure treats the time-dependent change of chemical structure

$$X_{ij} ; i=1,k ; j=1,m \qquad (2\text{-}45)$$

due to nucleosynthetic and convective processes by replacing time derivatives with differences. The subsequent model must again be relaxed. A number of such models separated in time is an evolutionary sequence.

REPLACING DIFFERENTIAL EQUATIONS BY DIFFERENCE EQUATIONS.

Kippenhahn et al divide the interval $M_s \geq M_r \geq M_o$ into m-2 mass shells with mesh points

$$\xi_1 = \xi(M_s), \xi_2, \xi_3, \ldots, \xi_{m-1} = \xi(M_o) \qquad (2\text{-}46)$$

Applying transformation (2-44) and replacing, say, (2-1) with a difference equation, the equations

$$\frac{x_{j+1} - x_j}{\xi_{j+1} - \xi_j} = \left[\frac{1}{4\pi r^2 \rho}\right]_{j+1/2} \frac{(dx/dr)_{j+1/2}}{(d\xi/dM_r)_{j+1/2}}, \qquad (2\text{-}47)$$

$$(j = 1, \ldots m-2),$$

are obtained. Subscripts $j + \frac{1}{2}$ indicate an average for the mass shell between the mesh points j and j + 1. A number of possible ways for determining these averages are available, those adopted are given below, alongside the forms used for the difference equations. Each of the m-2 mass shells provides four difference equations with the general form

$$G_i(x_j, l_j, p_j, t_j, \xi_j, x_{j+1}, l_{j+1}, p_{j+1}, t_{j+1}, \xi_{j+1}) = 0, \qquad (2\text{-}48)$$

$$(i = 1, \ldots 4;\ j = 1, \ldots m-2).$$

In addition these functions involve values of X_i and S° at j and j + 1 and Δt as parameters. As these 4(m-2) equations stand against the 4(m-1) unknowns $x_j, l_j, p_j, t_j;\ j = 1, \ldots m$, further equations must be obtained from the boundary conditions. We first write out the difference equations G_{ij}, i = 1,4 in the form used in the current programme, with the transformation (2-14) and (2-15).

$$G_1 = (x_{j+1} - x_j) + (\xi_{j+1} - \xi_j) \cdot \frac{M_*}{4\pi} \cdot 10^{(\xi_{j+1/2} - 3x_{j+1/2})} \Big/ \rho_{j+1/2} \qquad (2\text{-}49a)$$

$$G_2 = (l_{j+1} - l_j) + (\xi_{j+1} - \xi_j) \cdot \frac{M_*}{L_0 L'} \cdot 10^{(\xi_{j+1/2} - l_{j+1/2})} \cdot \varepsilon_{j+1/2} \qquad (2\text{-}49b)$$

$$G_3 = (p_{j+1} - p_j) + (\xi_{j+1} - \xi_j) \cdot \frac{GM_*^2}{4\pi} \cdot 10^{(\xi_{j+1/2} - p_{j+1/2} - 4x_{j+1/2})} \cdot (10^{\xi_{j+1/2}} - 1) \qquad (2\text{-}49c)$$

$$G_4 = (t_{j+1} - t_j) + (\xi_{j+1} - \xi_j) \cdot \frac{G M_*^2}{4\pi} \cdot 10^{(\xi_{j+1/2} - P_{j+1/2} - 4 x_{j+1/2})}$$

$$\times \left(10^{\xi_{j+1/2}} - 1\right) \cdot \nabla_{j+1/2} \qquad (2\text{-}49d)$$

where

$$\begin{aligned}
\xi_{j+1/2} &= (\xi_j + \xi_{j+1}) / 2 \\
x_{j+1/2} &= (x_j + x_{j+1}) / 2 \\
l_{j+1/2} &= (l_j + l_{j+1}) / 2 \\
P_{j+1/2} &= (P_j + P_{j+1}) / 2 \\
t_{j+1/2} &= (t_j + t_{j+1}) / 2 \\
\rho_{j+1/2} &= (\rho_j + \rho_{j+1}) / 2 \\
\nabla_{j+1/2} &= (\nabla_j + \nabla_{j+1}) / 2
\end{aligned} \qquad (2\text{-}50)$$

$$\varepsilon_{nuc\,j+1/2} = (\varepsilon_{nuc_j} \cdot \varepsilon_{nuc_{j+1}})^{1/2}$$

$$\varepsilon_{grav\,j+1/2} = \frac{(u^{\circ}_{j+1/2} - u_{j+1/2})}{\Delta t} + \frac{P_{j+1/2} \cdot (\rho_{j+1/2} - \rho^{\circ}_{j+1/2})}{\rho^2_{j+1/2} \cdot \Delta t}$$

$$\varepsilon_{j+1/2} = \varepsilon_{nuc\,j+1/2} + \varepsilon_{grav\,j+1/2}$$

$$u_{j+1/2} = (u_j + u_{j+1}) / 2$$

$$P_{j+1/2} = (P_j + P_{j+1}) / 2$$

Superscript o refers to the value in the previous model, Δt is the timestep between models.

THE CHOICE OF MESH POINTS

In order that the difference equations approximate the differential equations the stepwidths (e.g. $\Delta x = |x_j - x_{j+1}|$) in all variables must be sufficiently small. For economy of both computer time and memory, the mass-shells should not be too small. To satisfy both these conditions we adopt the following scheme to control the distribution of mesh-points. We start with the criteria

$$\begin{aligned}
\Delta q_{min} < \Delta q < \Delta q_{max} \qquad & \Delta q = |q_{j+1} - q_j| \\
\Delta x_{min} < \Delta x < \Delta x_{max} \qquad & \Delta x = |x_{j+1} - x_j| \\
\Delta l_{min} < \Delta l < \Delta l_{max} \qquad & \Delta l = |l_{j+1} - l_j| \\
\Delta p_{min} < \Delta p < \Delta p_{max} \qquad & \Delta p = |p_{j+1} - p_j| \\
\Delta t_{min} < \Delta t < \Delta t_{max} \qquad & \Delta t = |t_{j+1} - t_j| \\
\Delta X_{i\,min} < \Delta X_i < \Delta X_{i\,max} \qquad & \Delta X_i = |X_{ij+1} - X_{ij}|
\end{aligned} \tag{2-51}$$

where in this instance $q = M_r/M_*$, $l = L_r/L_*$ and values used for Δq_{min}, Δq_{max}, etc. are given in table 2.1 Each mass shell $[q_j, q_{j+1}]$; $j = 1, m$ is checked to see that (2-51) is satisfied. If one or more of the right-hand inequalities is violated a new mesh-point is inserted at a point defined by

$$q = (q_j + q_{j+1})/2 \tag{2-52}$$

Table 2.1 Upper and lower limits on step-sizes used for checking the distribution of mesh-points within the stellar model

Variable	Δq	Δx	Δl	Δp	Δt	ΔX_H	ΔX_{He}
min	0.01	0.05	0.05	0.05	0.02	0.03	0.03
max	0.02	0.20	0.20	0.20	0.10	0.10	0.10

Approximate values for all other quantities at this point are obtained by linear interpolation between existing values at mesh-points j and j + 1. If all of the left-hand inequalities fail then the meshpoint at q_{j+1} is deleted, providing that its omission violates none of the right-hand inequalities. Full details of an equivalent scheme are given by Kippenhahn et al (1967). No problems affecting the accuracy of our results arising from the distribution of mesh-points were encountered whilst using this scheme.

DIFFERENCE EQUATIONS FROM THE BOUNDARY CONDITIONS

We already have the conditions (2-41) which hold at $\xi = \xi_1$, yielding two equations

$$B_i(x_1, l_1, p_1, t_1) = 0 \quad , \quad i = 1,2 \tag{2-53}$$

or in particular :

$$B_1 = \eta_0 + \eta_1 p_1 + \eta_2 t_1 - r_1 = 0 \tag{2-54a}$$

$$B_2 = \iota_0 + \iota_1 p_1 + \iota_2 t_1 - l_1 = 0 \tag{2-54b}$$

We have also obtained equations (2-10) - (2-13) which determine the behaviour of the solution in a neighbourhood of the stellar centre. These may be rewritten in terms of the transformation (2-44) and rearranged to yield

$$C_i(x_{m-1}, l_{m-1}, p_{m-1}, t_{m-1}, p_m, t_m) = 0 \; ; \quad i = 1,4 \tag{2-55}$$

(Central values x_m and l_m are trivial and do not appear as arguments). The C_i under transformation (2-14) - (2-15) as used in the current programme are written out below. Note that the central values $\rho_m = \rho_c, \varepsilon_c, \nabla_c$, etc. are replaced by $\rho_{m-1/2}, \varepsilon_{m-1/2}, \nabla_{m-1/2}$, etc. where the subscript m - ½ represents an average of the values at meshpoints m and m - 1. This approximation is justified as follows. Equations (2-10) - (2-13) may be obtained by either of two methods. If (2-1) - (2-4) are integrated with constant values for $\rho, \varepsilon, \nabla$ over the interval M_c to M_o, then the means of the boundary values for ρ, etc. are better than the boundary values themselves. If (2-10) to (2-13) are obtained using the

truncated McLaurin series expansion, then taking the means of the boundary values for ρ, ε and ∇ in the interval M_c to M_0 allows for the neglect of higher order terms.

Regarding the choice of M_0, we use $M_0/M_\star = 10^{-3}$. Tests showed that using $M_0/M_\star = 10^{-4}$ gave rise to a change in the central pressure of $\delta \log P_c < 2 \times 10^{-4}$. Our form for the central conditions becomes :

$$C_1 = -X_{m-1} + \frac{1}{3} \log \left(\frac{3 M_0}{4\pi \rho_{m-1/2}} \right)$$

$$C_2 = -l_{m-1} + \log \left(1 + \frac{M_0}{L'} \cdot \varepsilon_{m-1/2} \right) \qquad (2\text{-}56)$$

$$C_3 = (p_m - p_{m-1}) - \left(\frac{4\pi}{3} \right)^{1/3} \cdot \frac{G}{2} \cdot \frac{M_0^{2/3}}{\ln 10} \cdot \rho_{m-1/2}^{4/3} \Big/ P_{m-1/2}$$

$$C_4 = (t_m - t_{m-1}) - (p_m - p_{m-1}) \cdot \nabla_{m-1/2}$$

Subscripts m - ½ represent averages of values at mass shells m - 1 and m, evaluated using the same conventions as in (2-50).

THE SYSTEM OF NON-LINEAR EQUATIONS

Following Kippenhahn et al, we now have a system of 4m - 2 non-linear equations;

$$B_i = 0 \quad : \quad i = 1, 2$$

$$G_{ij} = 0 \quad : \quad i = 1, \ldots 4 \; ; \; j = 1, \ldots m-2 \qquad (2\text{-}57)$$

$$C_i = 0 \quad : \quad i = 1, \ldots 4$$

for the 4m - 2 unknowns

$$(x_j, l_j, p_j, t_j \; ; \; j = 1, \ldots m-1), \; p_m, t_m$$

THE METHOD FOR SOLVING THE SYSTEM OF NON-LINEAR EQUATIONS

Kippenhahn et al (1967) give a detailed treatment of the solution of the system (2-57). In general, a system of non-linear equations

$$\begin{aligned} & E_1(y_1, y_2, \ldots y_n) = 0 \\ & E_2(y_1, y_2, \ldots y_n) = 0 \\ & \vdots \\ & E_3(y_1, y_2, \ldots y_n) = 0 \end{aligned} \qquad (2\text{-}58)$$

with an approximate solution

$$y_1^{(0)}, y_2^{(0)}, \ldots y_n^{(0)}$$

may be solved using a Newton-Raphson iteration. Corrections δy_i are found such that after s steps,

$$y_i^{(s+1)} = y_i^{(s)} + \delta y_i \quad ; i = 1, n \qquad (2\text{-}59)$$

will give a better approximation to the solution of (2-58), where the δy_i are determined by solving the system

$$\sum_{i=1}^{n} \left(\frac{\partial E_k}{\partial y_i}\right)^{(s)} \cdot \delta y_i = -E_k^{(s)} \quad ; k = 1, n \qquad (2\text{-}60)$$

where superscripts (s) indicate that the functions $\partial E_k/\partial y_i$ and E_k are evaluated from the $y_i^{(s)}$. Since (2-58) are non-linear, δy_i must be calculated and applied iteratively until some convergence criterion is satisfied.

If an approximate solution $x_j^{(0)}, l_j^{(0)}, p_j^{(0)}, t_j^{(0)}$ to the non-linear system (2-57) exists, then this method may be applied to obtain corrections from the system of <u>linear</u> equations of the form (2-60) :

$$\frac{\partial B_k}{\partial x_1}\delta x_1 + \frac{\partial B_k}{\partial l_1}\delta l_1 + \frac{\partial B_k}{\partial p_1}\delta p_1 + \frac{\partial B_k}{\partial t_1}\delta t_1 = -B_k \qquad (k = 1, 2)$$

$$\frac{\partial G_i}{\partial x_j}\delta x_j + \frac{\partial G_i}{\partial l_j}\delta l_j + \frac{\partial G_i}{\partial p_j}\delta p_j + \frac{\partial G_i}{\partial t_j}\delta t_j + \frac{\partial G_i}{\partial x_{j+1}}\delta x_{j+1}$$

$$+ \frac{\partial G_i}{\partial l_{j+1}}\delta l_{j+1} + \frac{\partial G_i}{\partial p_{j+1}}\delta p_{j+1} + \frac{\partial G_i}{\partial t_{j+1}}\delta t_{j+1} = -G_i$$

$$(i = 1, \ldots 4\,;\; j = 1, \ldots m-2)\,, \qquad (2\text{-}61)$$

$$\frac{\partial C_i}{\partial x_{m-1}}\delta x_{m-1} + \frac{\partial C_i}{\partial l_{m-1}}\delta l_{m-1} + \frac{\partial C_i}{\partial p_{m-1}}\delta p_{m-1} + \frac{\partial C_i}{\partial t_{m-1}}\delta t_{m-1}$$

$$+ \frac{\partial C_i}{\partial p_m}\delta p_m + \frac{\partial C_i}{\partial t_m}\delta t_m = -C_i$$

$$(i = 1, \ldots 4)\,.$$

All coefficients may be calculated from equations (2-49), (2-50), (2-54) and (2-56) using the approximate solution and the known parameters X_i, S° and Δt. At the present all derivatives of physical quantities (e.g. $\partial p_i/\partial p_j$, $\partial p_j/\partial t_j$, etc.) are obtained by first-order numerical differentiation. (2-61) represents a system of 4m - 2 inhomogeneous linear equations for 4m - 2 corrections which may be solved by familiar techniques. That used in the current programme is the one originally used by Henyey et al (1964) and described fully by Kippenhahn et al (1967). (2-61) may be rewritten in matrix form

$$\begin{pmatrix} \frac{\partial B_1}{\partial x_1} & \cdots & & \\ \vdots & & & \\ & & & \\ 0 & & \vdots & \\ & \cdots & \frac{\partial C_4}{\partial t_m} & \end{pmatrix} \cdot \begin{pmatrix} \delta x_1 \\ \vdots \\ \\ \vdots \\ \delta t_m \end{pmatrix} = \begin{pmatrix} -B_1 \\ \vdots \\ \\ \vdots \\ -C_4 \end{pmatrix}, \qquad (2\text{-}62)$$

where all non-trivial elements in the first matrix lie in overlapping blocks

along the leading diagonal. Corrections are determined as linear functions of the last two corrections in each block, e.g.

$$\delta p_j = U_{4j-1} \cdot \delta p_{j+1} + V_{4j-1} \cdot \delta t_j + W_{4j-1} , \qquad (2\text{-}63)$$

for which the 3(4m - 6) coefficients $(U_i, V_i, W_i, i = 1, 4m-6)$ are stored. The corrections $\delta p_{m-1}, \delta t_{m-1}, \delta p_m, \delta t_m$ are obtained directly from the last block, and are then used to substitute back, e.g. in (2-63), to yield all corrections

$$(\delta x_j, \delta l_j, \delta p_j \; \delta t_j ; j = 1, m-1), \delta p_m, \delta t_m .$$

2.5 RELAXATION OF ZERO-AGE MODELS

In order to use the Henyey code to solve the system of equations (2-57) to obtain a stellar model, an initial approximate solution must first exist. In the case of the first model of a sequence, this is normally a zero-age main-sequence or horizontal-branch star, for which evolution is slow and the approximation $T\partial S/\partial t = 0$ may be made. Another zero-age model, constructed with either different mass or composition parameters, is usually sufficient to provide an approximate solution within the range of convergence of the overall scheme. Where such a model does not exist, an approximate solution may be computed using either an integration scheme as described in §2.2, or some simplified stellar model such as a polytrope.

Once an approximate solution is established, surface conditions appropriate to it are obtained in the form (2-53). Coefficients for equation (2-62) are established, and the system is solved for corrections δx_i, etc. These are applied to the approximate solution, and the procedure is repeated. In our programme, when good convergence is obtained, each set of corrections falls by a factor of 10 with each iteration. Some constraints are applied to ensure convergence in as many cases as possible.

Consider δ_{max} to be the largest absolute correction to any variable, and $\hat{\delta}$ to be the r.m.s. correction to all variables. All corrections are multiplied by a constant f_δ before being applied. Values for f_δ and convergence criteria are given in terms of δ_{max} and $\hat{\delta}$ in table 2.2. The last condition tabulated is provided because in a few cases, convergence of the solution halts before δ_{max} and $\hat{\delta}$ have satisfied the previous criteria. $\hat{\delta}_o$ is the value for $\hat{\delta}$ from the previous iteration. While exhaustive attempts to improve convergence in these cases were considered unnecessary, it was noticed that δ_{max} was frequently associated with the C and O ionisation bumps at $T \simeq 10^6$K in the Carson opacity tables.

Table 2.2 Convergence criteria for solution of (2-60)

δ_{max}	$\hat{\delta}$	f_δ	other criteria	convergence
>1	-	0.1	-	-
<1	>0.5	0.5	-	-
<1	<0.5	1.0	-	-
$<5\times10^{-5}$	-	1.0	-	✓
-	$<1\times10^{-4}$	1.0	-	✓
-	$<5\times10^{-4}$	1.0	$\hat{\delta}/\delta_0 \simeq 1$	✓

After every 5 iterations, or when convergence has been established, the surface conditions are checked by finding λ and τ from (2-41) to determine whether they remain within the $(\lambda_i, \tau_i\ ;\ i=1,\ldots 3)$ triangle for which (2-41) is valid. In addition, M_s is tested to ensure that conditions (2-38) and (2-39) are satisfied. The scheme is illustrated in figure 2.1.
The best available solution for the model is written out regularly to allow the procedure to be restarted. When convergence has been established, and the surface conditions are consistent with the interior model, a solution to the stellar structure problem has been obtained.

Figure 2.1 Flowchart for the relaxation of the difference equations for zero age stellar structure.

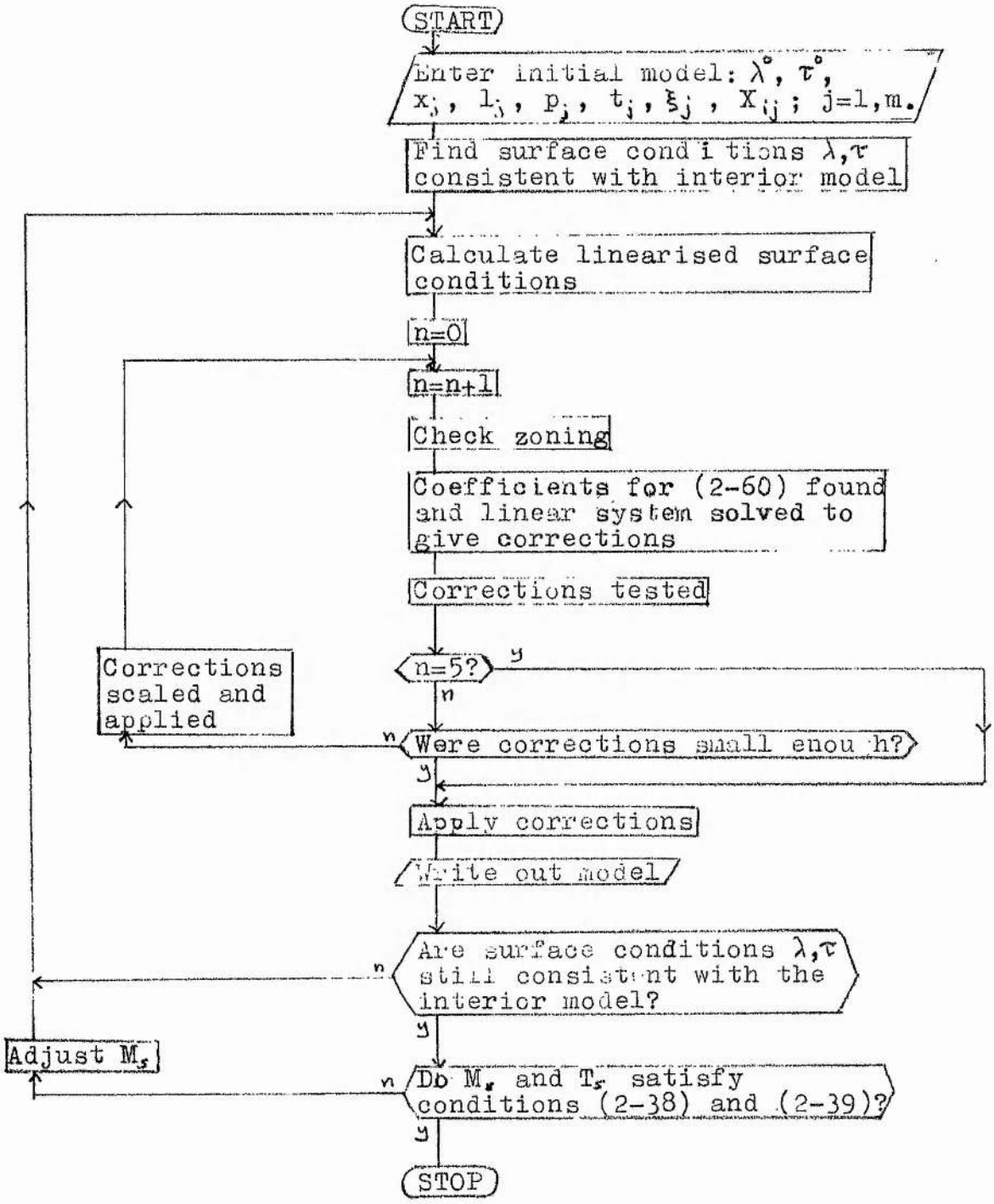

2.6 CONSTRUCTION OF EVOLUTIONARY SEQUENCES

Given a stellar model at time t_o, say, we may introduce time-dependent effects. Following Kippenhahn et al, a separate procedure is used to treat the changes in chemical structure due to equations (2-5) and (2-6) which are replaced by difference equations of the form

$$\frac{X_{ij} - X_{ij}^{o}}{\Delta t} = -\sum_{k'} \frac{\varepsilon_{k'}^{o}}{Q_{ik'}} + \sum_{k''} \frac{\varepsilon_{k''}^{o}}{Q_{ik''}} \quad (j=1,m;\ i=1,k) \tag{2-64}$$

where $\Delta t = t - t_o$ is the time interval between two models of ages t and t_o, and the superscript o refers to values from the model at time t_o. Applying (2-64) or its equivalent for convective regions, we obtain the chemical structure for the star at time t. The solution at t_o may be used as an approximate solution at time t. If a solution also exists at $t_o - \Delta t'$, a better approximation may be obtained by extrapolation. The approximate solution may then be relaxed as in § 2.5 to obtain a solution for the system (2-57). Energy released in a non-adiabatic expansion appears in (2-2) as $-T\,\partial S/\partial t$. In (2-50) the derivative has been replaced by a difference and rearranged using the first law of thermodynamics. Thus (2-2) becomes

$$\frac{\partial L_r}{\partial M_r} = \varepsilon_{nuc} + \frac{U^{o} - U}{\Delta t} + \frac{P(\rho - \rho^{o})}{\rho^{2}\Delta t} \tag{2-65}$$

The model is checked for chemical homogeneity in convective regions after each iteration for which $f_s = 1$. The timestep Δt is chosen to satisfy the requirements of good convergence, with a minimum number of timesteps providing a good distribution of points on an evolutionary sequence. In practice, this is achieved by limiting changes in central conditions to $\delta t_c < 0.02$, $\delta X_{ic} < 0.05$ (0.2 if the core is convective) and initial r.m.s. corrections to $\hat{\delta}_1 < 10^{-2}$. Near to the exhaustion of nuclear fuel in the core, the timestep is halved if $\delta X_i > X_i$. The timestep is doubled if convergence is very rapid.

Weigert's (1966) treatment of very thin shell sources as described by Kippenhahn et al (1967) is adopted, where the X profile is adjusted to satisfy

$$\frac{\partial X}{\partial M_r}\left(\frac{L_s}{X_c Q}\right) = \frac{\varepsilon}{Q} \tag{2-66}$$

where L_s is the nuclear energy released in the entire shell and X_e is the value of X in the region into which the shell is moving.

A method is included for restarting a timestep with Δt halved for situations where divergence is encountered.

Every tenth model is written out with its preceding model, to enable the sequence to be restarted if required. The overall scheme for constructing an evolutionary sequence is illustrated in fig. 2.2.

Figure 2.2 Flowchart for the construction of evolutionary sequences.

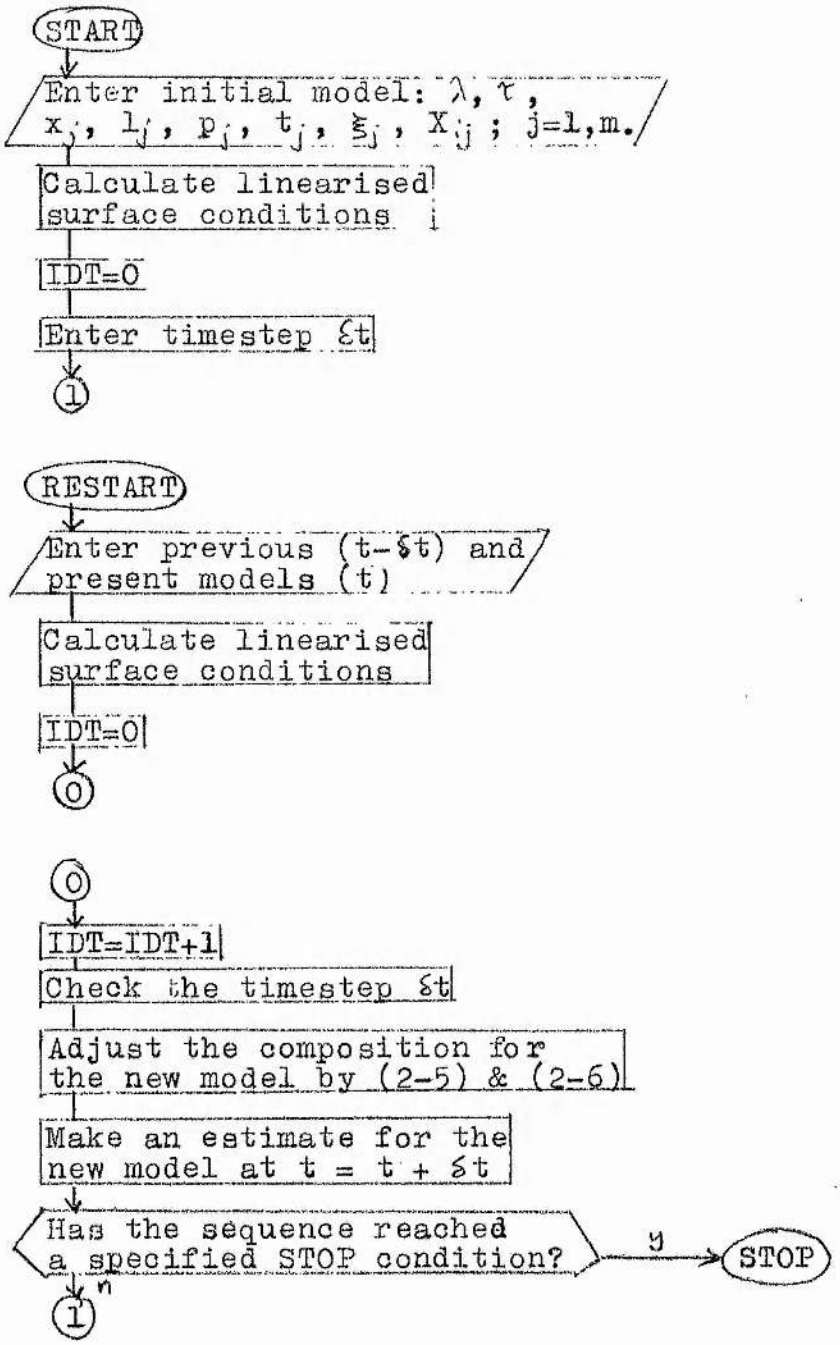

Figure 2.2 (contd.)

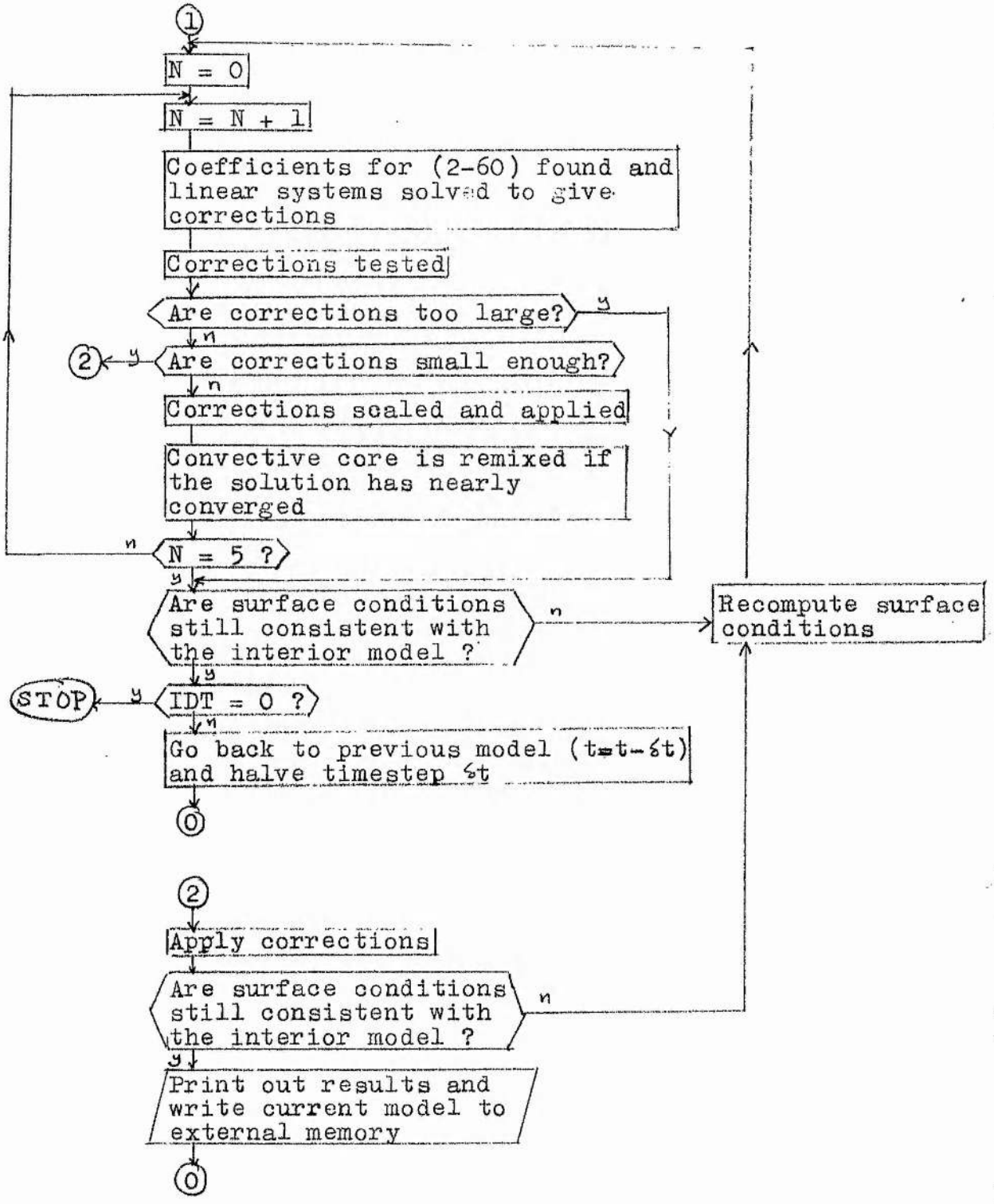

3 INPUT PHYSICS

3.1 THE EQUATIONS OF STATE

In order to calculate models for stellar structure, some description for the bulk properties of stellar material is required. Fairly general treatments of the equations of state under a number of conditions are given by Cox and Giuli (1968). After introducing the quantities required by our treatment we give details of our method for solving the equations of state for ionising material and electron degenerate material respectively. Further thermodynamic quantities required in the stellar structure calculations are also detailed. The method used to choose the appropriate equation of state is described.

The equations of state are solved knowing the total pressure, $P = P_t$, the temperature, T, and the chemical composition, X_k, where X_k is the relative abundance by weight of chemical isotope with atomic weight k. The total pressure is the sum of the total gas pressure and the radiation pressure,

$$P_t = P_r + P_g \tag{3-1}$$

where given the radiation constant a (= 7.564 x 10^{-15} erg cm^{-3} deg^{-1})

$$P_r = aT^4/3 \tag{3-2}$$

For a perfect gas the equation of state may be written in some form such as

$$P_g = n_p kT = (n_i + n_e) kT = \frac{N_o \rho}{\mu} kT \tag{3-3}$$

where k (= 1.38044 x 10^{-16} erg deg^{-1}) is Boltzmann's constant, n_p , n_i and n_e are the number densities of particles, ions and electrons respectively and N_o (= 6.0223 x 10^{23}) is Avogadro's number. μ is the mean atomic weight per particle. n_i is a simple function of the density, ρ , and the mean atomic weight per ion, μ_i ,

$$n_i = N_o \rho / \mu_i \tag{3-4}$$

where if M_k is the mass (in a.m.u) of each element

$$\mu_i^{-1} = \sum_k X_k / M_k \qquad (3\text{-}5)$$

The calculation of n_e is more complicated as the degree of ionisation is a non-linear function of T, ρ and X_k. The simple form of the perfect gas equation of state is further modified at high temperatures and densities by relativity and degeneracy.

In the current study, we do not encounter temperatures $T > 10^9 K$ or densities $\rho > 10^5$ gm cm^{-3}, and can therefore neglect relativistic effects (see fig. 24.4, Cox and Giuli, 1968). For densities at which electron-degeneracy becomes significant, temperatures are high enough to assume that the stellar material is fully ionised. Hence we have solved Saha's ionisation equation at low temperatures ($T/P_g^{0.1} < 5 \times 10^4$) to obtain equilibrium assuming no degeneracy. For higher temperatures we have assumed full ionisation in considering degeneracy effects on the solution of the equation of state. Quantities required from the equation of state are the mean atomic weight, μ, the total density, ρ, the electron density, n_e, the internal energy, U, the specific heats, C_V and C_P and the adiabatic gradient ∇_{ad}.

SAHA'S IONISATION EQUATION

Our treatment of ionisation equilibrium closely follows the discussions of Cox and Giuli (1968), and Mihalas (1978), where fuller derivations of the following equations may be found.

The Saha ionisation equation, an extension of the Boltzmann formula for occupation numbers of atomic energy levels, may be solved for the relative numbers of atoms and ions in successive stages of ionisation, and for the electron density, providing that the gas is in local thermodynamic equilibrium (LTE). The contribution of the excitation potential χ_{ijk} for bound levels to the total internal energy is neglected, while the ionisation energies $\chi_{I_{jk}}$ have been included. The Saha equation becomes

$$\frac{n_{jk}}{n_{j+1k}} = n_e \frac{U_{jk}(T)}{U_{j+1k}(T)} \left(\frac{h^2}{2\pi m k}\right)^{3/2} \frac{T^{-3/2}}{2} \exp\left(\frac{\chi_{Ijk}}{kT}\right) \qquad (3\text{-}6)$$

$$= n_e \tilde{\phi}_{jk}(T) \qquad (3\text{-}7)$$

where the $U_{jk}(T)$ are partition functions of the j^{th} ionisation state of atomic species k. Tests showed that using $U_{jk} = g_{ojk}$, the statistical weight of the lowest ground term was satisfactory. An earlier version of the equation of state treated the ionisation of H and He only. The treatment of partition functions followed that of Aller (1963), where

$$U_{jk} = \sum_n p_n g_n \exp(-\chi_n / kT) \qquad (3\text{-}8)$$

is the summation over energy states of the statistical weight g_n, representing number of available electron states obtained by summation of $g = 2J+1$ over all individual angular momentum states J available to an electron with principal quantum number n. The probability for the occupation of an energy state, p_n, may be approximated by

$$p_n = \exp\{-c(z) \cdot n_e \cdot n^6 \cdot 5040\} \qquad (3\text{-}9)$$

where $c(z)$ depends on the degree of ionisation. The excitation potentials must be obtained experimentally (e.g. Moore, 1949) or from some atomic model. Recursive application of (3 - 6) leads to the fraction of species k in ionisation stage j

$$f_{jk}(n_e, T) = \prod_{L=j}^{J_k - 1} (n_e \tilde{\phi}_{Lk}) \Big/ \sum_{m=0}^{J_k} \prod_{L=m}^{J_k - 1} (n_e \tilde{\phi}_{Lk}) \qquad (3\text{-}10)$$

$$= P_{jk}(n_e, T) / S_k(n_e, T) \qquad (3\text{-}11)$$

where J_k is the highest ionisation stage of species k considered.

Given P_g and T, the total number density, n_p, is known. If the relative abundance by number of species k, α_k, is such that the total number density of species k, $n_k = \alpha_k \cdot n_i$ where $\sum_k \alpha_k = 1$ and $\alpha_k = \mu_i X_k / M_k$ then the conditions of particle and charge conservation are given by

$$n_k = \alpha_k (n_p - n_e) \qquad (3\text{-}12)$$

$$n_e = (n_p - n_e) \sum_k \alpha_k \sum_{j=1}^{J_k} j f_{jk}(n_e, T) \qquad (3\text{-}13)$$

knowing n_p and T, n_e becomes the solution of a non-linear equation which we find using a generalised Newton-Raphson method first suggested by Auer and described by Mihalas (1978). An initial estimate for n_e° is used to obtain a value $n_e' \neq n_e^\circ$ from (3-13). If δn_e can be found such that $n_e = n_e^\circ + \delta n_e$, equation (3-13) will be satisfied exactly. This cannot be done exactly because the equation is non-linear. To first order, we have

$$\delta n_e = \left((n_p - n_e^\circ)\tilde{\Sigma} - n_e^\circ \right) \Big/ \left(1 + \tilde{\Sigma} - (N - n_e^\circ)\left(\partial\tilde{\Sigma}/\partial n_e\right) \right) \qquad (3\text{-}14)$$

$$\tilde{\Sigma} = \sum_k \alpha_k S_k^{-1} \sum_{j=1}^{J_k} j P_{jk} \qquad (3\text{-}15)$$

$$\frac{\partial\tilde{\Sigma}}{\partial n_e} = \sum_k \alpha_k \left(S_k^{-1} \sum_j j \left(\frac{\partial P_{jk}}{\partial n_e} \right) - S_k^{-2} \left(\frac{\partial S_k}{\partial n_e} \right) \sum_j j P_{jk} \right) \qquad (3\text{-}16)$$

The functions $P(n_e,T)$ and $S(n_e,T)$ may be rewritten

$$P_{jk}(n_e,T) = \prod_{\nu=j}^{J_k-1} \left(n_e \tilde{\phi}_{\nu k} \right) = n_e^{(J_k - j)} \Pi_{jk} \cdot \tilde{\phi}(T) \qquad (3\text{-}17)$$

$$S_k(n_e,T) = \sum_{j=J_k^\circ}^{J_k} P_{jk} = \sum_{j=J_k^\circ}^{J_k} n_e^{(J_k - j)} \Pi_{jk} \tilde{\phi}(T) \qquad (3\text{-}18)$$

which have simple forms for their derivatives $\partial P_{jk}/\partial n_e$ and $\partial S_k/\partial n_e$. Solving for δn_e, these equations are iterated using $n_e^i = n_e^{i-1} + \delta n_e$ as the i^{th} estimate for n_e until $\delta n_e / n_e$ drops below some specified value (e.g. 10^{-3}). The convergence of this procedure is quadratic, and with a good initial estimate we usually find 2 or 3 iterations to be sufficient.

In order to obtain a number of other thermodynamic properties of the stellar material, we must first have the gradients $(\partial n_e/\partial\rho)_{T,X_k}$ and $(\partial n_e/\partial T)_{\rho,X_k}$ in addition to the electron density n_e.

$$\left(\frac{\partial n_e}{\partial T}\right)_{\rho, X_k} = \tag{3-19}$$

$$\frac{(n_p - n_e)\sum_k \frac{\alpha_k}{S_k}\sum_{j=1}^{J_k} j\left(n_e^{J_k - j}\frac{\partial \Pi_{jk}}{\partial T} - \left(\sum_{l=0}^{J_k} n_e^{J_k - l}\frac{\partial \Pi_{lk}}{\partial T}\right)\cdot f_{jk}\right)}{1 - \left(\frac{n_p - n_e}{n_e}\right)\sum_k \frac{\alpha_k}{S_k}\sum_{j=1}^{J_k} j\left((J_k - j)P_{jk} - \left(\sum_{l=0}^{J_k}(J_k - l)P_{lk}\right)\cdot f_{jk}\right)}$$

$$\left(\frac{\partial n_e}{\partial \rho}\right)_{T, X_k} = \tag{3-20}$$

$$\frac{N_0 n_e / \mu_i (n_p - n_e)}{1 - \left(\frac{n_p - n_e}{n_e}\right)\sum_k \frac{\alpha_k}{S_k}\sum_{j=1}^{J_k} j\left((J_k - j)P_{jk} - \left(\sum_{l=0}^{J_k}(J_k - l)P_{lk}\right)\cdot f_{jk}\right)}$$

The mean atomic weight, μ, and density are now given by

$$\mu^{-1} = \sum_k X_k / M_k \cdot \left(1 + \sum_{j=1}^{J_k} j f_{jk}\right) \tag{3-21}$$

$$\rho = n_p \mu / N_0 \tag{3-22}$$

The internal energy per unit mass including kinetic energy, ionisation energy and radiation energy, is

$$U = \tfrac{3}{2} n_i (1 + \bar{f}) kT / \rho + \frac{n_i}{\rho}\sum_k \alpha_k \left(\sum_j f_{jk}\left(\sum_{m=1}^{j} \chi_{m-1\,jk}\right)\right) + \frac{aT^4}{\rho} \tag{3-23}$$

$$\bar{f} = \sum_k \alpha_k \left(\sum_j j f_{jk}\right) \tag{3-24}$$

The specific heats at constant volume, c_V , and at constant pressure, c_P and the temperature and density exponents, χ_T and χ_ρ, become

$$c_V \equiv \left(\frac{\partial U}{\partial T}\right)_\rho = \frac{3n_i k}{2\rho}\left(1 + \bar{f} + T\left(\frac{\partial \bar{f}}{\partial T}\right)_\rho\right) \tag{3-25}$$

$$+ \frac{n_i}{\rho}\left(\sum_k \alpha_k \sum_{j=1}^{J_k}\left(\left(\frac{\partial f_{jk}}{\partial T}\right)_\rho \sum_{i=1}^{j} \chi_{i-1,jk}\right)\right) + \frac{4aT^4}{\rho}$$

$$c_P \equiv c_V + \frac{P}{\rho T}\cdot\frac{\chi_T^2}{\chi_\rho} \tag{3-26}$$

$$\chi_T \equiv \left(\frac{\partial \ln P}{\partial \ln T}\right)_\rho = \left(\left(\frac{N_0\rho}{\mu_i} + \left(\frac{\partial n_e}{\partial T}\right)_\rho T + n_e\right)kT + 4P_r\right)/P \tag{3-27}$$

$$\chi_\rho \equiv \left(\frac{\partial \ln P}{\partial \ln \rho}\right)_T = \left(\frac{N_0}{\mu_i} + \left(\frac{\partial n_e}{\partial \rho}\right)_T\right)\frac{kT}{P} \tag{3-28}$$

The only adiabatic exponent (or gamma) required is the adiabatic gradient, ∇_{ad} , where

$$\nabla_{ad}^{-1} = \left(\frac{d\ln P}{d\ln T}\right)_{ad} = \frac{\Gamma_2}{\Gamma_2 - 1} = \chi_T + \chi_\rho \Big/ \left(\frac{P}{\rho T}\frac{\chi_T}{c_V}\right) \tag{3-29}$$

The treatment of local mixing-length theory adopted in this study also requires the quantity

$$\left(\frac{\partial \ln \mu}{\partial \ln T}\right)_{\rho,P} = -T\mu \sum_k \left(X_k / M_k \sum_{j=1}^{J_k} j\left(\frac{\partial f_{jk}}{\partial T}\right)\right) \tag{3-30}$$

where

$$\left(\frac{\partial f_{jk}}{\partial T}\right)_\rho = \left(\left(\frac{\partial n_e}{\partial T}\right)_\rho \left((J_k - j)P_{jk} - \sum_{L=0}^{J_k}(J_k - L)P_{Lk}f_{jk}\right)n_e^{-1}\right. \tag{3-31}$$

$$\left. + n_e^{J_k - j}\left(\frac{\partial \Pi_{jk}}{\partial T}\right)_\rho - \sum_{L=0}^{J_k} n_e^{J_k - L}\left(\frac{\partial \Pi_{Lk}}{\partial T}\right)_\rho f_{jk}\right) S_k^{-1}$$

and

$$\left(\frac{\partial \bar{f}}{\partial T}\right) = \sum_k \alpha_k \sum_{j=1}^{J_k} j\left(\frac{\partial f_{jk}}{\partial T}\right)_\rho \tag{3-32}$$

We have now collected the expressions for the thermodynamic properties of ionising stellar material required in our calculations of stellar structure. In practice, we treat the ionisation of elements H, He, C, N, O, Ne and Mg, where other elements are grouped equally with N and Mg in calculating their contribution to the ionisation equilibrium. We consider the negative ion

of each element, and all positive ions up to the seventh ionisation where appropriate. For all eqs. (3-10) to (3-32) care must be taken in the treatment of the summations over ionisation states. In tests, good agreement with the results of Vardya (1965) was achieved. The approximation of full ionisation at $T/P_g^{0.1} > 5\times10^4$ was found to be good for most common stellar envelope mixtures.

EQUATIONS OF STATE FOR A FULLY IONISED NON-RELATIVISTIC DEGENERATE GAS

Discussions of the treatment of the equation of state for electron degenerate gases may be found, for example, in Cox and Giuli (1968) and Hejlesen (1980). We describe the method we have adopted.

In deep stellar interiors, pressure effects alone will lead to a high degree of ionisation so that the stellar material becomes a neutral two-component plasma of nuclei and free electrons. Except in highly condensed stars (e.g. neutron stars), the positive component may be treated as a perfect gas. The negative component is an 'ideal' Fermi-Dirac electron gas, where the Pauli exclusion principle requires from statistical mechanics that the momentum distribution in the gas is given under the assumptions that electrons are non-interacting and are not in any appreciable potential fields by

$$n_e(p)\,dp = 8\pi p^2 dp/h^3 \cdot \left(\exp(-\eta + \varepsilon/kT) + 1\right)^{-1} \qquad (3\text{-}33)$$

Here $n_e(p)$ is the number density for electrons with momentum in the range $(p, p+dp)$, η is the degeneracy parameter, ε is the electron kinetic energy and h (= 6.6252 x 10^{-27} erg sec) is Planck's constant. The degeneracy parameter characterises the departure of the Fermi-Dirac distribution function from the Maxwell-Boltzmann distribution function for a perfect gas. At low densities, $\eta \ll 0$ and the perfect gas law may be used. Integrating over momentum states, (3-33) becomes

$$n_e = \frac{8\pi}{h^3}\int_0^\infty \frac{p^2 dp}{\exp(-\eta + \varepsilon/kT) + 1} \qquad (3\text{-}34)$$

Letting $x = \varepsilon/kT$ (= $p^2/2mkT$ in the non-relativistic case), then

$$n_e = \frac{2}{\pi^{1/2}} \cdot \frac{2(2\pi mkT)^{3/2}}{h^3} F_{1/2}(\eta) \tag{3-35}$$

where $$F_k(\eta) \equiv \int_0^\infty \frac{x^k dx}{\exp(-\eta+x)+1} \tag{3-36}$$

is the Fermi-Dirac integral, which has been tabulated by McDougall and Stoner (1939), and for which polynomial expansions have been derived, e.g. Cody and Thatcher (1967). We also obtain for the electron pressure

$$P_e = 1/3 \int_0^\infty n_e(p)\, p\, v(p)\, dp \tag{3-37}$$

$$= 2/3\, n_e kT \cdot F_{3/2}(\eta) / F_{1/2}(\eta) \tag{3-38}$$

In solving the equation of state, we know the gas pressure, P_g, temperature, T, the chemical composition, X_k, and assuming full ionisation, the mean atomic weights, μ, μ_i and μ_e. That is,

$$\mu = 2/(1 + 3X_H + X_{He}/2) \tag{3-39}$$

$$\mu_e = 2/(1 + X_H) \tag{3-40}$$

$$\mu_i^{-1} = \mu^{-1} - \mu_e^{-1}$$

Using $P_g = P_i + P_e$ we obtain

$$P_g = 4\pi \frac{(2\pi mkT)^{3/2}}{h^3} kT \left(\frac{\mu_e}{\mu_i} F_{1/2}(\eta) + 2/3\, F_{3/2}(\eta)\right) \tag{3-41}$$

In order to obtain an approximate value for η we attempt to satisfy

$$\tilde{F}(\eta) \le P_g' < \tilde{F}(\eta + \delta\eta) \quad (-4 < \eta < 20) \tag{3-42}$$

where $$P_g' = P_g / (4\pi/3 \cdot (2\pi mkT)^{3/2} kT) \tag{3-43}$$

and $$\tilde{F}(\eta) = \frac{\mu_e}{\mu_i} F_{1/2}(\eta) + \frac{2}{3} F_{3/2}(\eta) \tag{3-44}$$

If $\eta \le -4$ we assume a non-degenerate equation of state, in which case we obtain

$$\rho = \mu P_g / RT \tag{3-45}$$

$$\frac{\partial P_g}{\partial \rho} = RT/\mu \tag{3-46}$$

$$\frac{\partial P_g}{\partial \rho} = R\rho/\mu \tag{3-47}$$

If $\eta \geq 20$ we assume complete degeneracy in which case we obtain

$$P_g = \rho\left(\frac{RT}{\mu_i}\right) + \rho^{5/3}\,\frac{8\pi}{15h^3m}\left(\frac{3h^3N_0}{8\pi\mu_e}\right)^{5/3} \tag{3-48}$$

which may be solved for ρ using a Newton-Raphson iteration method.

If we then let

$$\Lambda = \frac{8\pi}{15h^3m}\cdot\left(\frac{3h^3N_0}{8\pi}\right)^{5/3}\cdot\left(\frac{\rho}{\mu_e}\right)^{2/3}\cdot\frac{1}{RT} \tag{3-49}$$

we obtain

$$\frac{\partial P_g}{\partial \rho} = RT\left(\frac{1}{\mu_i} + \frac{5\Lambda}{3\mu_e}\right) \tag{3-50}$$

$$\frac{\partial P_g}{\partial T} = R\rho/\mu_i \tag{3-51}$$

If $-4 < \eta < 20$ partial degeneracy holds and the degeneracy parameter is obtained as a solution of (3-41) by Newton-Raphson iteration. The density is then given by

$$\frac{\rho}{\mu_e} = \frac{2}{\pi^{1/2}}\cdot\frac{2(2\pi mkT)^{3/2}}{N_0h^3}F_{1/2}(\eta) \tag{3-52}$$

To obtain derivatives we define

$$\Lambda = {}^2/_3\,F_{3/2}(\eta)\,/\,F_{1/2}(\eta) \tag{3-53}$$

$$\mu_x = \left(F_{1/2}(\eta)\,/\,\frac{dF_{1/2}(\eta)}{d\eta} - \Lambda\right)/\mu_e \tag{3-54}$$

$$\mu_y = 1/\mu_i + \Lambda/\mu_e \tag{3-55}$$

in which case

$$\frac{\partial P_g}{\partial \rho} = RT\left(\mu_x + \mu_y\right) \tag{3-56}$$

$$\frac{\partial P_g}{\partial T} = R\rho\left(\mu_y - 1.5\mu_x\right) \tag{3-57}$$

We can then use standard forms for the internal energy, specific heats and temperature and density exponents, viz.,

$$U = \left(3/2\,P_g + 3R\right)/\rho \tag{3-58}$$

$$c_v = \left(3/2\,\frac{\partial P_g}{\partial T} + 12\,R/T\right)/\rho \tag{3-59}$$

$$c_p = c_v + \frac{P\,\chi_T^2}{\rho T\,\chi_\rho} \tag{3-26}$$

$$\chi_\rho = \frac{\partial P_g}{\partial \rho}\cdot\frac{\rho}{P} \tag{3-60}$$

$$\chi_T = \left(\frac{\partial P_g}{\partial T} \cdot T + 4 P_r \right) / P \qquad (3\text{-}61)$$

The adiabatic gradient $\nabla_{ad} = \Gamma_2 / \Gamma_2 - 1$ is given by (3-29) and the derivative $(\partial \ln \mu / \partial \ln T)_{P,\rho}$, vanishes under the assumption of full ionisation.

CHOOSING THE EQUATION OF STATE

We have already found that the full-ionisation approximation for $T/P_g^{0.1} > 5 \times 10^{-4}$ holds for most common stellar envelope mixtures. For stellar models constructed in the present work we do not encounter degeneracy effects for $T/P_g^{0.1} < 5 \times 10^{-4}$, and hence the separate treatment of ionisation equilibrium and non-relativistic degeneracy is valid. To ensure that all properties calculated from the equations of state and their derivatives are continuous we adopt the following procedure to select the appropriate method.

1) If $T/P_g^{0.1} < 5 \times 10^{-4}$ we obtain ionisation equilibrium from Saha's equation assuming no degeneracy effects.

2) If $T/P_g^{0.1} > 6.3 \times 10^{-4}$ we calculate the equation of state assuming full ionisation and non-relativistic degeneracy.

3) If $5 \times 10^{-4} < T/P_g^{0.1} < 6.3 \times 10^{-4}$ all quantities are obtained by interpolating between the results from both methods (1) and (2). To ensure continuous derivatives the interpolation is weighted by a cosine function over the interval (5×10^{-4} , 6.3×10^{-4}).

3.2 STELLAR OPACITY

Efforts to determine the opacity of stellar material to energy transfer are reviewed by Cox (1965) and by Carson (1976). Here we summarise the main features in the development of the theory, following Carson (1976). The Carson opacities and the method of interpolation are described. Alternative opacities are briefly mentioned.

In order to determine both the method and the rate of energy transport in stars the opacity to energy transfer, κ , must be known as a property of the stellar material. This opacity is the harmonic mean of radiative and conductive opacities,

$$\kappa^{-1} = \kappa_r^{-1} + \kappa_c^{-1} \tag{3-62}$$

following from the additivity of radiative and thermal conductivities,

$$K = K_r + K_c \tag{3-63}$$

where conductivity and opacity are related by the equation

$$K = 4acT^3 / 3\rho\kappa \tag{3-64}$$

In general, radiative transfer is the principal mode of energy transfer in the nondegenerate regime, while thermal conduction is more important in the degenerate regime.

The radiative opacity is itself a harmonic mean of the monochromatic radiative mass-absorption coefficient $\kappa(\nu)$ where ν is the photon frequency. In Local Thermodynamic Equilibrium, the Rosseland mean defined by

$$\kappa_r^{-1} = B^{-1}(T) \int \kappa^{-1}(\nu) \frac{\partial B(\nu,T)}{\partial T} d\nu \tag{3-65}$$

is appropriate where $B(\nu,T)$ and $B(T)$ are the monochromatic and integrated blackbody specific intensities, and $\kappa(\nu)$ comprises contributions from both absorption and scattering processes. The important atomic transitions contributing to the absorption coefficient will depend on the degree of ionisation of the material. Ionisation equilibrium, occupation numbers and cross-sections must be obtained from suitable atomic models.

Thermal conduction arises from the anisotropy in the energy distribution

of the constituent particles which arises when a temperature gradient exists in a medium. In LTE, equipartition of energy results in electrons carrying most of the heat energy. Traditional theories (see Carson (1971) for a summary) treat the temperature gradient as a perturbation in the Boltzmann equation for the electron distribution function

$$f(E) = \left(\exp\left(E/kT + \eta\right) + 1 \right)^{-1} \tag{3-66}$$

where η is a degeneracy parameter. With the collisional relaxation time τ, where

$$\tau^{-1} = N_s v \sigma_s , \tag{3-67}$$

N_s being the number density of scatterers, v their velocity and σ_s the momentum transfer total-scattering cross-section, the thermal conductivity becomes

$$K_c = \left(2m^3/h^3\right)\left(1(1)\,I(E') - I^2(E)\right) / T\,I(1) \tag{3-68}$$

$$I(x) = (4\pi/3) \int x \tau v^4 \frac{\partial f}{\partial E}\, dv \tag{3-69}$$

In analogy with the theory of metals, the thermal conductivity can also be expressed in some of the usual transport coefficients, S_{ij}, for the electric and thermal currents in the gas

$$K_c = \left(S_{11} S_{22} - S_{12} S_{21}\right) / T S_{11} \tag{3-70}$$

The Sij may be obtained from the collision cross-sections for electron-electron and electron-ion collisions (e.g. Lampe, 1968) with appropriate consideration given to collective electron effects.

Early models for radiative opacity adopted Kramers' semi-classical cross-sections for free-free and bound-free transitions (Eddington, 1926), quantum-mechanical cross-sections for electrons in a Coulomb field (Strömgren, 1932), and corrections for Coulomb screening and pressure ionisation (Morse, 1940). Keller and Meyerott (1955) made the first calculations with a programmed calculator, presenting results for 13 chemical compositions. With the development of high speed electronic computers, more sophisticated models were developed, largely by Cox and colleagues (Cox, 1965) at the Los Alamos Scientific Laboratory. In these

calculations energy levels were obtained, from observational data when available, otherwise from the Bohr theory with the aid of Slater screening constants and corrected for interactions with charged particles. For temperatures $T < 10^6 K$, Saha's ionisation equation was used to determine ionisation equilibrium. At higher temperatures only average atoms with average numbers of electrons in each shell were considered. The radiative absorption cross-sections for free-free, bound-free and bound-bound transitions were taken to be hydrogenic or Coulomb in form. The free electrons scatter according to the classical or Thomson cross section, modified for stimulated Compton-scattering (Sampson, 1959). At this stage, electron conduction was treated by the Mestel (1950) extension of the Marshak (1941) theory in which only electron-nuclei collisions with Rutherford cross-sections are considered. The first results of these calculations were given by Cox and Stewart (1962), Cox, Stewart and Eilers (1965) and Cox and Stewart (1965) for a total of 13 chemical mixtures. Further improvements over these calculations led Cox and Stewart (1969) to present results for 44 mixtures which included additional sources of absorption and improvements to the methods of calculation leading to results which differed by up to 40% at $T = 10^5 K$ from previous ones. Further improvements, including the effects of autoionisation broadening on absorption lines (Merts and Magee, 1972), the careful treatment of narrow lines (Magee, Merts and Huebner, 1975), the inclusion of more bound-bound transitions and the absorption due to many molecules (Merts, Magee and Beebe, 1973) have led to the publication of a further set of opacity tables by Cox and Tabor (1976). The general tendency of these successive improvements has been to increase the Cox-Stewart opacities, often by large factors.

THE CARSON OPACITIES

The most significant single physical approximation adopted in the opacity calculations discussed so far is the use of the 'hydrogenic' or 'Coulomb' approximation. Departures from the validity of this approximation will become important for many-electron and non-excited levels and at high densities, where departures from a strict Coulomb field are large. The validity of the hydrogenic approximation was examined by Carson and Hollingsworth (1968) using the standard atomic model, viz., the Wigner-Seitz ion sphere filled with a neutralising uniform density electron gas and numerically exact methods. Providing the effective nuclear charge was chosen in a particular way, they found that the hydrogenic approximation could be applied, but gave opacities increased by up to 40% above the corresponding Cox values. In a separate programme, Carson, Mayers and Stibbs (1968) carried out non-hydrogenic calculations. Using the generalised Thomas-Fermi atomic model for the charge distribution in the neighbourhood of each nucleus, solving the associated Poisson equation for the potential, and determining energy levels, wave functions and occupation numbers, it was found for the few comparison calculations performed that the opacity would be increased to a value two or three times the Cox values.

In addition to these uncertainties in the radiative opacity calculations, the assumptions of the standard Marshak-type theories of thermal conduction have been shown to be inadequate in some cases. In particular, the importance of electron-electron collisions was demonstrated by Spitzer and Harm (1953) for nondegenerate conditions, and by Lampe (1968) in degenerate conditions. Consequently Hubbard and Lampe (1968) have presented tables of the conductive opacity for a number of chemical compositions, with significant increases even for relatively high electron degeneracy.

These modifications to stellar opacity theory have been combined in a set of opacity tables for 28 stellar compositions computed by Carson. Hydrogen and Helium are treated 'exactly', while for heavier elements, the generalised Thomas-Fermi model, supplemented by experimental ionisation

energies, is used. At low temperatures, all negative ions and the formation of several molecules are considered in the ionisation equilibrium, while absorption by negative ions and Rayleigh scattering by all neutral atoms and molecules and by He^+ is included. The conductive opacity is calculated by means of the Hubbard and Lampe (1968) code.

The opacity tables are presented in Appendix A.2 in the form $\log \kappa$, ($\log T$, $\log \rho$) for up to 410 grid points in temperature and density and for the 28 chemical mixtures given in tables 3.1 and 3.2 respectively. The relative abundances of heavy elements (table 3.3) were taken from Cameron (1973) and represent an increase in the CNO component of the heavy element contribution over the Cox - Stewart (1969) opacities.

The validity of some opacity points is doubtful in regions of the (T, ρ) plane where the conduction code is invalid (i.e. the high density points). However these should not lead to difficulties as they lie well outside the range of (T, ρ) values normally encountered in calculations of stellar structure except in condensed objects such as white dwarfs. One possible temporary solution may be to set $\kappa_c = \infty$, where this would be reasonable. It will be evident from table 3.2 that population II compositions are not well represented by the opacity tables, in which $Z \in \{0.00, 0.01, 0.02, 0.04\}$ for Hydrogen mixtures. While making the comment that this is one area in which further opacity calculations would be desirable, we have considered it worthwhile to make studies for $Z < 0.01$ by interpolating in the existing data. Fortunately an opacity table does exist for one population II composition ($X = 0.745$, $Z = 0.005$), so we are able to compare an interpolated opacity table with the calculated table. Opacities for densities $\log \rho \in \{-10, -8, \ldots, 6\}$ are compared in figure 3.1. For temperatures and densities occurring in stellar models constructed in the present study the difference between the opacities obtained directly and by interpolation is always less than 25%, and usually less than $\sim 5\%$. Models of a stellar envelope for a horizontal-branch star calculated with the two sets of opacities (A. Bridger, 1982: private communication) show small differences

Table 3.1 Grid in temperature and density for which Carson opacities are tabulated.

log T	log ρ																		
	-12	-11	-10	-9	-8	-7	-6	-5	-4	-3	-2	-1	0	1	2	3	4	5	6	7	8
3.3	*	*	*	*	*	*	*	*	*	*											
3.4	*	*	*	*	*	*	*	*	*	*											
3.5	*	*	*	*	*	*	*	*	*	*											
3.6		*	*	*	*	*	*	*	*	*	*										
3.7		*	*	*	*	*	*	*	*	*	*										
3.8		*	*	*	*	*	*	*	*	*	*										
3.9		*	*	*	*	*	*	*	*	*	*										
4.0		*	*	*	*	*	*	*	*	*	*										
4.1			*	*	*	*	*	*	*	*	*	*									
4.2			*	*	*	*	*	*	*	*	*	*									
4.3			*	*	*	*	*	*	*	*	*	*									
4.4			*	*	*	*	*	*	*	*	*	*									
4.5			*	*	*	*	*	*	*	*	*	*									
4.6				*	*	*	*	*	*	*	*	*	*								
4.7				*	*	*	*	*	*	*	*	*	*								
4.8				*	*	*	*	*	*	*	*	*	*								
4.9				*	*	*	*	*	*	*	*	*	*								
5.0				*	*	*	*	*	*	*	*	*	*								
5.2					*	*	*	*	*	*	*	*	*	*							
5.4					*	*	*	*	*	*	*	*	*	*							
5.6						*	*	*	*	*	*	*	*	*	*						
5.8						*	*	*	*	*	*	*	*	*	*						
6.0						*	*	*	*	*	*	*	*	*	*						
6.2							*	*	*	*	*	*	*	*	*	*					
6.4							*	*	*	*	*	*	*	*	*	*					
6.6								*	*	*	*	*	*	*	*	*	*				
6.8								*	*	*	*	*	*	*	*	*	*				
7.0								*	*	*	*	*	*	*	*	*	*				
7.2									*	*	*	*	*	*	*	*	*	*			
7.4									*	*	*	*	*	*	*	*	*	*			
7.6										*	*	*	*	*	*	*	*	*	*		
7.8										*	*	*	*	*	*	*	*	*	*		
8.0										*	*	*	*	*	*	*	*	*	*		
8.2											*	*	*	*	*	*	*	*	*	*	
8.4											*	*	*	*	*	*	*	*	*	*	
8.6												*	*	*	*	*	*	*	*	*	*
8.8												*	*	*	*	*	*	*	*	*	*
9.0												*	*	*	*	*	*	*	*	*	*

Table 3.2 Naming conventions for the Carson opacity tables and the chemical mixtures for which they are available.

	Z	0.00	0.01	0.02	0.04
X = 1.00 - Z	Y = 0.00	C400	C401	C402	C404
X = 0.75 - Z	Y = 0.25	C310	C311	C312	C314
X = (1.0-Z)/2	Y = (1.0-Z)/2	C220	C221	C222	C224
X = 0.25	Y = 0.75 - Z	C130	C131	C132	C134
X = 0.00	Y = 1.00 - Z	C040	C041	C042	C044

X = 0.0	Z	C	O
Y = 0.0	C = O = 1.0	6004	8004
Y = 0.25	C = O = 0.75	6013	8013
Y = 0.50	C = O = 0.50	6022	8022
Y = 0.75	C = O = 0.25	6031	8031

Table 3.3

Relative abundances of elements within the heavy element component, taken from the compilation of Cameron (1973), considering the twelve most abundant elements :

Element	Zi	Ai	Ni	Xi
C	6	12.011110	0.26778311	0.19268399
N	7	14.006710	0.08246749	0.06919456
O	8	15.999380	0.48554122	0.46538115
Ne	10	20.211746	0.07991287	0.09433919
Na	11	22.989777	0.00135804	0.00187037
Mg	12	24.310013	0.02401470	0.03497370
Al	13	26.981537	0.00192389	0.00310976
Si	14	28.085617	0.02274267	0.03826527
S	16	32.064316	0.01149943	0.02206988
Ar	18	36.283112	0.00271767	0.00590718
Ca	20	40.077179	0.00167930	0.00403186
Fe	26	55.848541	0.02037624	0.06817431

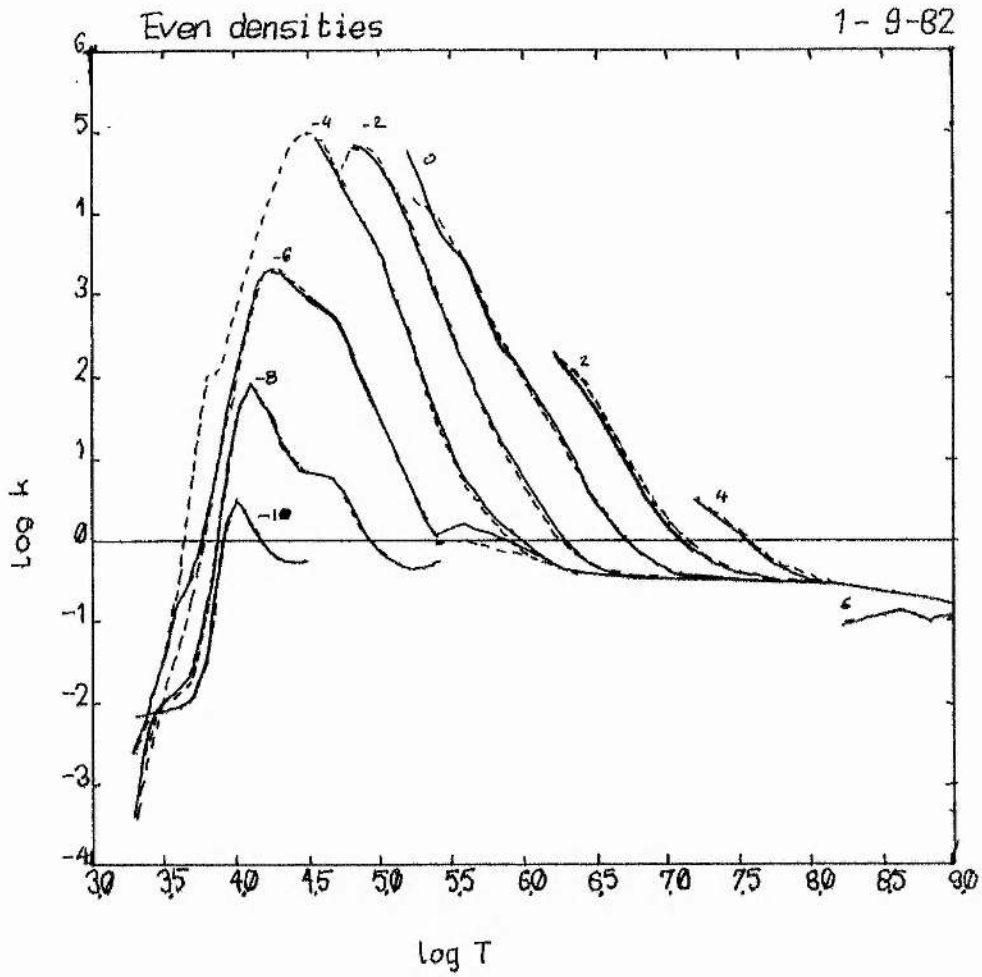

Figure 3.1 A comparison of the Carson opacities for a composition X = 0.745, Z = 0.005, 1) obtained by linear interpolation (dashed lines) between opacity tables for Z = 0 and Z = 0.01, and 2) calculated directly (solid lines). Opacities are plotted along lines of constant density (log ρ) as labelled.

in the stellar atmosphere structure. More significant differences occur for log T > 5 where the interpolated opacity is lower by approximately 5% than the calculated opacity. By the time a point one tenth of the stellar radius from the stellar centre is reached, the interpolated opacities have led to temperatures and pressures lower by 7% and 30% respectively than found with the calculated opacity. Significant opacity differences are encountered in the CNO ionisation region around log T = 6 which give rise to this result. We therefore adopt caution with respect to the interpretation of our results for population II mixtures.

A number of procedures of varying complexity and accuracy are available for interpolating amongst tabulated data. For the current problem, the simplest of these is a multi-dimensional linear interpolation in the existing tables. One improvement is to introduce a higher order interpolation or some form of spline function. Rood (1971) assesses the relative accuracy of different interpolation methods in opacity tables, and concludes that differences of up to 20% between a linear method and a four-point Lagrangian method can occur. Stothers (1974a) finds the effects of different interpolation methods on calculations of homogeneous stellar structure to be comparable to the effect of changing from Cox and Stewart to Carson opacities. Other authors (e.g. Hejlesen, 1980) have used a bicubic spline procedure to create new tables with an increased density of grid points (e.g. with $\Delta \log \rho = 0.3$), and have then adopted a linear interpolation in these new tables during stellar structure calculations. We have adopted a linear interpolation in ($\log T$, $\log \rho$, X_i) (where X_i represents the abundance of chemical element i). If more time had been available, a better strategy should possibly have been chosen - suggesting a possible extension of the current work.

The interpolation strategy operates as follows.

(1) We designate the hydrogen/helium/metals mixtures as (H, He, Z) and the helium/carbon/oxygen mixtures as (He, C, O). The (H, He, Z) mixtures are arranged in order of 1) increasing helium abundance (Y_k^{ν}) and

2) increasing metal abundance (Z_l). Given log T, log ρ and Xi, i = 1, j, we obtain Y and Z. If either the hydrogen abundance (X) is greater than 0 or $Z < 0.05$ then we choose four (H, He, Z) tables for which $Y_k^{l+1} < Y \leq Y_{k+1}^{l+1}$ and $Z_l < Z \leq Z_{l+1}$. For each table $\{(Y_k^l, Z_l), (Y_{k+1}^l, Z_l), (Y_k^{l+1}, Z_{l+1}), (Y_{k+1}^{l+1}, Z_{l+1})\}$ we obtain the opacity log κ_{kl} by linear interpolation in log T and log ρ. We then obtain log κ (H, He, Z) by linear interpolation in Y and Z between these four opacity values.

(2) The (He, C, O) tables are arranged in order of 1) increasing helium abundance (Y_k) and 2) increasing atomic number. If both X = 0 and $Z > 0.05$ then we assume that the metal component is mostly a mixture of carbon and oxygen. By assuming separately that the metal component is purely carbon or oxygen we obtain two values, log κ_c, log κ_o, by linear interpolation 1) in log T and log ρ in four opacity tables (Y_k, Z = C), (Y_{k+1}, Z = C), (Y_k, Z = O), (Y_{k+1}, Z = O) and 2) in Y between each pair of opacity values. The required opacity is then obtained by linear interpolation between log κ_c and log κ_o from the relative abundances of C and O.

(3) The above two procedures have a discontinuity at a point X = 0, Z = 0.05 (If X > 0, then Z is assumed not to exceed 0.04). Therefore if $Z < 0.05$ and X = 0 we follow both procedures to obtain log κ (H, He, Z) and log κ (He, C, O). We then interpolate linearly such that

$$\log \kappa (Z = 0) = \log \kappa (H, He, Z)$$

$$\log \kappa (Z = 0.05) = \log \kappa (He, C, O)$$

This procedure ensures that the opacity is continuous for all chemical mixtures which we are likely to encounter in this study.

An earlier version of the procedure neglected the discontinuity at Z = 0.05. The effect of changing the assumed contribution of carbon to the total metal abundance from 19% to 93% when Z = 0.03 is shown in figure 3.2. The earlier version always assumed that $Z_c = 0.19Z$ when $Z < 0.05$. The effect of this change on the helium-core in models of horizontal-branch stars is discussed in the next chapter.

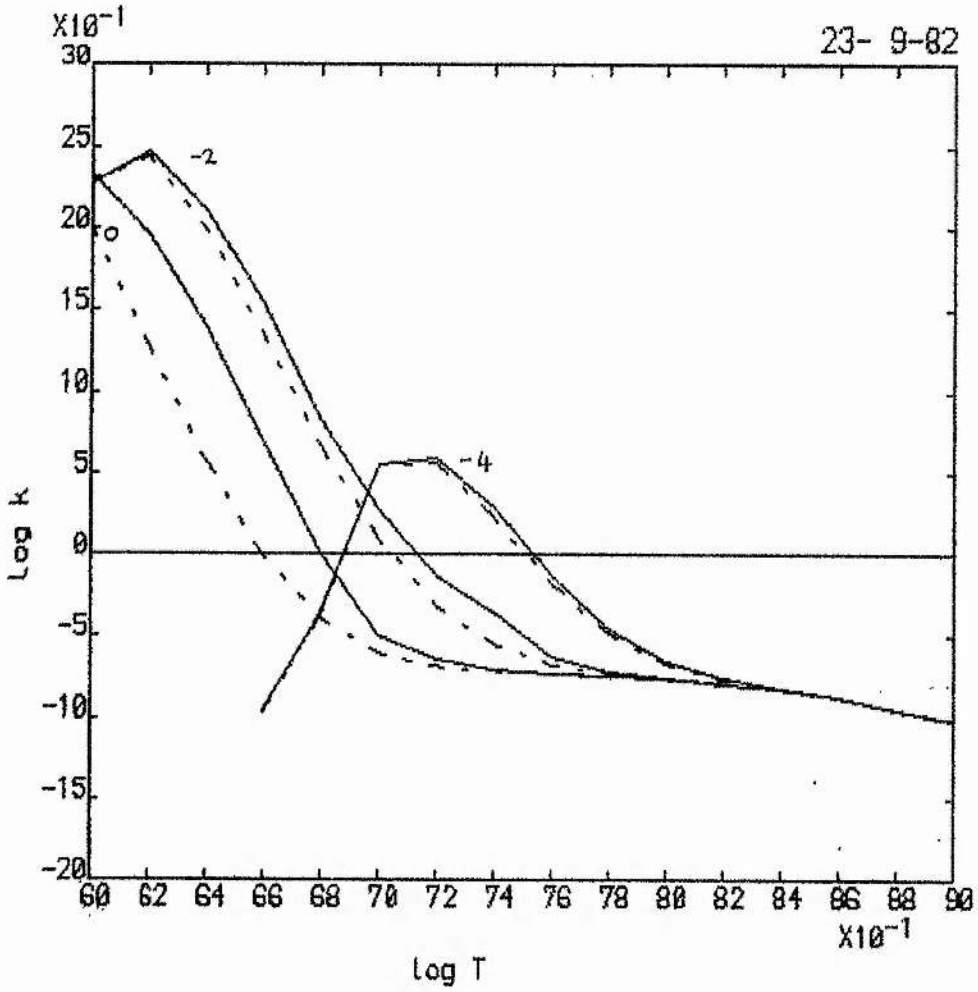

Figure 3.2 A comparison of the interpolated Carson opacities at helium-core temperatures and densities for Y = 0.97, Z = 0.03, with two metal compositions.

1) C = 0.19Z (dashed lines), where C is the relative abundance by mass of Carbon.

2) C = 0.028 (solid lines).

The second represents a carbon-enriched core immediately after the helium-flash more closely than the former. Opacities are plotted for constant densities ($\log \rho$) as labelled.

In figure 3.1 we showed the Carson opacity for composition ($X = 0.745$, $Z = 0.005$) as a function of temperature and at constant density. As the behaviour of the opacity for $\log T < 3.8$ at low densities is not regular (the opacity increases with decreasing density), we have replaced the Carson opacity at low temperatures with the Christy (1966) opacity formula, which is an analytic fit to the Cox and Stewart (1965) opacity data. This follows Carson, Stothers and Vemury (1981). For $\log T \leqslant 3.8$ we use the Christy opacity, for $\log T \geqslant 3.9$ we use the Carson opacity and we interpolate between the two for $3.8 < \log T < 3.9$. While this is not a particularly satisfactory method for obtaining low temperature opacities it has the advantage of providing a physically reasonable approximation until reliable Carson opacities at low temperatures become available. Models for zero-age main-sequence stars with a mass of approximately $0.8\ M_{\odot}$ constructed with the full Carson opacity are underluminous by a considerable amount ($\delta \log L \simeq -0.3$).

Several other opacity formulae are given in the literature, some of which have been useful in developing the stellar structure computer programme. In particular Kramers' laws (Schwarzschild, 1958; Eddington, 1926) give simple power law expressions for the opacity, while Stellingwerf (1975) gives an analytic opacity formula based on the Cox and Tabor (1976) opacity data. Although the Stellingwerf formula is optimised for densities and temperatures typical of Cepheid envelopes, errors of up to 25% outside this region should only lead to discrepancies in the stellar models comparable with those arising from the use of a linear interpolation procedure. Further discussion of tests run using the Stellingwerf opacity is deferred to chapter 5.

Carson and Stothers (1976) summarise the differences between the Carson opacities and the Cox-Stewart (1965) opacities for hydrogen-rich mixtures. Between $\log T = 3.8$ and 4.5 the Carson opacities are smaller than the Cox-Stewart opacities; the maximum difference occurs in the domain of hydrogen ionisation. From $\log T = 4.5$ to 5.4 the Carson opacities are

larger than the Cox-Stewart opacities, particularly in the region of second helium ionisation. Above log T = 5.4 a very large opacity due to the last stage of ionisation in the CNO group of elements is found with the Carson opacities, particularly at low densities. By log T = 6.5 both sets of opacities are close to the electron-scattering limit.

We have compared the Carson opacities with the Cox-Stewart (1969) opacities for hydrogen poor mixtures at temperatures and densities typical of horizontal-branch star helium-rich cores. The results are illustrated in figure 3.3 where log κ is plotted as a function of log T for densities log $\rho \in \{ 0, 2, 4 \}$. In general the Carson opacities are slightly larger than the Cox-Stewart opacities for $6 \lesssim \log T \lesssim 7$ and smaller for $7 \lesssim \log T \lesssim 8.2$, after which both reach the electron-scattering limit. Note that the Carson opacity takes account of the conductive opacity. For Helium poor mixtures the Carson opacities are very much smaller than the Cox-Stewart opacities for log $\rho = 0$.

Figure 3.3 A comparison of the tabulated Carson opacities (dashed lines) with the Cox-Stewart (1969) opacities (solid lines) for four compositions: 1) He, 2) He : C (1:1), 3) O, 4) C. Opacities are plotted for densities as labelled.

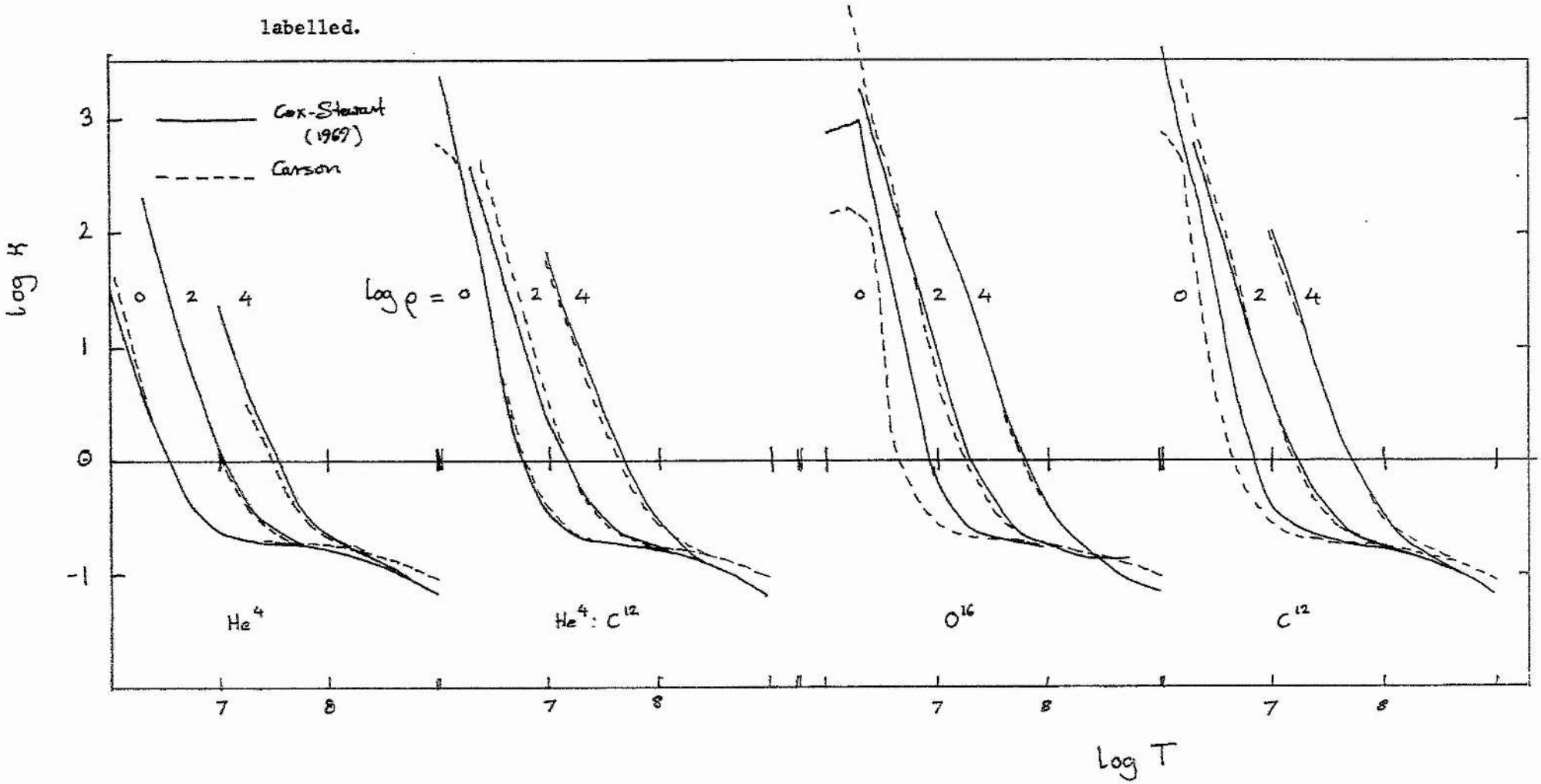

3.3 SUBATOMIC PROCESSES

One of the most significant stages in the development of the theory of stellar structure was the discovery that the stellar energy source must be linked to nuclear reactions in the stellar interior. Eddington (1926) traces the early development of the theory for the conversion of 4 hydrogen nuclei into 1 helium nucleus with the mass excess being converted to its equivalent energy. With successive advances in both theoretical and experimental nuclear physics, networks of nuclear reactions with reaction rates, r, and energy release Q, have been established for various stages of evolution. Reviews are given by Burbridge, Burbridge, Fowler and Hoyle (1958) Reeves (1965), Fowler, Caughlan and Zimmerman (1967) (FCZI), Cox and Giuli (1968) and Fowler, Caughlan and Zimmerman (1975) (FCZII) for thermonuclear reactions, and by Cox and Giuli (1968) and Beaudet, Petrosian and Salpeter (1967) for neutrino processes (amongst others). In this section we describe our treatment of nuclear reactions, nucleosynthesis and neutrino processes.

THERMONUCLEAR REACTIONS

For a gas composed of two types of particles, 1 and 2, the number of reactions per second per unit volume may be written

$$I_{12} = \int_0^\infty N(v)[v\sigma(v)]\,dv \qquad (3\text{-}71)$$

where v is the relative velocity between the two particles, $\sigma(v)$ is the nuclear cross-section for the reaction and N(v) is the number of pairs of particles with velocity v. In most cases a Maxwellian velocity distribution applies. If N_1 , N_2 are the number densities of particles 1 and 2, we can introduce the quantity $\langle\sigma v\rangle$, the reaction probability per unit pair 1, 2 in a unit volume per unit time,

$$\langle\sigma v\rangle_{12} = I_{12} / N_1 N_2 \qquad (3\text{-}72)$$

Hence we obtain a number of useful quantities, and in particular

$$r_{12} = \frac{N_1 N_2}{\rho} \frac{\langle\sigma v\rangle_{12}}{(1+\delta_{12})} \qquad (3\text{-}73)$$

is the reaction rate per unit mass for reactions of particles of type 1 and 2, where δ_{12} is the Kronecker delta function. Where these particles are atomic nuclei or protons, this reaction rate has to be modified for electron screening. Salpeter (1954) shows that the effective increase in r may be described in terms of a negative potential energy U_o

$$r_{12}' = r_{12} \cdot \exp\left(-U_o / kT\right) \tag{3-74}$$

If Q_{12} is the energy released per reaction, then the total energy generation rate is

$$\varepsilon_{12} = r_{12}\, Q_{12} \tag{3-75}$$

and the rate of change of relative abundance X_1 of atomic species 1 is given by

$$\left|\frac{\partial X_1}{\partial t}\right|_{12} = -(1+\delta_{12})\, A_1\, r_{12} / N_o \tag{3-76}$$

where N_o is Avogadro's number and A_1 is the atomic weight of species 1. If one of the products of the reaction is a neutrino, then a proportion of the energy Q_{12} will be lost.

Reaction rates and the energy released per reaction exclusive of neutrino energies for hydrogen and helium burning processes are taken from Fowler, Caughlan and Zimmerman (1975). Electron screening factors are taken from Reeves (1965). Reaction rates, etc. are given in table 3.4. Following Sweigart and Gross (1974), we determine the abundance of ^{14}N in the CNO cycle after Reeves (1965) and Caughlan and Fowler (1962) by setting the nitrogen abundance $X_{14} = X_{12} + X_{14} + X_{16}$ for $\log T > 7.235$ and $X_{14} = X_{12} + X_{14}$ for $\log T < 7.195$. In between these temperatures X_{14} is assigned a linear dependence on $\log T$.

We have assumed that all isotopes taking part in the thermonuclear reaction networks reach their equilibrium abundances instantaneously. This approximation is valid only when the evolutionary timescale of a star is long compared to the reaction time of the slowest reaction in a network. For rapidly evolving stars this is not the case. For most stellar models considered the former situation holds. The assumption also allows us to

make some deductions about rapid phases of evolution.

NEUTRINO PROCESSES

In considering further energy losses due to neutrino interactions, we have included contributions from photo-neutrino, pair neutrino and plasma neutrino processes via the analytic interpolation formula of Beaudet, Petrosian and Salpeter (1967) which we reproduce here. Defining the energy loss per unit mass in terms of the energy loss per unit volume

$$\varepsilon = Q/\rho, \tag{3-77}$$

expressing temperature in relativistic units

$$\lambda = \frac{kT}{mc^2} = \frac{T}{5.9302 \times 10^9} \tag{3-78}$$

we also define

$$\xi = (\rho/\mu_e)^{1/3}\ 10^{-3}\ \lambda^{-1} \tag{3-79}$$

$$f(\lambda,\xi) = \frac{(a_0 + a_1\xi + a_2\xi^2)e^{-c\xi}}{\xi^3 + b_1\lambda^{-1} + b_2\lambda^{-2} + b_3\lambda^{-3}} \tag{3-80}$$

The approximation to Q is then given as

$$Q = (\rho/\mu_e)^3 f_{pl} + (\rho/\mu_e)\lambda^5 f_{ph} + g(\lambda)e^{-(2/\lambda)} f_{pa} \tag{3-81}$$

$$g(\lambda) = 1 - 13.04\lambda^2 + 133.5\lambda^4 + 1534\lambda^6 + 918.6\lambda^8 \tag{3-82}$$

where f_{pl}, f_{ph} and f_{pa} are $f(\lambda,\xi)$ with different coefficients for plasma, photo and pair neutrino rates respectively. These coefficients are given in table 3.5.

Table 3.4 Reaction rates for the major nuclear processes considered in the stellar evolution program, from Fowler, Caughlan and Zimmerman (1975).

Nomenclature :

Q, R, : given in text as Qij, rij.
S : reaction cross-section .
ES : electron-screening factor (Reeves, 1965)
N0 : Avogadro's number
R0 : Density
Tn : Temperature (T/10**n)
Tnab : Tn**(a/b) (also R0ab)
Xm, Mm Relative abundance and atomic weight of species m

---

p-p chain

H1(P,E+NU)H2
```
Q = 13.116 * (1 + 1.412E8 * (1/X1 - 1) * EXP(-4.998/T913))
S = 4.21E-15/T923 * EXP(-3.380/T913) *
        (1 + 0.123*T913 + 1.09*T923 + 0.938*T9)
ES = 1 + 0.25 * R012/T612
R = R0 * N0 * (X1/M1)**2 * S*ES / 2
```

CN(O) cycle

N14(P,G)O15
```
Q = 24.970
S = 5.08E7/T923 * EXP(-15.228/T913 - (T9/3.090)**2)
        * (1 + 0.027*T913 - 0.778*T923 - 0.149*T9 + 2.10*T943 + 1.03*T953)
        + 2.28E3/T932 * EXP(-3.011/T9) + 1.65E4*T913 * EXP(-12.007/T9)
ES = 1 + 1.75 * R012/T612
X14 = X12 + X14 + (0 TO 1)*X16 (SEE TEXT)
R = R0 * N0 * (X1*X14)/(M1*M14) * S*ES
```

Table 3.4 (contd.)

α-processes

```
HE4(2A,G)C12    Q = 7.275
                S = 3.00E-8/T9**3 * EXP(-4.4109/T9) + (0.1)*1.35E-7/T932 * EXP(-24.811/T9)
                ES = EXP(2.4*R012/T632)
                R = R0**2 * N0 * (X4/M4)**3 * S*ES / 6

C12(A,G)O16     Q = 7.162
                S = 9.03E7/T9**2 * (1 + 0.621*T923)**3 / (1 + 0.047/T923)**2
                      * EXP(-32.120/T913 - (T9/5.863)**2)
                      + 2.74E7/T923 * EXP(-32.120/T913) + 1.25E3/T932 * EXP(-27.499/T9)
                      + 1.43E-2*T9**5 * EXP(-15.541/T9)
                ES = EXP(2.4*R012/T632)
                R = R0 * N0 * (X4*X12)/(M4*M12) * S*ES
```

Table 3.5 Coefficients for Pair neutrino, Photo-neutrino and Plasma neutrino rates in (3-80). Numbers in parentheses denote powers of 10. (Beaudet, Petrosian and Salpeter, 1967).

	a0	a1	a2	b1	b2	b3	c
Pair	6.002(19)	2.084(20)	1.872(21)	9.383(-1)	-4.141(-1)	5.829(-2)	5.5924
Photo	4.886(10)	7.580(10)	6.023(10)	6.290(-3)	7.483(-3)	3.061(-4)	1.5654
Plasma	2.320(-7)	8.449(-8)	1.787(-8)	2.581(-2)	1.734(-2)	6.990(-4)	0.56457

3.4 THE TEMPERATURE GRADIENT

The calculation of the stellar temperature gradient $\nabla \left(\equiv \frac{\partial \ln T}{\partial \ln P} \right)$ depends on the method and efficiency of the energy transport processes present in the stellar material. Radiation and conduction carry the energy flux if stability against convection is achieved. If not, the efficiency with which convection carries some or all of the flux must be determined. Further discussion may be found, e.g. in Cox and Giuli (1968).

The radiative gradient ∇_r is that which would exist if all energy is transported by radiation (and/or conduction) at a given point, and is given by

$$\nabla = \nabla_r = \frac{3}{16\pi acG} \cdot \frac{\kappa L_r P}{M_r T^4} \tag{3-83}$$

If all energy is transported wholly by the adiabatic motion of material, then the adiabatic gradient, ∇_{ad}, which has already been determined from the equation of state (3-29) applies, whence

$$\nabla = \nabla_{ad} \tag{3-84}$$

Schwarzschild (1906) pointed out that for the stellar material to be in radiative equilibrium, assuming uniform chemical composition and instantaneous chemical equilibrium, the condition for dynamical stability[1]

$$\nabla_r < \nabla_{ad}, \tag{3-85}$$

must be satisfied. If the chemical composition is non-uniform, Sakashita, Ono and Hayashi (1959) showed that this condition becomes

$$\nabla_r < \nabla_{ad} + \frac{\beta}{4 - 3\beta} \frac{d\ln \mu}{d\ln P} \qquad \left(\beta = P_r/P\right) \tag{3-86}$$

Various authors have investigated stellar evolution using this criterion, but for this investigation the Schwarzschild criterion has been adopted throughout.

If the stability criterion is not satisfied, convection will account for some or all energy transport. For convective regions in the deep stellar interior, the actual temperature gradient will be negligibly steeper than the adiabatic gradient, thus

$$\nabla = \nabla_{ad} \tag{3-87}$$

[1] see footnote on p. 68

In the outer layers of the envelope, this approximation fails and a better model of the complicated ensemble of moving elements is required. One such model, albeit a very simple one, is the local "mixing-length" theory of Böhm-Vitense (Vitense, 1953; Böhm-Vitense, 1958). The basic treatment adopted is described below.

The mixing length, Λ, whose physical interpration is the mean distance travelled by a moving element in the convective region, is defined as some number of pressure scale heights

$$\Lambda = l_p . H_p \tag{3-88}$$

where l_p is one major uncertainty of the theory, and the pressure scale height is

$$H_p = \left| \frac{\partial \ln P}{\partial r} \right| = \left(\frac{GM_r}{r^2} \right) \frac{\rho}{P} \tag{3-89}$$

The temperature gradient is then obtained by characterising the convective efficiency by a parameter ζ such that

$$\nabla = (1 - \zeta) \nabla_r + \zeta \nabla_{ad} \tag{3-90}$$

The efficiency ζ is the single real root ($0 \leq \zeta \leq 1$) of the cubic equation

$$\zeta^{1/3} + B \zeta^{2/3} + a_0 B^2 \zeta - a_0 B^2 = 0 \tag{3-91}$$

where $$B = \left[(A^2/a_0)(\nabla_r - \nabla_{ad}) \right]^{1/3} \tag{3-92}$$

a_0 is a constant depending on the version of the theory adopted, we use $a_0 = 9/4$ following Cox and Giuli (1968). The dimensionless quantity A represents the ratio of 'convective' to 'radiative' conductivities, and contains the "mixing-length" Λ.

Equation (3-90) is solved analytically, except in the case $B \ll 1$ where an iterative solution is used to obtain

$$\zeta = (a_0 B^2)^3 \left\{ 1 - 3B(a_0 B^2) - \left[3 - (9/a_0) \right] (a_0 B^2)^3 \ldots \right\} \tag{3-93}$$

This version of the mixing-length theory assumes hydrostatic equilibrium and the absence of energy sources in the convective region. It neglects turbulent pressure, which is a reasonable approximation if the convective velocities are not supersonic.

The major uncertainty in the "mixing-length" theory, as already

indicated, is the value for l_p, the mixing-length over the pressure scale height. In most of our calculations we have made an arbitrary choice for l_p with

$$1.0 \leq l_p \leq 2.0$$

Alternatively, models of convective envelopes using two-dimensional hydrodynamic calculations may be used to obtain a better estimate for the local value of the mixing-length (e.g. Deupree and Varner, 1980). This sort of treatment is impractical for stellar evolution calculations, but an analytic fit to the results of similar calculations may be a useful tool in resolving this uncertainty. For some models we have combined Deupree and Varner's fit with Deupree's (1979) modification to the local mixing-length theory. They find, to good agreement, that

$$\log(\Lambda/H_p) = -2.85(T_4 - 0.7) + 0.3 \quad (T_4 < 0.746)$$
$$= 6.36(T_4 - 0.97)^2 - 0.15 \quad (0.746 < T_4 < 1) \qquad (3\text{-}94)$$

where $T_4 = T/10^4$ K, and where the second form is applied for $T_4 > 1$ until Λ/H_p reaches a given value (e.g. 1.5) which is used for all higher temperatures. The modification suggested by Deupree (1979) allows for the difference between the horizontally averaged opacity and the opacity of the horizontally averaged temperature which can be considerable near the surface of stars. Assuming a horizontal temperature variation (ΔT_a), Deupree constructs the effective opacity

$$\frac{1}{\kappa_e} = \frac{f}{\kappa(T+\Delta T_a)} + \frac{(1-f)}{\kappa(T-\Delta T_a)} \qquad (3\text{-}95)$$

where f denotes the weighting fraction for upward and downward moving elements. We choose the simplest value $f = 1/2$. ∇_r is recomputed for the effective opacity and the convective flux fraction ζ is found as before from equation (3-90). The mixing-length horizontal temperature variation (Cox and Giuli, 1968) is then given by

$$\Delta T_c = \Lambda \Delta \nabla T = \Lambda [32 F_c^2 T / c_p^2 \rho^2 g \Lambda^4 Q]^{1/3} \qquad (3\text{-}96)$$

where Fc/F is the fractional convective flux

$$\frac{F_c}{F} = \zeta \frac{\nabla_r - \nabla_{ad}}{\nabla_r} \qquad (3\text{-}97)$$

This procedure is iterated until $\Delta T_c = \Delta T_a$.

The main effect that this modification has on the standard mixing-length theory is to reduce the actual gradient ∇ in the hydrogen ionisation zone.

1 Secular (ie thermal) convective stability is discussed by Unno, Osaki, Ando, and Shibahashi, 1979: Nonradial Oscillations of Stars, Tokyo University Press, p.189

4 STUDIES OF HORIZONTAL BRANCH STARS

4.1 AN INTRODUCTION TO THE THEORETICAL STATUS OF HORIZONTAL BRANCH STARS.

The general features of stellar evolution through the horizontal branch (HB) phase have been well established for some years (Iben and Rood, 1970b ; hereafter IR70). Stars on the horizontal branch of the HR diagrams for globular clusters are burning helium by the triple-alpha (3α) process in a convective region at the centre of a helium/metal core, and hydrogen by the CN and p-p processes in a thin shell at the base of a hydrogen-rich envelope. Their internal structure is determined by five parameters;
1) the total mass M; 2) the mass of the helium-core, M_c ;
3) the initial helium abundance, Ye; 4) the initial metal abundance, Ze;
5) the age of the star, t. In practice all five are not independent since, for real cluster stars, the core mass M_c depends almost entirely on the initial chemical composition, while the total mass M depends on initial composition and on age.

Early calculations of the zero-age location and evolutionary track topology of horizontal branch stars were carried out by Faulkner (1966), Faulkner and Iben (1966), Iben and Faulkner (1968), Rood and Iben (1968) and Castellani, Giannone and Renzini (1969), which succeeded in describing the dependence of these features on the initial core mass, total stellar mass, and chemical abundances in the envelope. Iben (1971) summarises these results qualitatively:
1) Given M_c , horizontal branch lifetime is approximately independent of total mass and envelope composition. However track shape is very sensitive to composition parameters.
2) For every value of Z_e, there exists a critical helium abundance Y_I such that if $Y_e < Y_I$, evolution during central helium burning is from blue to red, whereas if $Y_e > Y_I$, evolution is at first from blue to red, then to blue, and finally back to red. However if M is small enough, the first case always applies. For a given core mass and envelope composition,

the mass dividing the primarily redward and blueward evolution is known as the ' bifurcation ' mass. The difference in primary direction of evolution is related to the relative strength of the H-burning shell to the He-burning core. The smaller this ratio becomes, the greater the tendency for evolution from blue to red.

3) For models of the same total mass, core mass, and Ye , the lower Z_e is, the bluer is the average colour of the model. Iben and Rood (1970) describe the evolution of the interior and surface properties of a horizontal branch star with M = 0.625 $M_\odot$, M = 0.475 $M_\odot$, Ye = 0.3 and Ze = 0.001. Helium burning is concentrated in a small region at the centre of a convective core containing 0.11 $M_\odot$. During evolution the convective region grows slowly in mass until helium is nearly exhausted. As He is converted into carbon and thence into oxygen, the molecular weight of the entire convective region rises uniformly. Central and shell temperatures rise to maintain pressure balance, thus increasing the core luminosity L_{He} In addition, the hydrogen burning shell continues to add mass to the core.

In Iben and Rood's model, as L_{He} increases, the outer regions of the helium-core expand. The temperature at the base of the hydrogen-shell consequently drops, so that the decrease in the shell luminosity L_H almost exactly compensates for the increase in L_{He} . The increase in molecular weight within the H-burning shell means that the shell densities rise, the entire region between the base of the H-burning shell and the stellar surface contracts, and the star evolves to the blue. For models with weak H-shell sources (i.e. for $L_{He}/L > 0.55$) the shell density increase is not rapid enough to offset the core-induced expansion and evolution is continuously to the red until helium is exhausted at the centre.

Iben and Rood find that when the central helium abundance Yc drops to about 0.3, an increase in core temperature alone is not sufficient to maintain a flux balance, hence core densities must increase. Consequently the helium core contracts, the hydrogen-burning shell moves inwards and the envelope expands. The star evolves to the red in the H-R diagram and

and brightens. At this stage, both L_H and L_{He} are increasing.

As evolution continues, the central helium abundance eventually becomes so small that L_{He} begins to drop, although core temperatures and densities continue to rise. However the decrease in L_{He} is now more than offset by the increase in L_H, and the model continues to move upwards and to the red in the H.R. diagram.

Iben and Rood go on to examine stellar evolution as the region of maximum energy production by helium burning shifts from near the centre to a shell. This phase and subsequent evolution is thought to be related to stars on the Asymptotic Giant Branch, with which this study is not concerned.

In calculating an extensive grid of models for zero-age and evolved HB stars, Rood (1970) and IR70 adopted the Cox and Stewart (1969) opacities. Other features of the input physics are described in Iben and Rood (1970a). In particular they adopt $l_{mix}/H_{dens} = 0.5$ in their version of the mixing-length treatment of convection, metallicity abundances of C : N : O = 3:1:9 and $Z_{CNO} = 0.6Z$, and $\Theta_\alpha^2 = 0.078$ for the reduced α-particle width controlling the $^{12}C(\alpha,\gamma)^{16}O$ reaction.

Uncertainties in the distribution of heavy elements throughout the star are emphasized as being due to uncertainties in the amount of ^{12}C produced during the core-helium flash and to the amount of mixing of the enriched material immediately after the flash. Iben and Rood's assumption that Z is constant throughout the star requires that no mixing between core-material and the hydrogen-rich envelope takes place during or after the helium-flash.

Evolutionary tracks were calculated for parameters
$Ze = 10^{-3}, 10^{-4}$; $Ye = 0.1, 0.2, 0.3$; $0.45 \leq M_c/M_\odot \leq 0.6$; $0.5 < M_*/M_\odot < 0.9$.
For a star with $Ye = 0.3$, $Ze = 10^{-3}$, $M_c = 0.475\ M_\odot$ and $M_* = 0.625\ M_\odot$, whose evolutionary track contains a blueward loop through the instability strip, some properties are given in table 4.6.

Newell (1970) estimated the width in effective temperature (T_{eff}) for horizontal branches in several globular clusters. These estimates lead to the requirement that stellar structure theory must be able to account for

horizontal branch widths of up to 0.3 in $\log T_{eff}$. IR70 find all single evolutionary tracks are short compared to the required width in $\log T_{eff}$ and conclude that a variation of one or more parameters occurs within a cluster.

The helium-core mass Mc is almost entirely a function of initial composition (e.g. Eggleton, 1968). Since horizontal branch lifetime $t_{HB} \propto 1/M_c$, we consider $t_{HB} \simeq t_{HB}(Y_e, Z_e)$. Letting the red-giant lifetime $t_{RG}(L_{RG}, Y_e, Z_e)$ be the time required by a giant branch star to evolve to the red-giant tip from a luminosity L_{RG}, and choosing $L_{RG} = L_{RR}$ the mean luminosity of a theoretical RR Lyrae variable in the instability strip, we can construct t_{HB}/t_{RG} as a function of Ye and Ze. From observations of the numbers of stars on the horizontal branch (N_{HB}) and on the giant branch with luminosity $L \gtrsim L_{RG}$ (N_{RG}), it is possible to establish a relation between Ye and Ze by setting $N_{HB}/N_{RG} = t_{HB}/t_{RG}$. If Ze can be estimated from spectroscopic data, a value of Ye can be obtained for stars in a given cluster.

Assuming that the composition variation within a cluster is negligible, IR70 used this method to estimate the composition and initial core masses for several clusters. They find that a variation in total mass of 0.1 - 0.2 $M_\odot$ along the horizontal branch is necessary to account for the observed width in $\log T_{eff}$ in M3. They continue to discuss the mass distribution N(M) within the HB, but avoid a realistic analysis owing to a lack of observational and theoretical data. They also point out that a defensibly large variation in Ze or in Z_{CNO} within a cluster would also increase the width of the horizontal branch.

In concluding their study of horizontal branch stars with a calibration of Mc(Ye, Ze, M) from red-giant models, (Rood, 1972), Rood (1973) had hoped "to present the final solution to the appearance of the horizontal branch in the H-R diagram". However several developments had taken place during the course of these calculations which affected the interpretation of the H-R

Castellani, Giannone and Renzini (1971a, b) and Schwarzschild (1970) had discovered the importance of convective overshooting followed by semi-convective mixing at the outer boundary of the convective core. These effectively increase the amount of nuclear fuel available in the core, and hence increase the HB lifetime. Sweigart and Demarque (1972) and Robertson and Faulkner (1972) assume that overshooting and semiconvection occur to the maximum possible extent and find that the convective core size, and hence the HB lifetime, is doubled.

Despite the omission of overshooting and semiconvection from his earlier calculations, Rood (1973) obtains synthetic colour-magnitude diagrams for HB stars. He finds it easy to achieve a good fit to observed c-m diagrams and consequently cannot limit some of the parameters involved. Some results do, however, emerge. Details of evolutionary tracks have little effect on the appearance of the HB. As Ze varies from cluster to cluster, either the mean mass loss or the mean helium abundance must vary. Several candidates for the 'second parameter' emerge and cannot be eliminated. An effort to combine evolutionary theory with pulsation theory is unsuccessful - a result that Rood considers may be attributed to the sensitivity of the pulsation calculations to the opacity used. In the temperature range $4.0 > \log T_{eff} > 3.84$, the theoretical ($\log g$, $\log T_{eff}$) diagram gives a value $d \log g / d \log T_{eff} = 4.4$, in good agreement with observations by Newell (1970). The locus of the ($\log g$, $\log T_{eff}$) relation is only sensitive to the helium abundance, where $d \log g / d Y_e \simeq -0.2$ for $Y_e > 0.2$.

Meanwhile a number of other workers had been making more detailed studies of the evolutionary behaviour of HB stars. Lauterborn, Refsdal and Stabell (1972) consider separately the effects of changes in the He-core and in the H-burning shell, confirming the earlier work of other authors. Demarque and Mengel (1971) continued evolutionary sequences for red-giant models past the helium flash and obtained HB models with masses (0.5 - 0.65$M_\odot$) lower than previously adopted. The very blue ($\log T_{eff} \simeq 4.3$)

evolutionary tracks obtained correspond well with the hitherto unexplained very blue HB stars pointed out by Newell (1970). Demarque and Mengel (1972) extended their previous work to examine quantitatively the effects of opacity changes and the inclusion of semiconvection on HB evolution. The inclusion of semiconvection leads to (a) longer 'blue-loops', (b) a broader luminosity range and (c) an increase in t_{HB} by a factor of at least 1.6. By choosing an alternative interpolation scheme, Demarque and Mengel obtained reduced free-free opacities for C,O enriched core mixtures. Comparing results of HB calculations for the two interpolation schemes led to the conclusion that an increase in core free-free opacities would lead to the same results as the inclusion of semiconvection. This is because both modifications lead to an increase in the convective-core size.

Refsdal and Stabell (1972) (hereafter RS72) extended the study of the effect of opacity changes on horizontal branch models. The results of small opacity changes in restricted temperature ranges are given in table 4.1. The effect of small opacity changes in the helium core on the mass of the convective core M_{cc} is shown in table 4.2. The main result here is that while a constant opacity change throughout the core has little effect, differential opacity changes may modify M_{cc} considerably.

In order to extend the work of Iben and Rood (1970b) following the discovery of the importance of semiconvection, Sweigart and Gross (1974, 1976) made an extensive set of calculations of HB evolution, including semiconvection, for a larger grid of values for (M, M_c, Ye, Ze) than hitherto used in any single study, and based on a reference set of parameters
($M = 0.66\ M_\odot$, $M_c = 0.475\ M_\odot$, Ye = 0.3, Ze = 0.001).
The essential results of this investigation are as follows.
1) Track morphology in the HR diagram. For the reference set ($M_c = 0.475$, Ze = 0.001) the critical value of L_{He}/L separating redward and blueward evolutionary groups is about 0.55. For sequences in each combination of (M_c, Ye, Ze), the maximum length ($\Delta \log T_{eff}$) of the blueward loops is increased by an increase in either Ye or Ze, or by a

Table 4.1 The effect of artificial opacity increases in particular temperature ranges on properties of horizontal branch models, adapted from Refsdal and Stabell (1972)

log T	Teff	L_{He}/L	δTeff	δL
< 6.6	low		large, negative	small, negative
< 6.6	high		small, negative	" "
$6.6 < \log T < 7.45$		$\gtrsim 0.85$	negative	small, negative
$\simeq 7.2$		< 0.85	increases with L_{He}/L	decreases with L_{He}/L
$\simeq 7.4$			decreases with L_{He}/L	increases with L_{He}/L
> 7.45	(within helium core)		positive	negative
> 7.9	(within convective core)		no effect	

Table 4.2 Changes in the convective core mass Mcc due to artificial opacity changes $\delta\kappa$ at two core temperatures T_1 and T_2 (adapted from table 3, Refsdal and Stabell, 1972).

$\delta\kappa_1$ ($T_1 = 7.92$)	$\delta\kappa_2$ ($T_2 = 7.45$)	Mcc/Mc
0	0	0.222
0.1	0.1	0.224
0.1	0	0.257
-0.1	0	0.203
0	-0.1	0.251

Table 4.3 The dependence of horizontal branch lifetime on ZAHB parameters for HB evolution with semiconvection, adapted from Sweigart and Gross (1976).

$M/M_\odot$	$M_c/M_\odot$	Y_e	Z_e	t_{HB} / 10^7 years
$\sim$	0.475	0.3	0.001	$\sim$10
0.66	0.425	0.3	0.001	14.3
0.66	0.475	0.3	0.001	6.0
0.50	0.475	0.3	0.001	12.9
0.94	0.475	0.3	0.001	9.6
0.66	0.475	0.1	0.001	11.8
0.66	0.475	0.4	0.001	8.8

decrease in M_c.

2) Horizontal branch lifetimes. For the reference sequences ($M_c = 0.475 M_\odot$, Ye = 0.3, Ze = 0.001), $t_{HB} \simeq 10^8$ years in agreement with previous estimates. t_{HB} is found to increase significantly with decreasing total mass, particularly in the range $0.50 < M/M_\odot < 0.60$. An increase in t_{HB} is also found for a decrease in Ye or M_c. There is little dependence on Ze. Examples of t_{HB} variation are given in table 4.3. The variation of t_{HB} with Ye and M is easily understood as increasing either leads to an increase in shell luminosity. This means that M_c is increasing more rapidly, and t_{HB} is correspondingly reduced.

3) Interior characteristics. At zero-age, the convective core mass M_{cc} depends only on M_c. When the central helium abundance Y_c drops to 0.5 both M_{cc} and M_{sc}, the maximum extent in mass of the semiconvective region, increase for larger values of M and Ye. At maximum, $M_{sc} - M_{cc} \simeq 0.1 M_\odot$. With $\Theta_\alpha^2 = 0.085$ for the reduced α-particle width in the $^{12}C(\alpha,\gamma)^{16}O$ reaction, the convective core consists of roughly equal amounts of ^{12}C and ^{16}O when Ye = 0.05.

Further evolutionary studies by Sweigart and Gross (1978) of red-giant evolutionary sequences enabled Caloi, Castellani and Tornambé (1978) to construct 'evolutionary' zero-age HB sequences. where M_c is treated as a function of composition only, and the increase in the helium content (δY_e) of the envelope due to convective "dredge-up" during initial red-giant evolution is taken into account. For a given cluster age (10^{10} years), M_{RG}, M_c and δY_e are interpolated in Sweigart and Gross's (1978) results. Thus ZAHB sequences are constructed as functions of total mass and composition only. Two results emerge. 1) Increasing Ye increases the luminosity L for red ZAHB stars, but decreases L for blue ZAHB stars. 2) No RR Lyrae stars are allowed for extremely metal poor clusters with ages of 10^{10} years. In addition, it is clear that age has a comparatively small effect on the structure of ZAHB sequences. However it must be noted that the decreasing mass of the evolving giant stars for older clusters may reflect

itself in the ZAHB population through a changing mass distribution on the HB.

Recent theoretical studies have examined the effects of modified CNO abundances (Castellani and Tornambe 1977), metal rich envelopes (Gingold, 1977) rotation (Castellani, Ponte and Tornambé, 1980) and diffusion (Giannone and Rossi, 1981) on the structure and evolution of HB stars. Castellani and Tornambé (1981) publish the most recent theoretical attempt to understand the Oosterhoff dichotomy in RR Lyrae variables. Kippenhahn (1982) observes that the most pressing problems in the interpretation of HB stars are 1) to account for sufficient mass loss between red giant and horizontal branch phases, with a sufficient mass spread, to populate the HB and 2) to understand properly the amount of helium-burning, chemical mixing and mass loss caused by the core helium-flash. While most of the former studies discuss the effect of modifying one or two of the initial assumptions, and the latter underlines the need for studies of red-giant evolution and the helium-flash, we have to look back to the earlier work (e.g. of SG76) to obtain comparative studies if we also wish to investigate the effect of modifying an initial assumption. These recent studies are cited for completeness.

4.2 WHY MAKE STUDIES OF THE HORIZONTAL-BRANCH USING THE CARSON OPACITIES?

It is clear from the preceding survey that many uncertainties still exist in the theoretical status of horizontal branch stars. It may be regarded as presumptuous to consider examining the effect of new physics on equilibrium models while historical effects on the initial chemical structure are still poorly known. However we may obtain a qualitative view of the dependence of stellar structure upon the physics assumed by making a comparative study with the work of previous authors. We noted in § 3.2 that stellar opacity is one feature of astrophysics in which uncertainty remains. While RS72 discuss the effect of artificial opacity changes on equilibrium horizontal branch models, no study has been made of HB stars using opacities calculated independently of the Cox-Stewart opacities. The Carson opacities give us an opportunity to correct this omission.

Previous studies using the Carson opacities have led to a number of interesting results. Stothers (1974 a,b) compares models for zero-age main-sequence stars calculated with Carson opacities and with Cox-Stewart opacities. Although surface characteristics are not significantly altered, there are important structural differences. At high mass, Stothers (1976c) obtains substantial reddening of the ZAMS due to the development of a convective zone in the stellar envelope. Several classes of star in the luminous blue region of the HR diagram are found to be pulsationally unstable against the κ-mechanism due to large opacities at low densities in the CNO ionisation zone (Stothers, 1976b). The major successes with the Carson opacities have been in studies of stellar pulsation. Studies of classical Cepheids (Carson and Stothers, 1976; Stothers, 1976a; Vemury and Stothers, 1978) lead to better agreement for inferred masses and pulsational properties between evolutionary theory, pulsation theory and observation. Better agreement between theory and observations has also been achieved for the light curves and 'bump masses' of BL Herculis variables (Carson, Stothers and Vemury, 1981; Carson and Stothers, 1982). Using data from velocity and light curves only, Stothers (1981) obtains properties for RR Lyrae stars in

the range $M/M_{\odot} = 0.55 - 0.65$; $Y = 0.2 - 0.3$, and $\log L/L_{\odot} = 1.6 - 1.7$. Independent data corroborate these values. Cox-Stewart opacities lead to similar results, but derived masses are smaller by about 20%. It should be noted that pulsation studies provide tests primarily of the hydrogen and helium opacities.

It is therefore appropriate to extend studies of stellar structure with the Carson opacities to horizontal branch stars for two reasons. 1) If the Carson opacities represent an improvement on the Los Alamos opacities, we need to know how the theoretical picture of the horizontal branch is affected. 2) Models of horizontal branch stars give an opportunity to test the Carson opacities for evolved (Helium/Carbon/Oxygen) chemical compositions.

4.3 THE GRID OF HORIZONTAL BRANCH MODELS

We adopt a procedure similar to that of Sweigart and Gross (1974, 1976) in obtaining a number of zero-age and evolutionary sequences for horizontal branch stars which will permit a systematic comparison of the properties of HB stars as functions of their total mass M, their initial helium-core mass M_c and the relative mass abundances of helium Ye, and metals, Ze, in the hydrogen-rich envelope. The range of values for the parameters (M, M_c, Ye, Ze) has been taken from the grid

$$\begin{aligned} M/M_\odot &= 0.50(0.02)0.90 \\ M_c/M_\odot &= 0.475,\ 0.525,\ 0.575 \\ Ye &= 0.1,\ 0.2,\ 0.3 \\ Ze &= 0.,\ 0.001,\ 0.01 \end{aligned} \qquad (4\text{-}1)$$

The range of values is smaller than that used by Sweigart and Gross (1976), and not all combinations have been included in the grids of model sequences. In particular we have not made calculations with Ze typical of metal-poor globular clusters ($\log Ze = -4, -5$). As mentioned in §3.2 we only have limited confidence in opacities interpolated for $0.1 > Z > 0$. However a sufficient number of sequences are calculated to tell us about the variation of sequence properties over a wide range of (M, M_c, Ye, Ze).

The computational procedure and input physics have been discussed in chapters 2 and 3 respectively. The zero-age (equilibrium) structure and subsequent evolution of a horizontal branch star with
($M = 0.62\ M_\odot$, $M_c = 0.475\ M_\odot$, Ye = 0.3, Ze = 0.001)
are discussed in detail in §4.4. The grid of zero-age horizontal branch models, which were constructed for a wider range of parameters than used for the evolutionary sequences, are discussed in §4.5. The evolutionary sequences are presented in §4.6.

4.4 THE STRUCTURE AND EVOLUTION OF A 0.62 $M_\odot$ HORIZONTAL BRANCH STAR

In this section we present the results of calculations of the structure and evolution of a horizontal branch star with one set of parameter values in order to make a detailed study of the effect of changing the input physics and to make a comparison with the work of Iben and Rood (1970b) (IR70, hereafter) and Sweigart and Gross (1976) (SG76).

In the ZAHB models, the hydrogen shells are constructed so that the profile of the hydrogen abundance represents a half sine wave ($-\pi/2$ to $+\pi/2$) in a shell of thickness 5×10^{-4} $M_\odot$ with its base at M_c, the initial value for the helium-core mass. Although arbitrary, the hydrogen shell thickness agrees with calculations for red-giant models just prior to the helium-flash. Throughout the core, the initial helium abundance is set equal to 0.971, consistent with estimates of the initial (helium-flash) carbon enrichment (Demarque and Mengel, 1971). Rood (1970) and Gross (1973) have considered the importance of uncertainties in the initial core-helium abundance and the initial profile in the H-shell respectively. The chemical composition in the homogeneous envelope is specified by the two parameters Ye, Ze.

The structure and evolution of a 0.62 $M_\odot$ star with initial helium-core mass $M_c = 0.475\ M_\odot$ and envelope composition Ye = 0.3, Ze = 0.001 is followed through the horizontal-branch phase. The sequence is halted when the central helium abundance Y_c reaches 0.01 (Some authors choose a higher value of Y_c to end horizontal branch evolution, arguing that for lower values the star will occupy a 'supra-horizontal-branch' position in the HR diagram. This difference will be noted when features critical to the choice of 'TAHB' definition are discussed). This sequence (Z) will serve as a typical example of our HB sequences, and will be compared in detail with sequences calculated using different input physics.

Properties of the ZAHB model are given in table 4.4, selected properties of models at regular intervals in the evolutionary sequence are given in table 4.5. The behaviour of the surface characteristics in the ($\log T_{eff}$, $\log L/L_\odot$) plane is illustrated in figure 4.2 (sequence Z),

Table 4.4 Details of the internal structure of a zero-age horizontal branch star with mass 0.62 $M_\odot$, core mass 0.475 $M_\odot$, Ye = 0.3, Ze = 0.001, constructed using the Carson opacities. The following information is given :

1) mass zone number, J ;
2) relative mass, Mr/M_* ;
3) radius, $\log r$;
4) luminosity, $\log L_r/L_\odot$;
5) pressure, log P ;
6) temperature, log T ;
7) hydrogen abundance, X ;
8) helium abundance, Y ;
9) density, $\log \rho$;
10) opacity, $\log \kappa$;
11) energy generation rate, $\log \varepsilon$;
12) stability against convection (* if unstable).

Table 4.4

J	Mr/M*	log r	log Lr	log P	log T	X	Y	logρ	logκ	logε	∇
0	1.0000	11.5545	1.7414	3.6112	3.8395	0.699	0.300	-8.040	-0.457	0.000	
1	1.0000	11.5125	1.7415	5.8067	4.8111	0.699	0.300	-7.169	0.943	0.000	
4	1.0000	11.4949	1.7415	6.2483	4.9039	0.699	0.300	-6.815	0.872	0.000	
8	1.0000	11.4685	1.7415	6.7912	5.0311	0.699	0.300	-6.398	0.889	0.000	
11	1.0000	11.4466	1.7415	7.1641	5.1179	0.699	0.300	-6.110	0.835	0.000	
14	1.0000	11.4190	1.7415	7.5732	5.2075	0.699	0.300	-5.788	0.769	0.000	
18	0.9999	11.3807	1.7415	8.0658	5.3105	0.699	0.300	-5.395	0.652	0.000	
22	0.9998	11.3284	1.7415	8.6558	5.4221	0.699	0.300	-4.912	0.491	0.000	
26	0.9997	11.2853	1.7415	9.0900	5.5106	0.699	0.300	-4.564	0.448	0.000	
30	0.9994	11.2354	1.7415	9.5447	5.6037	0.699	0.300	-4.200	0.350	0.000	
34	0.9988	11.1772	1.7415	10.0248	5.7093	0.699	0.300	-3.825	0.336	0.000	
39	0.9978	11.1092	1.7415	10.5325	5.8144	0.699	0.300	-3.421	0.189	0.000	
43	0.9963	11.0454	1.7415	10.9787	5.9043	0.699	0.300	-3.063	0.136	0.000	
48	0.9938	10.9722	1.7415	11.4550	6.0114	0.699	0.300	-2.693	0.136	0.000	
50	0.9922	10.9348	1.7415	11.6839	6.0680	0.699	0.300	-2.521	0.162	0.000	
52	0.9906	10.9016	1.7415	11.8783	6.1157	0.699	0.300	-2.374	0.131	-9.764	
57	0.9859	10.8215	1.7415	12.3300	6.2079	0.699	0.300	-2.014	-0.092	-8.544	
62	0.9792	10.7347	1.7415	12.8104	6.3052	0.699	0.300	-1.630	-0.075	-7.322	
67	0.9697	10.6403	1.7415	13.3101	6.4169	0.699	0.300	-1.241	-0.129	-6.051	
70	0.9608	10.5684	1.7415	13.6759	6.5006	0.699	0.300	-0.959	-0.150	-5.158	
74	0.9479	10.4783	1.7415	14.1158	6.6036	0.699	0.300	-0.622	-0.184	-4.127	
78	0.9313	10.3775	1.7415	14.5878	6.7157	0.699	0.300	-0.261	-0.207	-3.076	
81	0.9157	10.2932	1.7415	14.9694	6.8036	0.699	0.300	0.033	-0.262	-2.284	
84	0.8969	10.2001	1.7415	15.3798	6.9019	0.699	0.300	0.345	-0.254	-1.457	
87	0.8744	10.0957	1.7415	15.8253	7.0093	0.699	0.300	0.683	-0.298	-0.601	
90	0.8474	9.9765	1.7414	16.3194	7.1279	0.699	0.300	1.058	-0.318	0.306	
93	0.8209	9.8620	1.7410	16.7792	7.2414	0.699	0.300	1.404	-0.325	1.196	
96	0.8030	9.7839	1.7391	17.0830	7.3173	0.699	0.300	1.632	-0.337	1.959	
99	0.7809	9.6855	1.7050	17.4610	7.4075	0.699	0.300	1.919	-0.376	3.324	
104	0.7679	9.6273	1.3782	17.6838	7.4500	0.699	0.300	2.098	-0.363	4.127	
106	0.7668	9.6222	1.2677	17.7037	7.4522	0.665	0.334	2.128	-0.365	4.174	
111	0.7665	9.6211	1.2354	17.7086	7.4527	0.454	0.545	2.211	-0.373	4.129	
116	0.7663	9.6204	1.2157	17.7121	7.4530	0.216	0.783	2.324	-0.483	3.958	
119	0.7662	9.6201	1.2091	17.7141	7.4531	0.055	0.944	2.421	-0.480	3.485	
120	0.7661	9.6200	1.2086	17.7148	7.4532	0.000	0.999	2.459	-0.477	0.000	
125	0.7304	9.5664	1.2086	18.1650	7.5015	0.000	0.971	2.859	-0.421	0.000	
131	0.6492	9.4938	1.2086	18.7008	7.6014	0.000	0.971	3.284	-0.429	0.000	
135	0.6054	9.4637	1.2086	18.8883	7.6452	0.000	0.971	3.424	-0.429	0.000	
140	0.5351	9.4202	1.2086	19.1233	7.7048	0.000	0.971	3.594	-0.449	0.000	
145	0.4599	9.3761	1.2086	19.3226	7.7580	0.000	0.971	3.735	-0.484	0.000	
150	0.3885	9.3339	1.2086	19.4816	7.8022	0.000	0.971	3.846	-0.521	0.000	
157	0.3005	9.2777	1.2086	19.6520	7.8536	0.000	0.971	3.962	-0.545	0.000	
163	0.2173	9.2148	1.2086	19.7970	7.9031	0.000	0.971	4.055	-0.576	0.000	
165	0.1831	9.1837	1.2087	19.8540	7.9247	0.000	0.971	4.090	-0.591	0.000	
166	0.1725	9.1731	1.2087	19.8716	7.9316	0.000	0.971	4.101	-0.596	0.000*	
169	0.1405	9.1375	1.2087	19.9243	7.9526	0.000	0.971	4.132	-0.611	-2.792*	
171	0.1070	9.0917	1.2086	19.9804	7.9748	0.000	0.971	4.166	-0.627	-0.067*	
173	0.0737	9.0312	1.2076	20.0381	7.9977	0.000	0.971	4.201	-0.644	0.995*	
176	0.0377	8.9267	1.1926	20.1062	8.0247	0.000	0.971	4.242	-0.655	2.145*	
179	0.0117	8.7502	1.0558	20.1676	8.0490	0.000	0.971	4.279	-0.666	3.123*	
181	0.0048	8.6190	0.8399	20.1897	8.0578	0.000	0.971	4.292	-0.670	3.463*	
183	0.0022	8.5034	0.5899	20.2007	8.0621	0.000	0.971	4.299	-0.672	3.629*	
184	0.0009	8.3735	0.2742	20.2081	8.0651	0.000	0.971	4.303	-0.673	3.741*	
185	0.0000	0.0000	0.0000	20.2166	8.0685	0.000	0.971	4.308	-0.675	3.867*	

Table 4.5 Details of the internal characteristics of a horizontal branch star with mass 0.62 $M_\odot$, core mass 0.475 $M_\odot$, Ye = 0.3, Ze = 0.001 during evolution from the zero-age horizontal branch to a point where the central helium abundance has dropped to 0.01. Evolution is calculated using the Carson opacities, and energy generation rates from Fowler, Caughlan and Zimmerman (1975).

Columns give the following information :

1) time from the zero-age model in 10^7 years, t_7 ;
2) log effective temperature, log Teff ;
3) total luminosity in solar units, log $L/L_\odot$;
4) surface gravity, log g ;
5) mass interior to the hydrogen-burning shell, $Mc/M_\odot$;
6) luminosity of the hydrogen shell, log $L_H/L_\odot$;
7) temperature at the base of the hydrogen-shell, log T_{sh} ;
8) density at the base of the hydrogen-shell, log ρ_{sh} ;
9) mass within the convective core, $Mcc/M_\odot$;
10) luminosity of the helium-core, log $L_{He}/L_\odot$;
11) central temperature, log T_c ;
12) central density, log ρ_c ;
13) central helium abundance, Y_c ;
14) central oxygen abundance $^{16}X_c$.

Table 4.5

$M = 0.62\ M_\odot$, $M_c = 0.475\ M_\odot$, $Y_e = 0.3$, $Z_e = 0.001$

t_7 (1)	Teff (2)	L (3)	g (4)	Msh (5)	L_H (6)	Tsh (7)	ρsh (8)	Mcc (9)	L_{He} (10)	Tc (11)	ρc (12)	Yc (13)	$^{\kappa}Xc$ (14)
0.000	3.8395	1.741	2.807	0.475	1.590	7.453	2.463	0.107	1.208	8.068	4.308	0.971	0.000
0.135	3.8336	1.746	2.778	0.475	1.595	7.454	2.464	0.107	1.213	8.070	4.307	0.950	0.001
0.435	3.8247	1.756	2.733	0.475	1.602	7.455	2.469	0.107	1.230	8.072	4.304	0.902	0.002
0.735	3.8254	1.759	2.732	0.475	1.599	7.456	2.479	0.113	1.248	8.075	4.302	0.853	0.003
1.035	3.8398	1.755	2.794	0.475	1.584	7.457	2.496	0.113	1.268	8.078	4.298	0.804	0.005
1.335	3.8595	1.747	2.881	0.475	1.561	7.457	2.514	0.113	1.289	8.081	4.295	0.752	0.009
1.585	3.8796	1.736	2.972	0.475	1.533	7.458	2.530	0.113	1.308	8.084	4.293	0.707	0.012
1.885	3.9027	1.722	3.078	0.475	1.495	7.458	2.545	0.113	1.331	8.088	4.291	0.651	0.017
2.135	3.9187	1.711	3.154	0.475	1.463	7.458	2.554	0.113	1.350	8.092	4.291	0.602	0.023
2.385	3.9335	1.700	3.224	0.475	1.427	7.457	2.561	0.113	1.369	8.096	4.291	0.551	0.029
2.585	3.9442	1.690	3.276	0.475	1.393	7.457	2.566	0.113	1.385	8.099	4.292	0.509	0.036
2.835	3.9527	1.682	3.319	0.475	1.358	7.457	2.565	0.113	1.403	8.104	4.295	0.455	0.045
3.085	3.9616	1.674	3.363	0.475	1.316	7.456	2.567	0.113	1.423	8.109	4.300	0.398	0.057
3.285	3.9665	1.668	3.387	0.475	1.282	7.456	2.566	0.113	1.438	8.114	4.306	0.351	0.069
3.485	3.9665	1.668	3.388	0.475	1.261	7.456	2.561	0.113	1.452	8.120	4.315	0.303	0.082
3.685	3.9674	1.667	3.392	0.475	1.234	7.456	2.560	0.113	1.467	8.127	4.327	0.254	0.099
3.885	3.9653	1.671	3.380	0.475	1.220	7.457	2.560	0.113	1.481	8.135	4.344	0.203	0.119
4.085	3.9594	1.680	3.347	0.475	1.220	7.460	2.562	0.113	1.495	8.145	4.368	0.152	0.145
4.285	3.9437	1.702	3.263	0.475	1.264	7.466	2.569	0.113	1.505	8.158	4.406	0.100	0.180
4.485	3.9035	1.749	3.055	0.475	1.376	7.478	2.588	0.113	1.510	8.178	4.472	0.050	0.231
4.710	3.7494	1.862	2.326	0.475	1.615	7.503	2.633	0.113	1.499	8.212	4.600	0.012	0.311

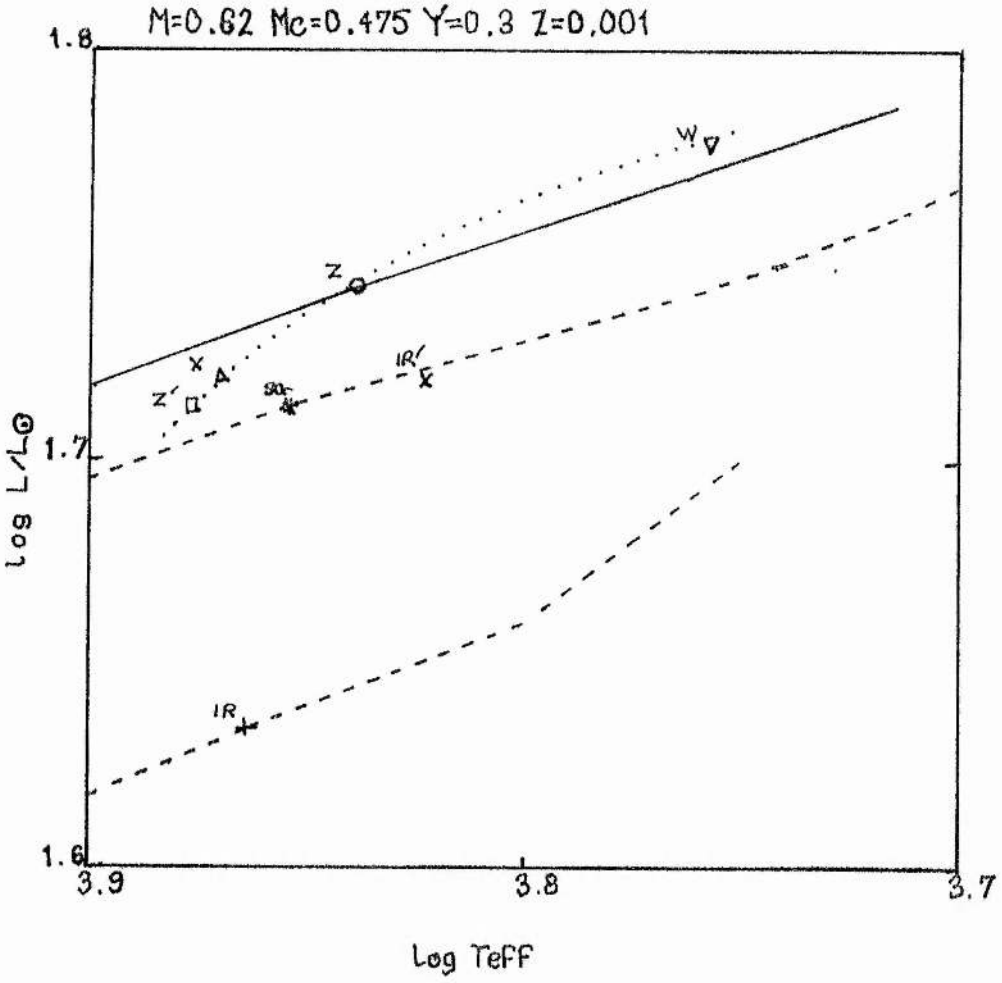

Figure 4.1 Positions of zero-age horizontal branch stars with masses of 0.62 $M_\odot$ and 0.625 $M_\odot$ (IR + IR′), calculated with different sets of input physics as described in the text. Models connected by a dotted line are constructed with the Carson opacities, others with the Cox-Stewart opacities. The solid line represents the ZAHB for models of different masses but the same physics as Z. The dashed lines represent the equivalent ZAHB corresponding to models SG and IR. Models SG, IR and IR′ are taken from Sweigart and Gross (1976), Iben and Rood (1970b) and Rood (1973).

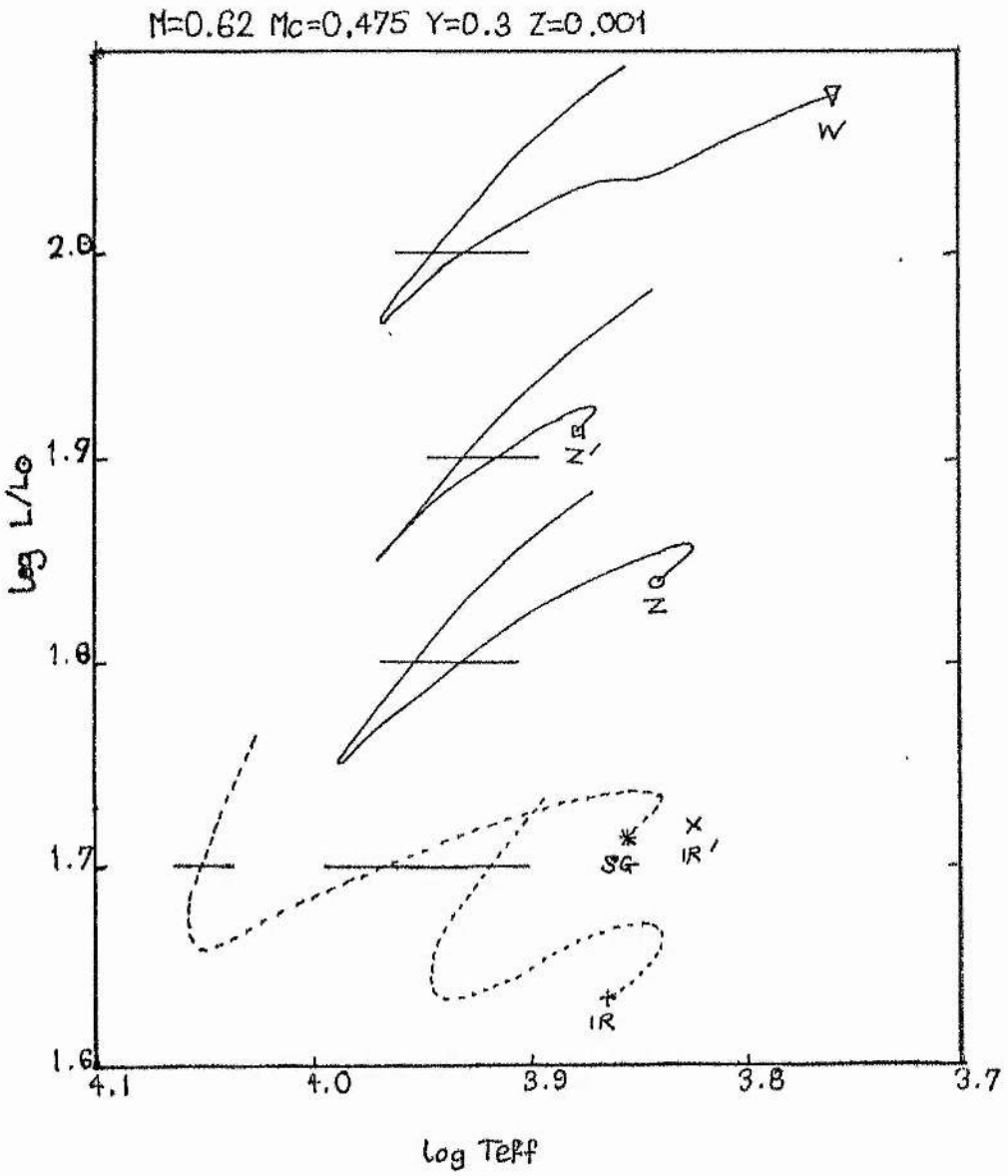

Figure 4.2 Evolutionary tracks for horizontal branch stars calculated with a number of assumptions about the input physics described in the text. The zero-age position of each track is marked and labelled. Tracks Z, Z′ and W are successively displaced by 0.1 in log $L/L_\odot$. Horizontal lines cutting the tracks mark the level of log $L/L_\odot = 1.7$. Tracks IR and SG are taken from Iben and Rood (1970), and Sweigart and Gross (1976) respectively. Track IR represents the evolutionary track of a 0.625 $M_\odot$ star. All other tracks are for a 0.62 $M_\odot$ star. IR′ is the zero-age position obtained by Rood (1973) for a 0.625 $M_\odot$ star.

Figure 4.3 The behaviour of selected quantities, as a function of time during the evolution of a 0.62 $M_\odot$ star, with M = 0.475 $M_\odot$, Ye = 0.3, Ze = 0.001. Quantities shown, with appropriate scales are ;

1) $3.75 < \log T_{eff} < 4.0$: Effective temperature,
2) $1.5 < \log L/L_\odot < 2.0$: Total luminosity,
3) $7.4 < \log T_{sh} < 7.65$: Temperature at base of H-shell,
4) $2.4 < \log \rho_{sh} < 2.65$: Density at base of H-shell,
5) $1.2 < \log L_H/L_\odot < 1.7$: Hydrogen-shell luminosity,
6) $8.0 < \log T_c < 8.25$: Central temperature,
7) $4.3 < \log \rho_c < 4.55$: Central density,
8) $1.0 < \log L_{He}/L_\odot < 1.5$: Helium-core luminosity,
9) $0. < Y_c < 1.0$: Central helium abundance,
10) $0. < {}^{16}X_c < 1.0$: Central oxygen abundance.

Figure 4.3

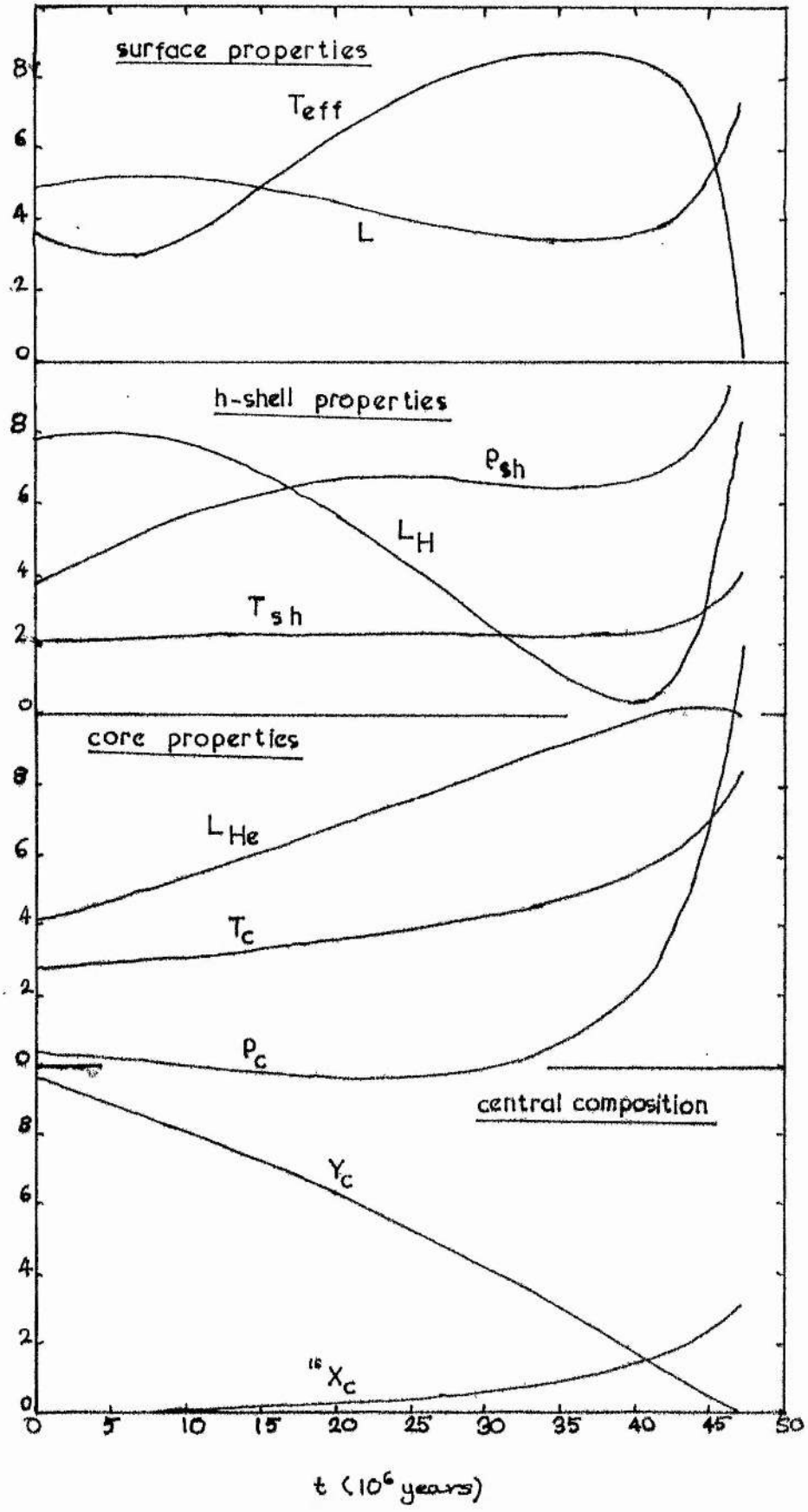
surface properties
T_{eff}
L
h-shell properties
P_{sh}
L_H
T_{sh}
core properties
L_{He}
T_c
P_c
central composition
Y_c
$^{16}X_c$
0
2
4
6
8
0
5
10
15
20
25
30
35
40
45
50
t (10^6 years)

and of certain interior characteristics in figure 4.3. Figure 4.2 also illustrates the evolution of a similar star with semiconvection using Cox-Stewart opacities (sequence SG), and the evolution of a 0.625 $M_\odot$ using Cox-Stewart opacities without semiconvection (sequence IR). Properties of several ZAHB models are illustrated in figure 4.1.

ZERO-AGE MODELS

With the models presented, it is not easy to deduce the quantitative effect of using the Carson opacities on the properties of horizontal branch models. In addition to properties of models calculated with different input physics by ourselves, table 4.6 contains details of models calculated by other authors who have used Cox-Stewart opacities.

Model IR (taken from IR70) was calculated using linear interpolation in the Cox-Stewart (1969) opacities and energy generation rates from FCZI. Model IR′ (from Rood, 1973) was calculated with a multipoint interpolation procedure for the opacities, and energy generation rates altered by 1) a 12% increase in the p-p reaction rate, 2) a factor 10^{-6} decrease in the $^{14}N(\alpha,\gamma)^{18}F$ rate, and 3) factor exp $(-0.138/T_9)$ decrease in the 3α rate. Model SG (from SG76) was calculated with similar physics to IR′ except that linear interpolation was used for the opacity. The surface properties of SG at zero-age agree well with those of IR′ (noting the mass difference), although the interior properties (e.g. L_{He}) do not agree so well.

The remaining models mentioned in table 4.6 were calculated using linear interpolation in the Carson opacity tables. Models Z, X and W were calculated with energy generation rates from FCZII. These adopt a smaller value for Θ_α^2 for the $^{12}C(\alpha,\gamma)^{16}O$ reaction than used by IR70 and SG76, and the 3α rate is reduced by a factor 1.41 exp $(-0.117/T_9)$ w.r.t. FCZI. The reduction for the 3α rate is $\sim$50% at central temperatures for HB stars, while the same reduction used in calculating models IR′ and SG is $\sim$70%.

Model Z′ was calculated with the 3α rate restored to the FCZI value.

Table 4.6. A summary of results for the horizontal branch structure and evolution of 1) a 0.62 $M_\odot$ star with Carson opacities (Z, Z′, X, W), 2) a 0.625 $M_\odot$ star with Cox-Stewart opacities (IR, IR′), 3) a 0.62 $M_\odot$ star with Cox-Stewart opacities and semi-convection (SG). All stars have M_c = 0.475 M , Ye = 0.3, Ze = 0.001. 2) and 3) are adapted from Iben and Rood (1970b) and Sweigart and Gross (1976) respectively. Physics for each sequence are described in the text.

Property		Sequence						
		Z	Z′	X	W	IR	IR′	SG
Mass ($/M_\odot$)		0.62	0.62	0.62	0.62	0.625	0.625	0.62
log Teff	(ZAHB)	3.840	3.877	3.870	3.758	3.864	3.823	3.854
log $L/L_\odot$	(ZAHB)	1.741	1.713	1.720	1.777	1.634	1.719	1.713
log $L_{He}/L_\odot$	(ZAHB)	1.208	1.218	1.159	1.143	1.173	1.215	1.183
log g	(ZAHB)	2.807	2.985	2.949	2.443	3.192	2.765	2.878
$Mcc/M_\odot$	(ZAHB)	0.107	0.107	0.100	0.100	0.110	0.110	0.109
log Tc	(ZAHB)	8.068	8.062	8.067	8.066	8.065	8.078	8.072
log ρc	(ZAHB)	4.308	4.280	4.315	4.322	4.291	4.323	4.327
t_{HB}	(10^7 yrs)	47.3	44.0		47.7	68.0		104.3
Mcc	(Yc=0.5)	0.113	0.113		0.100	0.119		†0.163
X_{16} c	(Yc=0.05)	0.231	0.163		0.235	0.5		0.504
δlog Teff (blue loop)		0.143	0.101		0.230	0.120		0.221
δlog $L/L_\odot$ (blue loop)		-0.092	-0.077		-0.127	-0.04		-0.07

†excluding semiconvective zone.

The result of increasing $r_{3\alpha}$ is to increase the core luminosity L_{He} and the central density and temperature. However the total luminosity L and, consequently, the stellar radius R are decreased. The drop in the hydrogen-shell luminosity L_H follows from the increase in the helium-core radius with L_{He}. Changing $r_{3\alpha}$ has no effect on the mass in the convective core, M_{cc}. The increase in L_{He} also leads to a decrease in the horizontal branch lifetime t_{HB}.

Model X was constructed in the same way as Z, except that a different method of interpolating between the opacity tables for core compositions was used, which led to an increase in the core opacity (as illustrated in figure 3.2). Since the increase is non-uniform, M_{cc} is altered (RS72 and table 4.2). In this case the larger increase occurs at a lower temperature, leading to a reduction in M_{cc}, in agreement with the results of RS72. In addition, the increased opacity leads to a drop in L_{He}, hence to an increase in L_H, L and R. This is in contradiction to the results of RS72 (see table 4.1).

Model W was constructed in the same way as X, except that the helium profile in the hydrogen-shell was modified by the addition of carbon in proportion to their relative core abundances. This represents the situation where helium and carbon are both fully mixed (in the post-helium flash phase) throughout the helium core and into the base of the hydrogen envelope, and will be discussed in the next section. For the present, we find that its immediate effect is to significantly increase the hydrogen-shell luminosity L_H. L_{He} is reduced. L and R are increased. Combined with the drop in L_{He} due to the increased core opacity, the reduced core mass leads to virtually no change in t_{HB} w.r.t. sequence Z.

With these results from the variation of the input physics we may now attempt to understand the effect of using Carson opacities instead of Cox-Stewart opacities on the properties of zero-age models. Models Z′ and IR represent those with the most nearly similar input physics, excluding

the opacity. The alterations to the input physics to produce IR′ and SG led to an increase in L and R. However in this case L_{He} was also increased.

By interpolating the behaviour of L and T_{eff} for models IR and IR′ to models with total mass M = 0.62 M , we see that a line in the (log L, log T_{eff}) plane connecting models constructed with Carson opacities, but with variations in other aspects of the input physics, lies above or to the left of that connecting similar models constructed with the Cox-Stewart (1969) opacities (figure 4.1). At log $T_{eff} \simeq 3.85$ this shift is approximately $\delta \log T_{eff} = 0.025$ at constant luminosity, or $\delta \log L = 0.02$ at constant temperature. It should be noted that this result is dissimilar to a similar comparison for main-sequence stars (Stothers, 1974a) where $\delta \log T_{eff} \simeq -0.01$. We also note that the small difference in the location of the ZAHB models is unlikely to create a significantly new picture of the ZAHB. We noted in section 3.2 that interpolating in the opacity tables for $0 < Z < 0.01$ may lead to an opacity which is too small. If this is the case, an increase in the envelope opacity will lead to a shift to lower luminosities and effective temperatures (Refsdal and Stabell, 1972) for all models constructed with the Carson opacities.

Interpreting the behaviour of the core-luminosity is more complicated. With the Cox-Stewart opacities the result of reducing $r_{3\alpha}$, and other reaction rates was to increase L_{He}, and also to increase L_H. With the Carson opacities, reducing $r_{3\alpha}$ led to a reduction in L_{He}, but an increase in L_H. The paradox appears to lie with the Cox-Stewart models, as in all other cases of increasing L_{He} we find a decrease in L_H. This may be caused by the reduction in r_{pp} used in calculating IR′. However the opposite effect on L_{He} of similar changes in the reaction rates still requires an explanation which lies beyond the scope of this present study. We may add that it seems unlikely to be an opacity effect, although this is the only obvious solution.

EVOLUTIONARY TRACKS

Evolutionary sequences are not available for models IR′ and X (In his paper on horizontal branch morphology, Rood (1973) transposed the track for IR onto the zero-age model IR′, doubling its length to take semiconvection into account). We may make some general observations concerning the remaining sequences.

Comparing sequence Z with Z′, we find that one effect of reducing $r_{3\alpha}$ is to increase slightly both t_{HB} and the extent of the blueward loop. With sequence W, the increased core opacity has little effect on t_{HB}. The extent of the blueward loop is increased by the carbon enriched shell. This may easily be accounted for by the greater initial L_H which is rapidly lost as the hydrogen-shell moves out into regions of normal CNO abundances. The irregular behaviour of sequence W at $\log T_{eff} \simeq 3.85$ is due to the change in the method of interpolation between the opacity tables. One further feature of this sequence is that the change in interpolation method artificially limits M_{cc} to its initial value. The negligible change in t_{HB} is due to a balance between the reduced M_{cc} and the reduced L_{He},

$$[M_{cc}(Z)/M_{cc}(W)]_{max} \simeq [L_{He}(Z)/L_{He}(W)]_{ZAHB}$$

For all sequences calculated using the Carson opacities the maximum value that the effective temperature attains is $\log T_{eff\,max} \simeq 3.97$. After the initial increase in luminosity the rate of change of luminosity with effective temperature during the blueward loop is

$$d\log L / d\log T_{eff} \simeq 0.65 \pm 0.10$$

Sequence IR has a similar blueward extent to Z, however both the luminosity change and t_{HB} are altered. For sequences IR and SG, calculated with the Cox-Stewart opacities, we find

$$d\log L / d\log T_{eff} \simeq 0.33 \pm 0.01$$

The difference in $d\log L/d\log T_{eff}$ for the two opacity sets is significant. In previous work (i.e. with Cox-Stewart opacities) the decrease in L_H almost compensates for the increase in L_{He}, and the evolutionary track

remains above the corresponding zero-age sequence in the (L-T) plane. However with the Carson opacities, after an initial rise in L, the drop in L_H is greater than necessary to compensate for the increase in L_{He}, eventually bringing the evolutionary track below the ZAHB. Comparing sequences Z and IR in more detail (using figure 3, IR70), we find that with the Carson opacities, the rate of increase of L_{He} w.r.t. the decrease in helium abundance Yc is increased by an amount

$$\frac{[\partial L_{He}/\partial Y_c]_Z}{[\partial L_{He}/\partial Y_c]_{IR}} \simeq 1.16$$

This result is independent of the value used for $Y_{3\alpha}$ (sequence Z′).

As L_{He} increases the radius of the helium-core increases. The temperature at the base of the hydrogen envelope remains roughly constant. However the increase in L_{He} means that the temperature gradient in the hydrogen shell increases ($\nabla_{rad} \propto \kappa L_r P/M_r T^4$) so that the mean temperature within the shell falls, and L_H also falls. The increase in L_{He} does not account fully for the drop in L_H. We can compare the rate of change of L_H with L_{He} for sequences Z and IR and find that

$$\frac{[\partial L_H/\partial L_{He}]_Z}{[\partial L_H/\partial L_{He}]_{IR}} = 1.45$$

Therefore the Carson opacities independently increase $\partial L_{He}/\partial Y_c$ and $\partial L_H/\partial L_{He}$, the combination leads to the increase in the total luminosity drop during blueward evolution for sequence Z over that for sequence IR (The total luminosity drop for SG is similar to that of Z. However semiconvection in SG increases the effective M_{cc}, and comparison is no longer straightforward). The difference in $\partial \log L/\partial \log T_{eff}$ between Z and IR is anticipated as $L(T_{eff})$ is known to be a sensitive function of the opacity.

As found by other authors, the central oxygen abundance X_{16C} does not rise appreciably until after Yc has dropped to 0.4, after which we obtain (sequence Z) an increase in X_{16C} from 0.05 (Yc = 0.4) to 0.32 (Yc = 0.01). SG76 and IR70, using $\Theta_\alpha^2 = 0.085$ and 0.078 respectively for the effective

cross-section factor in the $^{12}C(\alpha,\gamma)^{16}O$ reaction, obtain $X_{16C}(Y_c \to 0) \simeq 0.$
This important difference (the amount of ^{16}O produced during core-helium burning is important for determination of cosmic abundances and affects horizontal branch lifetimes and post horizontal-branch evolution) is due mainly to the reduced value for Θ_α^2 used by Fowler, Caughlan and Zimmerman (1975). (The effect of altering Θ_α^2 is investigated by both IR70 and SG76). However it was found (sequence Z′) that increasing $r_{3\alpha}$ and hence reducing t_{HB} also leads to a decrease in X_{16C}, we find $X_{16C}(Y_c = 0.01, Z') = 0.239$ Because of the differences in both $r_{3\alpha}$ and Θ_α^2 between our work and sequences IR and SG, it is not possible to determine whether opacity affects $X_{16C}(Y_c \to 0)$. Our work does highlight the importance of understanding reaction rates properly in order to determine relative abundances of chemical elements accurately. In this respect, we believe a value for $X_{16C}(Y_c \to 0) \simeq 0.3$ represents an improvement over SG76 as we have adopted more modern energy generation rates.

The horizontal branch lifetime $t_{HB} = 4.73 \times 10^7$ years is considerably shorter than those found by previous authors. As core properties for HB stars are virtually independent of M, t_{HB} for sequence IR may be compared directly with Z. We have

$$\left[t_{HB}(Z)/t_{HB}(IR)\right]_{calc} \simeq 0.7$$

We can account for this difference by considering a number of effects. As already noted, the opacity leads to a difference in the convective core size and hence to the amount of fuel available. Considering the maximum mass contained in the convective core we find

$$\left[\frac{M_{cc}(Z)}{M_{cc}(IR)}\right]_{max} \simeq \left[\frac{t_{HB}(Z)}{t_{HB}(IR)}\right]_{M_{cc}} \simeq 0.95$$

We also noted the difference in core luminosity between sequences Z and IR, which implies

$$\left[\frac{L_{He}(IR)}{L_{He}(Z)}\right] \simeq \left[\frac{t_{HB}(Z)}{t_{HB}(IR)}\right]_{L_{He}} \simeq 0.81$$

IR70 notes that $t_{HB} \propto (1 + 0.246\, X_{16C}(Y_c \to 0))$

With our value for $X_{16C}(Y_c \to 0)$, we also obtain

$$\left[\frac{t_{HB}(Z)}{t_{HB}(IR)}\right]_{X_{16C}} \simeq 0.96$$

To first order, we may estimate the expected t_{HB} by combining these effects to obtain

$$\left[\frac{t_{HB}(Z)}{t_{HB}(IR)}\right]_{pred} \simeq 0.74$$

on the basis of the amount of available nuclear fuel and the rate at which it is consumed. As a first order estimate, it is within reasonable agreement of the result obtained.

We have discussed results of calculations for the structure and evolution of a single horizontal branch star. Some important differences between the results of our work and earlier calculations have been indicated. We have attempted to understand these in terms of new opacities and energy generation rates. In particular we note that using the Carson opacities inctead of the Cox-Stewart opacities leads to the following results.

1) An increase in core-luminosity L_{He}.
2) A decrease in convective core mass $M_{c.c}$.
3) An increase in $L(T_{eff})_{ZAHB}$ for a given star, independent of other input physics, of $\delta \log L \simeq 0.02$ at $\log T_{eff} \simeq 3.85$.
   (Improved opacities at $Z_c = 0.001$ may alter this result).
4) An increase in $(d \log L / d \log T_{eff})$ during blueward evolution by a factor of 2.
5) An increase in $(\partial L_{He} / \partial Y_c)$ by a factor of 1.16.
6) An increase in $(\partial L_H / \partial L_{He})$ by a factor of 1.45 (This result may not be independent of ε changes between IR and Z).
7) A reduction in horizontal branch lifetime by a factor of $\simeq 0.77$
   (a further reduction is caused by a reduced value for Θ_α^2).

In the following sections we present further calculations for horizontal-branch star models over a wide range of values for the parameters (M, M_c, Y_c, Z_c).

4.5 ZERO AGE HORIZONTAL BRANCH MODELS

Tables 4.7 to 4.10 list important properties of several zero-age horizontal branch models. Each set of models is grouped according to Y_e , Z_e and Mc values. Each table represents a different set of assumptions concerning the input physics and chemical structure. Table 4.7 lists models constructed with the same set of assumptions used for the zero-age model of sequence Z in § 4.4, and provides the most direct comparison with the zero-age models reported in SG76 and Rood (1973). These models are labelled Z.

The bulk of the HB calculations were made with a modified set of assumptions, which were noted briefly in § 4.4.

1) The original method of interpolation between compositions in the opacity tables used the (H, He, Z) tables for $Z \lesssim 0.04$, and the (He, C, O) tables for $Z \gtrsim 0.05$, interpolating between the two methods for $0.04 < Z < 0.05$. This procedure neglects the contribution of the enriched carbon ($\sim$3%) in the zero-age helium-core, and overestimates the contribution of other elements to the total opacity. Further investigation showed this to be a misleading assumption as table 4.8 (models are labelled X) and the discussion in § 4.4 demonstrate.

2) In constructing the hydrogen profile in the hydrogen-burning shell, the hydrogen was replaced by both helium and carbon in their relative core abundances instead of by helium alone. This situation may arise if core-mixing at the helium-core flash extends into the base of the hydrogen envelope by a small amount (Early quasi-static calculations (Schwarzschild and Härm , 1966; Thomas, 1967) and dynamic calculations (Edwards, 1970) of the helium-core flash have not resolved the question of whether mixing takes place between helium-flash products and hydrogen-rich matter or not).

The effects these assumptions have on zero-age models are illustrated in figure 4.4b, while further data is given in table 4.9 (models are labelled W). Hence with reference to the sequence of standard zero-age models Z, sequences

X are constructed with an increased core opacity and sequences W use both an increased core opacity and, effectively, an increased C N cycle energy generation rate.

A small number of models (labelled DV, presented in table 4.10) were calculated by modifying the Böhm-Vitense treatment of the mixing-length theory of convection as discussed by Deupree (1979) and Deupree and Varner (1980).

Figure 4.5 demonstrates the dependence of zero-age horizontal branch models on core mass and envelope composition (using sequences W), while figure 4.6 illustrates the metallicity dependence of the ZAHB (using sequences X).

From figure 4.4a we find that the luminosity increase over SG76 reported for model Z in § 4.4 is extended to all models with metallicity Ze = 0.001, and from figure 4.4b we find that the luminosity and effective temperature differences due to the various sets of input physics are preserved for a given set of values for (Mc, Ye, Ze) over all M. However it is clear that these differences are not preserved when Ze (at least) is varied since for Ze = 0.001 we require a luminosity change of $\delta \log L > 0$ to transpose SG76 results onto our sequences Z, but for Ze = 0.01, the equivalent luminosity change becomes $\delta \log L < 0$. The effective temperature differences have the same sense for both metallicities. From our sequences X, we find that a change in core opacity leads to luminosity and effective temperature changes of the same sense for both metallicities, while increasing the carbon abundance in the hydrogen shell (sequences W) only increases the luminosity appreciably at lower Ze values. A closer comparison of the SG76 results with sequence Z shows that at Ze = 0.01, the new models have lower shell luminosities than the old by $\delta \log L_4 \simeq 0.03$, while at Ze = 0.001 the new models have shell luminosities which are larger than the earlier results by an equal amount. The core luminosities are greater at both metallicities for models using the Carson opacities. This difference may

be explained in terms of the opacities used. At the temperatures and densities encountered in the hydrogen-burning shell the Carson opacities are greater than the Cox-Stewart opacities for Ze = 0.01, but lower at Ze = 0.001 when using a linear interpolation scheme (see table 4.11). A decrease in the opacity leads to a decrease in the temperature gradient in the hydrogen shell, and hence to an increase in the total shell luminosity. The change in sign of the difference between Carson and Cox-Stewart opacities at two metallicities leads to the shell luminosity differences obtained. By extrapolating these results we expect an increase in $\delta \log L = (\log L_z - \log L_{SG76})$ for lower metallicities. More calculations are necessary to quantify this increase and to investigate the behaviour of $\log T_{eff}$ with decreasing metallicity for the Carson opacities.

It should be noted that the discrepancy found in § 3.2 between calculated and interpolated opacities for $Z_e = 0.005$ implies a value for opacity for $Z_e = 0.001$ that is too low. This is one point where the use of interpolation between the opacity tables for $0 < Ze < 0.01$ may be important, as noted in § 4.4. We therefore have less confidence in our results for the position of the ZAHB at Ze = 0.001 than at $Z_e = 0.01$.

The models constructed with the modified convection treatment serve to show that the uncertainty in the convection treatment and the uncertainty in the opacity carry a roughly equal share in the position of the redward limit for a ZAHB sequence.

By considering the larger set of zero-age models (W), we find the same general behaviour of model characteristics as functions of (M, Mc, Ye) as found with Cox-Stewart opacities. With the models constructed we have not

Table 4.11 Opacity at $\log T = 7$, $\log \rho = 2$, $Y = 0.5$

$\log \kappa$ / Ze :	10^{-2}	10^{-4}	0	10^{-3}	
				Tab.	Int.
Carson	0.291		0.159		0.172
Cox-Stewart(1969)	0.272	0.207		0.212	0.214

found any specific modification to the dependence on Ye or Mc with the Carson opacities in the sense that the L_H (Z) dependence is modified.

From calculations of a large number of zero-age horizontal branch models using Carson opacities we do not find any major modifications to the present theoretical status of such models. However we do note that the Carson opacities may lead to an increase in the sensitivity of the hydrogen-shell luminosity to the envelope metallicity for $10^{-2} > Ze > 10^{-3}$, which we expect to be true for lower Ze.

Tables 4.7 to 4.10

Sequences of models for zero-age horizontal-branch stars. Each table represents models constructed with a different set of input physics. Adopting the labels used in the text :

Table	Sequence	Modified physics (w.r.t. Z)
4.7	Z	
4.8	X	core κ
4.9	W	core κ , H-shell ε
4.10	DV	core κ , H-shell ε , envelope ∇

Models are grouped according to 1) helium-core mass, M_c , 2) envelope helium abundance, Ye, 3) envelope metallicity, Ze. For each mass, we give the surface properties L, Teff, g, the nuclear energy source strengths, L_H , L_{He} , and the convective core mass, M_{cc} .

Table 4.7

M*	log Teff	log L	log g	log LHe	log LH	Mcc
Mc=0.475 Y=0.3 Z=0.0100 Z						
0.54	3.9746	1.593	3.436	1.182	1.360	0.107
0.58	3.6233	1.703	1.951	1.176	1.550	0.107
Mc=0.475 Y=0.3 Z=0.0010 Z						
0.54	4.2244	1.425	4.602	1.222	0.997	0.107
0.58	4.0382	1.644	3.670	1.214	1.442	0.107
0.60	3.9373	1.703	3.222	1.212	1.534	0.107
0.62	3.8393	1.742	2.805	1.209	1.591	0.107
0.66	3.7150	1.786	2.291	1.205	1.654	0.107

Table 4.8

M*	log Teff	log L	log g	log LHe	log LH	Mcc
Mc=0.475 Y=0.3 Z=0.0100						
0.52	4.1915	1.349	4.531	1.145	0.923	0.100
0.54	4.0013	1.559	3.576	1.139	1.351	0.100
0.56	3.7479	1.647	2.490	1.135	1.487	0.100
0.58	3.6296	1.684	1.996	1.133	1.541	0.100
Mc=0.475 Y=0.3 Z=0.0010						
0.54	4.2319	1.576	4.681	1.173	0.948	0.100
0.56	4.1504	1.520	4.228	1.170	1.263	0.100
0.58	4.0571	1.616	3.773	1.165	1.426	0.100
0.60	3.9628	1.677	3.349	1.162	1.519	0.100
0.62	3.8699	1.720	2.949	1.159	1.580	0.100
0.64	3.7795	1.751	2.750	1.157	1.623	0.100
0.66	3.7252	1.772	2.346	1.555	1.567	0.100
0.68	3.7064	1.788	2.268	1.154	1.673	0.101
Mc=0.475 Y=0.3 Z=0.0000						
0.52	4.2985	1.210	5.097	1.165	0.203	0.100
0.54	4.2563	1.293	4.862	1.184	0.639	0.100
0.56	4.2125	1.377	4.618	1.195	0.911	0.100
0.58	4.1666	1.452	4.375	1.200	1.096	0.100
0.60	4.1198	1.512	4.142	1.202	1.220	0.100
0.62	4.0746	1.561	3.927	1.203	1.310	0.100
0.64	4.0318	1.602	3.729	1.203	1.381	0.100
0.66	3.9927	1.633	3.555	1.202	1.432	0.100
0.68	3.9563	1.661	3.394	1.202	1.476	0.101
0.70	3.9244	1.683	3.257	1.202	1.509	0.100

Table 4.9

Mx	log Teff	log L	log g	log Lne	log LH	Mcc
		Mc=0.475 Y=0.3 Z=0.0100				
0.50	4.2873	1.149	5.197	1.131	-0.242	0.101
0.52	4.1886	1.362	4.566	1.144	0.958	0.100
0.54	3.9942	1.566	3.541	1.138	1.363	0.100
0.56	3.7320	1.654	2.420	1.134	1.498	0.100
0.58	3.6275	1.688	1.985	1.132	1.547	0.100
0.60	3.6125	1.710	1.915	1.131	1.577	0.100
0.64	3.5997	1.740	1.862	1.129	1.618	0.100
0.68	3.5969	1.742	1.875	1.129	1.621	0.101
0.72	3.5954	1.759	1.877	1.128	1.643	0.100
0.76	3.5943	1.772	1.883	1.128	1.660	0.100
		Mc=0.475 Y=0.2 Z=0.0100				
0.50	4.2304	1.136	4.882	1.125	-0.466	0.101
0.52	4.1200	1.238	4.355	1.142	0.535	0.100
0.54	3.9545	1.379	3.566	1.143	1.001	0.100
0.56	3.7313	1.466	2.603	1.140	1.192	0.100
0.58	3.6424	1.499	2.231	1.139	1.250	0.100
0.60	3.6220	1.514	2.150	1.138	1.277	0.100
0.62	3.6125	1.530	2.108	1.138	1.304	0.100
0.64	3.6109	1.547	2.100	1.137	1.333	0.100
0.66	3.6084	1.548	2.093	1.137	1.335	0.100
0.70	3.6046	1.560	2.101	1.137	1.354	0.100
0.74	3.6024	1.577	2.099	1.136	1.382	0.101
		Mc=0.475 Y=0.1 Z=0.0100				
0.50	4.1644	1.126	4.626	1.119	-0.670	0.094
0.52	4.0279	1.178	4.046	1.135	0.152	0.100
0.54	3.8661	1.246	3.348	1.141	0.578	0.100
0.56	3.6925	1.304	2.612	1.142	0.797	0.100
0.58	3.6447	1.321	2.416	1.142	0.850	0.100
0.60	3.6307	1.339	2.359	1.142	0.901	0.100
		Mc=0.525 Y=0.3 Z=0.0100				
0.54	4.3582	1.502	5.261	1.501	-1.336	0.111
0.56	4.2789	1.558	4.903	1.328	0.182	0.111
0.58	4.1852	1.533	4.368	1.336	1.095	0.111
0.60	4.0252	1.697	3.597	1.332	1.452	0.111
0.62	3.8165	1.784	2.672	1.328	1.597	0.111
0.64	3.6450	1.826	1.957	1.326	1.661	0.111
0.66	3.6141	1.831	1.842	1.325	1.669	0.111
0.68	3.6052	1.847	1.803	1.325	1.692	0.111
0.70	3.5968	1.861	1.768	1.324	1.712	0.111
0.74	3.5956	1.865	1.784	1.324	1.718	0.111
0.78	3.5925	1.878	1.782	1.323	1.736	0.111
0.82	3.5910	1.893	1.785	1.322	1.757	0.111
		Mc=0.575 Y=0.3 Z=0.0100				
0.60	4.3408	1.479	5.059	1.476	-0.683	0.121
0.62	4.2742	1.540	4.746	1.496	0.524	0.122
0.64	4.1859	1.686	4.261	1.501	1.226	0.122
0.66	4.0491	1.819	3.595	1.498	1.537	0.121
0.68	3.8776	1.898	2.842	1.495	1.679	0.122
0.70	3.6881	1.940	2.055	1.493	1.748	0.122

$M_c = 0.475$ $Y_e = 0.3$ $Z_e = 0.001$

0.50	4.5415	1.146	5.515	"	"	0.101
0.52	4.2681	1.255	5.011	"	"	0.100
0.54	4.2163	1.441	4.556	"	"	0.100
0.56	4.1134	1.591	4.003	1.158	1.591	0.100
0.58	3.9992	1.681	3.477	1.152	1.529	0.100
0.60	3.8829	1.736	2.971	1.148	1.606	0.100
0.62	3.7576	1.777	2.443	1.143	1.662	0.100
0.64	3.7149	1.795	2.270	1.143	1.683	0.100
0.66	3.6981	1.814	2.195	1.141	1.710	0.100
0.68	3.6927	1.817	2.183	1.142	1.714	0.101
0.70	3.6858	1.826	2.160	1.141	1.726	0.100
0.74	3.6737	1.844	2.117	1.139	1.749	0.101
0.78	3.6718	1.858	2.119	1.139	1.766	0.101

Mc=0.475 Y=0.2 Z=0.0010

0.50	4.2994	1.137	5.156	1.130	-0.659	0.101
0.52	4.2312	1.213	4.825	1.153	0.524	0.100
0.54	4.1461	1.363	4.351	1.158	0.938	0.100
0.56	4.0659	1.431	3.978	1.161	1.097	0.100
0.58	3.9734	1.499	3.555	1.160	1.233	0.100
0.60	3.8644	1.559	3.074	1.156	1.340	0.100
0.62	3.7591	1.599	2.627	1.152	1.407	0.100
0.64	3.7286	1.606	2.512	1.155	1.416	0.100
0.66	3.7080	1.629	2.419	1.152	1.453	0.100
0.70	3.6891	1.659	2.340	1.149	1.498	0.100
0.74	3.6839	1.681	2.321	1.146	1.531	0.101

Mc=0.475 Y=0.1 Z=0.0010

0.50	4.2545	1.130	4.984	1.124	-0.733	0.101
0.52	4.1702	1.177	4.617	1.144	0.041	0.100
0.54	4.0933	1.232	4.271	1.156	0.438	0.100
0.56	4.0104	1.298	3.889	1.161	0.730	0.100
0.58	3.9159	1.361	3.463	1.160	0.930	0.100
0.60	3.8171	1.410	3.034	1.158	1.054	0.100
0.62	3.7432	1.416	2.843	1.162	1.062	0.100
0.64	3.7269	1.439	2.673	1.161	1.114	0.100
0.66	3.7119	1.458	2.606	1.161	1.153	0.100
0.68	3.7057	1.469	2.583	1.160	1.176	0.101

Mc=0.525 Y=0.3 Z=0.0010

0.54	4.4014	1.304	5.430	1.303	-1.334	0.111
0.56	4.3408	1.349	5.160	1.333	-0.093	0.111
0.58	4.2938	1.436	4.899	1.352	0.681	0.111
0.60	4.2315	1.584	4.518	1.356	1.195	0.111
0.62	4.1549	1.695	4.115	1.353	1.431	0.111
0.64	4.0650	1.781	3.683	1.349	1.580	0.111
0.66	3.9754	1.835	3.283	1.346	1.665	0.111
0.68	3.8821	1.877	2.881	1.342	1.727	0.111
0.70	3.7985	1.902	2.535	1.340	1.763	0.111
0.72	3.7275	1.921	2.244	1.339	1.789	0.111
0.74	3.7080	1.935	2.164	1.338	1.808	0.111

Mc=0.475 Y=0.3 Z=0.0000

0.50	4.3471	1.146	5.338	1.136	-0.497	0.101
0.52	4.2971	1.238	5.064	1.163	0.438	0.100
0.54	4.2379	1.402	4.680	1.170	1.019	0.100
0.56	4.1509	1.557	4.192	1.164	1.532	0.092
0.58	4.0658	1.637	3.787	1.161	1.460	0.100
0.62	3.8769	1.745	2.952	1.152	1.617	0.100
0.65	3.7439	1.785	2.401	1.148	1.671	0.100
0.68	3.7199	1.809	2.301	1.146	1.703	0.101
0.70	3.7100	1.822	2.261	1.145	1.719	0.100

Table 4.10

M*	log Teff	log L	log g	log LHe	log LH	Mcc
Mc=0.475 Y=0.3 Z=0.0100						
0.50	4.2873	1.149	5.097	1.131	-0.242	0.101
0.52	4.1886	1.362	4.506	1.144	0.958	0.100
0.54	3.9943	1.566	3.541	1.138	1.363	0.100
0.56	3.7322	1.654	2.421	1.134	1.498	0.100
0.58	3.6479	1.688	2.064	1.132	1.547	0.100
0.60	3.6345	1.711	2.002	1.131	1.578	0.100
0.62	3.6258	1.730	1.962	1.130	1.604	0.100

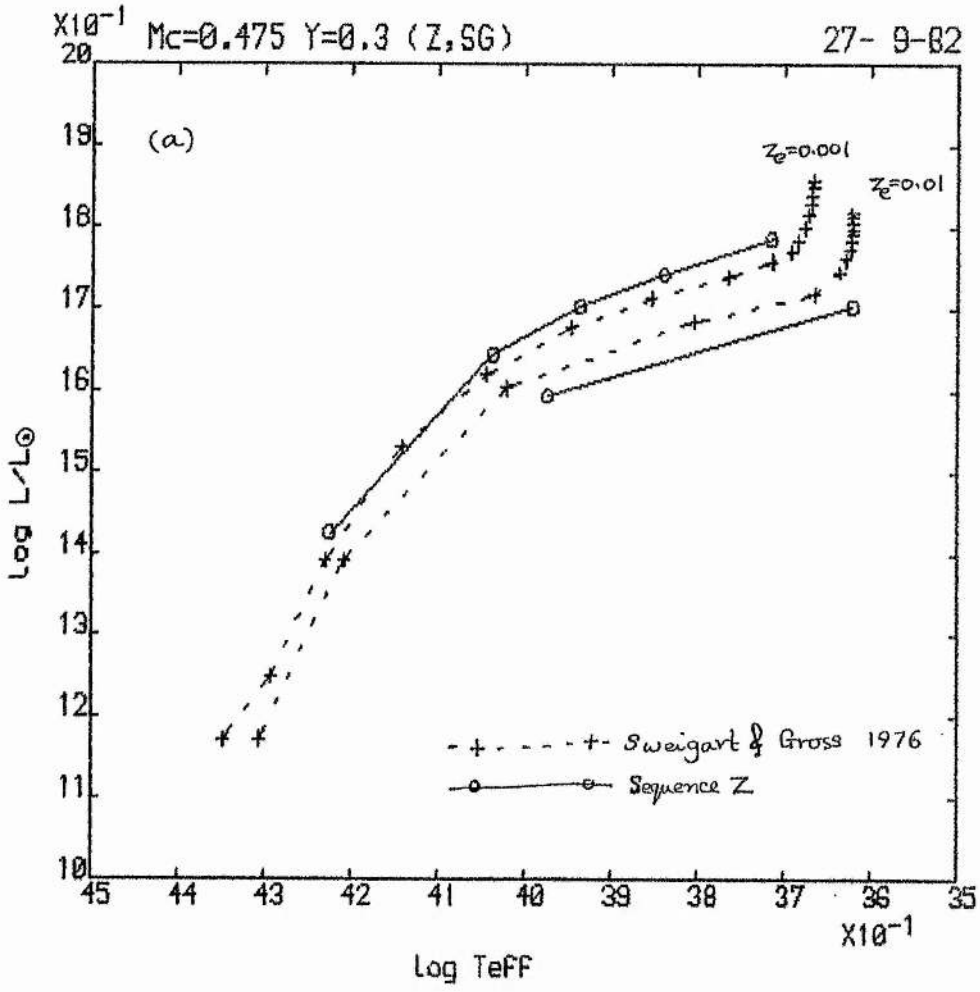

Figure 4.4 A comparison of ZAHB models for different sets of input physics.

(a) Carson opacities vs. Cox-Stewart opacities (from SG 76) for 2 metallicities.

(b) The effect of increased core opacities (X) and a carbon enriched H-shell (W) on the standard models (Z).

(c) Deupree's modification to the mixing-length theory for red ZAHB models.

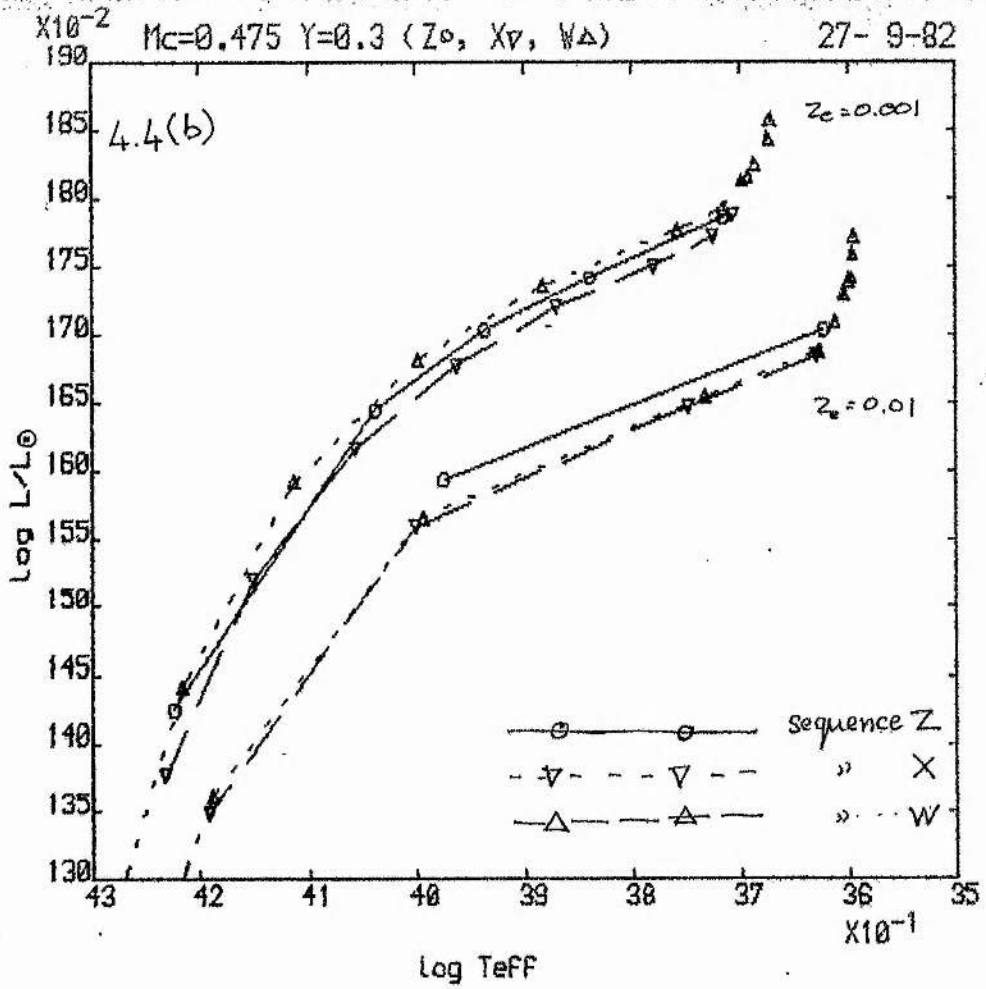
X10⁻²
Mc=0.475 Y=0.3 (Z○, X▽, W△)
27- 9-82
4.4(b)
Zc=0.001
Zc=0.01
Log L/L⊙
Sequence Z
» X
» W
Log TeFF
X10⁻¹

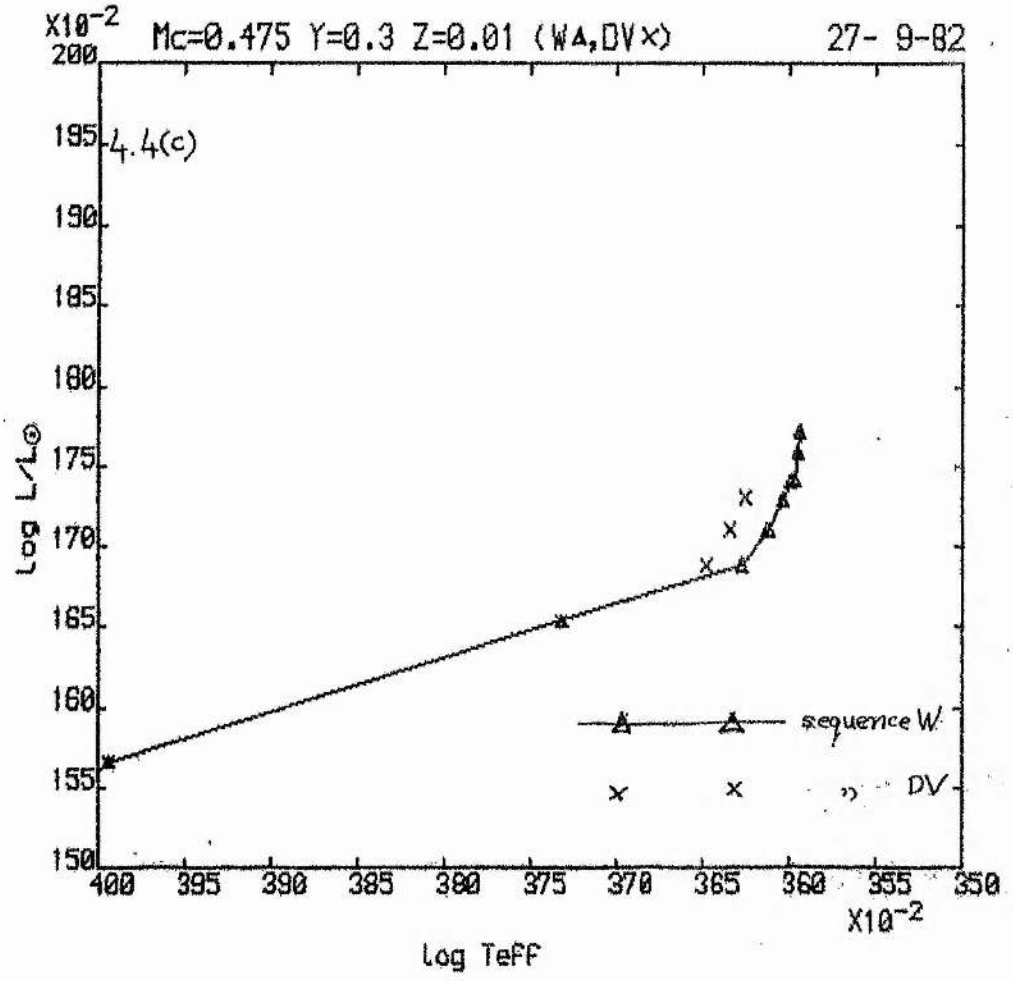
X10⁻²
Mc=0.475 Y=0.3 Z=0.01 (W△,DV×)
27- 9-82
4.4(c)
Log L/L⊙
sequence W
» DV
Log TeFF
X10⁻²

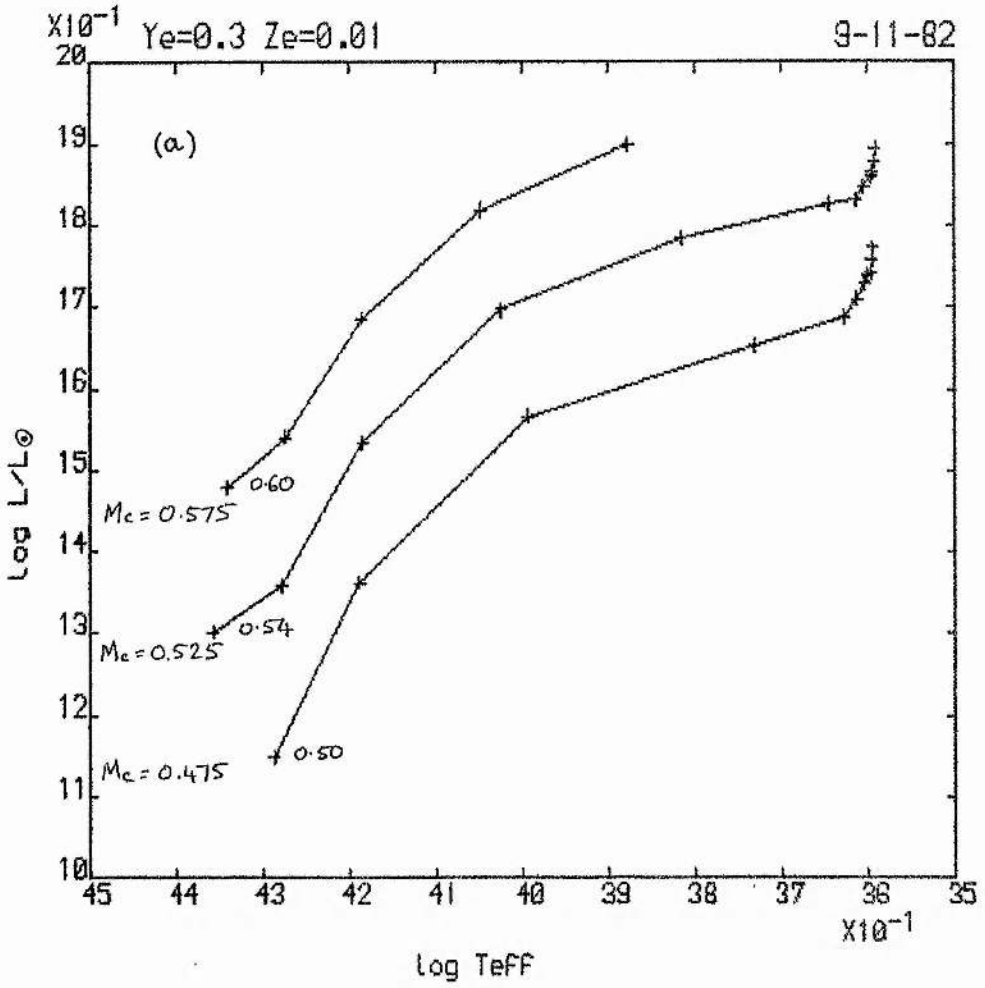

Figure 4.5 Characteristics of ZAHB models as a function of (a) helium core mass, (b) envelope helium abundance and (c) metallicity for models (W) with increased core opacities and a carbon enriched H-shell.

Parameters for each sequence are given in the diagrams with the mass (in $M_\odot$) of the bluest model in each sequence. The masses of other models in each sequence increase in steps of 0.02 $M_\odot$ towards the red. In figures 4.5 (b) and 4.5 (c), the lowest masses are 0.50 $M_\odot$ in all sequences.

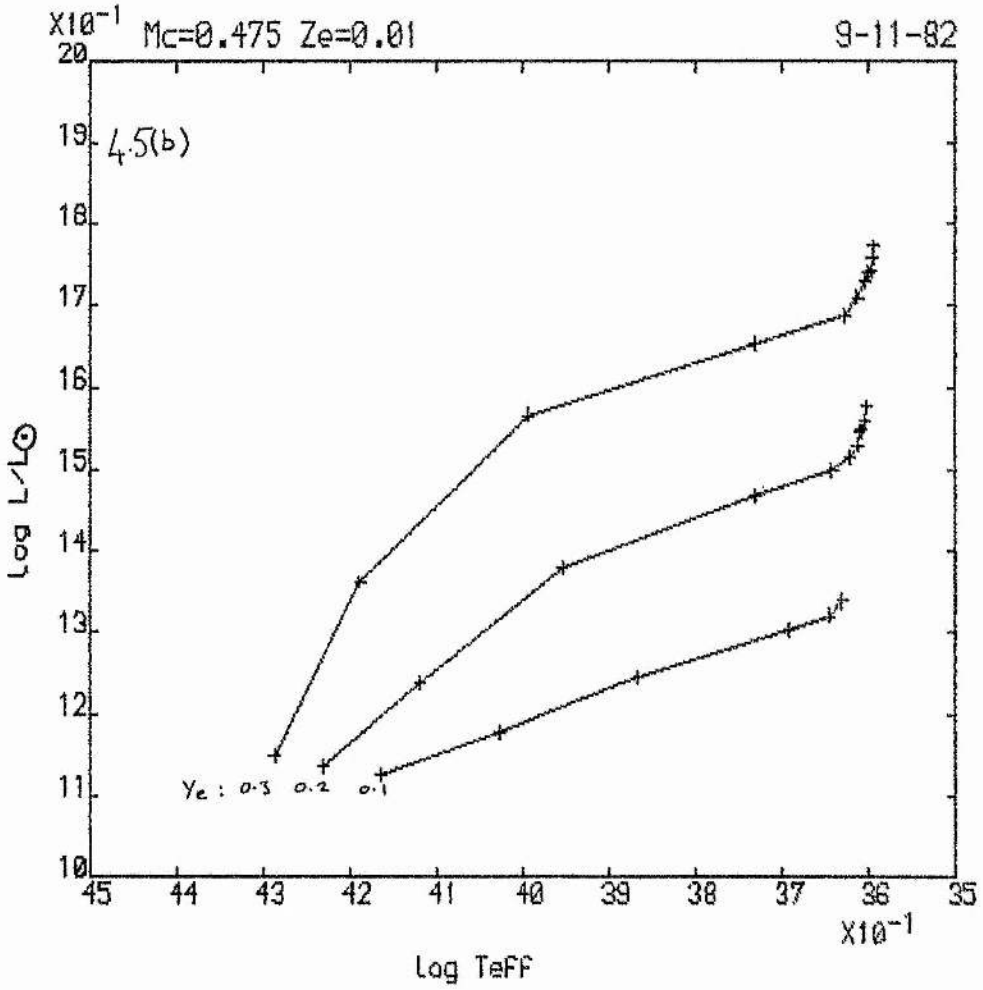
X10⁻¹
Mc=0.475 Ze=0.01
9-11-82
4.5(b)
Log L/L⊙
Ye : 0.3 0.2 0.1
Log TeFF
X10⁻¹

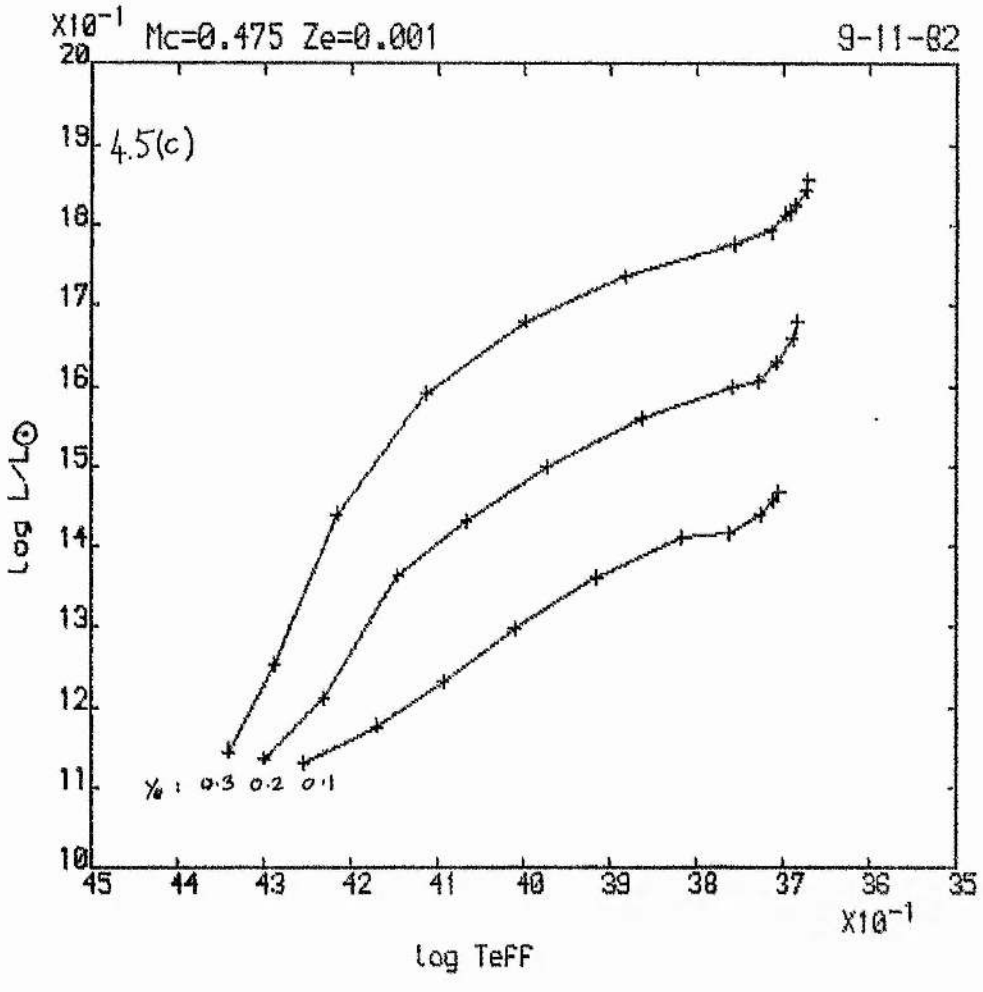
X10⁻¹
Mc=0.475 Ze=0.001
9-11-82
4.5(c)
Log L/L⊙
Ye : 0.3 0.2 0.1
Log TeFF
X10⁻¹

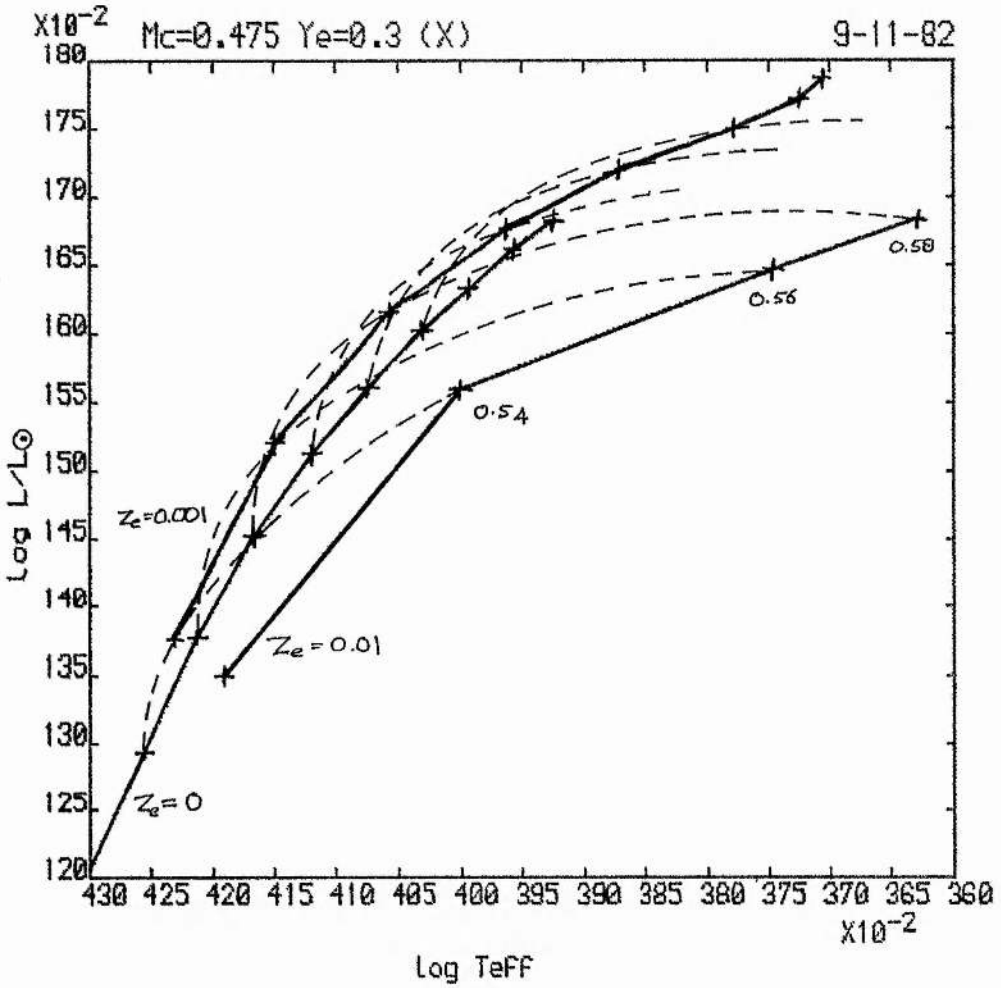

Figure 4.6 ZAHB models as a function of metallicity for models (X) with increased core opacities. Models of similar masses are connected by roughly interpolated dashed lines. Solid lines represent ZAHB sequences for the given metallicities. The mass interval between models is 0.02 $M_{\odot}$.

4.6 EVOLUTIONARY SEQUENCES FOR HORIZONTAL BRANCH STARS

Details of evolutionary sequences for horizontal branch stars calculated using the Carson opacities and the FCZII energy generation rates are given in tables 4.12 - 4.15. Table 4.12 gives overall properties for each evolutionary sequence for the standard models (Z), further details of each sequence are given in table 4.13. The same information is given in tables 4.14 and 4.15 for sequences (W) calculated with the modifications described at the beginning of § 4.5. Evolutionary tracks for both sets of sequences are shown in figures 4.7 and 4.8.

The major consequence of using the original opacity interpolation scheme (viz. interpolation in the H, He, Z tables for $Z < 0.04$) is to prevent the convective core from growing above its zero-age mass (M_{cc}^{o}). As the carbon abundance rises, the opacity interpolation alters to use the He, C, O tables and the opacity within the convective core drops steeply, causing a drop ($\sim 5\%$) in M_{cc}. M_{cc} subsequently rises, but on reaching $M_{cc} = M_{cc}^{o}$, $\kappa(M_r < M_{cc})$ has also risen to become significantly greater than $\kappa(M_r > M_{cc}^{o})$ where a large discontinuity in the opacity now occurs. Without convective overshooting no mixing will take place across the convective core boundary, and M_{cc} is unable to grow any further. With the new opacity interpolation scheme M_{cc} grows continuously until the rising composition difference between the radiative and convective regions of the core increases the size of the discontinuity in the opacity at the core boundary to an extent which prevents this growth (usually when Yc has dropped to approximately 0.82). For $M_e = 0.475\ M_\odot$ the main difference between evolutionary sequences Z and W is that maximum values for the convective core size are M_{cc}^{max} (Z) = 0.184 $M_\odot$ and M_{cc}^{max} (W) = 0.161 $M_\odot$.

The carbon enrichment in the hydrogen-shell has little effect on the overall evolution, but produces a luminosity and effective temperature difference in evolutionary stages where the hydrogen-shell has not burnt out through the region of carbon-enrichment. For stars in which the hydrogen-

shell is weak, and hence moving outwards less rapidly, the carbon enrichment has a correspondingly smaller effect on the total luminosity. The irregular early behaviour of red evolutionary tracks (W) (e.g. for $M > 0.60$, $Mc = 0.475$, $Ye = 0.3$, $Ze = 0.001$) is due to the rapid movement of the hydrogen shell away from its original position (figure 4.7).

Having accounted for the differences between evolutionary tracks in figures 4.7 and 4.8, we observe that the general features of both sets are morphologically similar. We therefore use the larger number of sequences available in set W to examine general sequence characteristics.

We have already noted (§ 4.4) the substantial luminosity drop during core-helium burning. This feature occurs in all sequences, but the luminosity drop increases with L_H (except for low T_{eff} where the effect is reduced). In contradiction to SG76, we find that as Ye increases to Ye = 0.3 evolutionary tracks do not deviate significantly from their ZAHB curves. Due to the drop in L_H, the increase in M_c due to hydrogen-burning is much lower when the Carson opacities are used than found previously. We do not find significant luminosity differences for stars at opposite ends of blueward loops within the instability strip. If there is a large mass spread in the HB population, the luminosity thickness of the HB is not found to vary significantly with increasing Y_e.

The division of HB tracks into two morphological groups depending on whether evolution is mainly to the blue or to the red (IR70) is still possible. We propose a method to identify the bifurcation point between redward and blueward evolutionary sequences for a given set of parameters (M, Ye, Z). The time-averaged T_{eff} is obtained from each evolutionary sequence by

$$\langle \log T_{eff} \rangle = \frac{\sum_{i=1}^{n} (\log T_{eff\,i} + \log T_{eff\,i-1})/2 \cdot (t_i - t_{i-1})}{t_{HB}} \qquad (4\text{-}2)$$

where $\log T_{eff_i}$ is the logarithm of the effective temperature at time t_i, and $t_{HB} = t_n - t_0$. By linear interpolation we obtain the mass of the

horizontal branch star for which $\log T_{eff}$ (ZAHB) = $< \log T_{eff} >$. Interpolating again we obtain L_{He}/L for the star at the bifurcation point. Stars for which $\log T_{eff}$ (ZAHB) $> < \log T_{eff} >$ are considered to evolve mainly to the red (This arbitrary definition of the bifurcation point means that some models which evolve partly to the blue may fall in the 'redward' evolution group). The bifurcation points for a number of combinations of (Mc, Ye, Ze) calculated from sequences W are given in table 4.16. For (M = 0.475, Ye = 0.1, Ze = 0.01), $L_{He}/L > 0.63$ for all M and there is no blueward evolution. The results obtained in table 4.16 agree with the conclusion of Lauterborn, Refsdal and Stabell (1972) that small and large values of L_{He}/L lead, respectively, to blueward and redward evolving sequences. For sequences W, the critical value of L_{He}/L separating the morphological groups is approximately 0.56. However our definition of the bifurcation point is sensitive to the definition of t_{HB}. If the end of HB evolution is chosen at Yc = 0.05 rather than Yc = 0.01, $< \log T_{eff} >$ for a given (Mc, Ye, Ze) will be increased. The 'bifurcation mass' will be reduced and the critical relative core luminosity L_{He}/L will be increased. From the small number of evolutionary sequences calculated we find that the different physics used in the Z sequences leads to an increase in the bifurcation mass and a decrease in the critical core luminosity fraction. The last entry in table 4.15 demonstrates this, but note that the interpolation is over an increased mass interval. We do not anticipate a significant change in the population of the morphological groups as a result of using the Carson opacities.

We find for all values of (M, Mc, Ye, Ze) used that HB lifetimes are considerably shorter than found previously, even after an allowance for the neglect of semiconvection has been made. The principal reasons for this result are discussed in §4.4. As earlier authors have found, t_{HB} is a sensitive function of core mass Mc. During HB evolution the behaviour of the hydrogen-shell may significantly modify Mc. As before, we find an

Table 4.16 Masses and Core-luminosity fractions at the bifurcation point between redward and blueward evolutionary sequences for model sequences W at constant (Mc, Ye, Ze).

Mc	Ye	Ze	M_b	L_{He}/L_b
0.475	0.3	0.01	0.523	0.57
0.475	0.2	0.01	0.544	0.56
0.475	0.1	0.01	-	-
0.475	0.3	0.001	0.540	0.53
0.475	0.2	0.001	0.550	0.58
0.525	0.3	0.01	0.586	0.58
(Z) 0.475	0.3	0.001	0.560	0.50

increase in Mc leads to a decrease in t_{HB}. Similarly, an increase in Ye leads to an increase in L_H and hence in dM_c/dt; a decrease in t_{HB} follows. Thus for (M = 0.60, Ye = 0.3, Ze = 0.01), t_{HB} drops from 5.2×10^7 years to 3.4×10^7 years as Mc increases from 0.475 $M_\odot$ to 0.525 $M_\odot$, and for (M = 0.54, Mc = 0.475, Ze = 0.01), t_{HB} drops from 5.3×10^7 years to 5.0×10^7 years as Y increases from 0.1 to 0.3. However the Carson opacities modify the behaviour of L_H as a function of M and Ze. In general, for Ye = 0.3 and a given pair (Mc, Ze), increasing M for stars with $\langle \log T_{eff} \rangle \gtrsim 4.0$ leads to a decrease in t_{HB}. For $4.0 \gtrsim \langle \log T_{eff} \rangle \gtrsim 3.8$, the increasing total drop in L_H during evolution with increasing M leads to an increase in t_{HB} with increasing M. For $\langle \log T_{eff} \rangle \lesssim 3.8$, the total drop in L_H decreases, and t_{HB} also decreases with increasing M. The region in which t_{HB} increases with increasing M vanishes as Ye drops below 0.3. This is best illustrated in table 4.14 by the set of evolutionary tracks for (Mc = 0.475, Ye = 0.3, Ze = 0.001). We find that L_H is very sensitive to the metal abundance Ze ($0.001 \leq Ze \leq 0.01$), and consequently for (M = 0.60, Mc = 0.475, Ye = 0.3), t_{HB} drops from 4.94×10^7 years to 4.45×10^7 years as Ze drops from 0.01 to 0.001. The change in physics causes lifetimes in set Z to be slightly shorter than those in set W.

From the evolutionary sequences calculated we find that the Carson opacities do not have a significant effect on the direction of evolution in the (L-T_{eff}) plane. However we find that they reduce the thickness of the theoretical horizontal branch for a given set (Mc, Ye, Ze) and lead to a substantial reduction in horizontal branch lifetimes. The dependence of t_{HB} on total mass and metallicity is also modified.

Table 4.12

Summary of evolutionary sequences for horizontal branch stars. The sequences are grouped according to 1) metallicity Ze; 2) helium-core mass, Mc ; and 3) envelope helium abundance Ye. Columns show 1) M_*, Total mass of star in solar units; 2) t_{HB}, horizontal branch lifetime in units of 10^7 years; 3) Fractional time spent in the RR Lyrae instability strip t_{RR}/t_{HB} ; 4),5),6) and zero-age values for the effective temperature, total luminosity, helium-core luminosity and surface gravity. Columns 8) 9) and 10) give the upper and lower limits and the range for the effective temperature during horizontal branch evolution. Columns 11) and 12) give the time averaged mean effective temperature and luninosity during horizontal-branch evolution. Columns 13) and 14) give the relative abundances by mass of ^{16}O and ^{4}He at the end of the evolutionary sequence. Effective temperatures and luminosities are given in logarithmic units, the luminosity is also in solar units.

Table 4.13

Extracts from evolutionary sequences for horizontal branch stars. The sequences are grouped as in table 4.11. The tables show (column 1) time in units of 10^7 years, (2) effective temperature, (3-5) total, helium-core and hydrogen-shell luminosities, (6) surface gravity, (7) central helium and (8) central oxygen relative mass abundances, (9) mass within the convective core and (10) mass interior to the hydrogen-burning shell. Masses are all given in solar units. Other units are as for table 4.12.

Table 4.14

Summary of evolutionary sequences for horizontal branch stars with limited convective core size and carbon-enriched hydrogen shell. Details are as for table 4.12.

Table 4.15

Extracts from evolutionary sequences for horizontal branch stars summarised in table 4.14.

Table 4.12

M*	thb	trr/Thb	Teff	L*	LHe	g	Mcc	TeMax	Temin	DTe	<Te>	<L>	X16c	Yc
				Mc=0.475 Y=0.3 Z=0.01										
0.54	5.342	0.00	3.9746	1.593	1.181	3.435	0.107	4.076	3.930	0.146	4.039	1.525	0.339	0.008
0.58	5.243	0.27	3.6233	1.703	1.176	1.951	0.100	3.836	3.614	0.223	3.725	1.656	0.341	0.009
				Mc=0.475 Y=0.3 Z=0.001										
0.54	4.675	0.00	4.2244	1.425	1.222	4.602	0.107	4.225	4.172	0.052	4.205	1.436	0.309	0.008
0.58	4.550	0.00	4.0386	1.644	1.214	3.671	0.107	4.084	3.932	0.152	4.060	1.618	0.301	0.009
0.62	4.710	0.27	3.8395	1.741	1.208	2.807	0.107	3.967	3.749	0.218	3.903	1.717	0.311	0.012
0.66	4.813	0.26	3.7150	1.786	1.205	2.291	0.107	3.865	3.681	0.184	3.778	1.773	0.330	0.009

Table 4.13

M=0.54 Mc=0.475 Y=0.3 Z=0.0100

t7	Teff	L	LHe	LH	g	Yc	X16c	Mcc	Msh
0.000	3.9746	1.593	1.181	1.380	3.435	0.971	0.005	0.107	0.475
0.455	3.9752	1.601	1.201	1.381	3.430	0.903	0.006	0.107	0.475
1.130	4.0046	1.578	1.240	1.311	3.570	0.801	0.010	0.113	0.475
1.780	4.0451	1.550	1.280	1.171	3.780	0.694	0.017	0.113	0.475
2.330	4.0674	1.491	1.314	1.016	3.908	0.597	0.027	0.113	0.475
2.830	4.0753	1.469	1.345	0.864	3.961	0.503	0.041	0.113	0.475
3.330	4.0739	1.462	1.373	0.730	3.964	0.404	0.060	0.113	0.475
3.830	4.0673	1.465	1.404	0.582	3.934	0.299	0.088	0.113	0.475
4.280	4.0594	1.478	1.428	0.514	3.890	0.202	0.125	0.113	0.475
4.730	4.0504	1.509	1.451	0.606	3.822	0.103	0.185	0.113	0.475
5.342	3.9301	1.740	1.456	1.421	3.110	0.008	0.339	0.113	0.475
5.342	3.9301	1.740	1.456	1.421	3.110	0.008	0.339	0.113	0.475

M=0.58 Mc=0.475 Y=0.3 Z=0.0100

t7	Teff	L	LHe	LH	g	Yc	X16c	Mcc	Msh
0.000	3.6233	1.703	1.176	1.550	1.951	0.971	0.005	0.100	0.475
0.480	3.6202	1.723	1.198	1.569	1.918	0.900	0.006	0.107	0.475
1.130	3.6321	1.706	1.243	1.523	1.983	0.801	0.010	0.114	0.475
1.730	3.6646	1.677	1.286	1.450	2.142	0.701	0.016	0.114	0.475
2.280	3.7179	1.648	1.325	1.368	2.384	0.602	0.027	0.114	0.477
2.780	3.7782	1.621	1.361	1.275	2.653	0.506	0.040	0.114	0.477
3.330	3.8175	1.598	1.399	1.163	2.832	0.394	0.063	0.114	0.480
3.730	3.8334	1.588	1.426	1.081	2.907	0.305	0.086	0.114	0.480
4.180	3.8334	1.590	1.456	1.014	2.904	0.205	0.124	0.114	0.480
4.605	3.8020	1.620	1.478	1.065	2.749	0.112	0.180	0.114	0.480
5.243	3.6137	1.836	1.482	1.582	1.779	0.009	0.341	0.114	0.480

M=0.54 Mc=0.475 Y=0.3 Z=0.0010

t7	Teff	L	LHe	LH	g	Yc	X16c	Mcc	Msh
0.000	4.2244	1.425	1.222	0.997	4.602	0.971	0.000	0.107	0.475
0.450	4.2237	1.418	1.243	0.939	4.606	0.896	0.002	0.107	0.475
1.050	4.2211	1.410	1.275	0.837	4.604	0.793	0.006	0.113	0.475
1.550	4.2177	1.407	1.301	0.743	4.593	0.705	0.012	0.113	0.475
2.050	4.2125	1.409	1.328	0.640	4.571	0.607	0.021	0.113	0.475
2.550	4.2058	1.416	1.356	0.527	4.537	0.506	0.035	0.113	0.475
3.050	4.1974	1.429	1.385	0.413	4.490	0.397	0.056	0.113	0.475
3.450	4.1900	1.444	1.410	0.321	4.445	0.304	0.080	0.113	0.475
3.850	4.1830	1.465	1.435	0.289	4.397	0.204	0.115	0.113	0.475
4.250	4.1804	1.497	1.462	0.386	4.354	0.093	0.177	0.113	0.475
4.675	4.1723	1.639	1.465	1.158	4.180	0.008	0.309	0.113	0.475
4.675	4.1723	1.639	1.465	1.158	4.180	0.008	0.309	0.113	0.475

Table 4.13 (contd.)

M=0.58 Mc=0.475 Y=0.3 Z=0.0010

t7	Teff	L	LHe	LH	q	Yc	X16c	Mcc	Msh
0.000	4.0386	1.644	1.214	1.442	3.671	0.971	0.000	0.107	0.475
0.450	4.0372	1.650	1.237	1.458	3.669	0.898	0.002	0.107	0.475
1.050	4.0438	1.645	1.272	1.406	3.691	0.799	0.006	0.114	0.475
1.600	4.0577	1.626	1.306	1.343	3.705	0.702	0.012	0.114	0.475
2.150	4.0714	1.604	1.343	1.259	3.842	0.598	0.023	0.114	0.475
2.650	4.0807	1.584	1.379	1.159	3.900	0.492	0.038	0.114	0.475
3.050	4.0857	1.573	1.408	1.073	3.922	0.400	0.056	0.114	0.475
3.450	4.0824	1.571	1.437	0.995	3.920	0.300	0.081	0.114	0.475
3.850	4.0761	1.581	1.467	0.944	3.984	0.191	0.120	0.114	0.475
4.150	4.0637	1.614	1.487	1.018	3.802	0.098	0.171	0.114	0.475
4.550	3.9319	1.813	1.477	1.544	3.076	0.009	0.301	0.114	0.475

M=0.62 Mc=0.475 Y=0.3 Z=0.0010

t7	Teff	L	LHe	LH	q	Yc	X16c	Mcc	Msh
0.000	3.8395	1.741	1.208	1.590	2.807	0.971	0.000	0.107	0.475
0.435	3.8247	1.756	1.230	1.602	2.753	0.902	0.002	0.107	0.475
1.085	3.8419	1.754	1.272	1.580	2.803	0.795	0.006	0.113	0.475
1.635	3.8836	1.734	1.312	1.527	2.990	0.698	0.015	0.113	0.475
2.135	3.9187	1.711	1.350	1.463	3.154	0.602	0.023	0.113	0.475
2.635	3.9444	1.690	1.387	1.391	3.278	0.498	0.038	0.113	0.475
3.085	3.9616	1.674	1.425	1.316	3.363	0.398	0.057	0.113	0.475
3.485	3.9665	1.668	1.452	1.261	3.386	0.303	0.082	0.113	0.475
3.885	3.9653	1.671	1.481	1.220	3.380	0.205	0.119	0.113	0.475
4.285	3.9437	1.702	1.505	1.264	3.263	0.100	0.180	0.113	0.475
4.710	3.7494	1.862	1.499	1.615	2.326	0.012	0.311	0.113	0.475

M=0.66 Mc=0.475 Y=0.3 Z=0.0010

t7	Teff	L	LHe	LH	q	Yc	X16c	Mcc	Msh
0.000	3.7150	1.786	1.205	1.654	2.291	0.971	0.000	0.107	0.475
0.450	3.7069	1.803	1.228	1.669	2.242	0.900	0.002	0.107	0.475
1.050	3.7124	1.804	1.269	1.654	2.203	0.803	0.006	0.114	0.475
1.625	3.7340	1.780	1.313	1.608	2.347	0.702	0.013	0.114	0.475
2.150	3.7788	1.765	1.357	1.550	2.567	0.602	0.023	0.114	0.475
2.650	3.8231	1.746	1.399	1.487	2.703	0.498	0.038	0.114	0.475
3.075	3.8463	1.734	1.433	1.433	2.868	0.403	0.057	0.114	0.475
3.525	3.8653	1.724	1.470	1.370	2.954	0.295	0.085	0.114	0.475
3.900	3.8594	1.730	1.497	1.348	2.924	0.204	0.120	0.114	0.475
4.337	3.8223	1.764	1.522	1.395	2.742	0.094	0.188	0.114	0.475
4.813	3.6810	1.929	1.512	1.719	2.012	0.009	0.330	0.114	0.475

Table 4.14

M*	thb	trr/Thb	Teff	L*	LHe	g	Mcc	TeMax	Temin	DTe	<Te>	<L>	X16c	Yc
					Mc=0.475 Y=0.1 Z=0.0100									
0.50	5.650	0.00	4.1644	1.126	1.119	4.628	0.094	4.164	4.069	0.096	4.113	1.227	0.329	0.008
0.52	5.400	0.00	4.0279	1.178	1.135	4.046	0.100	4.028	3.871	0.157	3.951	1.251	0.322	0.007
0.54	5.300	0.28	3.8661	1.246	1.141	3.348	0.100	3.867	3.681	0.185	3.790	1.281	0.318	0.009
0.56	5.200	0.00	3.6925	1.304	1.142	2.612	0.100	3.699	3.625	0.074	3.676	1.308	0.311	0.009
0.58	5.175	0.00	3.6447	1.321	1.142	2.418	0.100	3.649	3.611	0.037	3.641	1.322	0.315	0.007
0.60	5.188	0.00	3.6307	1.339	1.142	2.359	0.100	3.634	3.607	0.026	3.630	1.335	0.314	0.009
					Mc=0.475 Y=0.2 Z=0.0100									
0.50	5.550	0.00	4.2304	1.136	1.125	4.882	0.101	4.230	4.162	0.069	4.193	1.233	0.327	0.007
0.52	5.225	0.00	4.1200	1.238	1.142	4.355	0.100	4.120	4.032	0.088	4.078	1.279	0.312	0.008
0.54	5.150	0.01	3.9543	1.379	1.143	3.568	0.100	3.969	3.768	0.201	3.945	1.363	0.319	0.009
0.56	5.163	0.29	3.7313	1.468	1.140	2.603	0.100	3.809	3.651	0.158	3.772	1.437	0.303	0.019
0.58	5.163	0.00	3.6424	1.499	1.139	2.231	0.100	3.683	3.605	0.078	3.661	1.472	0.328	0.009
					Mc=0.475 Y=0.3 Z=0.0100									
0.50	4.871	0.00	4.2873	1.149	1.131	5.097	0.101	4.287	4.238	0.050	4.198	1.215	0.230	0.050
0.52	4.660	0.00	4.1884	1.361	1.144	4.506	0.100	4.192	4.154	0.037	4.101	1.307	0.227	0.050
0.54	4.710	0.00	3.9943	1.566	1.138	3.541	0.100	4.091	3.994	0.097	4.028	1.474	0.229	0.050
0.56	4.994	0.10	3.7320	1.654	1.134	2.420	0.100	3.978	3.731	0.248	3.884	1.585	0.250	0.050
0.58	4.919	0.39	3.6275	1.688	1.132	1.983	0.100	3.865	3.625	0.239	3.740	1.637	0.250	0.050
0.60	4.938	0.00	3.6125	1.710	1.131	1.915	0.100	3.709	3.610	0.099	3.634	1.667	0.252	0.050
0.62	4.894	0.00	3.6044	1.729	1.130	1.878	0.100	3.645	3.602	0.043	3.613	1.695	0.250	0.050

Table 4.14 (contd.)

M*	thb	trr/Thb	Teff	L*	LHe	g	Mcc	TeMax	Temin	DTe	<Te>	<L>	X16c	Yc
						Mc=0.475 Y=0.2 Z=0.0010								
0.50	5.125	0.00	4.2994	1.138	1.130	5.156	0.101	4.299	4.257	0.042	4.277	1.237	0.312	0.008
0.52	4.950	0.00	4.2312	1.213	1.153	4.825	0.100	4.231	4.175	0.056	4.202	1.277	0.314	0.009
0.54	4.925	0.00	4.1461	1.363	1.158	4.351	0.100	4.160	4.110	0.050	4.139	1.330	0.308	0.009
0.56	4.854	0.00	4.0659	1.431	1.161	3.978	0.100	4.089	4.000	0.089	4.073	1.389	0.308	0.009
0.58	4.850	0.00	3.9734	1.499	1.160	3.555	0.100	4.022	3.864	0.158	4.006	1.442	0.322	0.008
0.60	4.825	0.02	3.8644	1.559	1.156	3.074	0.100	3.954	3.734	0.220	3.932	1.493	0.321	0.007
						Mc=0.475 Y=0.3 Z=0.0010								
0.50	5.375	0.00	4.3413	1.146	1.135	5.315	0.101	4.350	4.309	0.042	4.323	1.244	0.316	0.009
0.52	5.025	0.00	4.2881	1.255	1.161	5.011	0.100	4.288	4.247	0.041	4.267	1.298	0.314	0.009
0.54	4.825	0.00	4.2163	1.441	1.164	4.553	0.100	4.230	4.185	0.044	4.216	1.385	0.311	0.008
0.56	4.700	0.00	4.1133	1.591	1.158	4.007	0.100	4.162	4.058	0.103	4.152	1.497	0.306	0.009
0.58	4.750	0.00	3.9992	1.680	1.152	3.477	0.100	4.101	3.927	0.174	4.075	1.594	0.320	0.009
0.60	4.531	0.00	3.8833	1.735	1.147	2.973	0.100	4.045	3.883	0.162	4.001	1.653	0.258	0.032
0.62	4.772	0.12	3.7575	1.777	1.143	2.443	0.100	3.987	3.723	0.264	3.919	1.706	0.321	0.010
0.64	4.750	0.16	3.7173	1.792	1.144	2.281	0.100	3.940	3.717	0.223	3.851	1.735	0.301	0.018
0.66	4.650	0.23	3.6981	1.814	1.141	2.195	0.100	3.884	3.698	0.186	3.796	1.758	0.246	0.052
0.68	4.825	0.12	3.6927	1.817	1.142	2.183	0.101	3.816	3.673	0.143	3.745	1.787	0.329	0.009
						Mc=0.525 Y=0.3 Z=0.0100								
0.54	3.900	0.00	4.3582	1.302	1.301	5.261	0.111	4.371	4.321	0.049	4.338	1.402	0.304	0.006
0.56	3.700	0.00	4.2789	1.358	1.328	4.903	0.111	4.279	4.218	0.061	4.247	1.437	0.306	0.006
0.58	3.525	0.00	4.1852	1.533	1.336	4.368	0.111	4.188	4.118	0.070	4.170	1.518	0.297	0.008
0.60	3.438	0.00	4.0252	1.697	1.332	3.579	0.111	4.087	3.920	0.167	4.062	1.642	0.287	0.009
0.62	3.600	0.22	3.8165	1.784	1.328	2.672	0.111	3.994	3.690	0.304	3.921	1.730	0.313	0.010
0.64	3.637	0.22	3.6450	1.826	1.326	1.957	0.111	3.879	3.643	0.236	3.773	1.780	0.268	0.031
0.66	3.525	0.00	3.6141	1.831	1.325	1.842	0.111	3.760	3.613	0.147	3.677	1.795	0.223	0.060

Table 4.15

M=0.50 Mc=0.475 Y=0.1 Z=0.0100

t7	Teff	L	LHe	LH	g	Yc	X16c	Mcc	Msh
0.000	4.1644	1.126	1.119	-0.670	4.628	0.971	0.005	0.094	0.475
0.525	4.1566	1.140	1.135	-0.801	4.563	0.894	0.006	0.094	0.475
1.125	4.1462	1.160	1.156	-0.878	4.522	0.804	0.009	0.100	0.475
1.825	4.1331	1.184	1.181	-0.978	4.445	0.697	0.017	0.101	0.475
2.425	4.1207	1.206	1.204	-1.132	4.373	0.601	0.028	0.101	0.475
3.025	4.1076	1.229	1.228	-1.409	4.298	0.500	0.043	0.101	0.475
3.625	4.0935	1.253	1.253	0.000	4.217	0.394	0.065	0.101	0.475
4.125	4.0816	1.276	1.275	-1.362	4.147	0.301	0.091	0.101	0.475
4.625	4.0718	1.299	1.299	0.000	4.084	0.203	0.128	0.101	0.475
5.125	4.0699	1.326	1.325	-1.312	4.050	0.098	0.191	0.101	0.475
5.650	4.1205	1.357	1.351	-0.506	4.222	0.008	0.329	0.101	0.475

M=0.52 Mc=0.475 Y=0.1 Z=0.0100

t7	Teff	L	LHe	LH	g	Yc	X16c	Mcc	Msh
0.000	4.0279	1.178	1.155	0.152	4.046	0.971	0.005	0.100	0.475
0.500	4.0195	1.183	1.151	0.034	4.008	0.896	0.006	0.094	0.475
1.100	4.0055	1.195	1.173	-0.111	3.940	0.802	0.009	0.100	0.475
1.700	3.9896	1.210	1.195	-0.259	3.862	0.707	0.016	0.100	0.475
2.300	3.9705	1.228	1.218	-0.415	3.768	0.607	0.027	0.100	0.475
2.900	3.9486	1.248	1.241	-0.548	3.660	0.503	0.042	0.100	0.475
3.500	3.9239	1.271	1.267	-0.767	3.538	0.393	0.064	0.100	0.475
4.000	3.9016	1.293	1.289	-0.745	3.427	0.296	0.091	0.100	0.475
4.500	3.8801	1.316	1.314	-1.022	3.318	0.194	0.131	0.100	0.475
4.900	3.8706	1.338	1.335	-0.824	3.253	0.107	0.182	0.100	0.475
5.400	3.9081	1.396	1.364	0.247	3.350	0.007	0.322	0.100	0.475

M=0.54 Mc=0.475 Y=0.1 Z=0.0100

t7	Teff	L	LHe	LH	g	Yc	X16c	Mcc	Msh
0.000	3.8661	1.246	1.141	0.578	3.348	0.971	0.005	0.100	0.475
0.450	3.8640	1.242	1.157	0.492	3.344	0.903	0.006	0.094	0.475
1.150	3.8539	1.242	1.184	0.339	3.304	0.792	0.010	0.100	0.475
1.750	3.8386	1.247	1.207	0.191	3.237	0.694	0.017	0.100	0.475
2.350	3.8169	1.257	1.231	0.021	3.140	0.591	0.029	0.100	0.475
2.850	3.7937	1.269	1.252	-0.147	3.055	0.501	0.042	0.100	0.475
3.450	3.7594	1.288	1.277	-0.314	2.879	0.388	0.065	0.100	0.475
3.950	3.7309	1.307	1.299	-0.432	2.746	0.289	0.093	0.100	0.475
4.350	3.7103	1.325	1.319	-0.538	2.646	0.206	0.125	0.100	0.475
4.850	3.6923	1.354	1.346	-0.385	2.545	0.094	0.191	0.100	0.475
5.300	3.6815	1.426	1.366	0.537	2.480	0.009	0.318	0.100	0.475

Table 4.15 (contd.)

M=0.50 Mc=0.475 Y=0.1 Z=0.0100

t7	Teff	L	LHe	LH	g	Yc	X16c	Mcc	Msh
0.000	3.6925	1.304	1.142	0.797	2.612	0.971	0.005	0.100	0.475
0.475	3.6968	1.296	1.159	0.728	2.637	0.899	0.006	0.094	0.475
1.075	3.6990	1.288	1.184	0.616	2.653	0.805	0.009	0.100	0.475
1.675	3.6968	1.284	1.208	0.490	2.649	0.707	0.016	0.100	0.475
2.275	3.6896	1.284	1.234	0.320	2.619	0.604	0.027	0.100	0.475
2.875	3.6791	1.292	1.259	0.156	2.570	0.495	0.045	0.100	0.475
3.375	3.6673	1.305	1.281	-0.003	2.512	0.399	0.062	0.100	0.475
3.875	3.6576	1.318	1.304	-0.161	2.458	0.299	0.090	0.100	0.475
4.375	3.6465	1.338	1.327	-0.264	2.394	0.195	0.131	0.100	0.475
4.775	3.6410	1.359	1.340	-0.243	2.350	0.102	0.185	0.100	0.475
5.200	3.6247	1.448	1.369	0.669	2.196	0.009	0.311	0.100	0.475

M=0.56 Mc=0.475 Y=0.1 Z=0.0100

t7	Teff	L	LHe	LH	g	Yc	X16c	Mcc	Msh
0.000	3.6447	1.321	1.142	0.850	2.418	0.971	0.005	0.100	0.475
0.475	3.6405	1.315	1.160	0.792	2.431	0.898	0.006	0.094	0.475
1.125	3.6452	1.307	1.188	0.687	2.447	0.794	0.010	0.100	0.475
1.725	3.6485	1.301	1.213	0.564	2.454	0.695	0.017	0.100	0.475
2.225	3.6474	1.299	1.235	0.436	2.451	0.606	0.026	0.100	0.475
2.825	3.6441	1.302	1.261	0.257	2.435	0.499	0.042	0.100	0.475
3.325	3.6398	1.310	1.282	0.105	2.410	0.403	0.061	0.100	0.475
3.825	3.6350	1.323	1.305	-0.068	2.376	0.302	0.088	0.100	0.475
4.325	3.6299	1.342	1.329	-0.188	2.338	0.195	0.129	0.100	0.475
4.725	3.6264	1.365	1.350	-0.104	2.301	0.104	0.183	0.100	0.475
5.175	3.6114	1.475	1.369	0.811	2.131	0.007	0.315	0.100	0.475

M=0.60 Mc=0.475 Y=0.1 Z=0.0100

t7	Teff	L	LHe	LH	g	Yc	X16c	Mcc	Msh
0.000	3.6307	1.339	1.142	0.901	2.359	0.971	0.005	0.100	0.475
0.462	3.6315	1.334	1.160	0.853	2.368	0.901	0.006	0.094	0.475
1.188	3.6328	1.325	1.190	0.752	2.382	0.787	0.010	0.100	0.475
1.688	3.6335	1.318	1.212	0.654	2.391	0.704	0.016	0.100	0.475
2.287	3.6335	1.314	1.238	0.520	2.395	0.599	0.027	0.100	0.475
2.887	3.6325	1.315	1.265	0.351	2.390	0.489	0.044	0.100	0.475
3.387	3.6307	1.322	1.287	0.211	2.377	0.392	0.064	0.100	0.475
3.887	3.6280	1.334	1.311	0.046	2.354	0.290	0.092	0.100	0.475
4.288	3.6253	1.349	1.330	-0.019	2.328	0.203	0.125	0.100	0.475
4.788	3.6211	1.379	1.357	0.075	2.280	0.087	0.196	0.100	0.475
5.188	3.6074	1.481	1.370	0.834	2.124	0.009	0.314	0.100	0.475

Table 4.15 (contd.)

M=0.50 Mc=0.475 Y=0.2 Z=0.0100

t7	Teff	L	LHe	LH	g	Yc	X16c	Mcc	Msh
0.000	4.2304	1.136	1.125	-0.466	4.882	0.971	0.005	0.101	0.475
0.500	4.2246	1.148	1.140	-0.591	4.847	0.897	0.006	0.094	0.475
1.100	4.2166	1.167	1.161	-0.696	4.796	0.806	0.009	0.100	0.475
1.800	4.2065	1.191	1.187	-0.847	4.751	0.697	0.017	0.101	0.475
2.400	4.1974	1.213	1.210	-0.949	4.673	0.600	0.028	0.101	0.475
3.000	4.1874	1.236	1.234	-1.102	4.610	0.497	0.043	0.101	0.475
3.600	4.1770	1.261	1.259	-1.077	4.544	0.389	0.066	0.101	0.475
4.100	4.1687	1.283	1.282	-1.355	4.488	0.295	0.092	0.101	0.475
4.600	4.1625	1.307	1.306	-1.331	4.439	0.195	0.132	0.101	0.475
5.100	4.1658	1.335	1.333	-1.005	4.425	0.087	0.199	0.101	0.475
5.550	4.2131	1.368	1.356	-0.197	4.581	0.007	0.327	0.101	0.475

M=0.52 Mc=0.475 Y=0.2 Z=0.0100

t7	Teff	L	LHe	LH	g	Yc	X16c	Mcc	Msh
0.000	4.1200	1.258	1.142	0.535	4.355	0.971	0.005	0.100	0.475
0.500	4.1167	1.235	1.159	0.441	4.346	0.894	0.006	0.094	0.475
1.100	4.1098	1.236	1.183	0.296	4.317	0.798	0.010	0.100	0.475
1.700	4.1005	1.243	1.206	0.155	4.273	0.701	0.017	0.100	0.475
2.300	4.0888	1.255	1.230	0.003	4.214	0.598	0.028	0.100	0.475
2.900	4.0749	1.271	1.255	-0.171	4.142	0.490	0.044	0.100	0.475
3.400	4.0618	1.289	1.277	-0.276	4.072	0.396	0.063	0.100	0.475
3.900	4.0479	1.309	1.300	-0.379	3.996	0.297	0.091	0.100	0.475
4.400	4.0354	1.332	1.324	-0.407	3.923	0.191	0.132	0.100	0.475
4.800	4.0323	1.356	1.347	-0.332	3.887	0.101	0.186	0.100	0.475
5.225	4.0446	1.456	1.369	0.715	3.836	0.008	0.312	0.100	0.475

M=0.54 Mc=0.475 Y=0.2 Z=0.0100

t7	Teff	L	LHe	LH	g	Yc	X16c	Mcc	Msh
0.000	3.9543	1.379	1.143	1.001	3.568	0.971	0.005	0.100	0.475
0.475	3.9607	1.370	1.162	0.950	3.603	0.898	0.006	0.094	0.475
1.075	3.9655	1.357	1.189	0.863	3.655	0.801	0.010	0.100	0.475
1.675	3.9687	1.344	1.215	0.754	3.661	0.701	0.017	0.100	0.475
2.275	3.9670	1.335	1.243	0.616	3.662	0.595	0.028	0.100	0.475
2.775	3.9607	1.334	1.266	0.495	3.639	0.503	0.041	0.100	0.475
3.275	3.9504	1.338	1.289	0.366	3.593	0.405	0.061	0.100	0.475
3.775	3.9354	1.350	1.314	0.251	3.522	0.302	0.088	0.100	0.475
4.275	3.9182	1.370	1.340	0.194	3.433	0.192	0.150	0.100	0.475
4.675	3.9041	1.400	1.362	0.323	3.346	0.097	0.187	0.100	0.475
5.137	3.7812	1.572	1.372	1.139	2.682	0.010	0.315	0.100	0.475
5.150	3.7678	1.583	1.371	1.170	2.617	0.009	0.319	0.100	0.475

Table 4.15 (contd.)

M=0.50 Mc=0.475 Y=0.2 Z=0.0100

t7	Teff	L	LHe	LH	g	Yc	X16c	Mcc	Msh
0.000	3.7313	1.468	1.140	1.192	2.603	0.971	0.005	0.100	0.475
0.450	3.7398	1.464	1.159	1.167	2.641	0.903	0.006	0.094	0.475
1.100	3.7567	1.454	1.188	1.115	2.718	0.802	0.010	0.100	0.475
1.700	3.7768	1.439	1.217	1.041	2.814	0.705	0.017	0.100	0.475
2.300	3.7959	1.422	1.246	0.945	2.907	0.603	0.028	0.100	0.475
2.850	3.8072	1.408	1.275	0.829	2.966	0.499	0.043	0.100	0.475
3.350	3.8088	1.401	1.301	0.714	2.979	0.399	0.063	0.100	0.475
3.850	3.7997	1.404	1.328	0.610	2.941	0.292	0.092	0.100	0.475
4.250	3.7842	1.415	1.349	0.564	2.868	0.201	0.126	0.100	0.475
4.650	3.7548	1.445	1.372	0.635	2.720	0.103	0.182	0.100	0.475
5.163	3.6514	1.579	1.382	1.141	2.172	0.019	0.303	0.100	0.475

M=0.50 Mc=0.475 Y=0.2 Z=0.0100

t7	Teff	L	LHe	LH	g	Yc	X16c	Mcc	Msh
0.000	3.6424	1.499	1.139	1.250	2.231	0.971	0.005	0.100	0.475
0.488	3.6442	1.498	1.159	1.232	2.240	0.897	0.006	0.094	0.475
1.088	3.6484	1.491	1.188	1.192	2.263	0.803	0.010	0.100	0.475
1.688	3.6563	1.478	1.217	1.133	2.308	0.705	0.016	0.100	0.475
2.287	3.6680	1.459	1.249	1.043	2.373	0.599	0.028	0.100	0.475
2.887	3.6782	1.442	1.282	0.931	2.431	0.484	0.045	0.100	0.475
3.287	3.6824	1.434	1.305	0.844	2.456	0.402	0.061	0.100	0.475
3.787	3.6817	1.432	1.332	0.745	2.455	0.294	0.090	0.100	0.475
4.188	3.6752	1.440	1.354	0.694	2.421	0.202	0.125	0.100	0.475
4.587	3.6595	1.471	1.377	0.760	2.328	0.102	0.181	0.100	0.475
5.150	3.6066	1.642	1.383	1.294	1.946	0.010	0.325	0.100	0.475
5.163	3.6052	1.651	1.383	1.314	1.931	0.009	0.328	0.100	0.475

M=0.50 Mc=0.475 Y=0.3 Z=0.0100

t7	Teff	L	LHe	LH	g	Yc	X16c	Mcc	Msh
0.000	4.2873	1.149	1.131	-0.242	5.097	0.971	0.005	0.101	0.475
0.500	4.2828	1.160	1.146	-0.339	5.067	0.896	0.006	0.094	0.475
1.100	4.2762	1.179	1.169	-0.464	5.022	0.799	0.009	0.098	0.475
1.700	4.2690	1.200	1.192	-0.539	4.973	0.699	0.016	0.100	0.475
2.300	4.2613	1.222	1.217	-0.719	4.919	0.593	0.027	0.101	0.475
2.900	4.2529	1.247	1.244	-0.915	4.861	0.479	0.044	0.101	0.475
3.300	4.2471	1.266	1.263	-0.896	4.819	0.397	0.060	0.101	0.475
3.700	4.2415	1.286	1.284	-1.052	4.776	0.308	0.082	0.101	0.475
4.200	4.2370	1.313	1.311	-1.025	4.731	0.199	0.122	0.101	0.475
4.700	4.2419	1.341	1.339	-0.997	4.723	0.090	0.190	0.101	0.475
5.150	4.2877	1.390	1.364	0.154	4.857	0.007	0.321	0.101	0.475

Table 4.15 (contd.)

M=0.52 Mc=0.475 Y=0.3 Z=0.0100

t7	Teff	L	LHe	LH	g	Yc	X16c	Mcc	Msh
0.000	4.1884	1.361	1.144	0.956	4.506	0.971	0.005	0.100	0.475
0.475	4.1911	1.342	1.163	0.871	4.536	0.897	0.006	0.094	0.475
1.075	4.1912	1.322	1.190	0.740	4.556	0.799	0.010	0.099	0.475
1.675	4.1883	1.310	1.216	0.599	4.556	0.697	0.017	0.100	0.475
2.275	4.1820	1.307	1.244	0.437	4.554	0.584	0.028	0.100	0.475
2.675	4.1762	1.311	1.264	0.322	4.507	0.503	0.039	0.100	0.475
3.275	4.1655	1.326	1.295	0.164	4.450	0.370	0.065	0.100	0.475
3.575	4.1599	1.337	1.312	0.085	4.416	0.301	0.083	0.100	0.475
4.075	4.1530	1.360	1.337	0.072	4.366	0.192	0.125	0.100	0.475
4.475	4.1529	1.390	1.360	0.214	4.335	0.098	0.182	0.100	0.475
4.950	4.1252	1.616	1.371	1.251	3.998	0.008	0.318	0.100	0.475

M=0.54 Mc=0.475 Y=0.3 Z=0.0100

t7	Teff	L	LHe	LH	g	Yc	X16c	Mcc	Msh
0.000	3.9943	1.566	1.138	1.363	3.541	0.971	0.005	0.100	0.475
0.450	4.0015	1.566	1.157	1.351	3.570	0.903	0.006	0.094	0.475
1.075	4.0231	1.548	1.189	1.298	3.674	0.806	0.009	0.100	0.475
1.675	4.0553	1.506	1.223	1.186	3.845	0.705	0.016	0.100	0.475
2.275	4.0789	1.463	1.258	1.038	3.982	0.596	0.028	0.100	0.475
2.775	4.0887	1.436	1.286	0.901	4.049	0.499	0.042	0.100	0.475
3.275	4.0912	1.421	1.314	0.760	4.073	0.396	0.062	0.100	0.475
3.675	4.0881	1.421	1.336	0.671	4.061	0.308	0.086	0.100	0.475
4.175	4.0805	1.438	1.365	0.628	4.013	0.190	0.130	0.100	0.475
4.575	4.0707	1.484	1.389	0.777	3.928	0.085	0.193	0.100	0.475
4.988	3.9578	1.712	1.393	1.428	3.248	0.011	0.313	0.100	0.475

M=0.56 Mc=0.475 Y=0.3 Z=0.0100

t7	Teff	L	LHe	LH	g	Yc	X16c	Mcc	Msh
0.000	3.7320	1.654	1.134	1.498	2.420	0.971	0.005	0.100	0.475
0.462	3.7326	1.665	1.154	1.505	2.411	0.902	0.006	0.094	0.475
1.112	3.7941	1.648	1.192	1.461	2.674	0.801	0.010	0.100	0.475
1.737	3.8728	1.610	1.231	1.375	3.026	0.699	0.017	0.100	0.475
2.313	3.9225	1.577	1.266	1.286	3.259	0.598	0.028	0.100	0.475
2.838	3.9511	1.551	1.296	1.198	3.399	0.499	0.043	0.100	0.475
3.287	3.9691	1.531	1.324	1.110	3.491	0.405	0.062	0.100	0.475
3.787	3.9765	1.521	1.353	1.027	3.531	0.301	0.090	0.100	0.475
4.262	3.9719	1.528	1.379	0.991	3.505	0.198	0.131	0.100	0.475
4.688	3.9533	1.564	1.400	1.062	3.395	0.106	0.188	0.100	0.475
5.238	3.8007	1.736	1.411	1.458	2.615	0.018	0.317	0.100	0.479

Table 4.15 (contd.)

M=0.58 Mc=0.475 Y=0.3 Z=0.0100

t7	Teff	L	LHe	LH	Q	Yc	X1oc	Mcc	Msh
0.000	3.6275	1.688	1.132	1.547	1.964	0.971	0.005	0.100	0.475
0.462	3.6254	1.703	1.153	1.559	1.959	0.902	0.006	0.094	0.475
1.112	3.6403	1.692	1.194	1.526	2.050	0.799	0.010	0.100	0.475
1.713	3.6711	1.668	1.232	1.470	2.177	0.700	0.017	0.100	0.475
2.262	3.7334	1.639	1.271	1.396	2.455	0.601	0.028	0.100	0.475
2.787	3.7942	1.612	1.305	1.317	2.725	0.500	0.043	0.100	0.475
3.262	3.8366	1.589	1.337	1.233	2.918	0.403	0.062	0.100	0.480
3.762	3.8577	1.577	1.368	1.159	3.014	0.297	0.092	0.100	0.480
4.212	3.8589	1.582	1.395	1.126	3.014	0.198	0.131	0.100	0.480
4.637	3.8257	1.619	1.417	1.189	2.845	0.103	0.191	0.100	0.480
5.050	3.6622	1.744	1.426	1.459	2.065	0.029	0.288	0.100	0.480

M=0.60 Mc=0.475 Y=0.3 Z=0.0100

t7	Teff	L	LHe	LH	Q	Yc	X1oc	Mcc	Msh
0.000	3.6125	1.710	1.151	1.577	1.915	0.971	0.005	0.100	0.475
0.462	3.6105	1.727	1.172	1.593	1.890	0.902	0.006	0.094	0.475
1.112	3.6161	1.714	1.195	1.557	1.926	0.802	0.010	0.100	0.475
1.713	3.6258	1.692	1.236	1.505	1.986	0.703	0.017	0.100	0.475
2.287	3.6450	1.670	1.275	1.446	2.078	0.600	0.028	0.100	0.477
2.838	3.6609	1.654	1.312	1.390	2.165	0.494	0.044	0.100	0.477
3.313	3.6819	1.639	1.345	1.331	2.264	0.396	0.064	0.100	0.477
3.738	3.6978	1.632	1.372	1.286	2.335	0.304	0.090	0.100	0.477
4.212	3.7073	1.633	1.402	1.248	2.372	0.200	0.131	0.100	0.477
4.663	3.6778	1.666	1.427	1.293	2.221	0.103	0.192	0.100	0.485
5.212	3.5976	1.874	1.454	1.678	1.692	0.009	0.341	0.100	0.485

M=0.62 Mc=0.475 Y=0.3 Z=0.0100

t7	Teff	L	LHe	LH	Q	Yc	X1oc	Mcc	Msh
0.000	3.6044	1.729	1.150	1.603	1.878	0.971	0.005	0.100	0.475
0.456	3.6020	1.746	1.151	1.619	1.852	0.903	0.006	0.094	0.475
1.106	3.6071	1.735	1.194	1.588	1.863	0.803	0.010	0.100	0.475
1.731	3.6158	1.713	1.238	1.536	1.931	0.699	0.017	0.100	0.476
2.281	3.6201	1.694	1.277	1.484	1.976	0.601	0.028	0.100	0.476
2.806	3.6240	1.685	1.311	1.446	2.001	0.500	0.045	0.100	0.476
3.306	3.6349	1.665	1.347	1.380	2.065	0.398	0.064	0.100	0.476
3.756	3.6443	1.655	1.379	1.327	2.112	0.299	0.091	0.100	0.484
4.206	3.6431	1.666	1.408	1.310	2.099	0.196	0.132	0.100	0.484
4.631	3.6311	1.694	1.431	1.351	2.020	0.102	0.192	0.100	0.484
5.056	3.6034	1.813	1.446	1.571	1.791	0.023	0.300	0.100	0.484

Table 4.15 (contd.)

M=0.50 mc=0.475 Y=0.2 Z=0.0010

t7	Teff	L	LHe	LH	g	Yc	X1oc	Mcc	Msh
0.000	4.2994	1.156	1.130	-0.601	5.156	0.971	0.000	0.101	0.475
0.525	4.2952	1.152	1.146	-0.711	5.125	0.892	0.002	0.094	0.475
1.225	4.2886	1.177	1.172	-0.764	5.074	0.779	0.007	0.100	0.475
1.625	4.2846	1.192	1.188	-0.846	5.043	0.712	0.011	0.100	0.475
2.225	4.2783	1.215	1.212	-0.947	4.995	0.608	0.022	0.101	0.475
2.825	4.2714	1.241	1.239	-1.097	4.941	0.496	0.038	0.101	0.475
3.425	4.2643	1.269	1.267	-1.069	4.885	0.373	0.062	0.101	0.475
3.825	4.2600	1.290	1.289	-1.348	4.848	0.286	0.087	0.101	0.475
4.225	4.2574	1.313	1.312	-1.325	4.813	0.192	0.122	0.101	0.475
4.625	4.2601	1.334	1.333	-1.304	4.802	0.106	0.174	0.101	0.475
5.125	4.2981	1.308	1.301	-0.428	4.920	0.006	0.312	0.101	0.475

M=0.52 mc=0.475 Y=0.2 Z=0.0010

t7	Teff	L	LHe	LH	g	Yc	X1oc	Mcc	Msh
0.000	4.2312	1.215	1.153	0.324	4.425	0.971	0.000	0.100	0.475
0.475	4.2274	1.214	1.169	0.207	4.389	0.896	0.002	0.094	0.475
1.075	4.2210	1.224	1.192	0.075	4.774	0.798	0.006	0.099	0.475
1.775	4.2122	1.241	1.220	-0.085	4.721	0.677	0.015	0.100	0.475
2.175	4.2062	1.254	1.237	-0.162	4.684	0.601	0.025	0.100	0.475
2.775	4.1964	1.276	1.264	-0.289	4.623	0.481	0.040	0.100	0.475
3.175	4.1894	1.294	1.284	-0.349	4.577	0.395	0.057	0.100	0.475
3.575	4.1821	1.314	1.306	-0.425	4.528	0.300	0.080	0.100	0.475
3.975	4.1769	1.333	1.326	-0.463	4.482	0.215	0.112	0.100	0.475
4.475	4.1764	1.362	1.354	-0.377	4.457	0.101	0.178	0.100	0.475
4.950	4.2056	1.423	1.378	0.416	4.512	0.009	0.314	0.100	0.475

M=0.54 mc=0.475 Y=0.2 Z=0.0010

t7	Teff	L	LHe	LH	g	Yc	X1oc	Mcc	Msh
0.000	4.1461	1.363	1.158	0.938	4.451	0.971	0.000	0.100	0.475
0.450	4.1536	1.315	1.179	0.745	4.449	0.900	0.002	0.094	0.475
1.050	4.1594	1.295	1.207	0.558	4.472	0.796	0.006	0.099	0.475
1.650	4.1544	1.294	1.233	0.411	4.455	0.695	0.015	0.100	0.475
2.150	4.1479	1.300	1.254	0.302	4.421	0.604	0.023	0.100	0.475
2.650	4.1400	1.311	1.277	0.186	4.379	0.508	0.037	0.100	0.475
3.150	4.1308	1.325	1.299	0.069	4.325	0.408	0.057	0.100	0.475
3.650	4.1214	1.344	1.323	-0.018	4.272	0.302	0.085	0.100	0.475
4.150	4.1128	1.367	1.349	-0.024	4.216	0.189	0.128	0.100	0.475
4.550	4.1111	1.394	1.373	0.066	4.160	0.091	0.188	0.100	0.475
4.925	4.1162	1.491	1.389	0.512	4.104	0.009	0.308	0.100	0.475

Table 4.15 (contd.)

M=0.56 Mc=0.475 Y=0.2 Z=0.0010

t7	Teff	L	LHe	LH	g	Yc	X16c	Mcc	Msh
0.000	4.0659	1.451	1.161	1.097	3.978	0.971	0.000	0.100	0.475
0.429	4.0823	1.395	1.162	0.991	4.077	0.903	0.002	0.094	0.475
1.029	4.0877	1.370	1.211	0.882	4.118	0.803	0.006	0.100	0.475
1.629	4.0882	1.367	1.239	0.774	4.151	0.701	0.013	0.100	0.475
2.179	4.0851	1.382	1.265	0.663	4.124	0.599	0.024	0.100	0.475
2.679	4.0801	1.365	1.289	0.556	4.103	0.501	0.038	0.100	0.475
3.179	4.0725	1.370	1.314	0.453	4.085	0.398	0.059	0.100	0.475
3.679	4.0626	1.385	1.340	0.357	4.013	0.288	0.089	0.100	0.475
4.079	4.0543	1.400	1.361	0.334	3.903	0.194	0.126	0.100	0.475
4.479	4.0470	1.431	1.384	0.442	3.903	0.091	0.187	0.100	0.475
4.854	3.9995	1.580	1.391	1.128	3.563	0.009	0.308	0.100	0.475

M=0.58 Mc=0.475 Y=0.2 Z=0.0010

t7	Teff	L	LHe	LH	g	Yc	X16c	Mcc	Msh
0.000	3.9734	1.499	1.160	1.253	3.555	0.971	0.000	0.100	0.475
0.425	4.0097	1.453	1.185	1.116	3.746	0.903	0.002	0.094	0.475
1.025	4.0178	1.438	1.215	1.042	3.794	0.803	0.006	0.100	0.475
1.675	4.0214	1.425	1.248	0.950	3.821	0.688	0.014	0.100	0.475
2.175	4.0214	1.419	1.273	0.875	3.827	0.593	0.024	0.100	0.475
2.675	4.0194	1.414	1.299	0.781	3.824	0.493	0.039	0.100	0.475
3.075	4.0153	1.415	1.320	0.706	3.807	0.408	0.056	0.100	0.475
3.575	4.0068	1.422	1.347	0.622	3.766	0.296	0.086	0.100	0.475
3.975	3.9974	1.436	1.369	0.591	3.714	0.200	0.122	0.100	0.475
4.375	3.9856	1.470	1.393	0.681	3.625	0.095	0.183	0.100	0.475
4.850	3.8639	1.650	1.393	1.300	2.906	0.006	0.322	0.100	0.475

M=0.60 Mc=0.475 Y=0.2 Z=0.0010

t7	Teff	L	LHe	LH	g	Yc	X16c	Mcc	Msh
0.000	3.8644	1.559	1.156	1.340	3.074	0.971	0.000	0.100	0.475
0.425	3.9243	1.511	1.184	1.234	3.362	0.903	0.002	0.094	0.475
1.025	3.9371	1.490	1.215	1.174	3.428	0.803	0.006	0.100	0.475
1.575	3.9448	1.485	1.244	1.114	3.469	0.708	0.012	0.100	0.475
2.175	3.9517	1.473	1.275	1.037	3.509	0.598	0.024	0.100	0.475
2.675	3.9542	1.465	1.303	0.950	3.527	0.496	0.039	0.100	0.475
3.175	3.9528	1.461	1.331	0.874	3.526	0.388	0.061	0.100	0.475
3.575	3.9479	1.463	1.354	0.809	3.514	0.296	0.086	0.100	0.475
3.975	3.9381	1.475	1.377	0.780	3.453	0.198	0.123	0.100	0.475
4.375	3.9151	1.512	1.400	0.869	3.323	0.090	0.186	0.100	0.475
4.825	3.7341	1.693	1.396	1.388	2.419	0.007	0.321	0.100	0.475

Table 4.15 (contd.)

M=0.50 Mc=0.475 Y=0.3 Z=0.0010

t7	Teff	L	LHe	LH	g	Yc	X16c	Mcc	Msh
0.000	4.3413	1.146	1.135	-0.456	5.315	0.971	0.000	0.101	0.475
0.475	4.3381	1.159	1.150	-0.529	5.290	0.899	0.002	0.094	0.475
1.075	4.3336	1.179	1.172	-0.617	5.252	0.805	0.005	0.100	0.475
1.775	4.3284	1.203	1.198	-0.738	5.207	0.694	0.014	0.101	0.475
2.375	4.3233	1.225	1.221	-0.813	5.165	0.594	0.025	0.101	0.475
2.975	4.3182	1.249	1.246	-0.913	5.120	0.489	0.041	0.101	0.475
3.475	4.3140	1.270	1.268	-1.068	5.082	0.396	0.061	0.101	0.475
3.975	4.3104	1.293	1.291	-1.045	5.045	0.300	0.088	0.101	0.475
4.475	4.3086	1.318	1.316	-1.020	5.013	0.197	0.128	0.101	0.475
4.875	4.3122	1.339	1.337	-0.999	5.006	0.109	0.179	0.101	0.475
5.375	4.3504	1.377	1.367	-0.266	5.120	0.009	0.316	0.101	0.475

M=0.52 Mc=0.475 Y=0.3 Z=0.0010

t7	Teff	L	LHe	LH	g	Yc	X16c	Mcc	Msh
0.000	4.2881	1.255	1.161	0.544	5.011	0.971	0.000	0.100	0.475
0.500	4.2853	1.246	1.179	0.401	5.008	0.891	0.002	0.094	0.475
1.000	4.2811	1.249	1.199	0.285	4.988	0.807	0.005	0.099	0.475
1.600	4.2753	1.259	1.223	0.160	4.955	0.705	0.012	0.100	0.475
2.200	4.2688	1.274	1.248	0.038	4.914	0.598	0.024	0.100	0.475
2.700	4.2629	1.290	1.270	-0.057	4.875	0.505	0.038	0.100	0.475
3.200	4.2569	1.308	1.292	-0.134	4.833	0.406	0.057	0.100	0.475
3.700	4.2511	1.329	1.316	-0.201	4.789	0.303	0.085	0.100	0.475
4.200	4.2472	1.353	1.342	-0.249	4.749	0.192	0.127	0.100	0.475
4.600	4.2500	1.379	1.365	-0.120	4.735	0.097	0.185	0.100	0.475
5.025	4.2784	1.464	1.387	0.675	4.763	0.009	0.314	0.100	0.475

M=0.54 Mc=0.475 Y=0.3 Z=0.0010

t7	Teff	L	LHe	LH	g	Yc	X16c	Mcc	Msh
0.000	4.2163	1.441	1.164	1.115	4.553	0.971	0.000	0.100	0.475
0.425	4.2287	1.383	1.187	0.943	4.661	0.903	0.002	0.094	0.475
1.000	4.2290	1.364	1.215	0.827	4.682	0.806	0.006	0.100	0.475
1.600	4.2257	1.358	1.242	0.728	4.674	0.702	0.013	0.100	0.475
2.100	4.2218	1.355	1.266	0.623	4.661	0.608	0.023	0.100	0.475
2.700	4.2157	1.360	1.294	0.509	4.632	0.490	0.040	0.100	0.475
3.100	4.2109	1.367	1.313	0.435	4.606	0.406	0.057	0.100	0.475
3.600	4.2044	1.382	1.339	0.356	4.565	0.296	0.086	0.100	0.475
4.000	4.2001	1.400	1.361	0.334	4.530	0.202	0.121	0.100	0.475
4.400	4.1993	1.430	1.385	0.423	4.496	0.100	0.179	0.100	0.475
4.825	4.1853	1.617	1.393	1.222	4.254	0.008	0.311	0.100	0.475

Table 4.15 (contd.)

M=0.56 Mc=0.475 Y=0.3 Z=0.0010

t7	Teff	L	LHe	LH	g	Yc	X16c	Mcc	Msh
0.000	4.1133	1.591	1.158	1.391	4.007	0.971	0.000	0.100	0.475
0.425	4.1486	1.524	1.187	1.256	4.216	0.903	0.002	0.094	0.475
1.025	4.1548	1.507	1.218	1.194	4.258	0.802	0.006	0.100	0.475
1.575	4.1589	1.490	1.247	1.122	4.291	0.706	0.013	0.100	0.475
2.175	4.1614	1.472	1.279	1.027	4.319	0.591	0.025	0.100	0.475
2.575	4.1614	1.464	1.301	0.959	4.328	0.509	0.037	0.100	0.475
3.075	4.1595	1.458	1.329	0.868	4.326	0.402	0.057	0.100	0.475
3.475	4.1562	1.460	1.352	0.803	4.310	0.310	0.081	0.100	0.475
3.875	4.1516	1.472	1.375	0.773	4.280	0.212	0.116	0.100	0.475
4.275	4.1448	1.509	1.399	0.859	4.216	0.105	0.174	0.100	0.475
4.700	4.0583	1.745	1.397	1.486	3.634	0.009	0.306	0.100	0.475

M=0.58 Mc=0.475 Y=0.3 Z=0.0010

t7	Teff	L	LHe	LH	g	Yc	X16c	Mcc	Msh
0.000	3.9992	1.680	1.152	1.527	3.477	0.971	0.000	0.100	0.475
0.425	4.0528	1.626	1.183	1.432	3.746	0.903	0.002	0.094	0.475
1.025	4.0627	1.616	1.215	1.396	3.795	0.805	0.006	0.100	0.475
1.625	4.0758	1.597	1.250	1.338	3.866	0.700	0.013	0.100	0.475
2.225	4.0877	1.576	1.285	1.265	3.936	0.587	0.026	0.100	0.475
2.625	4.0952	1.560	1.310	1.201	3.982	0.504	0.038	0.100	0.475
3.125	4.1003	1.545	1.342	1.117	4.017	0.393	0.060	0.100	0.475
3.525	4.1010	1.540	1.368	1.055	4.025	0.297	0.085	0.100	0.475
3.925	4.0971	1.550	1.393	1.032	3.999	0.194	0.123	0.100	0.475
4.325	4.0783	1.605	1.417	1.151	3.869	0.079	0.192	0.100	0.475
4.750	3.9271	1.827	1.407	1.619	3.042	0.009	0.320	0.100	0.475

M=0.60 Mc=0.475 Y=0.3 Z=0.0010

t7	Teff	L	LHe	LH	g	Yc	X16c	Mcc	Msh
0.000	3.8833	1.755	1.147	1.605	2.973	0.971	0.000	0.100	0.475
0.444	3.9521	1.693	1.180	1.534	3.290	0.901	0.002	0.094	0.475
1.031	3.9652	1.688	1.214	1.510	3.348	0.804	0.006	0.100	0.475
1.631	3.9873	1.671	1.251	1.463	3.454	0.700	0.013	0.100	0.475
2.131	4.0091	1.650	1.283	1.406	3.562	0.606	0.023	0.100	0.475
2.681	4.0300	1.624	1.321	1.325	3.672	0.491	0.040	0.100	0.475
3.081	4.0404	1.609	1.349	1.263	3.729	0.400	0.058	0.100	0.475
3.481	4.0448	1.601	1.376	1.208	3.753	0.303	0.083	0.100	0.475
3.881	4.0425	1.607	1.403	1.181	3.758	0.197	0.121	0.100	0.475
4.181	4.0258	1.640	1.422	1.236	3.639	0.110	0.169	0.100	0.475
4.531	3.9501	1.749	1.427	1.468	3.226	0.032	0.258	0.100	0.475

Table 4.15 (contd.)

M=0.62 Mc=0.475 Y=0.3 Z=0.0010

t7	Teff	L	LHe	LH	g	Yc	X16c	Mcc	Msh
0.000	3.7575	1.777	1.143	1.662	2.443	0.971	0.000	0.100	0.475
0.447	3.8538	1.736	1.178	1.595	2.868	0.901	0.002	0.094	0.475
1.072	3.8703	1.735	1.215	1.579	2.936	0.799	0.006	0.100	0.475
1.622	3.9010	1.719	1.251	1.538	3.075	0.703	0.013	0.100	0.475
2.172	3.9360	1.696	1.289	1.480	3.257	0.600	0.024	0.100	0.475
2.672	3.9610	1.676	1.323	1.421	3.358	0.499	0.039	0.100	0.475
3.222	3.9793	1.658	1.362	1.352	3.449	0.373	0.065	0.100	0.475
3.572	3.9864	1.651	1.388	1.308	3.464	0.288	0.089	0.100	0.475
3.872	3.9860	1.655	1.410	1.290	3.479	0.206	0.118	0.100	0.475
4.272	3.9610	1.691	1.431	1.345	3.342	0.105	0.178	0.100	0.475
4.772	3.7229	1.886	1.428	1.700	2.195	0.010	0.321	0.100	0.475

M=0.64 Mc=0.475 Y=0.3 Z=0.0010

t7	Teff	L	LHe	LH	g	Yc	X16c	Mcc	Msh
0.000	3.7173	1.792	1.144	1.681	2.281	0.971	0.000	0.100	0.475
0.425	3.7607	1.766	1.176	1.637	2.461	0.904	0.002	0.093	0.475
1.050	3.7700	1.770	1.213	1.629	2.513	0.803	0.006	0.100	0.475
1.625	3.8176	1.753	1.253	1.588	2.721	0.705	0.013	0.100	0.475
2.125	3.8575	1.755	1.288	1.543	2.899	0.609	0.023	0.100	0.475
2.625	3.8956	1.713	1.325	1.484	3.073	0.507	0.038	0.100	0.475
3.075	3.9196	1.697	1.359	1.450	3.165	0.409	0.057	0.100	0.475
3.525	3.9373	1.684	1.392	1.374	3.208	0.305	0.085	0.100	0.475
3.925	3.9388	1.687	1.419	1.350	3.272	0.207	0.121	0.100	0.475
4.325	3.9112	1.721	1.442	1.397	3.127	0.107	0.180	0.100	0.479
4.750	3.7284	1.864	1.446	1.655	2.253	0.018	0.301	0.100	0.479

M=0.66 Mc=0.475 Y=0.3 Z=0.0010

t7	Teff	L	LHe	LH	g	Yc	X16c	Mcc	Msh
0.000	3.6981	1.814	1.141	1.710	2.195	0.971	0.000	0.100	0.475
0.450	3.7152	1.789	1.176	1.668	2.289	0.901	0.002	0.094	0.475
1.075	3.7234	1.789	1.216	1.654	2.321	0.798	0.006	0.100	0.475
1.625	3.7448	1.776	1.255	1.620	2.420	0.702	0.013	0.100	0.475
2.150	3.7915	1.758	1.293	1.576	2.625	0.604	0.024	0.100	0.475
2.650	3.8350	1.739	1.332	1.523	2.817	0.501	0.039	0.100	0.475
3.100	3.8672	1.723	1.367	1.471	2.963	0.402	0.059	0.100	0.475
3.525	3.8790	1.718	1.399	1.434	3.015	0.305	0.085	0.100	0.478
3.950	3.8790	1.723	1.428	1.416	3.010	0.204	0.124	0.100	0.478
4.400	3.8390	1.761	1.451	1.469	2.812	0.100	0.190	0.100	0.478
4.650	3.7767	1.807	1.458	1.549	2.516	0.052	0.246	0.100	0.478

Table 4.15 (contd.)

M=0.68 Mc=0.475 Y=0.3 Z=0.0010

t7	Teff	L	LHe	LH	g	Yc	X16c	Mcc	Msh
0.000	3.6927	1.817	1.142	1.714	2.183	0.971	0.000	0.101	0.475
0.450	3.7025	1.801	1.175	1.684	2.239	0.901	0.002	0.094	0.475
1.050	3.7039	1.806	1.212	1.678	2.239	0.803	0.006	0.101	0.475
1.650	3.7169	1.793	1.256	1.644	2.305	0.700	0.013	0.101	0.475
2.175	3.7382	1.777	1.296	1.603	2.405	0.601	0.024	0.101	0.475
2.650	3.7673	1.765	1.334	1.564	2.534	0.504	0.039	0.101	0.477
3.200	3.8114	1.747	1.377	1.505	2.728	0.382	0.064	0.101	0.477
3.550	3.7935	1.757	1.398	1.507	2.647	0.295	0.087	0.101	0.477
3.900	3.7904	1.763	1.422	1.499	2.628	0.211	0.120	0.101	0.477
4.350	3.7576	1.792	1.451	1.528	2.468	0.100	0.187	0.101	0.477
4.825	3.6733	1.940	1.456	1.767	1.983	0.009	0.329	0.101	0.477

M=0.54 Mc=0.525 Y=0.3 Z=0.0100

t7	Teff	L	LHe	LH	g	Yc	X16c	Mcc	Msh
0.000	4.3582	1.302	1.301	-1.336	5.261	0.971	0.005	0.111	0.525
0.350	4.3548	1.315	1.314	-1.323	5.234	0.901	0.006	0.104	0.525
0.850	4.3491	1.339	1.338	-1.299	5.188	0.794	0.009	0.110	0.525
1.250	4.3445	1.358	1.358	0.000	5.149	0.709	0.015	0.111	0.525
1.750	4.3382	1.384	1.384	0.000	5.098	0.596	0.026	0.111	0.525
2.150	4.3328	1.407	1.406	-1.231	5.054	0.500	0.039	0.111	0.525
2.550	4.3274	1.430	1.430	0.000	5.009	0.399	0.057	0.111	0.525
2.950	4.3228	1.456	1.456	0.000	4.965	0.290	0.085	0.111	0.525
3.250	4.3211	1.477	1.477	0.000	4.937	0.202	0.116	0.111	0.525
3.550	4.3253	1.504	1.504	0.000	4.927	0.103	0.167	0.111	0.525
3.875	4.3639	1.540	1.539	-1.098	5.045	0.010	0.292	0.111	0.525
3.900	4.3705	1.543	1.542	-1.095	5.069	0.006	0.304	0.111	0.525

M=0.50 Mc=0.525 Y=0.3 Z=0.0100

t7	Teff	L	LHe	LH	g	Yc	X16c	Mcc	Msh
0.000	4.2789	1.358	1.328	0.182	4.903	0.971	0.005	0.111	0.525
0.325	4.2744	1.364	1.340	0.094	4.879	0.903	0.006	0.104	0.525
0.775	4.2666	1.380	1.363	-0.036	4.832	0.801	0.009	0.110	0.525
1.275	4.2575	1.399	1.389	-0.244	4.776	0.686	0.016	0.111	0.525
1.675	4.2492	1.417	1.410	-0.379	4.725	0.589	0.026	0.111	0.525
2.075	4.2402	1.438	1.433	-0.503	4.668	0.487	0.040	0.111	0.525
2.375	4.2331	1.455	1.451	-0.583	4.623	0.406	0.055	0.111	0.525
2.775	4.2239	1.481	1.478	-0.681	4.561	0.291	0.083	0.111	0.525
3.075	4.2185	1.503	1.501	-0.835	4.517	0.196	0.116	0.111	0.525
3.375	4.2211	1.533	1.529	-0.505	4.497	0.087	0.175	0.111	0.525
3.700	4.2603	1.598	1.561	0.510	4.589	0.006	0.306	0.111	0.525

Table 4.15 (contd.)

M=0.58 Mc=0.525 Y=0.3 Z=0.0100

t7	Teff	L	LHe	LH	g	Yc	X16c	Mcc	Msh
0.000	4.1852	1.533	1.336	1.095	4.368	0.971	0.005	0.111	0.525
0.350	4.1877	1.516	1.354	1.009	4.396	0.894	0.006	0.104	0.525
0.800	4.1876	1.498	1.381	0.871	4.413	0.789	0.009	0.110	0.525
1.200	4.1845	1.489	1.404	0.739	4.410	0.694	0.016	0.111	0.525
1.600	4.1785	1.487	1.428	0.591	4.388	0.592	0.025	0.111	0.525
2.000	4.1702	1.493	1.453	0.437	4.348	0.485	0.040	0.111	0.525
2.300	4.1624	1.502	1.473	0.312	4.308	0.399	0.056	0.111	0.525
2.700	4.1509	1.522	1.501	0.196	4.243	0.276	0.087	0.111	0.525
2.900	4.1454	1.535	1.517	0.144	4.207	0.209	0.110	0.111	0.525
3.200	4.1416	1.570	1.546	0.300	4.157	0.094	0.167	0.111	0.525
3.525	4.1184	1.743	1.567	1.266	3.891	0.008	0.297	0.111	0.525
3.525	4.1184	1.743	1.567	1.266	3.891	0.008	0.297	0.111	0.525

M=0.60 Mc=0.525 Y=0.3 Z=0.0100

t7	Teff	L	LHe	LH	g	Yc	X16c	Mcc	Msh
0.000	4.0252	1.697	1.332	1.452	3.579	0.971	0.005	0.111	0.525
0.325	4.0337	1.691	1.350	1.427	3.620	0.901	0.006	0.104	0.525
0.775	4.0494	1.673	1.380	1.364	3.700	0.801	0.009	0.110	0.525
1.225	4.0677	1.644	1.410	1.264	3.802	0.697	0.016	0.111	0.525
1.625	4.0810	1.617	1.439	1.144	3.882	0.594	0.026	0.111	0.525
2.025	4.0870	1.596	1.469	1.000	3.928	0.482	0.041	0.111	0.525
2.325	4.0865	1.588	1.492	0.885	3.933	0.392	0.057	0.111	0.525
2.625	4.0818	1.590	1.516	0.785	3.913	0.295	0.081	0.111	0.525
2.925	4.0733	1.605	1.541	0.742	3.864	0.188	0.117	0.111	0.525
3.125	4.0635	1.634	1.561	0.824	3.795	0.105	0.158	0.111	0.525
3.438	3.9204	1.866	1.576	1.554	2.991	0.009	0.287	0.111	0.525

M=0.62 Mc=0.525 Y=0.3 Z=0.0100

t7	Teff	L	LHe	LH	g	Yc	X16c	Mcc	Msh
0.000	3.8165	1.784	1.328	1.597	2.672	0.971	0.005	0.111	0.525
0.325	3.8227	1.788	1.346	1.593	2.693	0.902	0.006	0.104	0.525
0.800	3.8583	1.776	1.381	1.552	2.847	0.797	0.009	0.111	0.525
1.200	3.9104	1.746	1.412	1.476	3.085	0.704	0.015	0.111	0.525
1.600	3.9506	1.715	1.444	1.382	3.277	0.604	0.025	0.111	0.525
2.050	3.9807	1.683	1.481	1.253	3.430	0.482	0.042	0.111	0.525
2.350	3.9906	1.668	1.506	1.161	3.484	0.389	0.059	0.111	0.525
2.650	3.9942	1.661	1.532	1.071	3.506	0.287	0.083	0.111	0.525
2.900	3.9859	1.671	1.554	1.044	3.463	0.196	0.114	0.111	0.525
3.200	3.9607	1.711	1.577	1.135	3.321	0.098	0.172	0.111	0.525
3.600	3.6900	1.932	1.589	1.669	2.017	0.010	0.313	0.111	0.525

Table 4.15 (contd.)

M=0.64 Mc=0.525 Y=0.3 Z=0.0100

t7	Teff	L	LHe	LH	g	Yc	X16c	Mcc	Msh
0.000	3.6450	1.826	1.326	1.661	1.957	0.971	0.005	0.111	0.525
0.337	3.6433	1.836	1.345	1.667	1.941	0.900	0.006	0.104	0.525
0.788	3.6599	1.828	1.379	1.637	2.015	0.802	0.009	0.111	0.525
1.237	3.7267	1.802	1.416	1.572	2.309	0.699	0.016	0.111	0.525
1.662	3.7910	1.775	1.451	1.496	2.593	0.594	0.026	0.111	0.525
2.012	3.8339	1.752	1.480	1.420	2.787	0.501	0.039	0.111	0.525
2.375	3.8608	1.735	1.509	1.343	2.912	0.402	0.058	0.111	0.525
2.725	3.8752	1.724	1.536	1.270	2.980	0.303	0.084	0.111	0.525
3.063	3.8701	1.730	1.562	1.236	2.954	0.203	0.121	0.111	0.525
3.350	3.8401	1.763	1.587	1.286	2.800	0.104	0.178	0.111	0.525
3.637	3.6962	1.868	1.600	1.531	2.120	0.031	0.268	0.111	0.525

M=0.66 Mc=0.525 Y=0.3 Z=0.0100

t7	Teff	L	LHe	LH	g	Yc	X16c	Mcc	Msh
0.000	3.6141	1.831	1.325	1.669	1.842	0.971	0.005	0.111	0.525
0.325	3.6129	1.840	1.345	1.673	1.828	0.902	0.006	0.104	0.525
0.775	3.6184	1.837	1.379	1.651	1.854	0.804	0.009	0.111	0.525
1.225	3.6370	1.814	1.417	1.592	1.951	0.702	0.016	0.111	0.525
1.638	3.6552	1.796	1.451	1.535	2.042	0.601	0.026	0.111	0.525
2.025	3.6977	1.775	1.484	1.460	2.235	0.501	0.040	0.111	0.525
2.563	3.7461	1.753	1.531	1.355	2.449	0.345	0.071	0.111	0.528
2.713	3.7586	1.748	1.544	1.322	2.504	0.300	0.084	0.111	0.528
3.037	3.7546	1.753	1.570	1.289	2.483	0.202	0.120	0.111	0.528
3.365	3.7127	1.784	1.594	1.333	2.284	0.105	0.178	0.111	0.528
3.525	3.6658	1.822	1.604	1.418	2.058	0.060	0.223	0.111	0.528

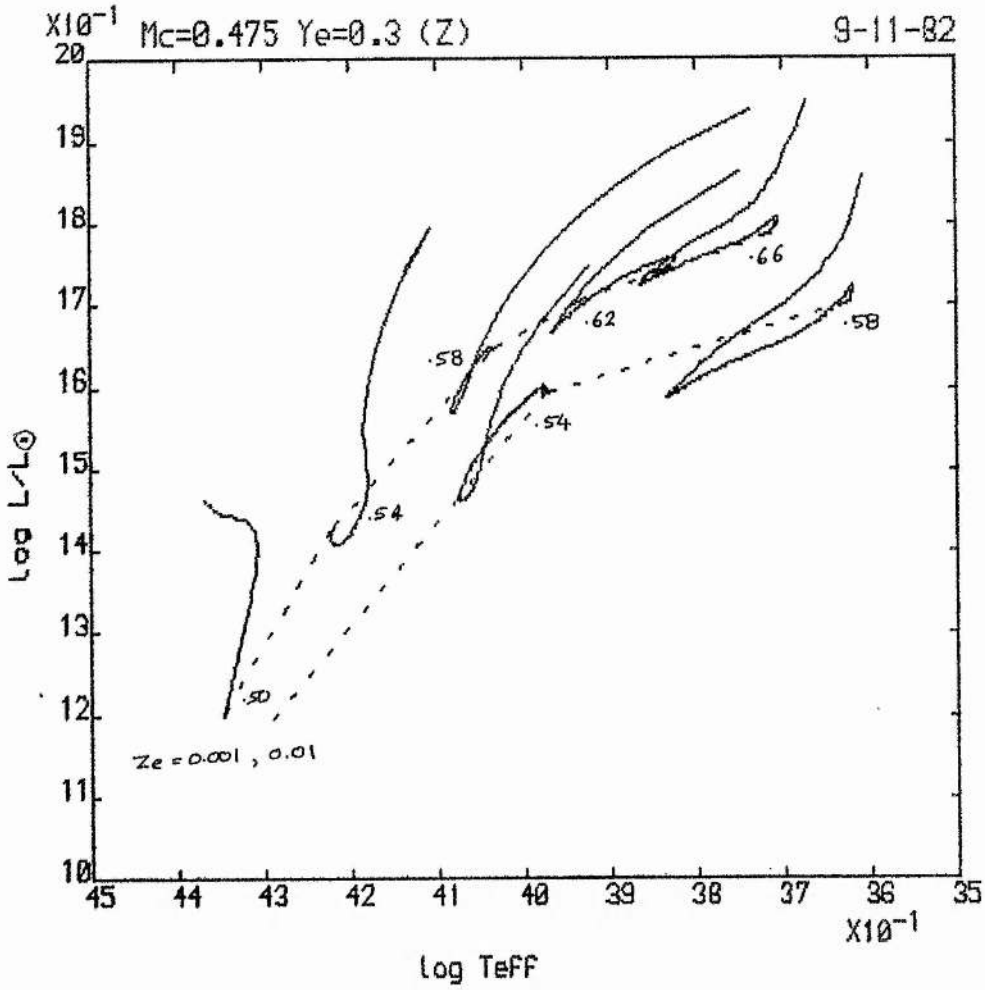

Figure 4.7 Evolutionary tracks for HB stars (Z), the ZAHB is shown as a dotted line. Evolutionary tracks are stopped when Y = 0.01. Model parameters are given in the diagram.

Figure 4.8 Evolutionary tracks for HB stars (W) with increased core opacities and initially carbon-enriched hydrogen shells. Following fig.4.7, parameters for each set of models are given in the appropriate diagram, but only one mass is given. All other masses differ by 0.02 M along the sequence. Some evolutionary tracks are calculated beyond core-helium exhaustion.

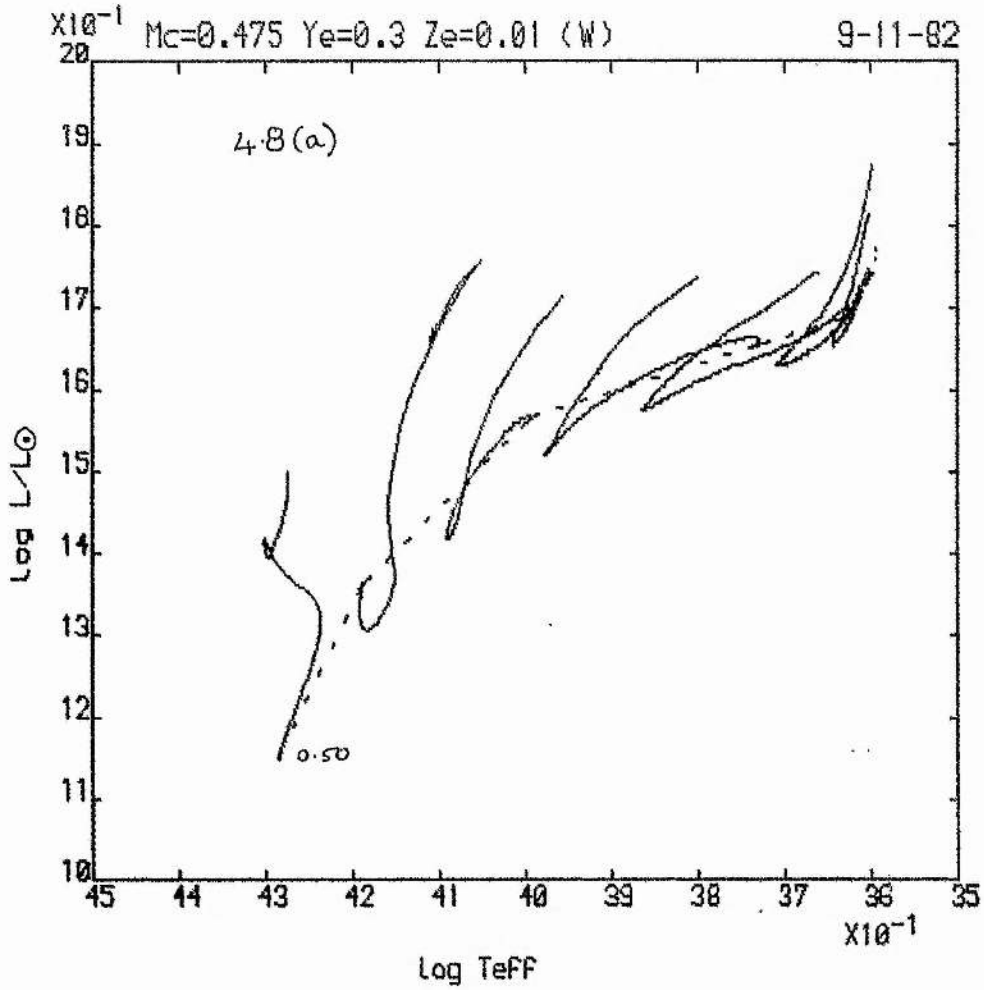
X10⁻¹ Mc=0.475 Ye=0.3 Ze=0.01 (W) 9-11-82
4.8(a)
0.50
Log L/L⊙
Log TeFF
X10⁻¹

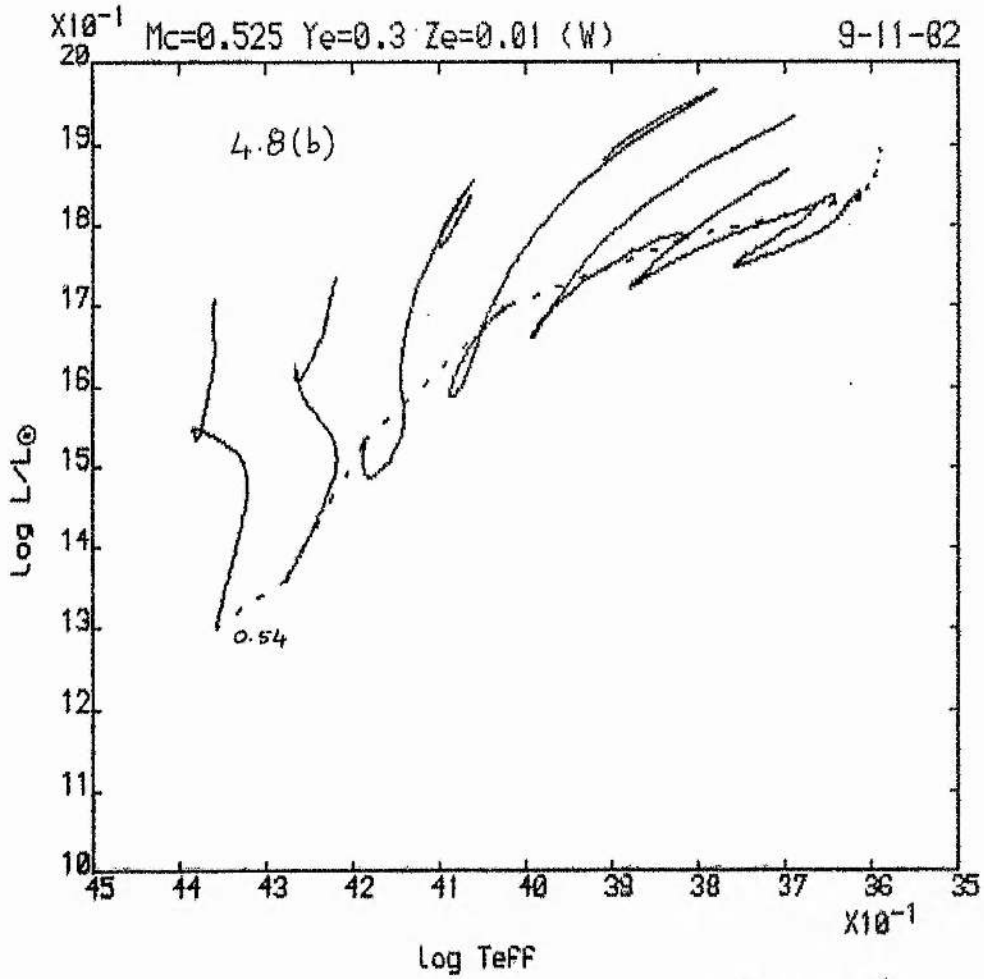
X10⁻¹ Mc=0.525 Ye=0.3 Ze=0.01 (W) 9-11-82
4.8(b)
0.54
Log L/L⊙
Log TeFF
X10⁻¹

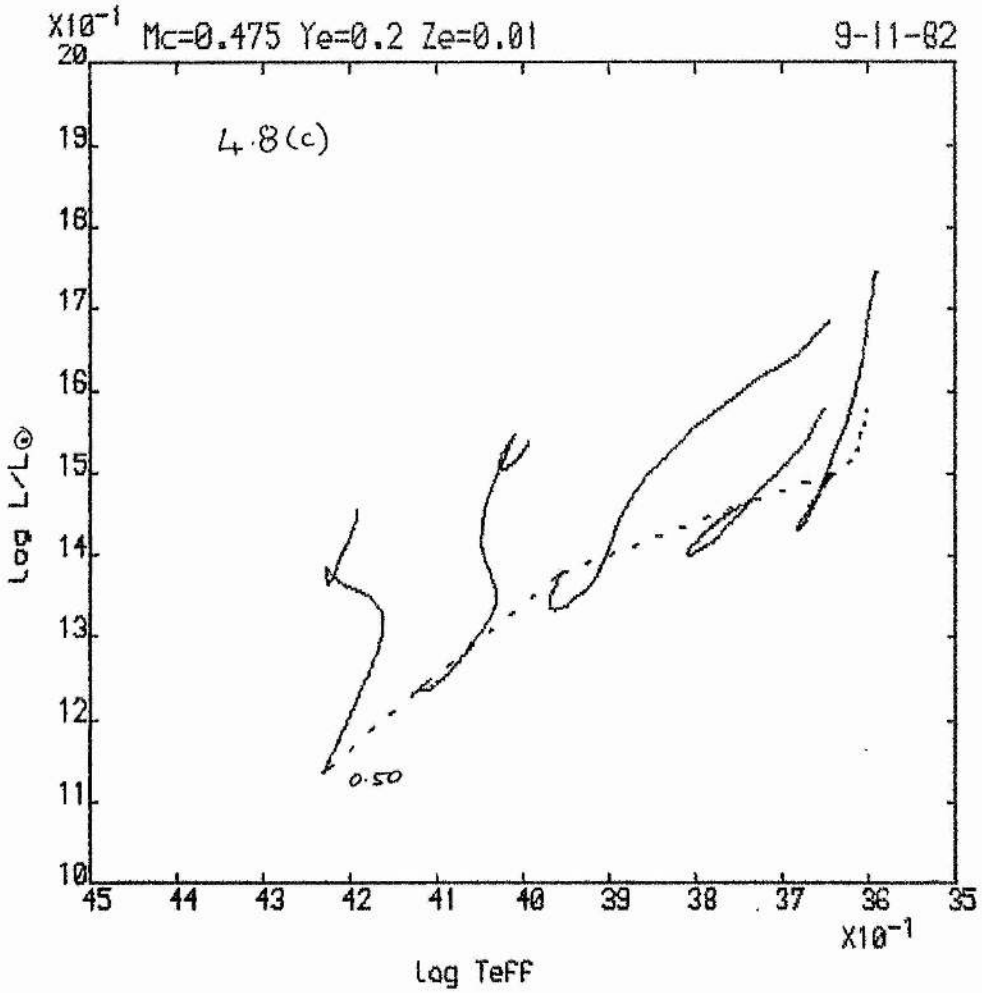
X10⁻¹
Mc=0.475 Ye=0.2 Ze=0.01
9-11-82
4.8(c)
Log L/L⊙
0.50
Log TeFF
X10⁻¹

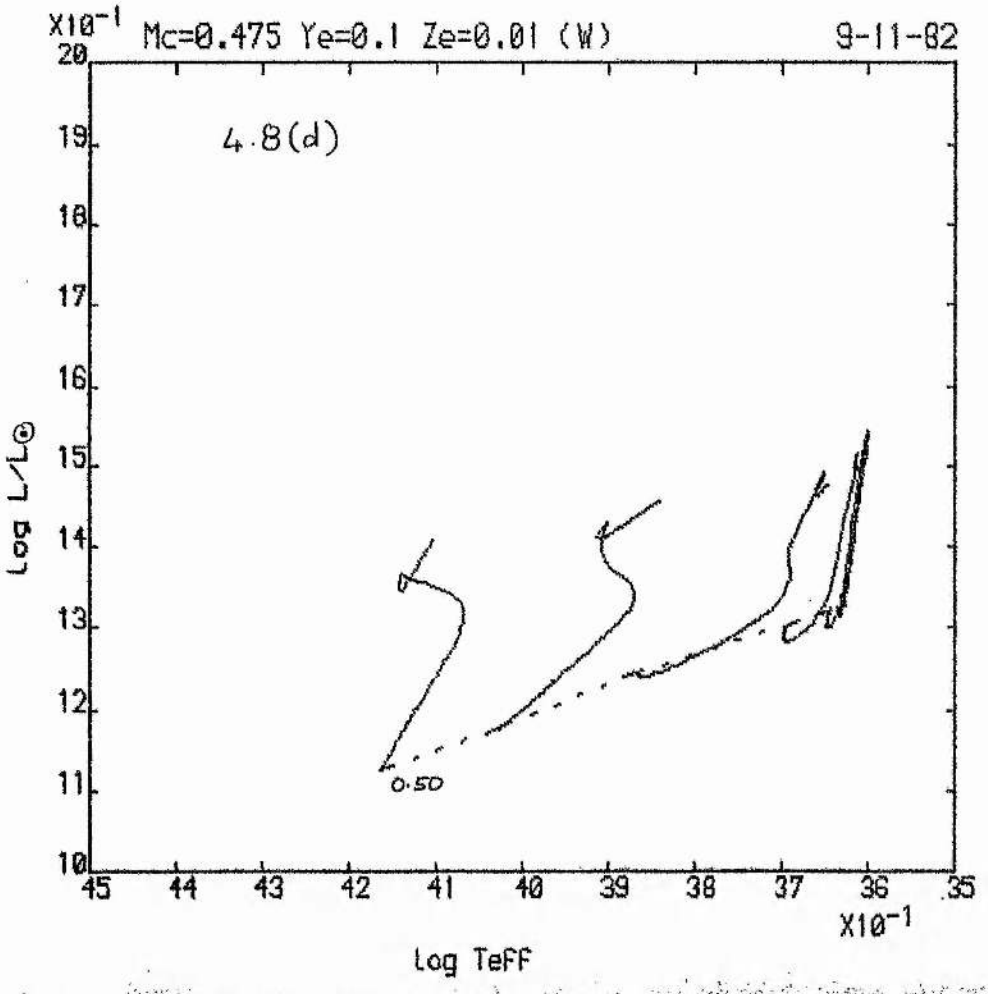
X10⁻¹
Mc=0.475 Ye=0.1 Ze=0.01 (W)
9-11-82
4.8(d)
Log L/L⊙
0.50
Log TeFF
X10⁻¹

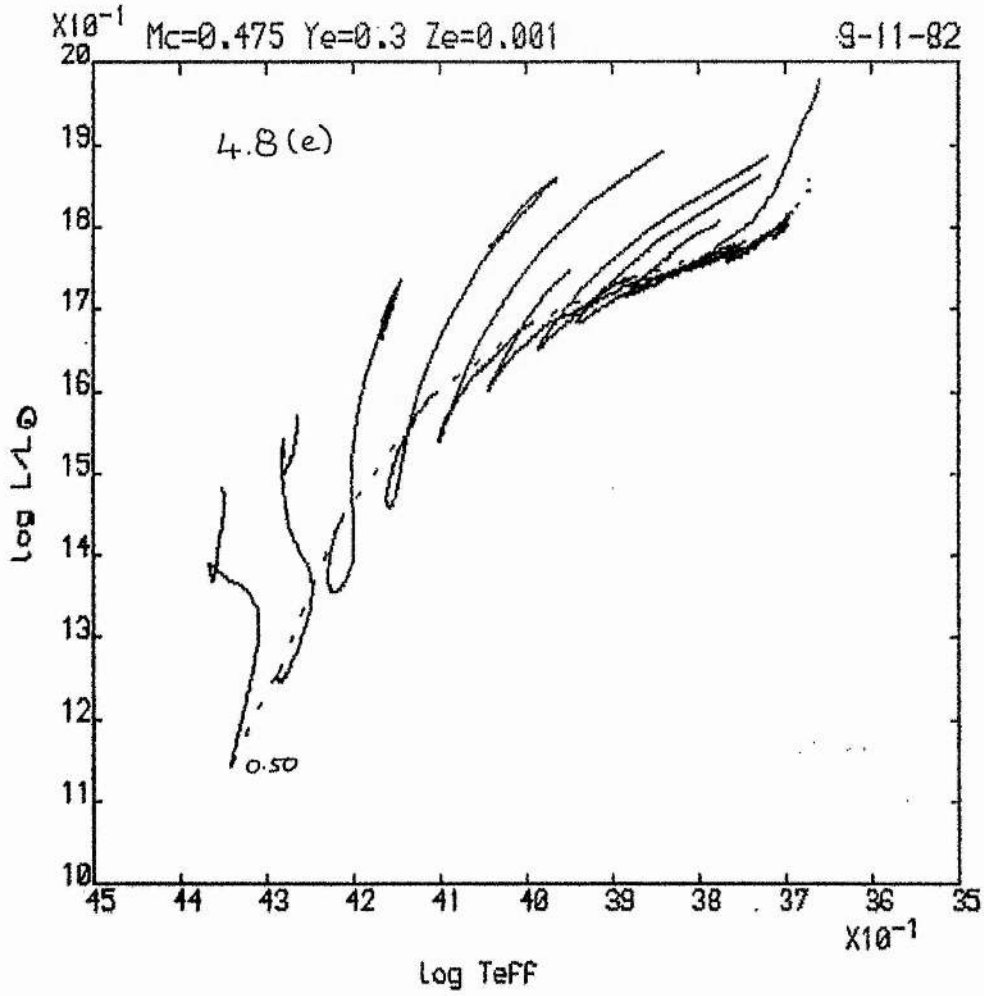
X10⁻¹ Mc=0.475 Ye=0.3 Ze=0.001 9-11-82
4.8(e)
Log L/L⊙
0.50
Log TeFF
X10⁻¹

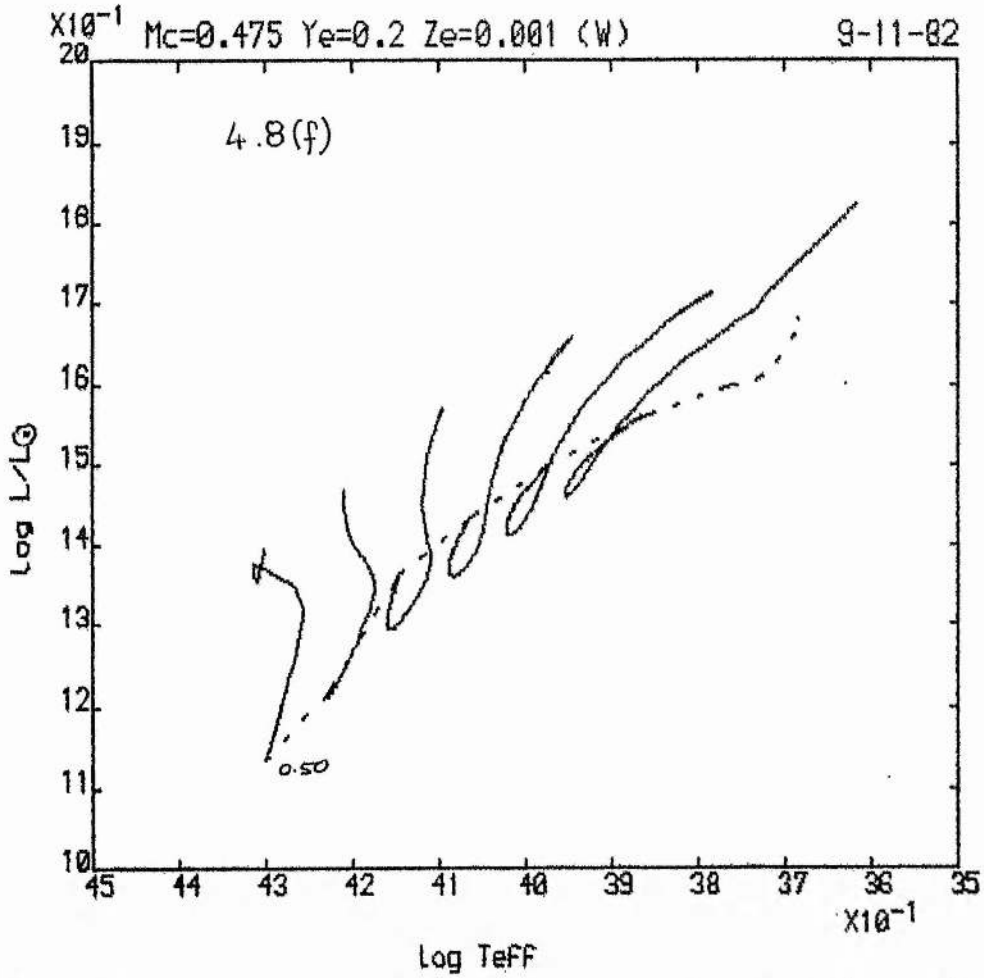
X10⁻¹ Mc=0.475 Ye=0.2 Ze=0.001 (W) 9-11-82
4.8(f)
Log L/L⊙
0.50
Log TeFF
X10⁻¹

5 STUDIES OF MAIN-SEQUENCE STARS

5.1 INTRODUCTION

The quantity of theoretical work published on the structure and evolution of main-sequence stars is considerable. For a wider discussion of theoretical and observational results the reader is referred to review papers by Iben (1967, 1974) and references therein.

Extensive calibrations of evolutionary tracks for hydrogen-burning phases have been made most recently by Mengel, Sweigart, Demarque and Gross (1979) and Hejlesen (1980). These calibrations are useful both as tools for the study of observational data for star-clusters (Iben, 1967) and (in the current study) as comparison models for the investigation of new input physics. Parsian, Refsdal and Stabell(1974) and Stabell (1975) investigate the influence of the opacity values and mixing-length on main-sequence stars, finding that 1) increased opacities anywhere in a main-sequence star lead to a decreased luminosity and effective temperature, especially when the opacity increase occurs in the hotter ($\log T > 6.5$) part of the star, 2) the slope of the main-sequence is unaffected by changes to the opacity data, but is influenced by the ratio of the mixing length to pressure scale height l/H_p , 3) an increase in the opacity throughout the star leads to an increase in the evolutionary timescale (for population II stars), but the change in the ZAMS position cancels out this effect when isochrones are constructed., 4) the value of l/H_p does influence the position of the isochrones leading to an uncertainty in the estimated age of M15, based on the position of the main-sequence turn-off point, of approximately 10% due to the uncertainty in the value of the mixing-length alone.

In the following sections we address three aspects of stellar structure and evolution in main-sequence stars.

1) Stothers (1974a) compares the structure of ZAMS models based on the Cox-Stewart (1965) and Carson opacities. He uses compositions $(X_e, Z_e) = (0.739, 0.021)$ and $(X_e, Z_e) = (0.602, 0.044)$ for models with

masses $1 \leq M/M_{\odot} \leq 120$. Differences between models based on the two sets of opacities are found to be similar to those produced by choosing a different interpolation procedure in the opacity tables. Assuming that the 'true' opacity lies between the Cox-Stewart and Carson opacities, this result implies that any significant uncertainty in the structure of the ZAMS is not due to errors in the opacity. We re-examine this claim, and extend the study to lower metallicities and lower masses, comparing the opacity uncertainty with the uncertainty in the treatment of convective envelopes.

2) In view of the sensitivity of hydrogen-burning shells to the opacity found for horizontal branch stars in chapter 4 we re-examine the evolution of main-sequence stars using the Carson opacities.

3) Gimenez and Garcia-Pelayo (1982) re-examine observations of the apsidal motion constant k_2 for a large number of eclipsing binary systems. They find a correlation between changes in k_2 and the surface gravity g during m-s evolution which indicates a marginal preference for theoretical values of k_2 for models constructed with the Carson opacities. We calculate k_2 during evolutionary sequences for a larger range in mass and composition than hitherto attempted in order to assess these results.

In the course of these studies a number of features with important consequences for the theory of hydrogen-burning stars have been established but for which time is not available for a full investigation to be undertaken. These features are noted at the appropriate points in the following discussion

5.2 ZERO-AGE MAIN-SEQUENCE MODELS

The zero-age main-sequence models have been calculated with the Henyey code described in chapter 2, and with the input physics described in chapter 3. The zero-age star is assumed to have a homogeneous composition and the CNO abundances in hydrogen-burning zones are assumed to be in equilibrium. The compositions and mixing-lengths used are described with the models in table 5.2

In an attempt to determine the effect of using the Carson opacities in the zero-age models, the Stellingwerf (1975) opacity formula was used to construct 3 ZAMS models (J82St). These are compared in table 5.1 and figure 5.1 with models constructed by Hejlesen (1980) (He80) using identical physics except in the opacity, and by Iben (1965) (Ib65) using much earlier physics. Using the Cox-Stewart (1965) opacity tables, Stothers (1974a) finds that the interpolation method (linear and quadratic interpolation, and an analytic fit to the tables are compared) leads to differences, $\delta \log T_{eff}$ and $\delta \log L$, between the resulting stellar models of the same order of magnitude as the choice of opacity table. The Stellingwerf opacity formula is an analytic fit based on the Cox and Tabor (1976) opacity tables. Hejlesen uses linear interpolation in the Cox-Stewart (1969) opacity tables with an increased grid-point density. In view of Stothers' findings and the different versions of the Los Alamos opacities used, the agreement between the models J82St and He80 is more fortunate than remarkable. We do not have enough data to study the sensitivity of the ZAMS to the method of opacity interpolation in the current programme. The significant difference ($\delta \log T_{eff}$, $\delta \log L$) found for models constructed with the Carson opacities (J82) may therefore be due partly to the interpolation method chosen. After Parsian et al (1974) we expect the higher Carson opacities to lead to some decrease in the luminosity and effective temperature.

Table 5.2 contains details of the ZAMS models constructed. Models are grouped according to their initial composition. For one composition (Xe = 0.7, Ze = 0.02) a number of values for the mixing length to pressure scale height l/H_p have been used. Columns (1-5) contain the stellar

Table 5.1 A comparison of main-sequence models using different input physics for composition (X = 0.708, Z = 0.02) and masses (3, 5, 9, 15) $M_\odot$. The first (Ib 65) models are from Iben (1965), the second (He 80) are interpolated from Hejlesen (1980). The remaining two sets are from the present study, using 1) the Stellingwerf analytic opacity formula (J82St) and 2) the Carson opacity data (J82Ca). The models are also shown in figure 5.1.

	Model							
	Ib65		He80		J82St		J82Ca	
Mass/$M_\odot$	log Teff	log $L/L_\odot$	log Teff	log $L/L_\odot$	log Teff	log $L/L_\odot$	log Teff	log $L/L_\odot$
3	4.14	1.97	4.116	1.968	4.109	1.897	4.091	1.901
5	4.29	2.80	4.254	2.776	4.256	2.767	4.226	2.724
9	4.41	3.65	4.394	3.624	4.397	3.643	4.360	3.595
15	4.51	4.32	-		-		4.457	4.282

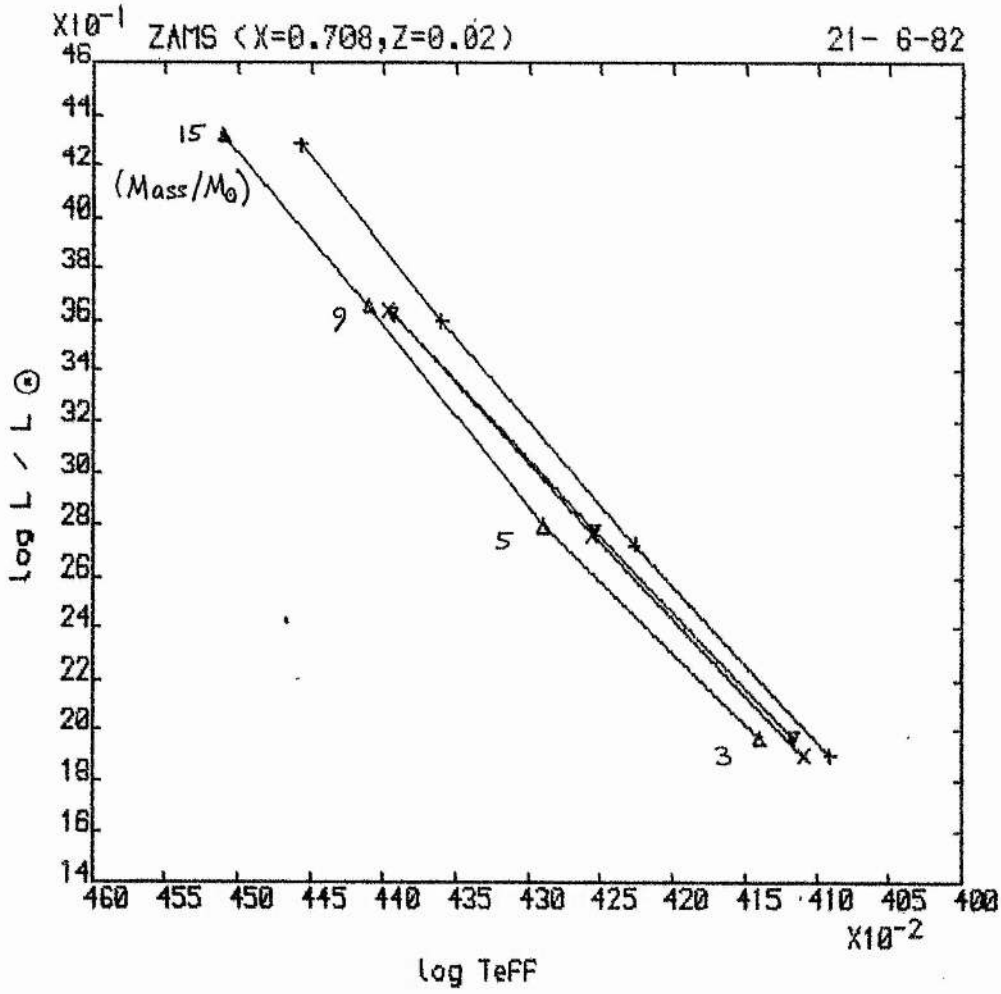

Figure 5.1 A comparison of the ZAMS models described in table 5.1, constructed with different sets of input physics.

Δ	Iben	1965	
∇	Hejlesen	1980	
×	Jeffery	1982	(Stellingwerf opacity)
+	Jeffery	1982	(Carson opacity)

The compositions used for MS models are given in the appropriate diagrams.

Table 5.2 Zero-age main-sequence models constructed with the Carson opacities. The models are grouped according to 1) hydrogen abundance, 2) metallicity abundance and 3) the treatment of convection. The contents of each column are described in the text.

M* (1)	log Teff (2)	log L (3)	log g (4)	log k2 (5)	Mcenv Mcc(*) (6)	Teff' (7)	L' (8)	d Te (9) (11)	d L (10) (12)
X=0.7 Z=0.0040			1/Hp=2						
0.50	3.6188	-1.212	4.784	-1.117	0.451	3.6374	-1.153	-0.0537	-0.059
1.00	3.8424	0.213	4.225	-1.936	0.004*	3.8382	0.2496	0.0042	-0.037
2.00	4.0829	1.456	4.574	-1.983	0.326*	4.0891	1.495	-0.0062	-0.040
5.00	4.3098	2.881	4.455	-1.870	1.340*	4.3247	2.893	-0.0148	-0.012
8.00	4.4054	3.536	4.386	-1.828	2.520*	4.4282	3.551	-0.0228	-0.015
10.00	4.4475	3.832	4.355	-1.813	3.450*	4.4717	3.848	-0.0242	-0.016
X=0.7 Z=0.0100			1/Hp=2						
0.50	3.5907	-1.342	4.801	-1.020	0.408	3.6172	-1.239	-0.0266	-0.103
0.60	3.6459	-0.989	4.748	-1.162	0.529	3.6499	-0.9101	-0.0400	-0.079
0.70	3.7009	-0.673	4.719	-1.268	0.642	3.6995	-0.595	0.0014	-0.078
0.80	3.7509	-0.394	4.699	-1.360	0.754	3.7746	-0.315	-0.0002	-0.078
1.00	3.8049	0.059	4.558	-1.747	0.993	3.8103	0.146	-0.0054	-0.087
1.40	3.9054	0.734	4.431	-2.128	0.091*	3.9199	0.804	-0.0145	-0.070
1.70	3.9715	1.067	4.447	-2.177	0.213*	3.9926	1.147	-0.0211	-0.080
2.00	4.0230	1.346	4.445	-2.145	0.288*	4.0460	1.420	-0.0230	-0.074
2.50	4.0883	1.719	4.429	-2.103	0.455*	4.1121	1.783	-0.0238	-0.064
3.00	4.1384	2.017	4.411	-2.070	0.651*	4.1622	2.070	-0.0238	-0.053
3.20	4.1558	2.121	4.405	-2.059	0.698*	4.1794	2.171	-0.0236	-0.050
4.00	4.2125	2.472	4.377	-2.025	0.940*	4.2371	2.514	-0.0246	-0.042
5.00	4.2661	2.814	4.347	-1.996	1.085*	4.2923	2.848	-0.0262	-0.034
6.00	4.3074	3.081	4.324	-1.972	1.608*	4.3355	3.115	-0.0281	-0.034
7.00	4.3410	3.303	4.304	-1.955	1.988*	4.3708	3.336	-0.0298	-0.022
8.00	4.3691	3.491	4.286	-1.942	2.400*	4.4017	3.523	-0.0326	-0.032
9.00	4.3931	3.653	4.270	-1.933	2.400*	4.4254	3.683	-0.0323	-0.030
10.00	4.4139	3.796	4.257	-1.926	3.300*	4.4477	3.826	-0.0338	-0.030
12.00	4.4483	4.037	4.233	-1.918	4.320*				
15.00	4.4874	4.319	4.204	-1.916	6.210*				
18.00	4.5166	4.538	4.181	-1.920	8.136*				
20.00	4.5323	4.660	4.167	-1.926	9.520*				
22.00	4.5455	4.767	4.154	-1.934	10.714*				
25.00	4.5619	4.906	4.137	-1.949	13.000*				
30.00	4.5826	5.095	4.110	-1.979	16.560*				
40.00	4.6076	5.373	4.057	-2.060	25.000*				
50.00	4.6209	5.573	4.006	-2.152	34.300*				
60.00	4.6271	5.728	3.956	-2.254	43.500*				
70.00	4.6288	5.853	3.905	-2.361	53.200*				
80.00	4.6267	5.957	3.850	-2.479	62.400*				
90.00	4.6227	6.046	3.796	-2.596	71.910*				
100.00	4.6170	6.123	3.742	-2.714	81.600*				

Table 5.2 (contd.)

M* (1)	log Teff (2)	log L (3)	log g (4)	log k2 (5)	Mcenv Mcc(*) (6)	Teff' (7)	L' (8)	d Te (9) (11)	d L (10) (12)
X=0.8 Z=0.0100			1/Hp=2						
0.50	3.5352	-1.569	4.806	-0.936	0.386				
1.00	3.7552	-0.194	4.613	-1.503	0.976				
2.00	3.9753	1.151	4.448	-2.156	0.212*				
3.20	4.1152	1.936	4.427	-2.062	0.640*				
5.00	4.2299	2.640	4.376	-1.986	1.175*				
8.00	4.3363	3.330	4.316	-1.923	2.272*				
10.00	4.3826	3.641	4.286	-1.902	3.150*				
12.00	4.4184	3.888	4.262	-1.890	4.140*				
X=0.6 Z=0.0200			1/Hp=2						
0.50	3.6145	-1.210	4.764	-1.120	0.436				
1.00	3.8236	0.192	4.499	-1.915	0.998				
2.00	4.0239	1.441	4.353	-2.203	0.326*				
5.00	4.2703	2.931	4.247	-2.072	1.175*				
10.00	4.4204	3.926	4.152	-2.037	3.450*				
X=0.7 Z=0.0200			1/Hp=2						
0.50	3.5572	-1.467	4.792	-0.979	0.386	3.5999	-1.323	-0.0427	-0.144
0.63	3.6200	-1.041	4.718	-1.160	0.549	3.6334	-0.942	-0.0133	-0.099
0.80	3.6956	-0.559	4.642	-1.370	0.750	3.7057	-0.454	-0.0101	-0.105
1.00	3.7727	-0.089	4.577	-1.592	0.976	3.7795	0.018	-0.0068	-0.107
								-0.042	-0.090
1.30	3.8375	0.451	4.410	-2.118	0.029*	3.8489	0.558	-0.0114	-0.107
1.70	3.9223	0.944	4.373	-2.235	0.180*	3.9463	1.050	-0.0240	-0.106
2.00	3.9751	1.228	4.370	-2.203	0.250*	4.0009	1.327	-0.0258	-0.099
								0.001	-0.016
3.20	4.1128	2.023	4.331	-2.121	0.640*	4.1404	2.095	-0.0276	-0.072
5.00	4.2294	2.739	4.275	-2.060	1.175*	4.2599	2.791	-0.0305	-0.052
								-0.001	0.002
8.00	4.3382	3.441	4.212	-2.017	2.272*	4.3745	3.486	-0.0363	-0.045
10.00	4.3849	3.757	4.181	-2.011	3.150*	4.4243	3.797	-0.0394	-0.040
								-0.010	0.006
12.00	4.4202	4.004	4.153	-2.014	4.320*				

Table 5.2 (contd.)

M* (1)	log Teff (2)	log L (3)	log g (4)	log k2 (5)	Mcenv Mcc(*) (6)	Teff' (7)	L' (8)	d Te (9) (11)	d L (10) (12)
X=0.7 Z=0.0200		1/Hp=2(BV)							
0.50	3.5579	-1.466	4.793	-0.978	0.386			-0.0007	-0.001
0.80	3.6858	-0.567	4.611	-1.422	0.758			0.0098	0.008
1.00	3.7532	-0.094	4.504	-1.737	0.989			0.0195	0.005
X=0.7 Z=0.0200		1/Hp=1.5							
0.50	3.5559	-1.469	4.789	-0.983	0.386			0.0013	0.002
0.63	3.6167	-1.046	4.709	-1.172	0.549			0.0033	0.005
0.80	3.6876	-0.566	4.617	-1.412	0.754			0.0080	0.007
1.00	3.7598	-0.093	4.529	-1.686	0.985			0.0129	0.004
1.30	3.8288	0.451	4.375	-2.205	0.029*			0.0087	0.000
1.70	3.9221	0.944	4.372	-2.236	0.180*			0.0002	0.000
X=0.7 Z=0.0200		1/Hp=1							
0.50	3.5533	-1.475	4.784	-0.989	0.391			0.0187	0.008
0.63	3.6098	-1.055	4.691	-1.198	0.556			0.0102	0.014
0.80	3.6771	-0.573	4.582	-1.472	0.766			0.0185	0.006
1.00	3.7379	-0.096	4.445	-1.865	0.996			0.0348	0.007
1.30	3.8221	0.451	4.348	-2.272	0.029*			0.0154	0.000
1.70	3.9221	0.944	4.372	-2.236	0.180*			0.0002	0.000
X=0.7 Z=0.0400		1/Hp=2							
0.50	3.5310	-1.590	4.811	-0.887	0.320				
1.00	3.7140	-0.296	4.550	-1.512	1.000				
1.30	3.8001	0.281	4.430	-1.904	1.296				
2.00	3.9202	1.090	4.290	-2.260	0.192*				
5.00	4.1832	2.633	4.196	-2.172	1.000*				
10.00	4.3466	3.697	4.086	-2.128	3.150*				

mass, effective temperature, luminosity, surface gravity and the apsidal motion constant k_2. Column (6) indicates the mass within the base of the convective envelope or within the convective core (only one model was found to have both). Columns (7-8) give the effective temperature and luminosity for a star with the same mass and composition interpolated in Hejlesen's (1980) results, where appropriate. Columns (9-10) give the differences

$$\begin{aligned} \delta \log T_{eff} &= \log T_{eff}(C) - \log T_{eff}(CS) \\ \delta \log L &= \log L(C) - \log L(CS) \end{aligned} \qquad (5\text{-}1)$$

where C indicates our models calculated with Carson opacities and CS indicates the Hejlesen models constructed with Cox-Stewart opacities. For the composition (Xe = 0.7, Ze = 0.02) the differences obtained by Stothers (1974a) for (Xe = 0.739, Ze = 0.021) are also given for comparison. For those models in which $l/H_p \neq 2$, columns (9-10) show the differences

$$\begin{aligned} \delta \log T_{eff}^{X} &= \log T_{eff}(2) - \log T_{eff}(l/H_p) \\ \delta \log L^{X} &= \log L(2) - \log T_{eff}(l/H_p) \end{aligned} \qquad (5\text{-}2)$$

where l/H_p is the appropriate value for the mixing-length ratio, or represents an alternative treatment of the mixing length theory.

For $12 > M/M_\odot > 2$ we obtain the same results as Stothers (1974), namely that $|\delta \log T_{eff}|$ increases as M increases. Table 5.3 compares the gradients

$$\left[\frac{\log L(10 M_\odot) - \log L(5 M_\odot)}{\log T_{eff}(10 M_\odot) - \log T_{eff}(5 M_\odot)}\right]_{ZAMS}$$

for a number of compositions. The result indicated is an increase in the gradient of the ZAMS when our opacity treatment is used. This feature is not anticipated by Parsian et al (1974).

Figure 5.2 compares luminosities and effective temperatures for our models with the Hejlesen (1980) models for the composition (Xe = 0.7, Ze = 0.02) and $l/Hp = 2$. Table 5.2 also demonstrates a marked change in the difference between the two sets of models at a mass of $\sim 1.5\ M_\odot$. This change roughly

Table 5.3 The gradient of the ZAMS as a function of composition for $10 > M/M_{\odot} > 5$. Data for Cox-Stewart (CS) opacities are taken from Hejlesen (1980). Gradients obtained by Stothers (1974a) are also given for one composition (S).

Ye	0.7	0.7	0.7	0.7	0.6	0.739 (S)
Ze	0.004	0.01	0.02	0.04	0.02	0.021
$\frac{\delta \log L\ (C)}{\delta \log Teff}$	5.76	6.65	6.54	6.51	6.63	6.50
$\frac{\delta \log L\ (CS)}{\delta \log Teff}$	7.73	6.29	6.12	5.76	6.17	6.09

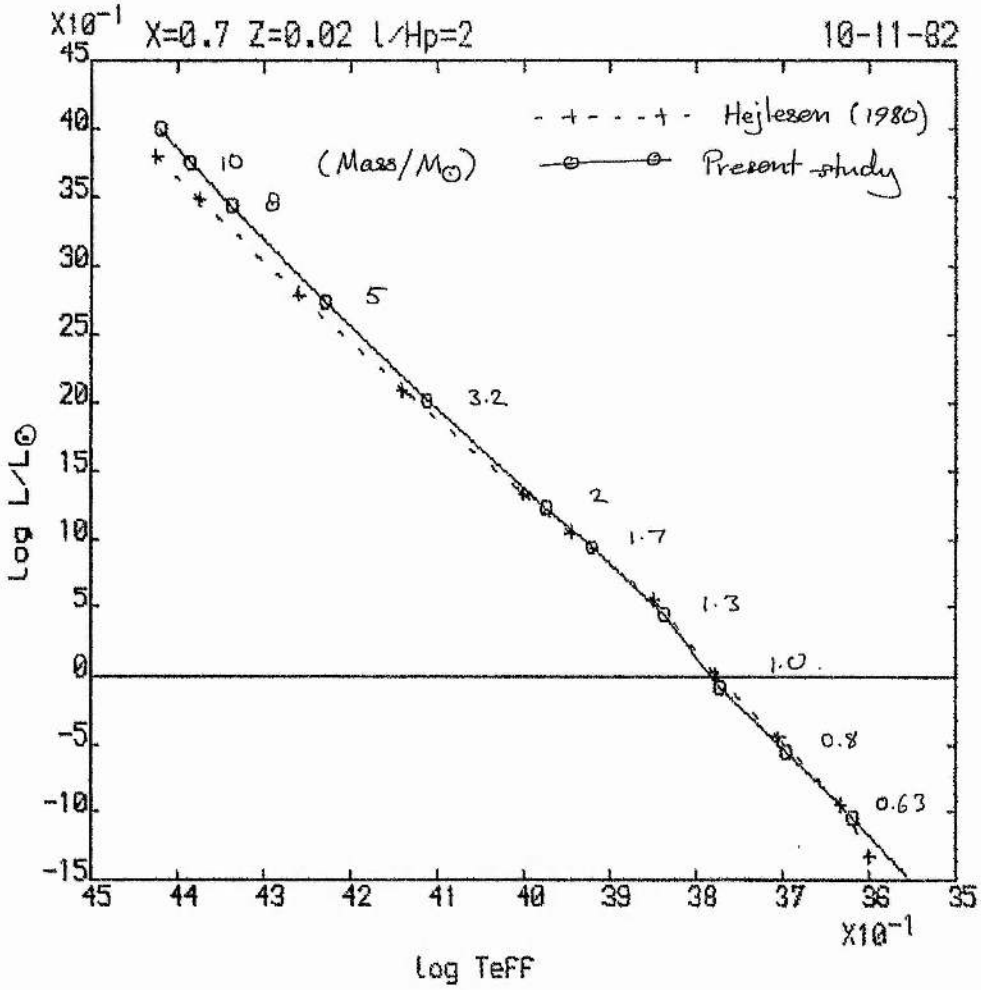

Figure 5.2 A comparison of ZAMS models constructed with Carson opacities (circles) in the current study with models constructed with Cox-Stewart opacities (crosses).
(Hejlesen, 1980).

coincides with a division between those stars having convective cores and radiative envelopes and those stars with radiative cores and convective envelopes. Parsian et al (1974) find that in addition to the strong opacity dependence for $\log T > 6.5$, main-sequence models for low-mass stars are sensitive to opacity changes at $\log T < 3.9$. For $\log T < 3.9$ we adopt the Christy (1966) analytic fit to the Cox-Stewart (1965) opacity tables which will tend to increase the luminosity and effective temperature of the models by acting in opposition to the effect of using Carson opacities in the interior. A change in the behaviour of $\delta \log L$, $\delta \log T_{eff}$ is therefore anticipated for low-mass stars. For $M \lesssim 0.7\ M_\odot$, uncertainties in the treatment of convection in the stellar atmosphere and envelope lead to very poor agreement between the models.

Stothers (1976c) studies the use of Carson opacities in luminous blue stars. For massive stars ($M \gtrsim 10\ M_\odot$) envelope densities are low and therefore the Carson opacities are large in the CNO ionisation zone. Stothers finds two effects not found with Cox-Stewart opacities; 1) the envelope structure becomes distended and giant-like; 2) convective instability breaks out in the layers with a high opacity. We have calculated one set of ZAMS models for composition ($X_e = 0.7$, $Z_e = 0.01$), $l/H_p = 2$ and for $100 \gtrsim M/M_\odot \gtrsim 0.5$. Table 5.2 contains details of these models. The maximum effective temperature attained is $\log T_{eff_{max}} \simeq 4.63$ which is consistent with Stothers' results for higher metallicities. The convective zones in the envelope occur typically between temperatures and densities

$$5.3 < \log T < 6.1\ ,\ -7.4 < \log \rho < -5.2\ , \qquad (100\ M_\odot),$$

$$5.4 < \log T < 5.8\ ,\ -6.2 < \log \rho < -5.4\ , \qquad (30\ M_\odot),$$

$$5.49 < \log T < 5.54\ ,\ -5.71 < \log \rho < -5.56\ , \qquad (15\ M_\odot),$$

but although extending through up to 30% of the stellar radius, contain less than 10^{-4} of the stellar mass. These results support Stothers' findings for massive main-sequence models with Carson opacities. Further

implications of these results on the interpretation of very massive stars are discussed by Stothers. These results are consistent with a steeper gradient for the ZAMS found earlier. There is some observational evidence (Underhill, 1980; Remie and Lamers, 1981) which lends support to the reddening of the ZAMS at high mass.

Figure 5.3 compares models with composition (Xe = 0.7, Ze = 0.02) for different treatments of the mixing-length theory of convection. Values of 1, 1.5 and 2 for the ratio of the mixing-length to the pressure scale height (l/H_p) are used. A few models are constructed using the modifications to the Böhm-Vitense treatment suggested by Deupree(1979) and by Deupree and Varner (1980), with a maximum value for $l/H_p = 2$. These models indicate that the uncertainty in the treatment of convection in the stellar envelope only leads to an ambiguity in the effective temperature of the star. However an uncertainty in the opacity, inasmuch as the core opacity is affected, also leads to an ambiguity in the stellar luminosity.

Using Hejlesen's (1980) isochrone analysis for main-sequence evolution, Mauder (1982) obtains a preference for the mixing length ratio $l/H_p = 2$ based on observational data for the sun and the eclipsing binary system CW Eri. We find that 1) improvements to the Böhm- Vitense treatment of the mixing length theory, regardless of the choice of the mixing length, and 2) the use of the Carson opacities will both have an effect on ZAMS models at least as great as the choice of the mixing length. Either change will shift both zero-age lines and subsequent isochrones and are likely to cast Mauder's results into some doubt. The determination of both stellar ages and the value of the mixing length are thus only as reliable as the opacities and the mathematical models for convection.

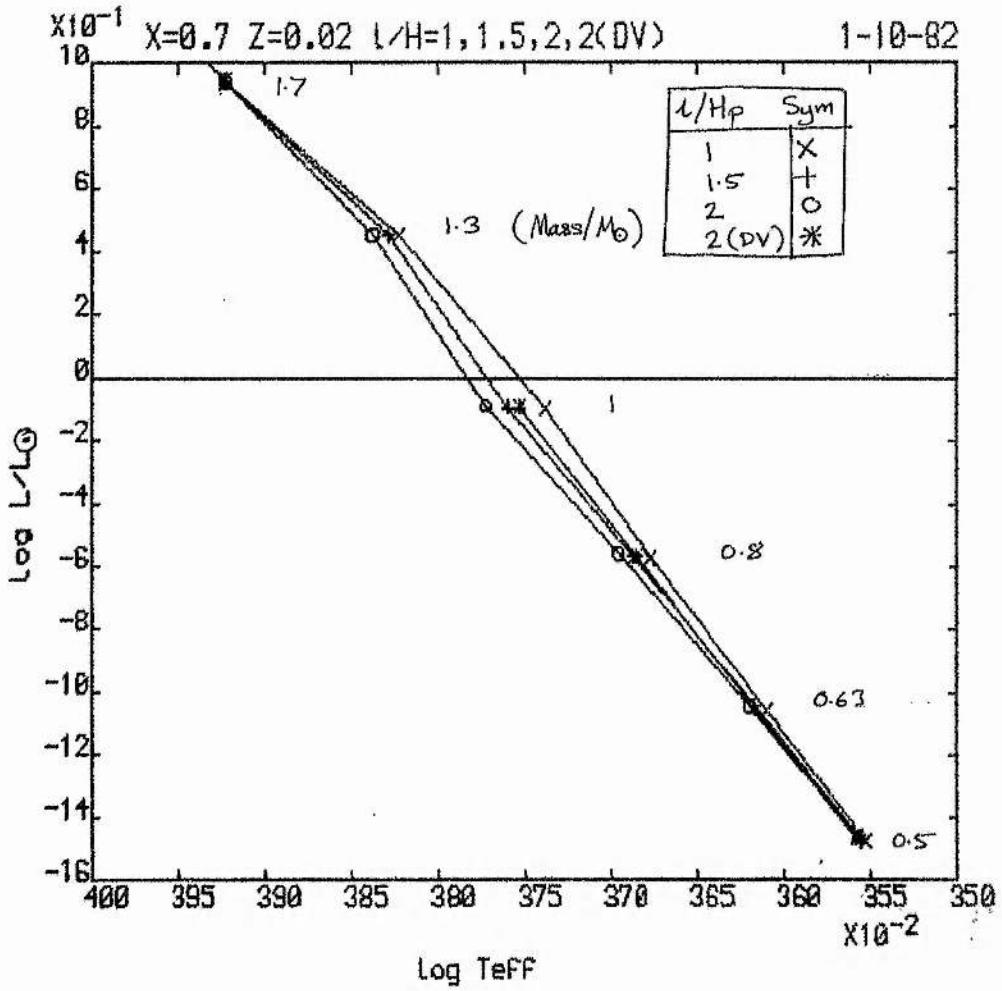

Figure 5.3 A comparison of ZAMS models for different values of the mixing-length to pressure scale-height ratio (l/H_p), and for the modified treatment due to Deupree et al (1979, 1980) (DV).

× l/H_p = 1 o l/H_p = 2

\+ l/H_p = 1.5 * l/H_p = 2 (DV)

5.3 MAIN-SEQUENCE EVOLUTION

Overall properties of evolutionary tracks for main-sequence stars are given in table 5.4. In addition to the mass and initial composition of each star the zero-age values of effective temperature, luminosity, surface gravity, the apsidal motion constant and the masses within the base of the convective envelope and within the convective core are given. The main-sequence lifetime t_{ms} is defined to be the time taken for a star to evolve from the zero-age main-sequence to complete core-hydrogen exhaustion. The blueward and redward limits of the evolutionary track (in effective temperature before core-hydrogen exhaustion are also given. Table 5.5 contains further details of the evolutionary sequences. Three compositions have been used; (Xe = 0.7, Ze = 0.02), (Xe = 0.7, Ze = 0.01) and (Xe = 0.8, Ze = 0.01). The time t_n is the time in 10^n years from the ZAMS position. Ye is the surface helium abundance, M_{sh} and L_c are the mass and luminosity of the hydrogen-exhausted core and L_{sh} is the luminosity of the hydrogen-burning shell.

The evolutionary tracks have no remarkable features and are not shown. We have compared the main-sequence lifetimes and the width (in effective temperature) of the main-sequence with the results of Mengel et al (1979).

Main-sequence lifetimes are compared in figure 5.4. The overlapping mass interval is unfortunately small, but allowing for differences in the initial composition and luminosity, there is no conflict in t_{ms} for $2 \lesssim M/M_\odot \lesssim 5$ when Ze = 0.01. We find that the convective core masses are similar for both sets of models, implying (Parsian et al, 1974) that there is no large differential effect in the difference between the Cox-Stewart and the Carson opacities at high temperatures. For $M/M_\odot = 1$ (Xe = 0.7, Ze = 0.01) we find $t_{ms} = 3.766 \times 10^9$ years. Interpolating, Mengel et al find $t_{ms} \simeq 5.45 \times 10^9$ years for the same mass and composition. Allowing for errors arising from the interpolation, this represents a major discrepancy. Thus for this star

$$t_{ms}(c) / t_{ms}(cs) \simeq 0.7 ,$$

where C and CS denote the opacities used, as before. As low-mass

Table 5.4 A summary of the evolutionary sequences for main-sequence stars. For each sequence we give : 1) the mass; 2) the main-sequence lifetime; 3) - 6) ZAMS values for the effective tempterature, the luminosity, the surface gravity, the apsidal motion constant and the masses interior to the convective core and convective envelope; 7) - 8) the maximum and minimum effective temperatures attained during m-s evolution.

Y=0.3 Z=0.0200

M*	Tms	Teff	L*	g	k2	Mcc	Mcenv	TeMax	Temin
1.0	4.720	3.7727	-0.089	4.577	-1.592	0.000	0.976	3.788	3.773
2.0	7.406	3.9751	1.228	4.370	-2.203	0.250	2.000	3.975	3.901
3.2	2.256	4.1128	2.023	4.331	-2.121	0.640	3.200	4.113	4.028
5.0	7.414	4.2294	2.739	4.275	-2.060	1.175	5.000	4.229	4.144
8.0	2.756	4.3382	3.441	4.212	-2.018	2.272	8.000	4.338	4.241
10.0	1.860	4.3849	3.756	4.181	-2.011	3.150	10.000	4.385	4.271
12.0	1.417	4.4202	4.004	4.153	-2.014	4.320	12.000	4.420	4.282

Y=0.3 Z=0.0100

M*	Tms	Teff	L*	g	k2	Mcc	Mcenv	TeMax	Temin
1.0	3.766	3.8074	0.059	4.568	-1.725	0.000	0.992	3.816	3.807
2.0	6.284	4.0234	1.346	4.446	-2.143	0.290	2.000	4.023	3.949
3.2	1.923	4.1558	2.121	4.405	-2.058	0.698	3.200	4.156	4.075
5.0	6.594	4.2663	2.814	4.348	-1.995	1.260	5.000	4.266	4.187
8.0	2.528	4.3693	3.491	4.286	-1.941	2.400	8.000	4.369	4.284
10.0	1.739	4.4141	3.797	4.257	-1.925	3.310	10.000	4.414	4.318
12.0	1.336	4.4483	4.037	4.233	-1.918	4.320	12.000	4.448	4.338

Y=0.2 Z=0.0100

M*	Tms	Teff	L*	g	k2	Mcc	Mcenv	TeMax	Temin
2.0	9.781	3.9753	1.151	4.448	-2.156	0.212	2.000	3.975	3.897
3.2	3.109	4.1152	1.936	4.427	-2.062	0.640	3.200	4.115	4.022
5.0	10.494	4.2299	2.640	4.376	-1.986	1.175	5.000	4.230	4.138
8.0	3.811	4.3363	3.330	4.316	-1.923	2.272	8.000	4.336	4.244
10.0	2.560	4.3826	3.641	4.286	-1.902	3.150	10.000	4.383	4.282
12.0	1.909	4.4184	3.888	4.262	-1.890	4.140	12.000	4.418	4.305

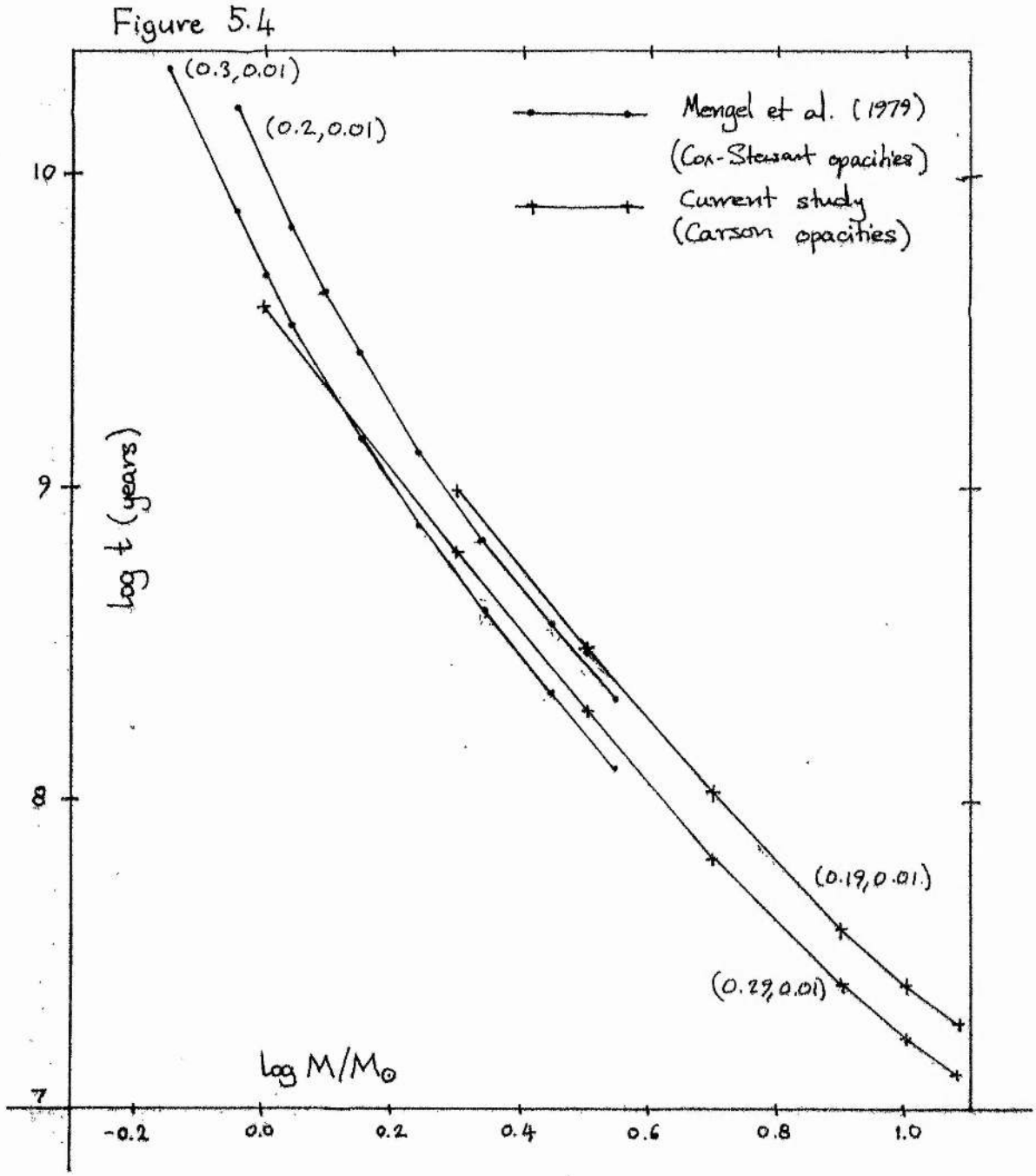

Figure 5.4 Main-sequence lifetime as a function of stellar mass and initial composition (Y, Z), compared for

1) Cox-Stewart opacities (Mengel et al, 1979),

2) Carson opacities.

main-sequence stars have radiative cores, we expect t_{ms} to be more sensitive to opacity changes than for stars with convective cores. An increase in the core opacity leads to an increased temperature gradient, the same luminosity can then be produced by more rapid hydrogen-burning in a less massive region of the star. This leads to a reduced value for t_{ms}. A contradiction arises here, as Stabell (1975) finds that a uniform increase in the opacity throughout the star will cause an increase in the main-sequence lifetime of a solar mass star. Stabell adds that the shift in the ZAMS position due to a uniform increase in opacity cancels the increased main-sequence lifetime when constructing isochrones. We note that our ZAMS position using the Carson opacities is moved relative to that using the Cox-Stewart opacities in a direction consistent with an opacity increase. A reduction in t_{ms}, according to Stabell, will therefore alter the position of isochrones significantly. The consequences for the determination of globular cluster ages from the relative positions of the main-sequence turn-off point and the horizontal branch are apparent. However, as we have calculated only two evolutionary sequences for stars with $M < 2\ M_{\odot}$, and only one gives coverage of the thick hydrogen-shell-burning phase, caution should be exercised in interpreting our results.

Figure 5.5 compares the width (in effective temperature) of the main-sequence. The redward and blueward extremes of the main-sequence evolutionary tracks for each star are connected by an arrow indicating the direction of evolution. For $\log M/M_{\odot} = 0.5$, the difference in $\delta \log T_{eff}$, where

$$\delta \log T_{eff} = \log T_{eff}\ (\text{blue}) - \log T_{eff}\ (\text{red}) \qquad (5\text{-}3)$$

between the two sets of models is

$$\delta \log T_{eff}\ (C) - \delta \log T_{eff}\ (CS) < 0.003,$$

which may be regarded as being mostly due to the small initial composition difference (δ Xe = 0.01). We have insufficient data to compare the evolution of low-mass stars in more detail.

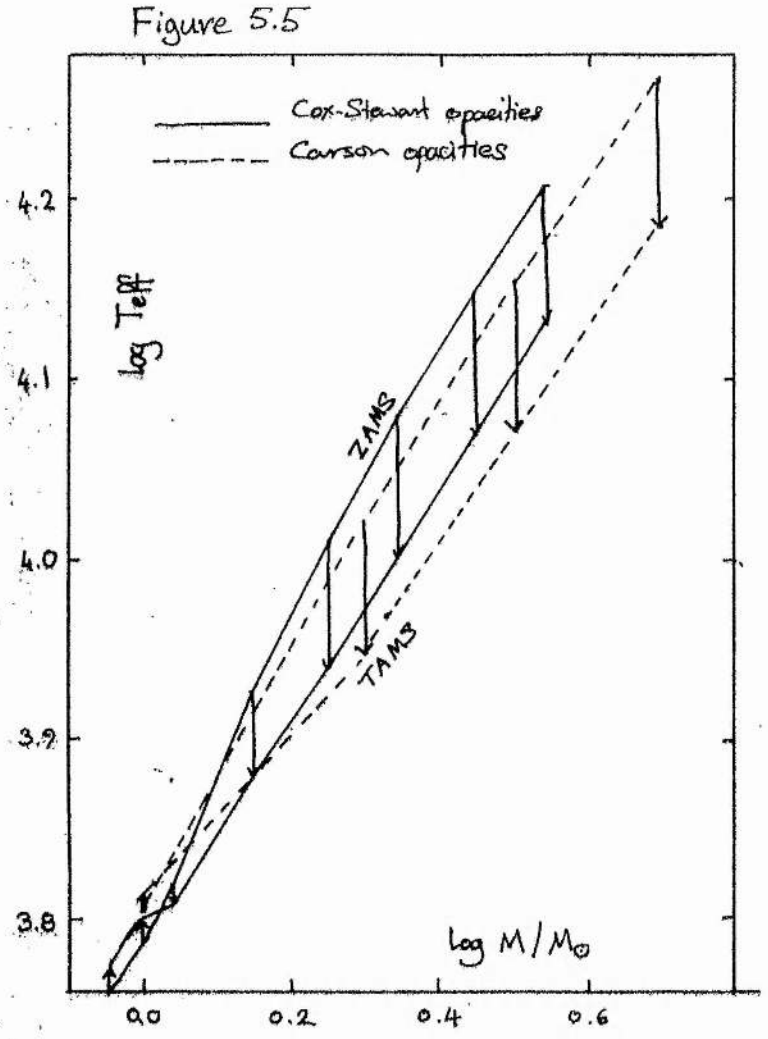

Figure 5.5 A comparison of changes in effective temperature during main-sequence evolution as a function of mass with

1) Cox-Stewart opacities (X = 0.3, Z = 0.01)
(Mengel et al, 1979)

2) Carson opacities (X = 0.29, Z = 0.01)

Arrows indicate evolution from ZAMS to TAMS.

At log $M/M_{\odot}$ = 0.5, the difference between δlog Teff for the two sets of opacities is less than 0.003.

Table 5.5

The evolutionary sequences for main-sequence stars. For each model extracted from the evolutionary sequences we list :

1) the time from the ZAMS, t_n , in 10^n years;
2) the effective temperature, log Teff ;
3) the luminosity, log L ;
4) the surface gravity, log g ;
5) the apsidal motion constant, log k_2 ;
6) the central helium abundance, Y_c ;
7) the mass within the convective core, M_{cc} ;
8) the envelope helium abundance, Ye ;
9) the mass within the convective envelope, $M_{c\,env}$;
10) the mass within the hydrogen-burning shell, M_{sh} ;
11) the helium-core luminosity, L_c ;
12) the hydrogen-shell luminosity, L_{sh} .

Table 5.5

M= 1.0 Y=0.3 Z=0.0200

t	Teff	L	g	k2	Yc	Mcc	Ye	Mcenv	Msh	Lc	Lsh
0.000	3.7727	-0.089	4.577	-1.592	0.280	0.000	0.280	0.976	0.000	0.000	0.000
0.160	3.7738	-0.080	4.572	-1.601	0.305	0.000	0.280	0.976	0.000	0.000	0.000
0.720	3.7778	-0.045	4.554	-1.636	0.395	0.000	0.280	0.980	0.000	0.000	0.000
1.360	3.7822	0.000	4.526	-1.684	0.498	0.000	0.280	0.980	0.000	0.000	0.000
2.000	3.7852	0.044	4.494	-1.734	0.599	0.000	0.280	0.983	0.000	0.000	0.000
2.800	3.7877	0.100	4.448	-1.785	0.708	0.006	0.280	0.983	0.000	0.000	0.000
3.440	3.7863	0.134	4.408	-1.797	0.809	0.014	0.280	0.018	0.000	0.000	0.000
3.760	3.7857	0.153	4.388	-1.805	0.891	0.006	0.280	0.980	0.000	0.000	0.000
3.920	3.7864	0.168	4.375	-1.820	0.935	0.001	0.280	0.983	0.000	0.000	0.000
4.080	3.7868	0.182	4.363	-1.833	0.961	0.000	0.280	0.983	0.000	0.000	0.000
4.320	3.7868	0.201	4.343	-1.846	0.974	0.000	0.280	0.983	0.000	0.000	0.000
4.800	3.7861	0.239	4.302	-1.868	0.980	0.000	0.280	0.980	0.000	0.000	0.000
5.200	3.7852	0.276	4.262	-1.881	0.980	0.000	0.280	0.980	0.002	-4.052	0.276
5.440	3.7844	0.301	4.234	-1.887	0.980	0.000	0.280	0.980	0.006	-3.840	0.301
5.840	3.7817	0.348	4.176	-1.883	0.980	0.000	0.280	0.976	0.022	-3.053	0.348
6.160	3.7750	0.397	4.100	-1.850	0.980	0.000	0.280	0.964	0.044	-2.844	0.397
6.560	3.7424	0.449	3.918	-1.586	0.980	0.000	0.280	0.872	0.096	-1.987	0.447
6.720	3.7132	0.506	3.744	-1.355	0.980	0.000	0.280	0.657	0.128	-1.797	0.504
6.770	3.7070	0.552	3.673	-1.309	0.980	0.000	0.280	0.571	0.133	-1.776	0.550
6.805	3.7041	0.599	3.614	-1.285	0.980	0.000	0.280	0.510	0.143	-1.715	0.597
6.867	3.6996	0.714	3.482	-1.258	0.980	0.000	0.280	0.401	0.160	-1.604	0.712
6.884	3.6985	0.744	3.448	-1.254	0.980	0.000	0.280	0.374	0.160	-1.629	0.742

M= 2.0 Y=0.3 Z=0.0200

t	Teff	L	g	k2	Yc	Mcc	Ye	Mcenv	Msh	Lc	Lsh
0.000	3.9751	1.228	4.370	-2.203	0.280	0.250	0.280	2.000	0.000	0.000	0.000
0.300	3.9740	1.235	4.359	-2.212	0.299	0.250	0.280	2.000	0.000	0.000	0.000
1.900	3.9667	1.273	4.292	-2.263	0.407	0.250	0.280	2.000	0.000	0.000	0.000
3.300	3.9579	1.306	4.224	-2.310	0.502	0.250	0.280	2.000	0.000	0.000	0.000
4.700	3.9449	1.337	4.141	-2.360	0.610	0.212	0.280	2.000	0.000	0.000	0.000
5.700	3.9311	1.358	4.065	-2.401	0.704	0.212	0.280	2.000	0.000	0.000	0.000
6.500	3.9166	1.374	3.991	-2.436	0.791	0.150	0.280	2.000	0.000	0.000	0.000
7.100	3.9019	1.388	3.918	-2.469	0.897	0.108	0.280	2.000	0.000	0.000	0.000
7.300	3.9025	1.403	3.906	-2.483	0.947	0.088	0.280	2.000	0.000	0.000	0.000
7.387	3.9233	1.442	3.949	-2.496	0.975	0.066	0.280	2.000	0.000	0.000	0.000
7.408	3.9357	1.469	3.972	-2.508	0.980	0.000	0.280	2.000	0.000	0.000	0.000
7.452	3.9312	1.485	3.938	-2.529	0.980	0.000	0.280	2.000	0.004	-1.911	1.485
7.502	3.9298	1.491	3.927	-2.537	0.980	0.000	0.280	2.000	0.018	-1.593	1.491
7.558	3.9284	1.498	3.915	-2.545	0.980	0.000	0.280	2.000	0.044	-1.373	1.497
7.708	3.9242	1.516	3.879	-2.569	0.980	0.000	0.280	2.000	0.066	-1.356	1.515
7.808	3.9186	1.529	3.844	-2.588	0.980	0.000	0.280	2.000	0.088	-1.243	1.528
7.908	3.9080	1.541	3.789	-2.613	0.980	0.000	0.280	2.000	0.108	-0.990	1.540
8.008	3.8827	1.548	3.681	-2.648	0.980	0.000	0.280	2.000	0.140	-0.574	1.545
8.070	3.8433	1.535	3.536	-2.677	0.980	0.000	0.280	2.000	0.160	-0.378	1.530

Table 5.5 (contd.)

M= 3.2 Y=0.3 Z=0.0200

t	Teff	L	g	k2	Yc	Mcc	Ye	Mcenv	Msh	Lc	Lsh
0.000	4.1128	2.023	4.331	-2.121	0.280	0.640	0.280	3.200	0.000	0.000	0.000
0.100	4.1118	2.031	4.319	-2.131	0.296	0.640	0.280	3.200	0.000	0.000	0.000
0.650	4.1038	2.076	4.242	-2.193	0.401	0.582	0.280	3.200	0.000	0.000	0.000
1.150	4.0922	2.121	4.150	-2.261	0.516	0.522	0.280	3.200	0.000	0.000	0.000
1.450	4.0819	2.150	4.080	-2.309	0.597	0.464	0.280	3.200	0.000	0.000	0.000
1.750	4.0668	2.181	3.989	-2.365	0.692	0.464	0.280	3.200	0.000	0.000	0.000
2.000	4.0484	2.208	3.888	-2.421	0.791	0.339	0.280	3.200	0.000	0.000	0.000
2.200	4.0279	2.235	3.779	-2.480	0.921	0.208	0.280	3.200	0.000	0.000	0.000
2.237	4.0325	2.252	3.780	-2.492	0.959	0.208	0.280	3.200	0.000	0.000	0.000
2.250	4.0442	2.271	3.809	-2.497	0.972	0.173	0.280	3.200	0.000	0.000	0.000
2.256	4.0663	2.314	3.854	-2.516	0.979	0.029	0.280	3.200	0.000	0.000	0.000
2.259	4.0562	2.313	3.815	-2.529	0.980	0.000	0.280	3.200	0.029	0.237	2.309
2.264	4.0507	2.330	3.775	-2.555	0.980	0.000	0.280	3.200	0.029	-0.491	2.329
2.274	4.0472	2.337	3.755	-2.567	0.980	0.000	0.280	3.200	0.106	-0.073	2.335
2.285	4.0438	2.343	3.734	-2.579	0.980	0.000	0.280	3.200	0.106	-0.297	2.342
2.301	4.0368	2.354	3.696	-2.600	0.980	0.000	0.280	3.200	0.173	0.074	2.352
2.321	4.0180	2.366	3.608	-2.638	0.980	0.000	0.280	3.200	0.208	0.153	2.363
2.341	3.9604	2.362	3.382	-2.704	0.980	0.000	0.280	3.200	0.256	0.609	2.354
2.349	3.8851	2.319	3.124	-2.739	0.980	0.000	0.280	3.200	0.307	0.856	2.304

M= 5.0 Y=0.3 Z=0.0200

t	Teff	L	g	k2	Yc	Mcc	Ye	Mcenv	Msh	Lc	Lsh
0.000	4.2294	2.739	4.275	-2.060	0.280	1.175	0.280	5.000	0.000	0.000	0.000
0.500	4.2278	2.750	4.257	-2.076	0.304	1.090	0.280	5.000	0.000	0.000	0.000
2.300	4.2200	2.796	4.180	-2.145	0.405	1.000	0.280	5.000	0.000	0.000	0.000
3.700	4.2104	2.837	4.101	-2.211	0.503	0.910	0.280	5.000	0.000	0.000	0.000
4.900	4.1978	2.875	4.012	-2.280	0.605	0.815	0.280	5.000	0.000	0.000	0.000
5.900	4.1820	2.911	3.913	-2.350	0.707	0.725	0.280	5.000	0.000	0.000	0.000
6.700	4.1621	2.945	3.799	-2.425	0.814	0.530	0.280	5.000	0.000	0.000	0.000
7.200	4.1447	2.974	3.701	-2.488	0.916	0.425	0.280	5.000	0.000	0.000	0.000
7.350	4.1477	2.992	3.695	-2.507	0.959	0.375	0.280	5.000	0.000	0.000	0.000
7.400	4.1647	3.015	3.740	-2.512	0.975	0.375	0.280	5.000	0.000	0.000	0.000
7.415	4.1839	3.048	3.783	-2.528	0.980	0.110	0.280	5.000	0.000	0.000	0.000
7.424	4.1664	3.048	3.714	-2.555	0.980	0.000	0.280	5.000	0.110	1.321	3.040
7.437	4.1554	3.071	3.647	-2.600	0.980	0.000	0.280	5.000	0.165	1.037	3.067
7.438	4.1549	3.071	3.644	-2.602	0.980	0.000	0.280	5.000	0.165	1.007	3.067

Table 5.5 (contd.)

M= 8.0 Y=0.3 Z=0.0200

t	Teff	L	g	k2	Yc	Mcc	Ye	Mcenv	Msh	Lc	Lsh
0.000	4.3382	3.441	4.212	-2.018	0.280	2.272	0.280	8.000	0.000	0.000	0.000
0.150	4.3371	3.451	4.198	-2.033	0.298	2.272	0.280	8.000	0.000	0.000	0.000
0.850	4.3294	3.504	4.114	-2.122	0.398	2.016	0.280	8.000	0.000	0.000	0.000
1.450	4.3180	3.558	4.014	-2.221	0.507	1.744	0.280	8.000	0.000	0.000	0.000
1.850	4.3055	3.600	3.923	-2.306	0.599	1.600	0.280	8.000	0.000	0.000	0.000
2.250	4.2852	3.648	3.793	-2.419	0.715	1.456	0.280	8.000	0.000	0.000	0.000
2.550	4.2584	3.693	3.641	-2.540	0.836	1.000	0.280	8.000	0.000	0.000	0.000
2.650	4.2460	3.711	3.573	-2.592	0.894	0.848	0.280	8.000	0.000	0.000	0.000
2.725	4.2418	3.733	3.535	-2.635	0.954	0.848	0.280	8.000	0.000	0.000	0.000
2.744	4.2492	3.744	3.553	-2.641	0.969	0.848	0.280	8.000	0.000	0.000	0.000
2.757	4.2769	3.783	3.625	-2.660	0.980	0.112	0.280	8.000	0.520	3.215	3.646
2.760	4.2412	3.783	3.482	-2.726	0.980	8.000	0.280	8.000	0.520	2.573	3.755
2.762	4.2243	3.800	3.398	-2.783	0.980	8.000	0.280	8.000	0.520	2.444	3.780
2.764	4.2036	3.813	3.302	-2.840	0.980	8.000	0.280	8.000	0.520	2.332	3.798

M=10.0 Y=0.3 Z=0.0200

t	Teff	L	g	k2	Yc	Mcc	Ye	Mcenv	Msh	Lc	Lsh
0.000	4.3849	3.756	4.181	-2.011	0.280	3.150	0.280	10.000	0.000	0.000	0.000
0.100	4.3837	3.767	4.165	-2.029	0.298	3.150	0.280	10.000	0.000	0.000	0.000
0.580	4.3755	3.825	4.074	-2.133	0.399	2.840	0.280	3.150	0.000	0.000	0.000
0.980	4.3630	3.882	3.968	-2.250	0.507	2.520	0.280	3.150	0.000	0.000	0.000
1.300	4.3455	3.935	3.844	-2.377	0.618	2.180	0.280	3.150	0.000	0.000	0.000
1.540	4.3227	3.983	3.705	-2.508	0.729	2.000	0.280	3.150	0.000	0.000	0.000
1.660	4.3053	4.011	3.607	-2.594	0.797	1.630	0.280	10.000	0.000	0.000	0.000
1.780	4.2802	4.043	3.475	-2.706	0.890	1.450	0.280	10.000	0.000	0.000	0.000
1.840	4.2710	4.068	3.414	-2.774	0.955	1.250	0.280	10.000	0.000	0.000	0.000
1.855	4.2839	4.082	3.450	-2.777	0.973	1.250	0.280	10.000	0.000	0.000	0.000
1.860	4.3098	4.118	3.519	-2.798	0.980	0.540	0.280	10.000	0.000	0.000	0.000
1.863	4.2470	4.124	3.261	-2.935	0.980	2.350	0.280	1.930	0.850	3.037	4.087
1.864	4.2331	4.129	3.201	-2.971	0.980	2.350	0.280	1.930	0.850	2.974	4.097

M=12.0 Y=0.3 Z=0.0200

t	Teff	L	g	k2	Yc	Mcc	Ye	Mcenv	Msh	Lc	Lsh
0.000	4.4202	4.004	4.153	-2.014	0.280	4.320	0.280	12.000	0.000	0.000	0.000
0.090	4.4187	4.018	4.134	-2.039	0.302	4.140	0.280	12.000	0.000	0.000	0.000
0.450	4.4096	4.078	4.036	-2.159	0.403	3.780	0.280	12.000	0.000	0.000	0.000
0.730	4.3967	4.133	3.930	-2.284	0.503	3.408	0.280	3.600	0.000	0.000	0.000
0.970	4.3778	4.188	3.800	-2.429	0.612	3.024	0.280	3.600	0.000	0.000	0.000
1.130	4.3568	4.230	3.674	-2.561	0.703	2.820	0.280	4.140	0.000	0.000	0.000
1.290	4.3206	4.280	3.479	-2.747	0.824	2.184	0.280	12.000	0.000	0.000	0.000
1.370	4.2896	4.313	3.322	-2.889	0.914	1.956	0.280	12.000	0.000	0.000	0.000
1.405	4.2833	4.333	3.277	-2.951	0.961	1.740	0.280	12.000	0.000	0.000	0.000
1.414	4.2979	4.347	3.321	-2.953	0.975	1.740	0.280	12.000	0.000	0.000	0.000
1.417	4.3221	4.376	3.390	-2.967	0.980	1.272	0.280	12.000	0.000	0.000	0.000
1.418	4.3102	4.388	3.329	-3.027	0.980	3.876	0.280	2.400	1.272	3.734	4.279
1.419	4.2878	4.383	3.245	-3.059	0.980	4.008	0.280	2.400	1.272	3.594	4.306

Table 5.5 (contd.)

M= 1.0 Y=0.3 Z=0.0100

t	Teff	L	g	k2	Yc	Mcc	Ye	Mcenv	Msh	Lc	Lsh
0.000	3.8074	0.059	4.568	-1.725	0.290	0.000	0.290	0.992	0.000	0.000	0.000
0.050	3.8076	0.063	4.565	-1.730	0.300	0.000	0.290	0.992	0.000	0.000	0.000
0.550	3.8103	0.106	4.533	-1.797	0.409	0.000	0.290	0.994	0.000	0.000	0.000
0.950	3.8122	0.141	4.505	-1.849	0.495	0.000	0.290	0.995	0.000	0.000	0.000
1.450	3.8145	0.187	4.468	-1.913	0.597	0.001	0.290	0.996	0.000	0.000	0.000
2.050	3.8154	0.239	4.420	-1.967	0.697	0.012	0.290	0.997	0.000	0.000	0.000
2.850	3.8119	0.297	4.348	-1.988	0.802	0.044	0.290	0.996	0.000	0.000	0.000
3.450	3.8080	0.334	4.296	-1.981	0.910	0.050	0.290	0.994	0.000	0.000	0.000
3.650	3.8084	0.357	4.274	-2.007	0.955	0.031	0.290	0.995	0.000	0.000	0.000
3.725	3.8120	0.388	4.258	-2.081	0.979	0.012	0.290	0.997	0.000	0.000	0.000
3.831	3.8136	0.432	4.219	-2.141	0.990	0.000	0.290	0.997	0.000	0.000	0.000
4.006	3.8118	0.451	4.194	-2.137	0.990	0.000	0.290	0.997	0.001	-3.850	0.451
4.256	3.8093	0.481	4.153	-2.135	0.990	0.000	0.290	0.996	0.012	-3.357	0.481
4.456	3.8068	0.510	4.115	-2.132	0.990	0.000	0.290	0.996	0.031	-2.769	0.510
4.881	3.7918	0.599	3.965	-1.985	0.990	0.000	0.290	0.982	0.075	-2.322	0.598
5.069	3.7737	0.632	3.860	-1.657	0.990	0.000	0.290	0.901	0.110	-1.702	0.630

M= 2.0 Y=0.3 Z=0.0100

t	Teff	L	g	k2	Yc	Mcc	Ye	Mcenv	Msh	Lc	Lsh
0.000	4.0234	1.346	4.446	-2.143	0.290	0.290	0.290	2.000	0.000	0.000	0.000
0.100	4.0230	1.349	4.442	-2.146	0.297	0.290	0.290	2.000	0.000	0.000	0.000
1.400	4.0174	1.390	4.378	-2.199	0.397	0.290	0.290	2.000	0.000	0.000	0.000
2.600	4.0097	1.428	4.309	-2.252	0.492	0.290	0.290	2.000	0.000	0.000	0.000
3.800	3.9976	1.467	4.222	-2.311	0.606	0.250	0.290	2.000	0.000	0.000	0.000
4.600	3.9860	1.492	4.150	-2.354	0.693	0.212	0.290	2.000	0.000	0.000	0.000
5.400	3.9686	1.519	4.054	-2.406	0.801	0.192	0.290	2.000	0.000	0.000	0.000
6.000	3.9511	1.542	3.961	-2.452	0.911	0.150	0.290	2.000	0.000	0.000	0.000
6.200	3.9513	1.560	3.944	-2.470	0.961	0.130	0.290	2.000	0.000	0.000	0.000
6.262	3.9633	1.581	3.971	-2.476	0.980	0.108	0.290	2.000	0.000	0.000	0.000
6.288	3.9941	1.639	4.036	-2.496	0.990	0.028	0.290	2.000	0.000	0.000	0.000
6.296	3.9857	1.640	4.001	-2.510	0.990	0.000	0.290	2.000	0.012	-0.649	1.638
6.302	3.9834	1.650	3.982	-2.521	0.990	0.000	0.290	2.000	0.018	-0.793	1.648
6.331	3.9789	1.660	3.954	-2.538	0.990	0.000	0.290	2.000	0.044	-0.988	1.659
6.409	3.9707	1.676	3.905	-2.564	0.990	0.000	0.290	2.000	0.088	-0.953	1.675
6.553	3.9337	1.700	3.733	-2.634	0.990	0.000	0.290	2.000	0.150	-0.460	1.697
6.553	3.9337	1.700	3.733	-2.634	0.990	0.000	0.290	2.000	0.150	-0.460	1.697

M= 3.2 Y=0.3 Z=0.0100

t	Teff	L	g	k2	Yc	Mcc	Ye	Mcenv	Msh	Lc	Lsh
0.000	4.1558	2.121	4.405	-2.058	0.290	0.698	0.290	3.200	0.000	0.000	0.000
0.050	4.1552	2.125	4.398	-2.064	0.299	0.698	0.290	3.200	0.000	0.000	0.000
0.500	4.1489	2.170	4.328	-2.125	0.393	0.640	0.290	3.200	0.000	0.000	0.000
0.900	4.1399	2.215	4.247	-2.189	0.495	0.582	0.290	3.200	0.000	0.000	0.000
1.300	4.1249	2.265	4.137	-2.268	0.621	0.464	0.290	3.200	0.000	0.000	0.000
1.500	4.1128	2.293	4.060	-2.317	0.703	0.464	0.290	3.200	0.000	0.000	0.000
1.700	4.0958	2.324	3.962	-2.376	0.799	0.339	0.290	3.200	0.000	0.000	0.000
1.850	4.0769	2.351	3.859	-2.433	0.909	0.272	0.290	3.200	0.000	0.000	0.000
1.900	4.0754	2.368	3.836	-2.454	0.959	0.240	0.290	3.200	0.000	0.000	0.000
1.919	4.0893	2.390	3.870	-2.460	0.982	0.208	0.290	3.200	0.000	0.000	0.000
1.925	4.1150	2.437	3.926	-2.479	0.990	0.045	0.290	3.200	0.000	0.000	0.000
1.927	4.1020	2.436	3.875	-2.497	0.990	0.000	0.290	3.200	0.045	0.402	2.432
1.929	4.0967	2.452	3.837	-2.522	0.990	0.000	0.290	3.200	0.045	-0.006	2.450
1.936	4.0893	2.465	3.795	-2.546	0.990	0.000	0.290	3.200	0.106	0.010	2.463
1.946	4.0808	2.475	3.751	-2.569	0.990	0.000	0.290	3.200	0.173	0.201	2.473
1.968	4.0478	2.493	3.601	-2.633	0.990	0.000	0.290	3.200	0.240	0.527	2.488

t	Teff	L	g	k2	Yc	Mcc	Ye	Mcenv	Msh	Lc	Lsh
0.000	4.2663	2.814	4.348-1.995		0.290	1.260	0.290	5.000	0.000	0.000	0.000
0.100	4.2660	2.816	4.344-1.998		0.295	1.260	0.290	5.000	0.000	0.000	0.000
1.900	4.2588	2.868	4.263-2.072		0.401	1.090	0.290	5.000	0.000	0.000	0.000
3.300	4.2493	2.914	4.179-2.144		0.504	0.910	0.290	5.000	0.000	0.000	0.000
4.300	4.2386	2.952	4.099-2.208		0.598	0.815	0.290	5.000	0.000	0.000	0.000
5.300	4.2217	2.996	3.987-2.289		0.717	0.725	0.290	5.000	0.000	0.000	0.000
5.900	4.2056	3.027	3.892-2.353		0.811	0.625	0.290	5.000	0.000	0.000	0.000
6.300	4.1904	3.053	3.804-2.409		0.900	0.530	0.290	5.000	0.000	0.000	0.000
6.500	4.1866	3.073	3.770-2.440		0.957	0.425	0.290	5.000	0.000	0.000	0.000
6.550	4.1916	3.082	3.780-2.446		0.973	0.425	0.290	5.000	0.000	0.000	0.000
6.599	4.2247	3.130	3.865-2.461		0.990	0.165	0.290	5.000	0.000	0.000	0.000
6.607	4.2070	3.132	3.792-2.490		0.990	0.000	0.290	5.000	0.165	1.608	3.119
6.614	4.1982	3.153	3.736-2.530		0.990	0.000	0.290	5.000	0.165	1.275	3.147
6.626	4.1895	3.164	3.690-2.557		0.990	0.000	0.290	5.000	0.220	1.141	3.160

M= 8.0 Y=0.3 Z=0.0100

t	Teff	L	g	k2	Yc	Mcc	Ye	Mcenv	Msh	Lc	Lsh
0.000	4.3693	3.491	4.286-1.941		0.290	2.400	0.290	8.000	0.000	0.000	0.000
0.050	4.3689	3.495	4.282-1.946		0.296	2.400	0.290	8.000	0.000	0.000	0.000
0.700	4.3626	3.547	4.204-2.027		0.393	2.144	0.290	8.000	0.000	0.000	0.000
1.300	4.3521	3.603	4.105-2.124		0.507	1.880	0.290	8.000	0.000	0.000	0.000
1.700	4.3401	3.648	4.012-2.208		0.607	1.600	0.290	8.000	0.000	0.000	0.000
2.000	4.3259	3.687	3.917-2.289		0.701	1.456	0.290	8.000	0.000	0.000	0.000
2.250	4.3073	3.726	3.804-2.378		0.804	1.160	0.290	8.000	0.000	0.000	0.000
2.450	4.2858	3.764	3.679-2.472		0.923	1.000	0.290	8.000	0.000	0.000	0.000
2.500	4.2853	3.780	3.662-2.497		0.963	0.848	0.290	8.000	0.000	0.000	0.000
2.519	4.2944	3.791	3.687-2.501		0.980	0.848	0.290	8.000	0.000	0.000	0.000
2.530	4.3207	3.826	3.757-2.516		0.990	0.264	0.290	8.000	0.000	0.000	0.000
2.533	4.2912	3.827	3.638-2.567		0.990	0.000	0.290	8.000	0.432	2.608	3.800
2.535	4.2725	3.852	3.539-2.634		0.990	0.000	0.290	8.000	0.520	2.497	3.832
2.537	4.2570	3.863	3.466-2.675		0.990	0.000	0.290	8.000	0.600	2.448	3.846

M=10.0 Y=0.3 Z=0.0100

t	Teff	L	g	k2	Yc	Mcc	Ye	Mcenv	Msh	Lc	Lsh
0.000	4.4141	3.797	4.257-1.925		0.290	3.310	0.290	10.000	0.000	0.000	0.000
0.020	4.4139	3.799	4.254-1.929		0.294	3.310	0.290	10.000	0.000	0.000	0.000
0.500	4.4069	3.858	4.167-2.026		0.397	2.840	0.290	10.000	0.000	0.000	0.000
0.900	4.3958	3.917	4.064-2.134		0.511	2.520	0.290	10.000	0.000	0.000	0.000
1.140	4.3846	3.958	3.978-2.219		0.598	2.350	0.290	10.000	0.000	0.000	0.000
1.380	4.3665	4.007	3.857-2.330		0.708	2.000	0.290	10.000	0.000	0.000	0.000
1.540	4.3469	4.045	3.740-2.428		0.804	1.630	0.290	10.000	0.000	0.000	0.000
1.660	4.3250	4.079	3.618-2.527		0.902	1.450	0.290	10.000	0.000	0.000	0.000
1.730	4.3245	4.111	3.584-2.586		0.978	1.250	0.290	10.000	0.000	0.000	0.000
1.740	4.3563	4.149	3.673-2.601		0.990	0.750	0.290	10.000	0.000	0.000	0.000
1.742	4.3181	4.154	3.516-2.678		0.990	2.520	0.290	1.970	0.850	3.154	4.108
1.744	4.2711	4.180	3.302-2.802		0.990	2.350	0.290	1.960	1.060	3.087	4.143

M=12.0 Y=0.3 Z=0.0100

t	Teff	L	g	k2	Yc	Mcc	Ye	Mcenv	Msh	Lc	Lsh
0.000	4.4483	4.037	4.233-1.918		0.290	4.320	0.290	12.000	0.000	0.000	0.000
0.030	4.4479	4.041	4.227-1.926		0.298	4.320	0.290	12.000	0.000	0.000	0.000
0.370	4.4411	4.098	4.142-2.026		0.394	3.960	0.290	4.140	0.000	0.000	0.000
0.650	4.4307	4.153	4.046-2.134		0.496	3.600	0.290	4.140	0.000	0.000	0.000
0.890	4.4152	4.209	3.928-2.259		0.606	3.012	0.290	3.600	0.000	0.000	0.000
1.050	4.3977	4.252	3.815-2.370		0.702	2.820	0.290	3.600	0.000	0.000	0.000
1.170	4.3771	4.290	3.695-2.480		0.792	2.400	0.290	3.600	0.000	0.000	0.000
1.290	4.3431	4.338	3.511-2.640		0.920	1.956	0.290	3.600	0.000	0.000	0.000
1.320	4.3380	4.355	3.474-2.683		0.963	1.956	0.290	4.140	0.000	0.000	0.000
1.330	4.3433	4.363	3.486-2.691		0.977	1.728	0.290	4.140	0.000	0.000	0.000
1.337	4.3758	4.397	3.582-2.703		0.990	1.260	0.290	4.140	0.000	0.000	0.000
1.340	4.3092	4.417	3.296-2.872		0.990	4.320	0.290	2.520	1.500	3.577	4.349
1.340	4.2709	4.428	3.132-2.956		0.990	4.140	0.290	2.520	1.620	3.549	4.366

Table 5.5 (contd.)

M= 2.0 Y=0.2 Z=0.0100

t	Teff	L	g	k2	Yc	Mcc	Ye	Mcenv	Msh	Lc	Lsh
0.000	3.9753	1.151	4.448	-2.156	0.190	0.212	0.190	2.000	0.000	0.000	0.000
0.200	3.9749	1.155	4.443	-2.161	0.202	0.212	0.190	2.000	0.000	0.000	0.000
1.800	3.9713	1.193	4.390	-2.206	0.301	0.212	0.190	2.000	0.000	0.000	0.000
3.200	3.9659	1.225	4.337	-2.246	0.391	0.212	0.190	2.000	0.000	0.000	0.000
4.800	3.9569	1.259	4.267	-2.294	0.498	0.230	0.190	2.000	0.000	0.000	0.000
6.200	3.9462	1.286	4.197	-2.336	0.596	0.212	0.190	2.000	0.000	0.000	0.000
7.400	3.9333	1.307	4.124	-2.375	0.692	0.192	0.190	2.000	0.000	0.000	0.000
8.600	3.9147	1.327	4.030	-2.418	0.807	0.150	0.190	2.000	0.000	0.000	0.000
9.400	3.8984	1.342	3.950	-2.453	0.912	0.130	0.190	2.000	0.000	0.000	0.000
9.700	3.9014	1.363	3.941	-2.469	0.969	0.108	0.190	2.000	0.000	0.000	0.000
9.750	3.9102	1.378	3.961	-2.474	0.980	0.108	0.190	2.000	0.000	0.000	0.000
9.789	3.9410	1.439	4.024	-2.496	0.990	0.008	0.190	2.000	0.000	0.000	0.000
9.803	3.9316	1.439	3.986	-2.508	0.990	0.000	0.190	2.000	0.012	-1.004	1.437
9.841	3.9265	1.450	3.955	-2.524	0.990	0.000	0.190	2.000	0.028	-1.307	1.449
10.277	3.8663	1.473	3.690	-2.614	0.990	0.000	0.190	2.000	0.130	-0.731	1.470

M= 3.2 Y=0.2 Z=0.0100

t	Teff	L	g	k2	Yc	Mcc	Ye	Mcenv	Msh	Lc	Lsh
0.000	4.1152	1.936	4.427	-2.062	0.190	0.640	0.190	3.200	0.000	0.000	0.000
0.100	4.1144	1.942	4.418	-2.069	0.204	0.640	0.190	3.200	0.000	0.000	0.000
0.700	4.1090	1.981	4.357	-2.120	0.294	0.582	0.190	3.200	0.000	0.000	0.000
1.300	4.1007	2.022	4.283	-2.175	0.398	0.522	0.190	3.200	0.000	0.000	0.000
1.800	4.0904	2.058	4.205	-2.229	0.500	0.464	0.190	3.200	0.000	0.000	0.000
2.200	4.0781	2.089	4.126	-2.279	0.597	0.400	0.190	3.200	0.000	0.000	0.000
2.600	4.0589	2.122	4.016	-2.339	0.719	0.339	0.190	3.200	0.000	0.000	0.000
2.800	4.0443	2.139	3.941	-2.375	0.800	0.307	0.190	3.200	0.000	0.000	0.000
3.000	4.0256	2.157	3.847	-2.418	0.904	0.240	0.190	3.200	0.000	0.000	0.000
3.075	4.0229	2.172	3.822	-2.437	0.958	0.208	0.190	3.200	0.000	0.000	0.000
3.094	4.0283	2.183	3.833	-2.442	0.974	0.208	0.190	3.200	0.000	0.000	0.000
3.111	4.0626	2.243	3.910	-2.462	0.990	0.029	0.190	3.200	0.000	0.000	0.000
3.114	4.0494	2.235	3.865	-2.472	0.990	0.000	0.190	3.200	0.029	0.049	2.232

M= 5.0 Y=0.2 Z=0.0100

t	Teff	L	g	k2	Yc	Mcc	Ye	Mcenv	Msh	Lc	Lsh
0.000	4.2299	2.640	4.376	-1.986	0.190	1.175	0.190	5.000	0.000	0.000	0.000
0.300	4.2293	2.645	4.369	-1.993	0.201	1.175	0.190	5.000	0.000	0.000	0.000
3.000	4.2221	2.696	4.289	-2.062	0.312	1.090	0.190	5.000	0.000	0.000	0.000
4.600	4.2156	2.729	4.230	-2.110	0.392	0.910	0.190	5.000	0.000	0.000	0.000
6.200	4.2059	2.766	4.154	-2.166	0.490	0.815	0.190	5.000	0.000	0.000	0.000
7.800	4.1906	2.807	4.051	-2.236	0.613	0.725	0.190	5.000	0.000	0.000	0.000
9.000	4.1718	2.843	3.941	-2.303	0.734	0.625	0.190	5.000	0.000	0.000	0.000
9.600	4.1577	2.863	3.864	-2.346	0.811	0.530	0.190	5.000	0.000	0.000	0.000
10.200	4.1397	2.887	3.768	-2.398	0.915	0.425	0.190	5.000	0.000	0.000	0.000
10.400	4.1392	2.902	3.751	-2.416	0.963	0.375	0.190	5.000	0.000	0.000	0.000
10.475	4.1513	2.919	3.783	-2.421	0.982	0.325	0.190	5.000	0.000	0.000	0.000
10.502	4.1754	2.957	3.841	-2.437	0.990	0.070	0.190	5.000	0.000	0.000	0.000
10.515	4.1551	2.957	3.760	-2.463	0.990	0.000	0.190	5.000	0.110	1.145	2.950
10.517	4.1533	2.961	3.748	-2.471	0.990	0.000	0.190	5.000	0.110	1.066	2.955

Table 5.5 (contd.)

M= 8.0 Y=0.2 Z=0.0100

t	Teff	L	g	k2	Yc	Mcc	Ye	Mcenv	Msh	Lc	Lsh
0.000	4.3363	3.330	4.316	-1.923	0.190	2.272	0.190	8.000	0.000	0.000	0.000
0.100	4.3358	3.334	4.309	-1.929	0.199	2.272	0.190	8.000	0.000	0.000	0.000
0.950	4.3304	3.378	4.243	-1.993	0.291	2.016	0.190	8.000	0.000	0.000	0.000
1.750	4.3219	3.426	4.162	-2.068	0.399	1.744	0.190	8.000	0.000	0.000	0.000
2.350	4.3116	3.468	4.079	-2.137	0.501	1.456	0.190	8.000	0.000	0.000	0.000
2.850	4.2981	3.507	3.986	-2.211	0.610	1.304	0.190	8.000	0.000	0.000	0.000
3.150	4.2859	3.534	3.910	-2.265	0.692	1.160	0.190	8.000	0.000	0.000	0.000
3.450	4.2680	3.564	3.808	-2.334	0.795	1.000	0.190	8.000	0.000	0.000	0.000
3.700	4.2467	3.596	3.691	-2.409	0.914	0.768	0.190	8.000	0.000	0.000	0.000
3.775	4.2458	3.612	3.672	-2.433	0.964	0.768	0.190	8.000	0.000	0.000	0.000
3.800	4.2548	3.623	3.696	-2.437	0.980	0.680	0.190	8.000	0.000	0.000	0.000
3.813	4.2787	3.655	3.760	-2.450	0.990	0.176	0.190	8.000	0.000	0.000	0.000
3.818	4.2474	3.656	3.634	-2.497	0.990	0.000	0.190	8.000	0.264	2.105	3.644
3.824	4.2243	3.678	3.519	-2.561	0.990	0.000	0.190	8.000	0.432	2.061	3.667

M=10.0 Y=0.2 Z=0.0100

t	Teff	L	g	k2	Yc	Mcc	Ye	Mcenv	Msh	Lc	Lsh
0.000	4.3826	3.641	4.286	-1.902	0.190	3.150	0.190	10.000	0.000	0.000	0.000
0.100	4.3819	3.649	4.276	-1.913	0.204	3.000	0.190	10.000	0.000	0.000	0.000
0.660	4.3765	3.695	4.208	-1.984	0.294	2.840	0.190	10.000	0.000	0.000	0.000
1.220	4.3672	3.749	4.118	-2.073	0.407	2.350	0.190	10.000	0.000	0.000	0.000
1.620	4.3560	3.793	4.028	-2.154	0.512	2.180	0.190	10.000	0.000	0.000	0.000
1.940	4.3416	3.835	3.929	-2.237	0.617	1.820	0.190	10.000	0.000	0.000	0.000
2.180	4.3245	3.870	3.825	-2.318	0.720	1.630	0.190	10.000	0.000	0.000	0.000
2.340	4.3071	3.898	3.728	-2.387	0.808	1.450	0.190	10.000	0.000	0.000	0.000
2.460	4.2898	3.922	3.635	-2.451	0.891	1.250	0.190	10.000	0.000	0.000	0.000
2.540	4.2832	3.946	3.584	-2.500	0.966	1.060	0.190	10.000	0.000	0.000	0.000
2.555	4.2948	3.959	3.618	-2.503	0.983	1.060	0.190	10.000	0.000	0.000	0.000
2.561	4.3164	3.988	3.675	-2.519	0.990	0.540	0.190	10.000	0.000	0.000	0.000
2.565	4.2696	3.989	3.487	-2.594	0.990	1.820	0.190	1.750	0.650	2.755	3.963
2.566	4.2599	3.997	3.440	-2.621	0.990	3.000	0.190	2.840	0.750	2.774	3.970

M=12.0 Y=0.2 Z=0.0100

t	Teff	L	g	k2	Yc	Mcc	Ye	Mcenv	Msh	Lc	Lsh
0.000	4.4184	3.888	4.262	-1.890	0.190	4.140	0.190	12.000	0.000	0.000	0.000
0.050	4.4179	3.893	4.255	-1.898	0.199	3.972	0.190	12.000	0.000	0.000	0.000
0.510	4.4118	3.946	4.177	-1.984	0.299	3.600	0.190	3.972	0.000	0.000	0.000
0.910	4.4023	4.001	4.085	-2.080	0.411	3.216	0.190	3.780	0.000	0.000	0.000
1.150	4.3931	4.038	4.010	-2.153	0.492	3.024	0.190	3.780	0.000	0.000	0.000
1.390	4.3790	4.081	3.911	-2.245	0.592	2.616	0.190	3.780	0.000	0.000	0.000
1.630	4.3546	4.132	3.763	-2.369	0.726	2.184	0.190	3.780	0.000	0.000	0.000
1.750	4.3352	4.161	3.657	-2.451	0.811	1.956	0.190	3.780	0.000	0.000	0.000
1.870	4.3065	4.198	3.504	-2.564	0.933	1.500	0.190	12.000	0.000	0.000	0.000
1.900	4.3090	4.214	3.498	-2.590	0.975	1.500	0.190	12.000	0.000	0.000	0.000
1.910	4.3397	4.250	3.585	-2.607	0.990	0.900	0.190	12.000	0.000	0.000	0.000
1.910	4.3428	4.254	3.593	-2.610	0.990	3.972	0.190	3.600	0.780	3.740	4.095
1.912	4.3133	4.239	3.491	-2.632	0.990	3.024	0.190	2.184	0.900	3.360	4.177
1.912	4.2906	4.249	3.390	-2.688	0.990	2.820	0.190	2.184	1.020	3.294	4.198

5.4 THE APSIDAL MOTION CONSTANT

The main purpose in constructing evolutionary sequences for main-sequence stars was to extend the number of theoretical calculations of the apsidal constant k_2, for evolved stars. The line of apsides in a close binary system precesses at a rate governed by the density distribution within the two components. Theoretical values for k_2, corresponding to the second harmonic of the mutual tidal distortion (of chief importance in practice), are obtained by integrating the standard Radau equation

$$\frac{d^2c}{dr^2} + \frac{2U}{r}\frac{dc}{dr} - \frac{2(3-U)}{r^2}c = 0 \qquad (5\text{-}4)$$

which has the boundary condition

$$\frac{dc}{dr} = 0 \quad \text{at} \quad r = 0, \qquad (5\text{-}5)$$

and in which U is the homology invariant (2-23), r is the radius and Mr the mass contained within a sphere of radius r (Schwarzschild, 1958). (5-4) is integrated over the entire star from r = 0 to r = R. The surface condition then yields the apsidal constant

$$k_2 = \left[\frac{3c - r\,dc/dr}{4c + 2r\,dc/dr}\right]_{r=R} \qquad (5\text{-}6)$$

Several authors have computed values of k_2, for main-sequence stellar models and have made comparisons with values of k_2 derived from observations of binary systems. Early results (Schwarzschild, 1958: Kopal, 1965) showed a wide discrepancy between theory and observation. Improvements in both theory (Petty, 1973; Odell, 1974; Stothers, 1974b, and references therein) and observations (Monet, 1980; Gimenez and Garcia-Pelayo, 1982; and references therein) have led to considerably improved agreement. Where Monet (1980) finds a significant discrepancy between values of k_2 obtained from the analysis of spectroscopic and eclipsing binary orbits and the values of k_2 for homogeneous main-sequence stars given by Stothers, Gimenez et al attempt to resolve the conflict by considering changes in k_2 due to the evolution of the binary star components. Theoretical determinations of k_2 for evolving m-s stars are given by Petty, Stothers and Odell. Stothers

claims that assuming relative changes of physical quantities along an evolutionary sequence are independent of mass, observed values of k_2 for Y Cyg α Vir, AG Per, CO Lac and CW Cep are in good agreement with predictions based on the evolutionary state of the systems when the Carson opacities are used. Further calculations of k_2 for evolved systems are needed in order to test Stothers' assumption.

We have calculated the apsidal motion constant k_2 for each stellar model during the construction of both zero-age and evolutionary sequences. The stellar models have already been discussed in sections 5.2 and 5.3, where values for k_2 are given in tables 5.2, 5.4 and 5.5. Figure 5.6 compares our results for k_2 in homogeneous stars with those of Stothers (1974b) confirming his results for $2 \leq M/M_\odot \leq 10$.

Since age is a difficult parameter to measure accurately in binary systems, Gimenez et al (1982) adopt the age-sensitive quantity R, the stellar radius, as an observable age indicator. The surface gravity ($g = GM/R^2$) is an equivalent parameter. Choosing zero-age main sequence values for k_2 and g from theoretical ZAMS models of an appropriate mass, Gimenez et al construct and plot the differences

$$\begin{aligned} \Delta \log g &= \log g_{obs} - \log g_{ZAMS}, \\ \Delta \log k_2 &= \log k_{2\,obs} - \log k_{2\,ZAMS} \end{aligned} \qquad (5\text{-}7)$$

For stars which have not evolved beyond core-hydrogen exhaustion (TAMS), the observed values of k_2 and g give a slope $c \simeq 1$ for the relation

$$\Delta \log k_2 = c . \Delta \log g, \qquad (5\text{-}8)$$

independently of the theoretical ZAMS models chosen. When the observations are split into two groups, Gimenez et al find that the group with higher statistical weight, which is also that of higher mean mass, has a slightly larger slope ($c = 1.04 \pm 0.09$) than obtained for the group with lower weight ($c = 0.96 \pm 0.06$ for both groups combined). Including stars with very large values of $\Delta \log k_2$, the slope is reduced to $c \simeq 0.8$. These systems may represent stars which have evolved beyond the TAMS.

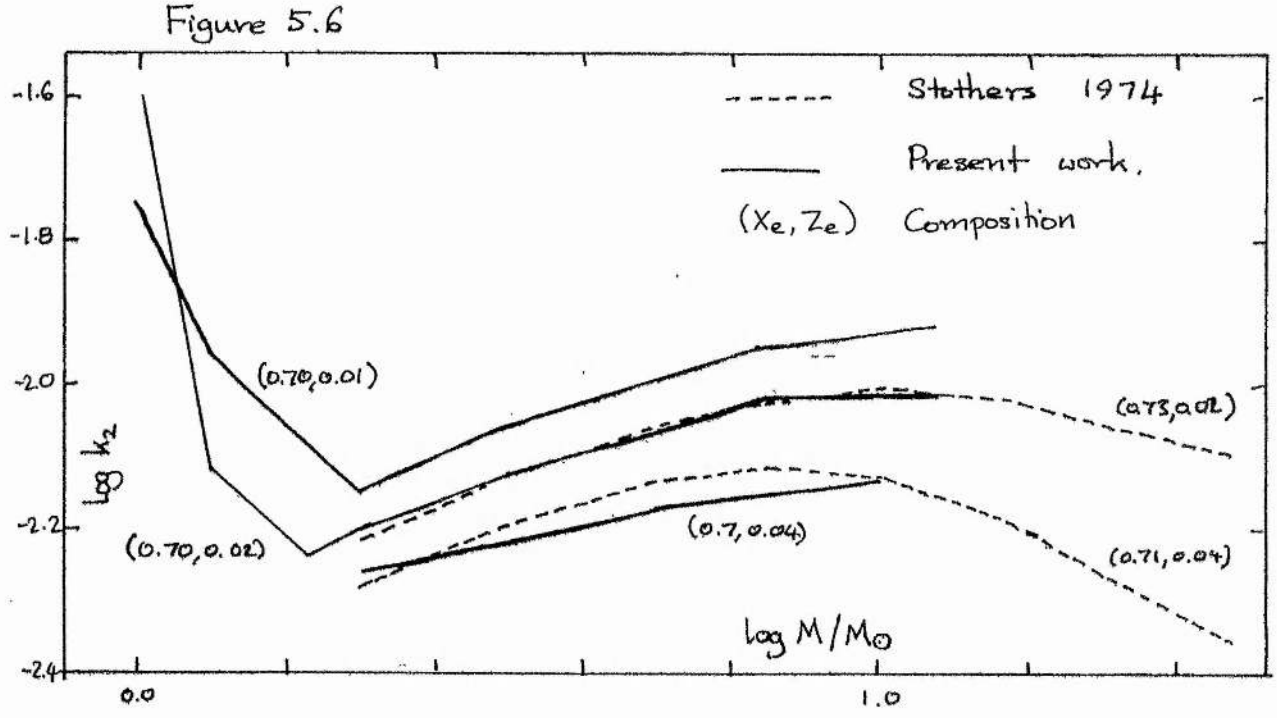

Figure 5.6 The apsidal motion constant k_2 as a function of mass and composition for ZAMS models. Values obtained by Stothers (1974b) are also shown (broken lines). The interpolated lines for log $M/M_\odot < 0.3$ should be disregarded.

In figure 5.7 we present $\Delta \log k_2$ as a function of $\Delta \log g$ from our evolutionary sequences for 3 initial compositions and masses $12 \geq M/M_\odot \geq 2$. The point ($\Delta \log g = 0, \Delta \log k_2 = 0$) corresponds to the ZAMS models, the horizontal 'hooks' correspond to the blueward loops in the evolutionary tracks where $0.05 > X_c > 0$, where X_c is the central hydrogen abundance. The line

$$\Delta \log k_2 = \Delta \log g$$

is also shown. We find that for core-hydrogen-burning stars ($X_c > 0.05$) the slope c is considerably less than unity for low-mass stars and increases with increasing mass in the range $12 \geq M/M_\odot \geq 2$. Typical values for c are given in table 5.6, but it should be noted that c is not a constant during m-s evolution for any given model. After TAMS ($X_c = 0$), c is considerably reduced. For the range of compositions considered we find that a star for which

$$\Delta \log k_2 \lesssim -0.4$$

and (5-9)

$$\Delta \log k_2 \gtrsim -0.7 + 0.5\, Xe + \Delta \log g \,/\, (0.46 + Ze)$$

is likely to be in a post main-sequence evolutionary phase. We have not investigated the use of different opacities on the shape and length of the ($\log k_2$: $\log g$) curves.

These results are in good general agreement with the observational results of Gimenez et al (1982), including the difference in c detected for lower-mass stars. Agreement with Stothers' (1974b) results for the evolution of a 10.9 $M_\odot$ star is also achieved. Stothers' assumption that relative changes in physical quantities are independent of mass appears to be false, casting doubt upon the success of his interpretation of k_2 for AG Per ($M \simeq 5\ M_\odot$) and CO Lac ($M \simeq 4\ M_\odot$). Assuming the same ages and masses for these systems as Stothers, predicted values for $\log k_2$ are recalculated as functions of Ze using the data in table 5.5. These are compared with Stothers' values and observed values given by Petty (1973) in table 5.7

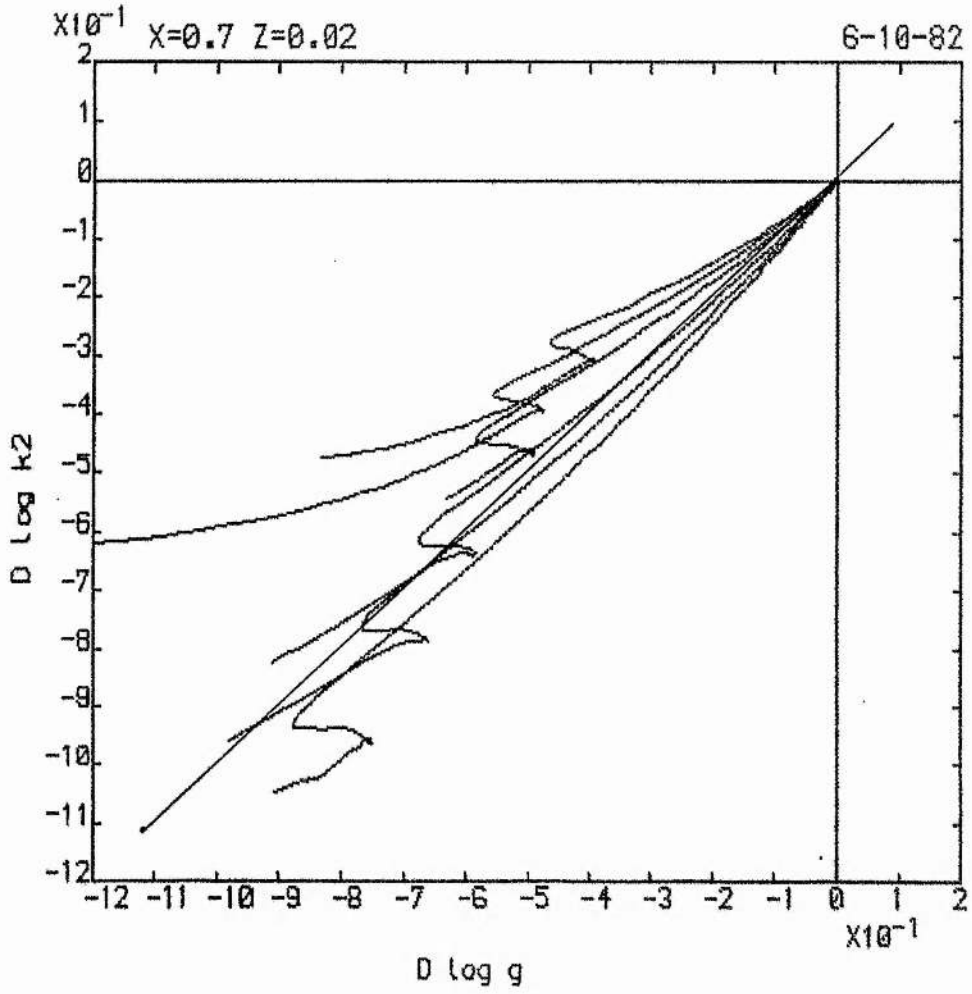

Figure 5.7 Changes in the apsidal motion constant k_2 during m-s evolution are plotted against the corresponding change in surface gravity, g for masses $M/M_\odot \in \{2, 3.2, 5, 8, 10, 12\}$ and three compositions indicated in the diagrams. The line $\Delta \log k_2 = \Delta \log g$ is also shown.

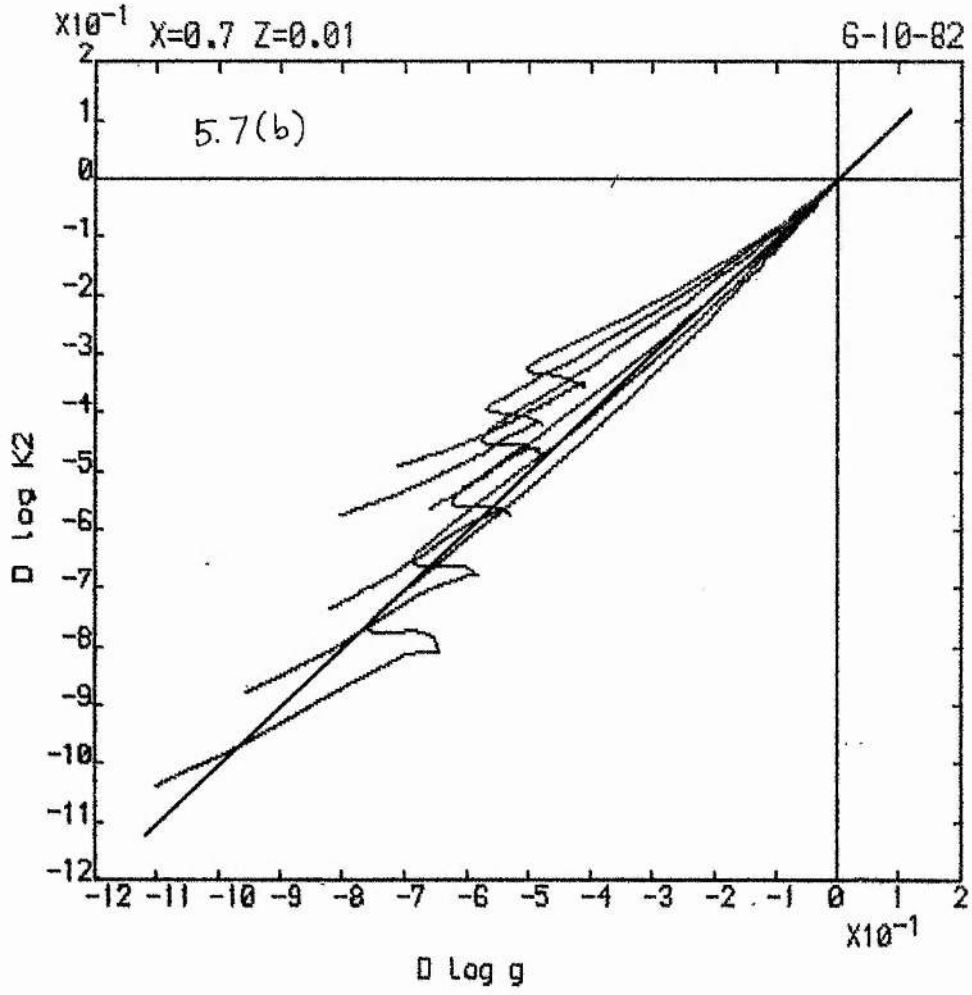
X10⁻¹
X=0.7 Z=0.01
6-10-82
5.7(b)
D Log K2
D Log g
X10⁻¹

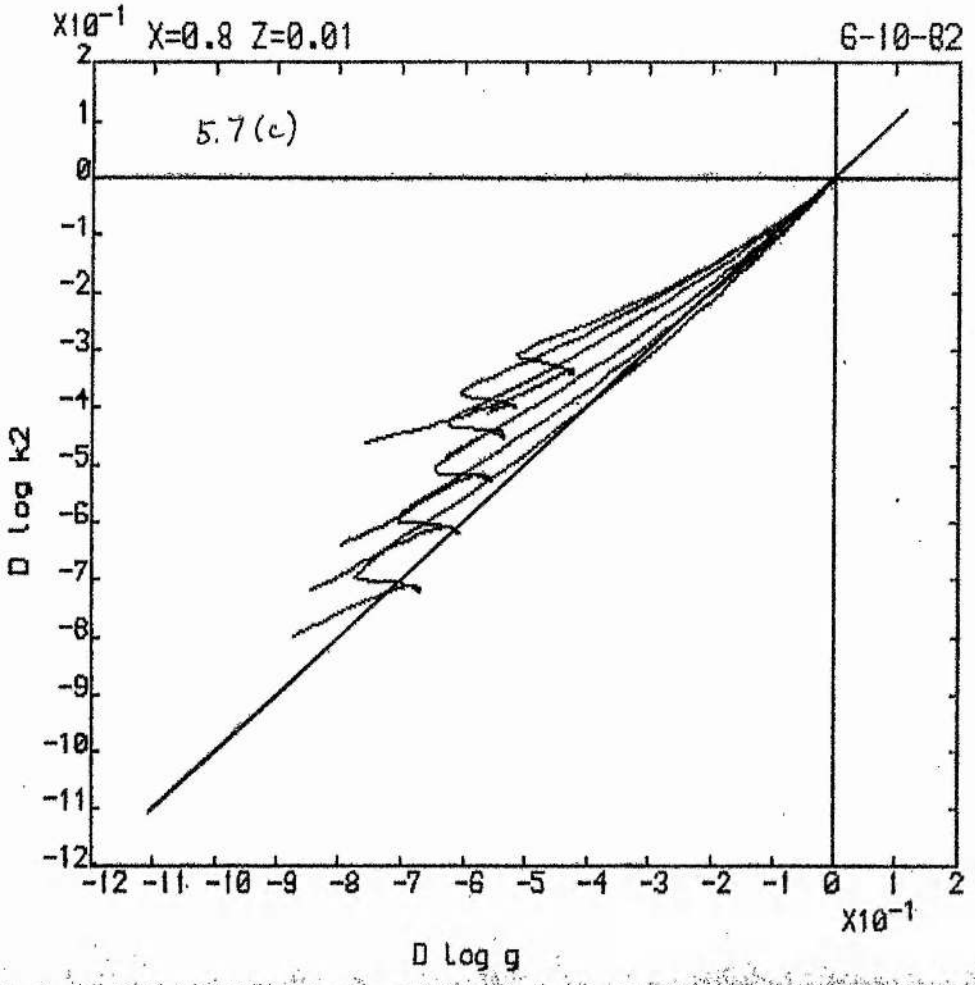
X10⁻¹
X=0.8 Z=0.01
6-10-82
5.7(c)
D Log K2
D Log g
X10⁻¹

Table 5.6 Values of c for the approximate relation $\Delta \log k_2 = c.\Delta \log g$ for main-sequence evolution, tabulated as a function of mass and composition. c is obtained from evolutionary tracks by comparing the models for Xc = Xe and for Xc ≃ 0.10. Note that the relation is not linear throughout main-sequence evolution.

Mass ($M_* / M_\odot$)	Composition		
	X = 0.7, Z = 0.02	X = 0.7, Z = 0.01	X = 0.8, Z = 0.01
2	0.59	0.64	0.60
3.2	0.65	0.69	0.62
5	0.75	0.76	0.68
8	0.90	0.87	0.78
10	0.98	0.94	0.84
12	1.05	1.00	0.89
1	1.13	0.94	-

Table 5.7 Predicted and observed values of the apsidal motion constant for two eclipsing binary systems.

System	Mass ($M_\odot^{-1}$)	t/tms	log k_2		
			Petty (1973)	Stothers (1974b)	Current
AG Per	~5	(0.4-5×Ze)	-2.20[a]	-2.20-3×(Ze-0.03)	-2.20-8×(Ze-0.0
CO Lac	~4	(0.4-7×Ze)	-2.37[b]	-2.34-7×(Ze-0.03)	-2.20-3×(Ze-0.0

Sources: a Kopal (1965) b Semeniuk (1967)

The different range in Ze for which we interpolate has a small effect which may partly account for the small discrepancy in the predicted values of log k_2 for AG Per. Since AG Per is a well determined system in a relatively unevolved state it is reasonable that both our method and Stothers' method (based on an assumption equivalent to setting c = 1 for all stars) should lead to good agreement with observations.

This situation no longer holds for CO Lac. Petty (1973) finds that the observed values of the stellar radii obtained from spectroscopic studies of the orbit by Smak (1967) imply that CO Lac is close to the ZAMS, while the observed value of k_2 (Semeniuk, 1967) implies that CO Lac has evolved some distance away from the ZAMS. By dropping the assumption that c = 1 we find that the Carson opacities fail to resolve this conflict, contradicting Stothers' result. An examination of the observational data is instructive. CO Lac has a spectrum with broad and diffuse metallic lines and possibly strong line-blending. Smak obtained spectra at a dispersion of approximately 39 Å/mm. His analysis gives a mean value for the radii of the two components of 2.63 $R_\odot$. If we assume that the apsidal motion constant obtained by Semeniuk is correct, we can obtain an estimate of the expected mean radius of the components. Assuming a mass of $\simeq 4\ M_\odot$, Xe = 0.7, our evolutionary tracks give

$$\log K_2 \simeq -1.98 - 5\ Ze - 0.4\ t/t_{ms} \qquad (5\text{-}10)$$

$$\log R/R_\odot \simeq 0.30 + 2\ Ze + 0.28\ t/t_{ms} \qquad (5\text{-}11)$$

where t/t_{ms} is the age of the system in terms of its main-sequence lifetime. Eliminating t/t_{ms} gives

$$\log R/R_\odot \simeq -1.09 - 1.5\ Ze - 0.7 \log K_2 \qquad (5\text{-}12)$$

and with the observed value for $\log K_2 = -2.37$,

$$\log R/R_\odot \simeq 0.57 - 1.5\ Ze \qquad (5\text{-}13)$$

If we assume a metallicity of $\simeq 3\%$ then the observed k_2 requires an increase in the observed radii corresponding to an increase in the orbital elements K_1 and K_2 of

$$\frac{(K_1 + K_2)_{expected}}{(K_1 + K_2)_{observed}} \simeq 1.27$$

Allowing for the highly approximate nature of this argument, an error of at least $\pm$ 0.05 is likely. In view of possible line-blending effects which may have been overlooked in Smak's analysis, an increase of 20% or more in the observed values of K_1 and K_2 is possible (Hilditch, 1982: private communication). While theoretical studies have mostly failed to interpret the apsidal motion in CO Lac, we consider it more likely to be resolved by an improvement in the observational data, particularly a spectroscopic redetermination of the orbit, than by changes to theoretical models of stellar evolution.

Gimenez et al (1982) attempt to determine a test for the opacity by assuming that the slope c in the $\Delta \log k_2 - \Delta \log g$ relation is equal to unity. As the mean error in the observations is greater than the difference between models constructed with Cox-Stewart and with Carson opacities, they attach little weight to their marginal preference for the Carson opacities. As already indicated the assumption c = 1 is false, reducing the validity of this preference still further.

We have shown that most observed values of the apsidal motion constant k_2 in binary systems may be accounted for by considering the evolution of their components. In one of those systems (CO Lac) in which this is not the case it is likely that better observational data will resolve the problem. The evolution of k_2 is mass-dependent.

5.5. SUMMARY

Our results of calculations of stellar structure and evolution for main-sequence stars are largely of an exploratory nature. Some establish known features of stellar models constructed with the Carson opacities. These are as follows :

1) Carson opacities have little effect on the zero-age main-sequence for $M < 12\ M_\odot$, although its gradient is slightly increased for $M \gtrsim 2\ M_\odot$ (Stothers, 1974a).

2) For $M \gtrsim 10\ M_\odot$, Carson opacities lead to distended envelopes and convective instability in the CNO ionisation zone (Stothers, 1976c).

3) The central condensation of m-s stars is increased when the Carson opacities are used. This leads to lower values for the apsidal motion constant k_2 (Stothers, 1974b).

Evolutionary studies with the Carson opacities give the following results :

1) The main-sequence evolution of stars with $2 < M/M_\odot < 10$ is unaffected.

2) The main-sequence lifetime of stars with radiative cores is reduced by a factor possibly as small as 0.7.

Studies of the evolution of the apsidal motion constant k_2 show good general agreement with the observations. The detailed agreement found by Stothers (1974b) is not upheld for all binary systems. The conflict between theory and observation for CO Lac is not resolved by using the Carson opacities.

6 CONCLUSION

We have examined a number of aspects of stellar structure and evolution. In view of the apparent success of the Carson opacities in theoretical studies of stellar pulsation we have adopted the Carson opacities in theoretical studies of both main-sequence and horizontal-branch stars.

While pulsation studies provide a test for the envelope opacity, stellar evolution studies test the opacity at higher temperatures and densities. However the test may determine only that the opacity gives results consistent with other opacities and with observations, and not that it is "better" than other opacities. Many of the results inferred from our calculations are therefore consequences of the adopted opacity, and not tests for the opacity. More extensive calculations (and, in some cases, better observations) may alter this situation.

In chapter 4 we found that the opacity value has a small effect on the position of the zero-age horizontal branch. Due to the lack of opacity data for population II metallicities, the apparent increase in the sensitivity of the zero-age position to the metallicity found with the Carson opacities may be an artefact of the interpolation procedure. The increase in the initial core luminosity and the decrease in the initial convective core mass appears to be a real consequence of using the Carson opacities rather than the Cox-Stewart opacities. A reduction of approximately 25% in the horizontal branch lifetime follows from these changes. The behaviour of the hydrogen-shell luminosity (L_H) during the evolution of the helium-core is also modified. An increase in $|\partial L_H / \partial L_{He}|$ means that 'blueward' evolving horizontal branch stars lie below the zero-age horizontal branch for most of their lifetime. For a given core mass and composition this means that the time-averaged luminosity of horizontal branch stars is reduced. The inclusion of semi-convection in the evolution calculations is unlikely to alter these results significantly.

In chapter 5 we confirmed that the Carson opacities have a marked

influence upon the structure of zero-age main-sequence stars only for massive stars. Stothers found a convective region in the CNO ionisation zone and a substantial reddening of the ZAMS for masses greater than 10 $M_\odot$ For lower mass stars there is only a small reduction in both luminosity and effective temperature. The main-sequence evolution of stars with masses $2 \lesssim M/M_\odot \lesssim 10$ appears to be unaffected by the change in opacity. For stars with convective envelopes ($M/M_\odot \lesssim 2$) the method chosen to treat convection has an effect on the zero-age positions of main-sequence stars comparable with that of choosing the opacity. However only the change in opacity leads to significantly lower luminosities. For the few evolutionary sequences calculated, main-sequence lifetimes for stars with radiative cores are reduced by approximately 30%.

An investigation of the behaviour of the apsidal motion constant, k_2 during main-sequence evolution demonstrates that most observed values of k_2 may be explained in terms of the evolution of the binary components. One exception (CO Lac) may be resolved by a redetermination of the orbital semi-amplitudes.

Any comprehensive study of stellar evolution concerned with population II stars should eventually be able to interpret the observed properties of globular cluster stars. In our study we have looked in some detail at the properties of theoretical horizontal branch stars, we have followed the evolution of two low mass main-sequence stars, and have not examined evolution on the red-giant branch.

The usual method for estimating the helium abundance in globular clusters relies on a spectroscopic determination of the cluster metallicity and the ratio of the numbers of horizontal branch stars to the number of red giants with luminosities greater than that of the RR Lyrae variables in the cluster. Evolutionary calculations give the ratio of the lifetimes of horizontal branch stars to those of the red giants as a function of the helium abundance and metallicity, from which the helium abundance may be obtained. We have already noted that stellar evolution calculations for stars burning

nuclear fuel in radiative zones are seriously affected by changing the opacity. Without studies of red giant evolution with the Carson opacities, we cannot estimate cluster helium abundances using this method. In order to avoid any reduction in the estimated helium abundance, the time taken for a star to evolve from the RR Lyrae luminosity to the red giant tip must be reduced by an amount equal to the relative reduction in the horizontal branch lifetime (approx. 25%).

Studies of red giants are also required to determine 1) the helium-core mass of horizontal branch stars as a function of initial composition and 2) the helium enrichment of the envelope due to convective 'dredge-up' during giant branch evolution. Both of these are required before 'evolved' horizontal branches may be constructed.

In order to account for the observed width in both luminosity ($\delta \log L \simeq 0.2$) and effective temperature ($\delta \log T_{eff} \simeq 0.3$) of the horizontal branch we need to assume that there is a variation in total mass and, possibly, composition amongst the cluster stars. The Carson opacities lead to longer evolutionary tracks (e.g. $\delta \log T_{eff} \simeq 0.2$ without semi-convection, see figure 4.2) and smaller deviation from the zero-age horizontal branch ($\delta \log L \simeq 0.1$). The first result implies that a smaller variation in total mass may be needed to account for the observed width in effective temperature than that indicated by the Cox-Stewart opacities. The second result suggests that a composition variation (e.g. $\delta Ye \simeq 0.02$) must exist within the cluster in addition to any mass variation. It may be easier to account for composition inhomogeneities in the "protocluster" than for large variations in mass-loss between stars of similar mass and composition.

Observations of the difference between the luminosity level of the horizontal branch and of the main-sequence turnoff point lead to an age determination for a globular cluster when combined with theoretical isochrones for the main-sequence evolution of low mass stars. More evolutionary sequences calculated using the Carson opacities are required before a full

grid of isochrones can be constructed. For the two sequences we have calculated for 1 $M_\odot$ stars, comparisons with Hejlesen's (1980) results show a shift in the isochrones for an age $\simeq 5 \times 10^9$ years of $\delta \log L \simeq 0.2$ at the main-sequence turnoff point. The corresponding shift at a fixed turnoff luminosity is a drop in age of $\delta \log t \simeq 0.3$. The reduction in main-sequence lifetimes of approximately 30% may represent a lower limit to the shift of the isochrones, and our estimate of $\delta \log t \simeq 0.3$ may represent an upper limit to the combined effects of the shift in the ZAMS position and the reduced lifetime. With the limited data available we anticipate that the Carson opacities imply a reduction by 40% $\pm$ 10% in the estimated ages of globular clusters.

The significance of reducing the age of the globular cluster system by such an amount lies in the implicit lower age limit for the universe. Using Hejlesen's main-sequence isochrones, Nissen (1982) derives a lower age limit of 1.6×10^{10} years from Strömgren photometry of turnoff stars in NGC 6397. Using the models of Sweigart and Gross (1976, 1978), Sandage (1982) obtains an absolute age for the globular cluster system of $(1.7 \pm 0.2) \times 10^{10}$ years from extensive observations of RR Lyrae variables in clusters. For a given value of the Hubble constant H_o, it is well known that the age of the universe is a function of the present mass density ρ_o. A lower age limit of 1.6×10^{10} years excludes values for $H_o \simeq 100$, while $H_o \simeq 50$ is consistent with this age limit if $\Omega = \rho_o / \rho_c < 0.2$, where ρ_c is the critical density and this value for Ω implies an open universe. Lower values of H_o lead to the possibility of a closed universe. Observational determinations of the Hubble constant fall into two categories. Sandage and Tammann (1982) obtain a value of $H_o = 50 \pm 7$ km s^{-1} Mpc^{-1}. This is consistent with Sandage's age for the globular cluster system, added to $t = 0.2\ H_o^{-1}$ for the formation time for galactic nuclei, to give $H_o = 46 \pm 4$ km s^{-1} Mpc^{-1}. However de Vancouleurs (1982) obtains $H_o = 95 \pm 10$ km s^{-1} Mpc^{-1}. If a reduction in globular cluster ages of the magnitude suggested by our results can be achieved, values for $H_o \gg 50$ need not be contradictory to them

The tantalising nature of this last result indicates the importance of further study of stellar evolution with the Carson opacities. We have already mentioned the lack of data for red giant evolution, and the paucity for low-mass main-sequence evolution. We hope that the Carson opacities will be augmented by data for a larger range of population II compositions, and that improvements to high density and low temperature values will become available. More extensive studies of horizontal-branch evolution with semiconvection would then be worthwhile, in particular in obtaining models for low metallicities characteristic of clusters with blue horizontal branches.

APPENDIX A.1

REFERENCES

Aller, L.H., 1963. 'The Atmospheres of the Sun and Stars', 2nd ed., Ronald Press, New York.

Baade, W., 1944. Astrophys. J., 100, 137.

Beaudet, G., Petrosian, V. & Salpeter, E.E., 1967. Astrophys.J., 150, 979.

Bell, R.A., Gustaffson, B., Erikson, K. & Nordlund, A., 1976. Astr. Astrophys. Suppl., 23, 37.

Bethe, H., 1939. Phys. Rev., 55, 434.

Böhm-Vitense, E., 1958. Z. Astrophysik, 46, 108.

Burbidge, E.M., Burbidge, G.R., Fowler, W.A. & Hoyle, F., 1957. Rev. mod. Phys., 29, 547.

Caloi, V., Castellani, V. & Tornambe, A., 1978. Astr. Astrophys. Suppl., 33, 1978.

Cameron, A.G.W., 1973. Space Sci. Rev., 15, 121.

Carson, T.R., 1971. In 'Progress in High Temperature Physics and Chemistry', Vol. 3, p.99, ed. Rouse, C.A., Pergamon, Oxford and New Yor

Carson, T.R., 1976. A. Rev. Astr. Astrophys., 14, 95.

Carson, T.R. & Hollingsworth, H.M., 1968. Mon.Not.R.Astr.Soc. 141, 77.

Carson, T.R., Mayers, D.F. & Stibbs, D.W.N., 1968, Mon. Not. R. Astr. Soc., 140, 483.

Carson, T.R. & Stothers, R., 1976. Astrophys. J., 204, 461.

Carson, T.R. & Stothers, R., 1982. Astrophys. J., 259, 740.

Carson, T.R., Stothers, R. & Vemury, S.K., 1981. Astrophys. J., 244, 230.

Castellani, V., Giannone, P. & Renzini , A., 1969. Astr. Space Sci., 4, 103.

Castellani, V., Giannone, P. & Renzini , A., 1971a. Astr. Space Sci., 10, 340.

Castellani, V., Giannone, P. & Renzini , A., 1971b. Astr. Space Sci., 10, 355.

Castellani, V. & Tornambé, A., 1977. Astr. Astrophys., 61, 427.

Castellani, V. & Tornambé, A., 1981. Astr. Astrophys., 96, 207.

Castellani, V., Ponte, G. & Tornambé, A., 1980. Astr. Space Sci., 73, 11.

Caughlan, G.R. & Fowler, W.A., 1962. Astrophys. J., 136, 453.

Chandrasekhar, S., 1939. 'An Introduction to the Study of Stellar Structure', University of Chicago Press, Chicago.

Christy, R.F., 1966. Astrophys. J., 144, 108.

Cody, W.J. & Thatcher, H.C., 1967. Math. Comput., 21, 30.

Cox, A.N., 1965. In 'Stars and Stellar Systems': Vol. 8, p.195, eds. Aller, L.H. & McLaughlin, D.B., University of Chicago Press, Chicago.

Cox, A.N. & Stewart, J.N., 1962. Astr. J., 67, 113.

Cox, A.N. & Stewart, J.N., 1965. Astrophys. J. Suppl. Ser., 6, 167.

Cox, A.N. & Stewart, J.N., 1969. Astrophys. J. Suppl. Ser.19, 243, 261.

Cox, A.N., Stewart, J.N. & Eilers, D.D., 1965. Astrophys. J. Suppl., Ser. 11, 1.

Cox, A.N. & Tabor, J.E., 1976. Astrophys. J. Suppl. Ser., 31, 271.

Cox, J.P. & Giuli, R.T., 1968. 'Principles of Stellar Structure', Vol.1, Gordon and Breach, New York.

Demarque, P. & Mengel, J.G., 1971. Astrophys. J., 164, 317.

Demarque, P. & Mengel, J.G., 1972. Astrophys. J., 171, 583.

Demarque, P., King, C.R. & Diaz, A., 1982. Astrophys. J., 259, 154.

Deupree, R.G., 1979. Astrophys. J., 234, 228.

Deupree, R.G. & Varner, T.M., 1980. Astrophys. J., 237, 558.

de Vaucouleurs, G., 1982. Observatory, 102, 178.

Eddington, A.S., 1926. 'The Internal Constitution of the Stars', Cambridge, England.

Edwards, A.C., 1970. Mon. Not. R. Astr. Soc., 146, 445.

Eggleton, P.P., 1968. Mon. Not. R. Astr. Soc., 140, 387.

Eggleton, P.P., 1971. Mon. Not. R. Astr. Soc., 151, 351.

Emden, R., 1907. 'Gaskugeln', Leipzig.

Ezer, D. & Cameron, A., 1963. Icarus, 1, 422.

Faulkner, J., 1966. Astrophys. J., 144, 978.

Faulkner, J. & Iben, I., Jr., 1966. Astrophys. J., 144, 995.

Fowler, W.A., Caughlan, G.R. & Zimmerman, B.A., 1967.
A. Rev. Astr. Astrophys., 5. 525, (FCZI).

Fowler, W.A., Caughlan, G.R. & Zimmerman, B.A., 1975.
A. Rev. Astr. Astrophys., 13, 69, (FCZII).

Giannone, P. & Rossi, L., 1981. Astr. Astrophys., 102, 386.

Gimenez, A. & Garcia-Pelayo, J.M., 1982. IAU Coll., 69, 37.

Gingerich, O., Noyes, R.W., Kalkofen, W. & Cuny, Y., 1971.
Sol. Phys., 18, 347.

Gingold, R.A., 1977. Mon. Not. R. Astr. Soc., 178, 533.

Gross, P.G., 1973. Mon. Not. R. Astr. Soc., 164, 65.

Haselgrove, C.B. & Hoyle, F., 1956. Astrophys. J., 116, 515.

Hayashi, C., Hōshi, R. & Sugimoto, D., 1962. Suppl.Progress theor.Phys., 22.

Hejlesen, P.M., 1980a. Astr. Astrophys., 84, 135.

Hejlesen, P.M., 1980b. Astr. Astrophys. Suppl., 39, 347.

Henyey, L.G., Forbes, J.M. & Gould, N.L., 1964. Astrophys. J., 139, 306.

Henyey, L.G., Vardya, M.S. & Bodenheimer, P., 1965. Astrophys. J., 142, 841.

Henyey, L.G., Wilets, L., Böhm, K.H., Lehevier, R. & Levee, R.D., 1959.
Astrophys. J., 129, 628.

Hubbard, W.B. & Lampe, M., 1968. Astrophys. J. Suppl. Ser., 18, 297.

Iben, I. Jr., 1967. A. Rev. Astr. Astrophys., 5. 571.

Iben, I. Jr., 1971. Astrophys. J., 166, 131.

Iben, I. Jr., 1971. Publ. astr. Soc. Pacific., 83, 697.

Iben, I. Jr., 1974. A. Rev. Astr. Astrophys., 12, 215.

Iben, I. Jr. & Faulkner, J., 1968. Astrophys. J., 153. 101.

Iben, I. Jr. & Rood, R.T., 1970a. Astrophys. J., 159, 605.

Iben, I. Jr. & Rood, R.T., 1970b. Astrophys. J., 161, 587, (IR79).

Keller, G. & Meyerott, R.F., 1955. Astrophys. J., 122, 32.

Kippenhahn, R., 1982. IAU Coll., 69, 3.

Kippenhahn, R., Weigert, A. & Hofmeister, E., 1967. Methods in Computational Physics, 7, 129.

Kopal, Z., 1965. Adv. Astr. Astrophys., 3. 89.

Kramers, N.A., 1923. Phil. Mag., 46, 836.

Krishna-Swamy, K.S., 1966. Astrophys. J., 145, 174.

Lampe, M., 1968. Phys. Rev., 170, 306; 174, 276.

Lauterborn, D., Refsdal, S. & Stabell, R., 1972. Astr.Astrophys.,17, 113.

McDougall, J. & Stoner, E.C., 1939. Phil. Trans. R. Soc. Lond., 237, 67.

Magee, N.H. Jr., Merts, A.L. & Huebner, W.F., 1974. Astrophys.J., 196, 617.

Marshak, R.E., 1941. Ann. NY Acad. Sci., 51, 49.

Mauder, H., 1982. IAU Coll., 69, 217.

Mengel, J.G., Sweigart, A.V., Demarque, P. & Gross, P.G., 1979. Astrophys. J. Suppl. Ser., 40, 733.

Merts, A.L. & Magee, N.H. Jr., 1972. Astrophys. J., 177, 137.

Merts, A.L., Magee, N.H. Jr. & Beebe, R., 1973. Bull. am. astr. Soc.,5, 443.

Mestel, L., 1950. Proc. Camb. phil. Soc., 46, 331.

Mihalas, D., 1978. 'Stellar Atmospheres', 2nd ed., W.H. Freeman & Co., San Francisco.

Monet, D.G., 1980. Astrophys. J., 237, 513.

Moore, C.E., 1949. Circular of the National Bureau of Standards, 467.

Morse, P.M., 1940. Astrophys. J., 92, 27.

Newell, E.B., 1970. Astrophys. J., 159, 443.

Nissen, P.E., 1982. Messenger, 28, 4.

Odell, A.P., 1974. Astrophys. J., 192, 417.

Parsian, I., Resfsdal, S. & Stabell, R., 1974. Astr.Astrophys., 30, 275.

Petty, A.F., 1973. Astr. Space Sci., 21, 189.

Reeves, H., 1965. In 'Stars and Stellar Systems': Vol.8, p.113, eds. Aller, L.H. & McLaughin, D.B., University of Chicago Press, Chicago.

Refsdal, S. & Stabell, R., 1972. Astr. Astrophys., 20, 19, (RS72).

Remie, H. & Lamers, H.J.G.L.M., 1982. Astr. Astrophys., 105, 85.

Robertson, J.W. & Faulkner, D.J., 1972. Astrophys. J., 171, 309.

Rood, R.T., 1971. Astrophys. J., 161, 191.

Rood, R.T., 1972. Astrophys. J., 177, 681.

Rood, R.T., 1973. Astrophys. J., 184, 815.

Rood, R.T. & Iben, I. Jr., 1968. Astrophys. J. 154, 215.

Sakashita, S., Ono, Y. & Hayashi, C., 1959. Progress theor.Phys., 21, 315.

Salpeter, E.E., 1954. Austr. J. Phys., 7, 373.

Sampson, D.H., 1959. Astrophys. J., 129, 734.

Sandage, A., 1982. Astrophys. J., 252, 553.

Sandage, A. & Tammann, G.A., 1982. Astrophys. J., 256, 339.

Schwarzschild, K., 1906. Gottinger Nachrichten, p.41.

Schwarzschild, M., 1958. 'Structure and Evolution of the Stars', Princeton University Press.

Schwarzschild, M., 1970. Q.J.R. astr. Soc., 11, 12.

Schwarzschild, M. & Härm, R., 1966. Astrophys. J., 145, 496.

Semeniuk, I., 1967. Acta astr., 17, 223.

Smak, J., 1967. Acta astr., 17, 245.

Spitzer, L. Jr., & Härm, R., 1953. Phys. Rev. 89, 977.

Stabell, R., 1975. Astr. Astrophys., 44, 315.

Stellingwerf, R.F., 1975. Astrophys. J., 195, 441.

Stothers, R., 1974a. Astrophys. J., 194, 695.

Stothers, R., 1974b. Astrophys. J., 194, 651.

Stothers, R., 1976a. Astrophys. J., 204, 461.

Stothers, R., 1976b. Astrophys. J., 204, 853.

Stothers, R., 1976c. Astrophys. J., 209, 800.

Stothers, R., 1981. Astrophys. J., 247, 941.

Strömgren, B., 1932. Z. Astrophys., 4, 118.

Sweigart, A.V. & Demarque, P., 1972. Astr. Astrophys., 20, 445.

Sweigart, A.V. & Gross, P.G., 1974. Astrophys. J. 190, 101.

Sweigart, A.V. & Gross, P.G., 1976. Astrophys. J. Suppl. Ser., 32, 367, (SG76).

Sweigart, A.V. & Gross, P.G., 1978. Astrophys.J.Suppl.Ser., 36, 405.

Thomas, H.C., 1967. Z. Astrophys., 67, 420.

Underhill, A.B., 1980. Astrophys. J., 239, 220.

Vardya, M.A., 1965. Mon. Not. R. astr. Soc., 129, 205.

Vemury, S.K. & Stothers, R., 1978. Astrophys. J., 225, 939.

Vitense, E., 1953. Z. Astrophys., 32, 135.

Weigert, A., 1966. Z. Astrophys., 64, 395.

Wilson, R.E., 1981. Astr. Astrophys., 99, 43.

APPENDIX A.2

THE CARSON OPACITIES

The Carson opacities tabulated for 28 chemical mixtures are presented here with the kind permission of Dr T.R. Carson. The mixtures are described in table 3.2 and in each table heading. Logarithms are used throughout to give the Rosseland mean opacity due to the radiative and conductive opacities as a function of temperature and density. The format in which the tables are presented is originally due to Carson et al (1981). Further discussion of the tables may be found in §3.2.

Opacity c400 for composition : H=1.000, He=0.000, Z=0.000

Log Opacity (cms2/gm)

Log Rho / Log T	I	I	I+1	I+2	I+3	I+4	I+5	I+6	I+7	I+8	I+9
3.3	-12	-2.0415	-2.1673	-2.4882	-2.9251	-3.3997	-3.8775	-4.3584	-4.8980	-5.8009	-4.0852
3.4	-12	-1.9987	-1.9998	-2.0092	-2.0816	-2.3353	-2.7413	-3.2029	-3.6643	-4.1948	-3.8068
3.5	-12	-1.9730	-1.9730	-1.9731	-1.9744	-1.9871	-2.0766	-2.3538	-2.7614	-3.1650	-3.0942
3.6	-11	-1.9380	-1.9373	-1.9347	-1.9266	-1.9043	-1.8629	-1.8556	-1.7972	-1.1182	1.1004
3.7	-11	-1.8543	-1.8461	-1.7839	-1.6274	-1.3346	-0.8996	-0.3650	0.1267	0.7700	2.3584
3.8	-11	-1.2863	-1.3113	-1.0833	-0.6657	-0.1583	0.3605	0.9359	1.3991	2.0912	3.2940
3.9	-11	-0.0749	0.0131	0.1707	0.4224	0.7446	1.1336	1.6157	2.2155	2.9536	3.9376
4.0	-11	0.0848	0.7560	1.3115	1.5803	2.0607	1.8119	2.4108	2.8908	3.5654	4.3824
4.1	-10	0.4428	1.3602	2.1579	2.6457	2.9081	3.1616	3.5135	4.1111	4.3551	5.0177
4.2	-10	0.0913	0.8894	1.8935	2.8439	3.4520	3.8150	4.1285	4.6317	4.7436	5.2284
4.3	-10	-0.1102	0.5030	1.4770	2.5608	3.5528	4.3383	4.6772	5.0731	5.1245	5.5592
4.4	-10	-0.1767	0.2689	1.1656	2.2552	3.3701	4.3562	5.0635	5.1955	5.4705	5.9282
4.5	-10	-0.2040	0.1717	0.9769	2.0413	3.1878	4.4220	5.1516	5.5115	5.5003	6.1021
4.6	-9	0.0732	0.8272	1.8520	2.9573	4.0568	4.8814	5.4150	5.5340	4.6700	2.1151
4.7	-9	-0.0776	0.5603	1.5246	2.5460	3.4423	4.3369	5.0135	5.3031	4.9075	2.5146
4.8	-9	-0.3006	0.2105	1.0117	1.9790	2.7837	3.7126	4.4996	4.5446	4.8075	2.5431
4.9	-9	-0.3453	-0.0777	0.5136	1.3917	2.1529	3.1028	3.9647	4.4766	4.6397	2.8019
5.0	-9	-0.4004	-0.2496	0.1529	0.8504	1.7771	2.5055	3.4397	4.1046	4.4558	3.1962
5.2	-8	-0.3749	-0.2601	0.1044	0.9303	1.4325	2.4471	3.2250	3.6187	4.2020	1.4896
5.4	-8	-0.3987	-0.3731	-0.2488	0.2995	0.5297	1.5222	2.3572	3.0807	3.9758	2.0327
5.6	-7	-0.3968	-0.3651	-0.0962	0.0233	0.7108	1.4942	2.5424	3.2858	2.7228	0.3950
5.8	-7	-0.4005	-0.3942	-0.2959	-0.2331	0.1591	0.7544	1.5951	2.4976	3.1623	0.5571
6.0	-7	-0.4012	-0.3994	-0.3944	-0.3565	-0.2286	0.1980	0.8872	1.7398	2.6444	1.4968
6.2	-6	-0.4015	-0.3995	-0.3889	-0.3324	-0.1527	0.5120	1.0109	1.9358	2.3162	-0.2693
6.4	-6	-0.4024	-0.4003	-0.3975	-0.3871	-0.3226	-0.0657	0.4035	1.2191	1.9994	0.2092
6.6	-5	-0.4034	-0.4000	-0.3976	-0.3785	-0.2670	-0.0154	0.5855	1.4282	1.0465	-1.3763
6.8	-5	-0.4050	-0.4005	-0.3996	-0.3934	-0.3556	-0.2467	0.1056	0.7947	1.2815	-0.9444
7.0	-5	-0.4075	-0.4075	-0.4075	-0.4070	-0.3987	-0.3550	-0.1895	0.2490	0.8754	-0.2758
7.2	-4	-0.4115	-0.4115	-0.4115	-0.4100	-0.4001	-0.3557	-0.1139	0.3955	0.4955	-2.0773
7.4	-4	-0.4176	-0.4176	-0.4176	-0.4174	-0.4154	-0.4009	-0.3220	-0.0327	0.2453	-1.5250
7.6	-3	-0.4271	-0.4271	-0.4272	-0.4268	-0.4231	-0.3958	-0.2649	-0.0375	-0.6719	-3.1258
7.8	-3	-0.4415	-0.4415	-0.4414	-0.4414	-0.4410	-0.4355	-0.3953	-0.2739	-0.3864	-2.7150
8.0	-3	-0.4622	-0.4622	-0.4622	-0.4622	-0.4624	-0.4622	-0.4533	-0.4155	-0.4550	-2.0211
8.2	-2	-0.4919	-0.4919	-0.4919	-0.4920	-0.4924	-0.4922	-0.4868	-0.5163	-1.1066	-3.0291
8.4	-2	-0.5323	-0.5323	-0.5323	-0.5323	-0.5325	-0.5335	-0.5361	-0.5912	-0.9467	-5.2304
8.6	-1	-0.5842	-0.5842	-0.5842	-0.5843	-0.5848	-0.5875	-0.6170	-0.8465	-2.3071	-4.8021
8.8	-1	-0.6476	-0.6476	-0.6476	-0.6476	-0.6479	-0.6493	-0.6643	-0.9650	-1.7093	-4.4590
9.0	-1	-0.7217	-0.7217	-0.7217	-0.7217	-0.7218	-0.7225	-0.7300	-0.8667	-1.5149	-3.7147

Opacity c310 for composition : H=0.750, He=0.250, Z=0.000

Log Opacity (cms2/gm)

Log Rho / Log T	I	I	I+1	I+2	I+3	I+4	I+5	I+6	I+7	I+8	I+9
3.3	-12	-2.1602	-2.2651	-2.5630	-2.9886	-3.4534	-3.9099	-4.3142	-4.6813	-4.7986	-4.0259
3.4	-12	-2.1230	-2.1238	-2.1310	-2.1890	-2.4168	-2.8085	-3.2615	-3.7100	-4.1916	-3.9458
3.5	-12	-2.0974	-2.0974	-2.0975	-2.0985	-2.1081	-2.1807	-2.4331	-2.8290	-3.2319	-3.2377
3.6	-11	-2.0624	-2.0619	-2.0596	-2.0525	-2.0324	-1.9909	-1.9695	-1.9228	-1.3144	0.7272
3.7	-11	-1.9769	-1.9737	-1.9192	-1.7759	-1.4965	-1.0772	-0.5444	-0.0404	0.5861	2.0571
3.8	-11	-1.3889	-1.4443	-1.2423	-0.8371	-0.3412	0.1771	0.7523	1.2098	1.9013	3.0426
3.9	-11	-0.2203	-0.1239	0.0275	0.2704	0.5942	0.9837	1.4676	2.0338	2.7513	4.7080
4.0	-11	-0.0968	0.5263	1.1356	1.4266	1.6671	1.9245	2.2684	2.7253	3.3804	4.7001
4.1	-10	0.2295	1.1346	1.9512	2.4840	2.7766	3.0580	3.3601	3.9210	4.7654	3.0615
4.2	-10	-0.0549	0.6924	1.6682	2.6353	3.2947	3.6976	3.9836	4.4471	4.7269	3.3681
4.3	-10	-0.2328	0.3343	1.2721	2.3131	3.3092	4.1169	4.4627	3.6825	4.9414	3.7050
4.4	-10	-0.2874	0.1184	0.9801	2.0394	3.1441	4.2600	4.8093	5.2055	5.2601	4.0265
4.5	-10	-0.2510	0.0634	0.8199	1.8495	2.9825	4.1936	4.9828	5.4484	5.2698	4.4336
4.6	-9	0.0694	0.8100	1.7621	2.8272	3.9915	4.8626	5.4689	5.4676	5.0877	2.1746
4.7	-9	-0.1639	0.6175	1.6823	2.6700	3.6463	4.5275	5.2435	4.2905	5.0005	2.3651
4.8	-9	-0.3333	0.1900	1.1501	2.2870	3.2457	4.1551	4.9051	4.8122	4.9659	2.6641
4.9	-9	-0.3652	-0.0737	0.6955	1.7584	2.7679	3.8245	4.6083	4.8322	5.0732	2.9770
5.0	-9	-0.4272	-0.2042	0.3939	1.3752	2.3698	3.4952	4.3500	4.6703	4.8396	3.3262
5.2	-8	-0.4065	-0.1329	0.5625	1.4627	2.4476	3.5177	3.9724	3.9921	4.2253	1.5413
5.4	-8	-0.4532	-0.4051	-0.1815	0.4378	1.1407	2.0491	2.9509	3.4618	3.9773	2.1386
5.6	-7	-0.4509	-0.4052	-0.2433	0.3986	0.9777	1.9447	2.8195	3.3601	2.9089	0.4669
5.8	-7	-0.4576	-0.4500	-0.3636	-0.0240	0.2149	1.0566	1.7708	2.5949	3.1805	0.9449
6.0	-7	-0.4587	-0.4567	-0.3962	-0.4487	-0.2378	0.3047	0.9769	1.8259	2.0422	1.6103
6.2	-6	-0.4590	-0.4566	-0.4437	0.2355	-0.1320	0.3310	1.0698	1.9271	2.3374	-0.2140
6.4	-6	-0.4599	-0.4578	-0.4554	-0.1209	-0.3635	-0.0917	0.4256	1.2045	1.9956	0.3793
6.6	-5	-0.4609	-0.4575	-0.4549	-0.4346	-0.3122	-0.0284	0.5581	1.4007	1.2356	-1.3048
6.8	-5	-0.4625	-0.4581	-0.4572	-0.4520	-0.4099	-0.2849	0.0655	0.7559	1.2897	-0.8547
7.0	-5	-0.4651	-0.4651	-0.4650	-0.4644	-0.4549	-0.4133	-0.2577	0.2071	0.8550	-0.1667
7.2	-4	-0.4690	-0.4690	-0.4690	-0.4675	-0.4536	-0.3887	-0.1598	0.3562	0.5128	-2.0056
7.4	-4	-0.4751	-0.4752	-0.4751	-0.4751	-0.4720	-0.4529	-0.3589	-0.0592	0.2566	-1.4210
7.6	-3	-0.4847	-0.4847	-0.4847	-0.4842	-0.4801	-0.4503	-0.3168	-0.0644	-0.4707	-3.0635
7.8	-3	-0.4989	-0.4989	-0.4989	-0.4989	-0.4985	-0.4918	-0.4475	-0.3249	-0.3709	-2.6071
8.0	-3	-0.5197	-0.5197	-0.5198	-0.5198	-0.5199	-0.5196	-0.5090	-0.4655	-0.4728	-1.9110
8.2	-2	-0.5494	-0.5494	-0.5495	-0.5495	-0.5497	-0.5490	-0.5399	-0.5513	-1.0601	-3.7703
8.4	-2	-0.5898	-0.5898	-0.5898	-0.5899	-0.5900	-0.5907	-0.5917	-0.6311	-0.9501	-3.1282
8.6	-1	-0.6418	-0.6418	-0.6418	-0.6418	-0.6425	-0.6442	-0.6661	-0.8591	-2.0751	-4.8110
8.8	-1	-0.7052	-0.7052	-0.7052	-0.7052	-0.7054	-0.7066	-0.7186	-0.9595	-1.6866	-4.3517
9.0	-1	-0.7792	-0.7792	-0.7792	-0.7792	-0.7795	-0.7799	-0.7860	-0.8945	-1.4966	-3.6021

Opacity c220 for composition : H=0.500, He=0.500, Z=0.000

Log Opacity (cms2/gm)

Log T \ Log Rho	I	I	I+1	I+2	I+3	I+4	I+5	I+6	I+7	I+8	I+9
3.3	-12	-2.3295	-2.4085	-2.6716	-3.0788	-3.5291	-3.9574	-4.3021	-4.5548	-4.5927	-4.0501
3.4	-12	-2.2980	-2.2985	-2.3034	-2.3449	-2.5360	-2.9043	-3.3442	-3.7743	-4.0967	-4.0171
3.5	-12	-2.2724	-2.2724	-2.2725	-2.2731	-2.2796	-2.3325	-2.5487	-2.9249	-3.3226	-3.4005
3.6	-11	-2.2374	-2.2371	-2.2352	-2.2293	-2.2118	-2.1718	-2.1343	-2.0909	-1.5663	0.2867
3.7	-11	-2.1478	-2.1521	-2.1072	-1.9807	-1.7255	-1.3224	-0.7938	-0.2687	0.3415	1.6952
3.8	-11	-1.5280	-1.6251	-1.4589	-1.0729	-0.5855	-0.0726	0.4976	1.0004	1.6395	2.7306
3.9	-11	-0.4209	-0.3163	-0.1706	0.0647	0.3873	0.7807	1.2689	1.7898	2.0123	3.4393
4.0	-11	-0.3711	0.2307	0.8866	1.2203	1.4797	1.7453	2.1269	2.5179	3.2077	4.0104
4.1	-10	-0.0575	0.7865	1.6597	2.2624	2.5997	2.9199	3.1978	3.7460	4.2704	3.1794
4.2	-10	-0.2345	0.4464	1.3705	2.3479	3.0823	3.5466	3.8788	4.3571	4.3212	3.5376
4.3	-10	-0.3838	0.1320	1.0263	2.0002	2.9749	3.8168	4.4606	4.5202	4.7015	3.6629
4.4	-10	-0.4277	-0.0611	0.7523	1.7840	2.8524	3.9394	4.9595	5.0160	5.0710	4.2007
4.5	-10	-0.4611	-0.0840	0.6183	1.6068	2.7138	3.9474	5.0708	5.2552	5.2120	4.7057
4.6	-9	-0.0011	0.7092	1.5939	2.5865	3.8382	4.8600	5.3599	5.4604	4.9987	2.2056
4.7	-9	-0.2135	0.5657	1.6339	2.5626	3.5842	4.6348	5.2108	4.1149	5.0259	2.4502
4.8	-9	-0.3965	0.0981	1.0975	2.2520	3.2844	4.5246	4.9406	4.9327	5.0225	2.7971
4.9	-9	-0.4662	-0.1577	0.5895	1.6740	2.8280	3.8261	4.6845	4.9714	5.2268	3.1260
5.0	-9	-0.4747	-0.2670	0.3038	1.2932	2.4309	3.5352	4.4929	4.8548	5.0166	3.4850
5.2	-8	-0.4488	-0.1275	0.6263	1.5910	2.6373	3.6902	4.1979	4.1453	4.2412	1.6265
5.4	-8	-0.5167	-0.4507	-0.1603	0.5014	1.3240	2.2271	3.1392	3.7721	3.9914	2.2614
5.6	-7	-0.5149	-0.4548	-0.1878	0.5059	1.1135	2.0961	2.7542	3.4121	3.1323	0.5526
5.8	-7	-0.5238	-0.5137	-0.4541	0.3926	0.2771	1.1669	1.6629	2.0556	3.1856	1.0694
6.0	-7	-0.5251	-0.5228	-0.5121	-0.3394	0.8742	0.3407	1.0235	1.6747	2.6128	1.7395
6.2	-6	-0.5254	-0.5225	-0.4653	0.3438	-0.1413	0.3305	1.1003	1.8950	2.3628	-0.1230
6.4	-6	-0.5265	-0.5241	-0.5212	-0.0688	-0.4350	-0.1272	0.4253	1.1699	1.9857	0.5076
6.6	-5	-0.5272	-0.5241	-0.5205	-0.4992	-0.3725	-0.0560	0.5157	1.3660	1.4262	-1.2207
6.8	-5	-0.5289	-0.5244	-0.5232	-0.5170	-0.4766	-0.3324	0.0147	0.7096	1.2909	-0.7090
7.0	-5	-0.5314	-0.5314	-0.5313	-0.5309	-0.5207	-0.4722	-0.2947	0.1597	0.8253	-0.0462
7.2	-4	-0.5353	-0.5353	-0.5351	-0.5333	-0.5182	-0.4504	-0.2131	0.3067	0.5221	-1.9198
7.4	-4	-0.5416	-0.5416	-0.5416	-0.5414	-0.5379	-0.5174	-0.4185	-0.1166	0.2492	-1.2901
7.6	-3	-0.5510	-0.5510	-0.5510	-0.5505	-0.5459	-0.5135	-0.3773	-0.0991	-0.2871	-2.9901
7.8	-3	-0.5652	-0.5652	-0.5652	-0.5652	-0.5647	-0.5569	-0.5098	-0.3704	-0.3594	-2.4641
8.0	-3	-0.5861	-0.5861	-0.5861	-0.5861	-0.5862	-0.5855	-0.5734	-0.5200	-0.4966	-1.7917
8.2	-2	-0.6158	-0.6158	-0.6158	-0.6159	-0.6159	-0.6145	-0.6018	-0.5949	-1.0267	-3.6945
8.4	-2	-0.6562	-0.6562	-0.6562	-0.6562	-0.6565	-0.6567	-0.6561	-0.6801	-0.9558	-3.0059
8.6	-1	-0.7081	-0.7081	-0.7081	-0.7082	-0.7085	-0.7098	-0.7255	-0.8840	-1.8567	-4.7486
8.8	-1	-0.7715	-0.7715	-0.7715	-0.7715	-0.7717	-0.7727	-0.7817	-0.9676	-1.6682	-4.2275
9.0	-1	-0.8456	-0.8456	-0.8456	-0.8456	-0.8456	-0.8461	-0.8509	-0.9341	-1.4817	-3.4657

Opacity c130 for composition : H=0.750, He=0.250, Z=0.000

Log Opacity (cms2/gm)

Log Rho / Log T	I	I	I+1	I+2	I+3	I+4	I+5	I+6	I+7	I+8	I+9
3.3	-12	-2.6214	-2.6670	-2.8671	-3.2354	-3.6572	-4.0394	-4.3097	-4.4706	-4.4730	-4.0350
3.4	-12	-2.5958	-2.5961	-2.5985	-2.6209	-2.7526	-3.0724	-3.4847	-3.8809	-4.1518	-4.0590
3.5	-12	-2.5704	-2.5704	-2.5704	-2.5707	-2.5740	-2.6031	-2.7579	-3.0913	-3.4704	-3.5955
3.6	-11	-2.5351	-2.5351	-2.5338	-2.5294	-2.5160	-2.4800	-2.4210	-2.3627	-1.9277	-0.2861
3.7	-11	-2.4351	-2.4523	-2.4211	-2.3192	-2.0957	-1.7155	-1.1992	-0.6680	-0.0377	1.1984
3.8	-11	-1.7551	-1.9136	-1.8091	-1.4866	-0.9853	-0.4771	0.0866	0.5637	1.2168	2.2641
3.9	-11	-0.7705	-0.6433	-0.4997	-0.2728	0.0515	0.4554	0.9547	1.3991	2.0372	3.0443
4.0	-11	-0.7785	-0.2699	0.4366	0.8591	1.1638	1.4547	1.8657	2.1809	2.6895	3.7031
4.1	-10	-0.4923	0.2501	1.1536	1.8792	2.2948	2.6786	2.9028	3.2722	4.2622	3.4040
4.2	-10	-0.4700	0.1131	0.9232	1.8739	2.7097	3.2845	3.5440	3.8296	4.7759	3.7346
4.3	-10	-0.5822	-0.1370	0.7110	1.5653	2.4391	3.2553	3.9718	4.2207	5.3499	4.0656
4.4	-10	-0.6190	-0.2959	0.4743	1.4396	2.4480	3.3891	4.3696	4.6149	5.5241	4.5127
4.5	-10	-0.5283	-0.2505	0.3579	1.2711	2.3536	3.4994	4.5469	4.8695	5.0129	4.9169
4.6	-9	-0.0669	0.5757	1.3447	2.2499	3.3947	4.4529	5.0327	5.2131	4.9516	2.3811
4.7	-9	-0.3280	0.4755	1.4972	2.3758	3.2550	4.1715	4.9952	4.6807	4.9943	2.6629
4.8	-9	-0.4785	-0.0282	0.9839	2.1790	3.1156	4.0147	4.8018	5.0039	5.3959	2.9955
4.9	-9	-0.5339	-0.2755	0.4441	1.5485	2.7137	3.8286	4.6460	5.0370	5.3053	3.3339
5.0	-9	-0.5398	-0.3584	0.1699	1.1489	2.3123	3.5970	4.5296	4.9443	5.1286	3.8271
5.2	-8	-0.5117	-0.1722	0.5842	1.6290	2.7049	3.7691	4.2991	4.2555	4.2607	1.7608
5.4	-8	-0.5925	-0.5110	-0.1771	0.5071	1.5426	2.3113	3.2235	3.8833	3.9453	2.4090
5.6	-7	-0.5909	-0.5184	-0.2275	0.6095	1.1222	2.1574	2.8261	3.1750	3.3563	0.6566
5.8	-7	-0.6018	-0.5894	-0.5080	0.1201	1.4883	1.1873	1.9074	2.5655	3.1442	1.2179
6.0	-7	-0.6035	-0.6009	-0.5878	-0.3927	-0.2456	0.3264	1.0578	1.8088	2.5440	1.9528
6.2	-6	-0.6037	-0.6004	-0.5527	0.3455	-0.2034	0.3081	1.0560	1.8301	2.3872	0.0256
6.4	-6	-0.6046	-0.6024	-0.6000	-0.5783	-0.5055	-0.1810	0.3840	1.1117	1.9666	0.6610
6.6	-5	-0.6056	-0.6022	-0.5974	-0.5648	-0.4434	-0.1106	0.4359	1.3238	1.4987	-1.1116
6.8	-5	-0.6072	-0.6027	-0.6020	-0.5942	-0.5508	-0.3973	-0.0489	0.6601	1.2827	-0.5595
7.0	-5	-0.6098	-0.6097	-0.6097	-0.6089	-0.6016	-0.5458	-0.3633	0.1038	0.7830	0.2168
7.2	-4	-0.6137	-0.6137	-0.6135	-0.6125	-0.5962	-0.5241	-0.2775	0.2441	0.5258	-1.7774
7.4	-4	-0.6199	-0.6199	-0.6199	-0.6200	-0.6166	-0.5958	-0.4894	-0.1859	0.2367	-1.1235
7.6	-3	-0.6293	-0.6293	-0.6294	-0.6291	-0.6237	-0.5885	-0.4492	-0.1445	-0.2976	-2.0972
7.8	-3	-0.6435	-0.6436	-0.6436	-0.6437	-0.6428	-0.6338	-0.5839	-0.4289	-0.3627	-2.3594
8.0	-3	-0.6644	-0.6644	-0.6644	-0.6645	-0.6645	-0.6652	-0.6496	-0.5868	-0.5262	-1.5321
8.2	-2	-0.6942	-0.6942	-0.6942	-0.6943	-0.6941	-0.6920	-0.6755	-0.6823	-1.0096	-3.5469
8.4	-2	-0.7345	-0.7345	-0.7345	-0.7346	-0.7346	-0.7347	-0.7325	-0.7418	-0.9585	-2.8546
8.6	-1	-0.7865	-0.7865	-0.7865	-0.7865	-0.7867	-0.7874	-0.7965	-0.9175	-1.8351	-4.6691
8.8	-1	-0.8499	-0.8499	-0.8499	-0.8499	-0.8501	-0.8508	-0.8570	-0.9922	-1.6447	-4.0809
9.0	-1	-0.9239	-0.9239	-0.9239	-0.9239	-0.9240	-0.9243	-0.9278	-0.9871	-1.4660	-3.1916

Opacity c040 for composition : H=0.000, He=1.000, Z=0.000

Log Opacity (cms2/gm)

Log Rho / Log T	I	I	I+1	I+2	I+3	I+4	I+5	I+6	I+7	I+8	I+9
3.3	-12	-4.4437	-4.4442	-4.4442	-4.4440	-4.4438	-4.4435	-4.4427	-4.4369	-4.3952	-4.0692
3.4	-12	-4.4261	-4.4265	-4.4264	-4.4262	-4.4260	-4.4257	-4.4250	-4.4209	-4.3919	-4.1798
3.5	-12	-4.4188	-4.4184	-4.4181	-4.4179	-4.4176	-4.4173	-4.4167	-4.4139	-4.3936	-4.2353
3.6	-11	-4.3657	-4.3654	-4.3651	-4.3647	-4.3643	-4.3637	-4.3614	-4.3478	-4.2414	-3.3912
3.7	-11	-4.3326	-4.3327	-4.3326	-4.3326	-4.3326	-4.3323	-4.3308	-4.3203	-4.2381	-3.5665
3.8	-11	-4.1836	-4.1884	-4.1894	-4.1887	-4.1859	-4.1784	-4.1587	-3.9826	-3.7656	-3.1057
3.9	-11	-3.6398	-3.8380	-3.9240	-3.9335	-3.5319	-3.1004	-2.5078	-2.3958	-2.1558	-1.5677
4.0	-11	-2.2535	-2.6384	-2.7717	-2.5062	-2.0355	-1.4950	-0.9115	-0.7558	-0.5753	-0.2403
4.1	-10	-1.3046	-1.3164	-1.0518	-0.6351	-0.1213	0.4563	0.5970	0.7305	0.9549	1.5662
4.2	-10	-0.8398	-0.4326	0.1165	0.5489	1.0309	1.5892	1.7166	1.8192	1.9502	2.2603
4.3	-10	-0.9252	-0.6268	0.0234	0.6797	1.0830	1.3465	1.6963	2.1467	2.7907	2.8129
4.4	-10	-0.9363	-0.7782	-0.3182	0.5028	1.4387	2.0070	2.5004	2.9429	3.5398	3.2979
4.5	-10	-0.6235	-0.5087	-0.2575	0.5168	1.2733	2.1207	2.9576	3.5524	4.1195	3.2751
4.6	-9	-0.1854	0.3768	0.8330	1.3972	1.9995	3.0599	3.9902	4.2310	4.0444	2.8552
4.7	-9	-0.4198	0.3262	1.2684	1.9436	2.3738	2.9859	4.1663	4.6255	4.7552	2.9042
4.8	-9	-0.5928	-0.1804	0.8267	1.9881	2.8627	3.4124	4.2756	4.9091	5.2115	3.5137
4.9	-9	-0.6216	-0.4131	0.2593	1.3676	2.5780	3.5999	4.4646	4.9853	5.2751	3.7600
5.0	-9	-0.6255	-0.4771	-0.0004	0.9507	2.1350	3.4088	4.5024	4.9549	3.1946	4.2564
5.2	-8	-0.5929	-0.2578	0.4751	1.3305	2.7318	3.7973	4.5461	4.2982	4.2561	1.9366
5.4	-8	-0.6859	-0.5908	-0.2257	0.4991	1.4240	2.8192	3.2502	3.8291	3.9515	2.5756
5.6	-7	-0.6845	-0.5998	-0.3069	0.3053	2.0685	2.1558	3.0365	3.1920	3.3520	0.7969
5.8	-7	-0.6972	-0.6825	-0.6080	-0.1366	1.4289	1.1565	2.2601	2.5602	3.0445	1.4035
6.0	-7	-0.6992	-0.6963	-0.6809	-0.4756	0.8398	0.3351	0.9665	1.7976	2.4207	2.2416
6.2	-6	-0.6995	-0.6955	-0.6242	0.2890	-0.2245	0.2506	1.0556	1.7251	2.4066	0.2067
6.4	-6	-0.7002	-0.6981	-0.6771	-0.6695	-0.5527	-0.2652	0.3421	1.0244	1.9347	0.3526
6.6	-5	-0.7012	-0.6978	-0.6917	-0.6485	-0.5321	-0.1726	0.5748	1.2706	1.5391	-0.9725
6.8	-5	-0.7029	-0.6984	-0.6971	-0.6676	-0.6472	-0.4755	-0.1299	0.5995	1.2615	-0.5735
7.0	-5	-0.7054	-0.7054	-0.7053	-0.7058	-0.6956	-0.6352	-0.4490	0.0366	0.7215	0.5556
7.2	-4	-0.7094	-0.7094	-0.7092	-0.7091	-0.6905	-0.6150	-0.3589	0.1595	0.5399	-1.6116
7.4	-4	-0.7156	-0.7156	-0.7156	-0.7154	-0.7117	-0.6876	-0.5776	-0.2711	0.1945	-0.9502
7.6	-3	-0.7250	-0.7250	-0.7252	-0.7249	-0.7187	-0.6806	-0.5571	-0.2069	-0.2504	-2.7743
7.8	-3	-0.7392	-0.7392	-0.7392	-0.7394	-0.7383	-0.7279	-0.6744	-0.5047	-0.5655	-2.1662
8.0	-3	-0.7601	-0.7601	-0.7601	-0.7603	-0.7602	-0.7580	-0.7430	-0.6748	-0.5699	-1.2371
8.2	-2	-0.7898	-0.7898	-0.7899	-0.7899	-0.7896	-0.7867	-0.7665	-0.7406	-1.0277	-3.3095
8.4	-2	-0.8302	-0.8302	-0.8302	-0.8302	-0.8302	-0.8300	-0.8261	-0.8216	-0.9762	-2.6727
8.6	-1	-0.8822	-0.8822	-0.8822	-0.8822	-0.8823	-0.8824	-0.8856	-0.9675	-1.8207	-4.5619
8.8	-1	-0.9456	-0.9456	-0.9456	-0.9456	-0.9457	-0.9461	-0.9496	-1.0387	-1.6191	-3.9002
9.0	-1	-1.0196	-1.0196	-1.0196	-1.0196	-1.0196	-1.0199	-1.0222	-1.0621	-1.4551	-2.7662

Opacity c401 for composition : H=0.990, He=0.000, Z=0.010

Log Opacity (cms2/gm)

Log Rho / Log T	I	I	I+1	I+2	I+3	I+4	I+5	I+6	I+7	I+8	I+9
3.3	-12	-2.0449	-2.1700	-1.6841	-2.9212	-3.3522	-3.3398	-2.5352	-1.5794	-0.5226	1.2940
3.4	-12	-2.0022	-2.0011	-2.0090	-2.0677	-2.2616	-2.4018	-1.9610	-1.0169	0.0612	1.2186
3.5	-12	-1.9760	-1.9728	-1.9649	-1.9313	-1.8293	-1.6492	-1.3718	-0.6340	0.3068	1.0692
3.6	-11	-1.9389	-1.9285	-1.8689	-1.6516	-1.1826	-0.5383	0.0987	0.7847	1.6968	3.1208
3.7	-11	-1.8554	-1.8418	-1.7567	-1.5089	-0.9754	-0.2005	0.5754	1.2503	1.9306	3.2145
3.8	-11	-1.2873	-1.3111	-1.0794	-0.6466	-0.1205	0.4453	1.0794	1.6091	2.2977	3.4179
3.9	-11	-0.0790	0.0130	0.1684	0.4257	0.7537	1.1460	1.6351	2.2366	2.9752	3.9705
4.0	-11	0.0961	0.7471	1.3029	1.5711	1.8067	2.0607	2.4522	2.9048	3.6192	4.5571
4.1	-10	0.4396	1.3497	2.1492	2.6374	2.9072	3.1765	3.5765	4.1351	4.4554	5.0199
4.2	-10	0.0896	0.8867	1.8881	2.8414	3.4495	3.8201	4.1435	4.6476	4.8209	5.2515
4.3	-10	-0.1072	0.5040	1.4698	2.5595	3.5382	4.3373	4.6738	5.0838	5.1774	5.5961
4.4	-10	-0.1668	0.2698	1.1713	2.2476	3.3679	4.5124	5.0678	5.2674	5.5089	5.9514
4.5	-10	-0.1735	0.1825	0.9906	2.0547	3.2136	4.4244	5.1493	5.5225	5.5154	6.2599
4.6	-9	0.2217	0.8829	1.8707	2.9716	4.0460	4.8740	5.4156	5.5361	4.8328	5.1000
4.7	-9	-0.0334	0.7484	1.6564	2.6118	3.5063	4.5384	5.0097	5.5033	4.9165	5.3103
4.8	-9	-0.2407	0.5758	1.2944	2.1694	2.9712	3.7674	4.4975	4.6212	4.8259	5.5474
4.9	-9	-0.1864	0.2532	0.7242	1.7763	2.5144	3.2539	3.9927	4.4725	4.6615	5.0043
5.0	-9	-0.2890	-0.0167	0.3331	1.5875	2.1452	2.8455	3.5238	4.1110	4.4744	3.1969
5.2	-8	-0.3066	0.0677	0.6557	1.4421	2.1181	2.7723	3.5330	3.6869	4.2108	1.4736
5.4	-8	-0.1555	-0.0992	0.8678	0.7706	1.4564	2.0038	2.6246	3.1691	3.9778	2.0394
5.6	-7	0.4138	0.4994	0.3812	0.6660	1.4054	2.0123	2.5034	3.5157	2.7330	0.4010
5.8	-7	0.5778	0.2609	0.2443	0.3852	0.8180	1.4652	2.0612	2.6445	3.1749	0.6455
6.0	-7	0.1754	0.0946	0.1493	0.1684	0.1885	0.9506	1.6401	2.1482	2.7125	1.5089
6.2	-6	-0.1503	-0.1247	-0.1535	-0.0476	0.3498	1.2036	1.7007	2.1550	2.3556	-0.2210
6.4	-6	-0.3374	-0.3213	-0.2685	-0.2517	-0.0638	0.5872	1.1245	1.5411	2.0486	0.2783
6.6	-5	-0.3910	-0.3846	-0.3752	-0.2898	0.0154	0.5041	0.9627	1.5097	1.8639	-1.3024
6.8	-5	-0.4049	-0.3994	-0.3984	-0.3864	-0.3091	-0.0125	0.3856	0.9039	1.5194	-0.9541
7.0	-5	-0.4082	-0.4074	-0.4070	-0.4073	-0.3932	-0.2962	-0.0454	0.3670	0.9220	-0.2073
7.2	-4	-0.4133	-0.4131	-0.4123	-0.4067	-0.3782	-0.2622	-0.0165	0.4448	0.5155	-2.0625
7.4	-4	-0.4197	-0.4197	-0.4197	-0.4189	-0.4140	-0.3708	-0.2526	0.0288	0.2887	-1.5127
7.6	-3	-0.4293	-0.4293	-0.4294	-0.4285	-0.4215	-0.3923	-0.2427	-0.0129	-0.6575	-3.1106
7.8	-3	-0.4435	-0.4435	-0.4435	-0.4435	-0.4428	-0.4342	-0.3659	-0.2753	-0.3705	-2.7051
8.0	-3	-0.4644	-0.4644	-0.4644	-0.4644	-0.4645	-0.4634	-0.4525	-0.4049	-0.4397	-2.0106
8.2	-2	-0.4941	-0.4941	-0.4941	-0.4942	-0.4944	-0.4936	-0.4860	-0.5093	-1.0795	-3.8225
8.4	-2	-0.5345	-0.5345	-0.5345	-0.5345	-0.5347	-0.5353	-0.5373	-0.5889	-0.9372	-3.2256
8.6	-1	-0.5864	-0.5864	-0.5864	-0.5865	-0.5870	-0.5893	-0.6175	-0.8403	-2.2958	-4.5571
8.8	-1	-0.6498	-0.6498	-0.6498	-0.6498	-0.6500	-0.6513	-0.6659	-0.7600	-1.7015	-4.4315
9.0	-1	-0.7238	-0.7238	-0.7238	-0.7239	-0.7239	-0.7246	-0.7319	-0.8652	-1.5095	-3.7065

Opacity c311 for composition : H=0.740, He=0.250, Z=0.010

Log Opacity (cms2/gm)

Log T \ Log Rho	I	I+1	I+2	I+3	I+4	I+5	I+6	I+7	I+8	I+9
3.3 -12	-2.1650	-2.2688	-2.5643	-2.9838	-3.3873	-3.2252	-2.3386	-1.3554	-0.3577	1.1142
3.4 -12	-2.1276	-2.1264	-2.1317	-2.1761	-2.3403	-2.4340	-1.9130	-0.9487	0.1209	1.6931
3.5 -12	-2.1015	-2.0984	-2.0696	-2.0560	-1.9480	-1.7434	-1.3940	-0.6053	0.3308	1.6054
3.6 -11	-2.0641	-2.0533	-1.9918	-1.7718	-1.2950	-0.6367	0.0526	0.6469	1.6336	2.8802
3.7 -11	-1.9791	-1.9699	-1.8910	-1.6465	-1.1024	-0.3150	0.4728	1.5758	1.9305	3.0288
3.8 -11	-1.3919	-1.4457	-1.2373	-0.8177	-0.2961	0.2752	0.9219	2.8545	2.1575	4.9954
3.9 -11	-0.2259	-0.1274	0.0246	0.2710	0.6008	1.2711	1.4907	2.0624	2.7780	4.0630
4.0 -11	-0.0958	0.5244	1.1305	1.4229	1.6688	1.9394	2.3581	2.9327	3.4134	4.4766
4.1 -10	0.2256	1.1197	1.9476	2.4826	2.7806	3.0803	3.4423	3.9363	4.5691	5.0862
4.2 -10	-0.0558	0.6882	1.6632	2.6344	3.3030	3.7159	4.0118	4.4578	4.9197	5.3751
4.3 -10	-0.2285	0.3397	1.2718	2.3118	3.3118	4.1226	4.4966	4.1818	4.9424	5.7129
4.4 -10	-0.2813	0.1271	0.9892	2.0445	3.1525	4.2661	4.6787	5.2065	5.2573	4.0366
4.5 -10	-0.2167	0.0812	0.8555	1.8695	2.9956	4.1961	4.9690	5.4458	5.3053	4.4457
4.6 -9	0.1740	0.8670	1.7629	2.8439	3.9936	4.8800	5.4503	5.5225	5.0063	2.1782
4.7 -9	-0.1239	0.7916	1.7328	2.6876	3.6731	4.5294	5.2411	4.3545	5.0005	2.5867
4.8 -9	-0.2243	0.5516	1.2096	2.5391	3.2863	4.1673	4.9054	4.8163	4.9665	2.6709
4.9 -9	-0.2043	0.1824	0.7832	1.9053	2.8506	3.8502	4.6138	4.8340	5.0760	2.9825
5.0 -9	-0.3161	-0.0413	0.6064	1.6060	2.5148	3.5365	4.3657	4.6740	4.8447	3.5540
5.2 -8	-0.3292	0.0998	0.8916	1.7111	2.6207	3.5532	4.9899	4.0016	4.2264	1.5466
5.4 -8	-0.1755	-0.1004	0.1573	0.8476	1.6905	2.2783	3.0416	3.4962	3.9840	2.1465
5.6 -7	0.4042	0.3970	0.3685	0.8995	1.4757	2.2116	2.7617	3.3856	2.9216	0.4735
5.8 -7	0.5784	0.2554	0.2255	0.4642	0.8780	1.5634	2.1418	2.7126	3.1921	0.9534
6.0 -7	0.1525	0.0787	0.1234	0.1705	0.2594	0.9697	1.6620	2.1988	2.6976	1.6179
6.2 -6	-0.1755	-0.1610	-0.1910	0.5672	0.3391	1.1924	1.7022	2.1217	2.3452	-0.2050
6.4 -6	-0.3894	-0.3939	-0.3346	-0.0442	-0.1001	0.5691	1.1176	1.5405	2.0357	0.3890
6.6 -5	-0.4472	-0.4406	-0.4514	-0.3507	-0.0774	0.4799	0.9457	1.4786	1.2496	-1.2966
6.8 -5	-0.4624	-0.4569	-0.4557	-0.4432	-0.3620	-0.0536	0.3434	0.8693	1.3126	-0.8242
7.0 -5	-0.4659	-0.4650	-0.4645	-0.4646	-0.4490	-0.3417	-0.0885	0.3337	0.6949	-0.1574
7.2 -4	-0.4711	-0.4709	-0.4700	-0.4650	-0.4536	-0.3138	-0.0589	0.4051	0.5314	-1.9949
7.4 -4	-0.4776	-0.4776	-0.4775	-0.4770	-0.4712	-0.4269	-0.2958	-0.0168	0.2829	-1.4121
7.6 -3	-0.4871	-0.4871	-0.4872	-0.4862	-0.4787	-0.4344	-0.2933	-0.0404	-0.4568	-3.0560
7.8 -3	-0.5013	-0.5013	-0.5014	-0.5013	-0.5005	-0.4907	-0.4399	-0.3107	-0.3532	-2.5977
8.0 -3	-0.5222	-0.5222	-0.5222	-0.5222	-0.5223	-0.5215	-0.5086	-0.4580	-0.4606	-1.9040
8.2 -2	-0.5519	-0.5519	-0.5519	-0.5520	-0.5521	-0.5507	-0.5394	-0.5456	-1.0559	-3.7630
8.4 -2	-0.5923	-0.5923	-0.5923	-0.5924	-0.5925	-0.5928	-0.5932	-0.6294	-0.9470	-3.1205
8.6 -1	-0.6442	-0.6442	-0.6443	-0.6443	-0.6447	-0.6464	-0.6669	-0.8574	-2.0647	-4.6053
8.8 -1	-0.7076	-0.7076	-0.7076	-0.7077	-0.7078	-0.7086	-0.7204	-0.9567	-1.6652	-4.5457
9.0 -1	-0.7817	-0.7817	-0.7817	-0.7817	-0.7818	-0.7824	-0.7883	-0.8942	-1.4949	-3.5956

Opacity c221 for composition : H=0.495, He=0.495, Z=0.010

Log Opacity (cms2/gm)

Log Rho / Log T	I	I	I+1	I+2	I+3	I+4	I+5	I+6	I+7	I+8	I+9
3.3	-12	-2.3326	-2.4109	-2.6717	-3.0726	-3.4636	-3.8156	3.1144	-1.4596	-0.4580	0.9059
3.4	-12	-2.3007	-2.2995	-2.3018	-2.3303	-2.4549	-2.5308	2.6524	-1.0505	0.0090	1.5060
3.5	-12	-2.2732	-2.2716	-2.2618	-2.2279	-2.1130	-1.8842	-1.4938	-0.7041	0.2314	1.4894
3.6	-11	-2.2371	-2.2250	-2.1633	-1.9376	-1.4505	-0.7808	-0.0840	0.6410	1.5340	2.6458
3.7	-11	-2.1474	-2.1445	-2.0725	-1.8294	-1.2669	-0.4694	0.3297	1.0576	1.8159	2.8150
3.8	-11	-1.5029	-1.6238	-1.4509	-1.0449	-0.5296	0.0525	0.7140	1.3351	1.9755	2.9565
3.9	-11	-0.4242	-0.3166	-0.1705	0.0687	0.3984	0.8033	1.3031	1.8343	2.6167	3.4656
4.0	-11	-0.3565	0.2320	0.8825	1.2343	1.4909	1.7604	2.2134	2.7421	3.1920	4.0530
4.1	-10	-0.0587	0.7817	1.6604	2.2636	2.6085	2.9475	3.2845	3.7369	4.2626	3.1865
4.2	-10	-0.2259	0.4517	1.3713	2.3505	3.0915	3.5666	3.9112	4.3160	4.5401	3.5432
4.3	-10	-0.3754	0.1394	1.0301	2.0045	2.9843	3.8342	4.4765	4.5337	4.7122	3.6670
4.4	-10	-0.4153	-0.0539	0.7616	1.8049	2.8629	3.9522	4.9866	5.0226	5.0724	4.2057
4.5	-10	-0.4211	-0.0572	0.6567	1.6363	2.7325	3.9538	5.0870	5.2569	5.2095	4.7749
4.6	-9	0.0390	0.7593	1.6208	2.6150	3.8514	4.8570	5.3582	5.4586	4.9966	2.2003
4.7	-9	-0.0642	0.7402	1.6821	2.5849	3.6012	4.6279	5.1962	4.1787	5.0245	2.4035
4.8	-9	-0.2936	0.4914	1.1532	2.2968	3.3217	4.3196	4.9398	4.9347	5.0215	2.8026
4.9	-9	-0.3092	0.1089	0.6978	1.8316	2.8875	3.8516	4.0856	4.9710	5.2213	3.1303
5.0	-9	-0.3099	-0.1078	0.5138	1.4703	2.5136	3.5685	4.4956	4.8464	5.0058	3.4066
5.2	-8	-0.3738	0.0808	0.7574	1.7712	2.7444	3.7115	4.2044	4.1476	4.2432	1.6502
5.4	-8	-0.2135	-0.1252	0.1728	0.8858	1.7656	2.3830	3.1966	3.7822	3.9960	2.2671
5.6	-7	0.4272	0.4030	0.3461	0.9617	1.5434	2.2975	2.8569	3.4326	3.1414	0.5542
5.8	-7	0.5734	0.2890	0.2092	0.6720	0.8821	1.6079	2.1624	2.7659	3.2001	1.0760
6.0	-7	0.1265	0.0542	0.0888	0.1556	1.0065	0.9682	1.0631	2.2103	2.6529	1.7449
6.2	-6	-0.2156	-0.1955	-0.2108	0.4446	0.3160	1.1676	1.7019	2.0048	2.3730	-0.1152
6.4	-6	-0.4479	-0.4295	-0.3906	-0.0021	-0.1662	0.5094	1.1008	1.5202	2.0313	0.5152
6.6	-5	-0.5110	-0.5037	-0.4943	-0.4099	-0.1396	0.4507	0.8935	1.4542	1.4397	-1.2151
6.8	-5	-0.5275	-0.5210	-0.5203	-0.5082	-0.4286	-0.1015	0.3025	0.8328	1.3154	-0.7006
7.0	-5	-0.5309	-0.5299	-0.5295	-0.5299	-0.5138	-0.4041	-0.1584	0.2914	0.8671	-0.0342
7.2	-4	-0.5364	-0.5362	-0.5351	-0.5306	-0.4990	-0.3669	-0.0965	0.3591	0.5395	-1.9108
7.4	-4	-0.5430	-0.5430	-0.5429	-0.5424	-0.5360	-0.4900	-0.3451	-0.0696	0.2754	-1.2819
7.6	-3	-0.5524	-0.5524	-0.5524	-0.5514	-0.5435	-0.4970	-0.3510	-0.0742	-0.2781	-2.9651
7.8	-3	-0.5667	-0.5667	-0.5667	-0.5666	-0.5657	-0.5547	-0.5007	-0.3553	-0.3421	-2.4767
8.0	-3	-0.5875	-0.5875	-0.5875	-0.5876	-0.5876	-0.5855	-0.5719	-0.5135	-0.4857	-1.7842
8.2	-2	-0.6173	-0.6173	-0.6173	-0.6174	-0.6175	-0.6152	-0.6002	-0.5885	-1.0241	-3.6665
8.4	-2	-0.6576	-0.6576	-0.6576	-0.6577	-0.6578	-0.6577	-0.6566	-0.6779	-0.9516	-2.9982
8.6	-1	-0.7096	-0.7096	-0.7096	-0.7096	-0.7099	-0.7109	-0.7256	-0.8819	-1.8558	-4.7451
8.8	-1	-0.7730	-0.7730	-0.7730	-0.7730	-0.7731	-0.7738	-0.7826	-0.9651	-1.6669	-4.2218
9.0	-1	-0.8470	-0.8470	-0.8470	-0.8470	-0.8471	-0.8476	-0.8522	-0.9339	-1.4800	-3.4563

Opacity c151 for composition : H=0.250, He=0.740, Z=0.010

Log Opacity (cms2/gm)

Log Rho / Log T	I	I	I+1	I+2	I+3	I+4	I+5	I+6	I+7	I+8	I+9
3.3	-12	-2.6193	-1.6802	-2.8633	-3.2250	-3.5867	-3.4307	-2.5626	-1.5955	-0.5816	0.7058
3.4	-12	-2.5923	-1.9496	-2.5905	-2.6007	-1.0207	-2.6849	-2.1197	-1.1813	-0.1279	1.2962
3.5	-12	-2.5647	-2.1427	-2.5518	-2.5171	-2.3917	-2.1237	-1.6426	-0.8306	0.0928	1.3211
3.6	-11	-2.3172	-2.5135	-2.4480	-2.2109	-1.7143	-1.0005	-0.2650	0.4808	1.4033	2.3017
3.7	-11	-2.4267	-2.4352	-2.3732	-2.1266	-1.5268	-0.7107	0.1084	0.8529	1.6400	2.5166
3.8	-11	-1.7520	-1.9047	-1.7899	-1.4391	-0.8953	-0.2871	0.4026	1.0478	1.7151	2.6327
3.9	-11	-0.7685	-0.6373	-0.4919	-0.2629	0.0733	0.4956	1.0112	1.4792	2.1161	3.1090
4.0	-11	-0.7587	-0.2374	0.4405	0.8769	1.1727	1.4937	1.9974	2.5340	2.7575	3.7406
4.1	-10	-0.4813	0.2558	1.1634	1.6787	2.3075	2.7162	3.0162	3.3158	4.2530	3.4072
4.2	-10	-0.4585	0.1190	0.9334	1.8854	2.7243	3.3058	3.5919	3.6724	4.7387	3.7571
4.3	-10	-0.5686	-0.1231	0.7197	1.5835	2.4578	3.2859	4.0067	4.2629	5.3096	4.0866
4.4	-10	-0.6030	-0.2727	0.4903	1.4629	2.4724	3.4204	4.4080	4.6320	5.5606	4.5195
4.5	-10	-0.4793	-0.2296	0.3899	1.5120	2.3865	3.5250	4.5606	4.8674	5.0735	4.9177
4.6	-9	-0.0406	0.6385	1.3779	2.2918	3.4109	4.4620	5.0404	5.2240	4.9520	2.5822
4.7	-9	-0.1724	0.6628	1.5481	2.3992	3.2808	4.1890	5.0003	4.6853	4.9949	2.6647
4.8	-9	-0.3736	0.3986	1.0455	2.2268	3.1688	4.0329	4.8134	4.7951	5.3629	2.9957
4.9	-9	-0.3684	0.0001	0.5648	1.7186	2.7812	3.8510	4.6500	5.0361	5.3023	3.3370
5.0	-9	-0.4340	-0.2885	0.3913	1.5432	2.3976	3.6261	4.5526	4.9426	5.1261	3.6515
5.2	-8	-0.4510	0.0588	0.6763	1.7848	2.8021	3.7823	4.3020	4.2555	4.2618	1.7657
5.4	-8	-0.2541	-0.1835	0.1448	0.8874	1.8585	2.4438	3.2679	3.8882	3.9512	2.4118
5.6	-7	0.4187	0.3970	0.2811	1.0059	1.5340	2.3327	3.1425	3.1492	3.1429	0.6626
5.8	-7	0.5624	0.3175	0.1860	0.5150	1.6085	1.5905	2.1964	2.6948	3.1571	1.2218
6.0	-7	0.0922	0.0328	0.0535	0.1546	0.1980	0.9260	1.6495	2.1656	2.6210	1.9574
6.2	-6	-0.2599	-0.2418	-0.2395	0.4597	0.2438	1.1315	1.6689	2.0513	2.4049	0.0295
6.4	-6	-0.5165	-0.4973	-0.4487	-0.4054	-0.1857	0.4352	1.0705	1.4776	2.0269	0.6659
6.6	-5	-0.5854	-0.5772	-0.5687	-0.4725	-0.2112	0.4061	0.8569	1.4305	1.5168	-1.1056
6.8	-5	-0.6038	-0.5984	-0.5962	-0.5850	-0.5014	-0.1507	0.2565	0.7984	1.3254	-0.5559
7.0	-5	-0.6062	-0.6066	-0.6056	-0.6064	-0.5927	-0.4887	-0.1944	0.2564	0.8348	0.2227
7.2	-4	-0.6133	-0.6150	-0.6117	-0.6081	-0.5757	-0.3918	-0.1563	0.3057	0.5551	-1.7711
7.4	-4	-0.6199	-0.6199	-0.6198	-0.6196	-0.6135	-0.5620	-0.4117	-0.1325	0.2658	-1.1165
7.6	-3	-0.6293	-0.6293	-0.6294	-0.6285	-0.6202	-0.5696	-0.4186	-0.1169	-0.2868	-2.6912
7.8	-3	-0.6436	-0.6436	-0.6436	-0.6437	-0.6425	-0.6297	-0.5644	-0.4122	-0.5464	-2.5546
8.0	-3	-0.6644	-0.6644	-0.6645	-0.6645	-0.6645	-0.6617	-0.6464	-0.5807	-0.5126	-1.5502
8.2	-2	-0.6942	-0.6942	-0.6942	-0.6943	-0.6941	-0.6904	-0.6726	-0.6746	-1.0048	-3.5416
8.4	-2	-0.7345	-0.7345	-0.7345	-0.7346	-0.7346	-0.7356	-0.7315	-0.7385	-0.9559	-2.6316
8.6	-1	-0.7865	-0.7865	-0.7865	-0.7865	-0.7867	-0.7870	-0.7952	-0.9145	-1.8345	-4.6643
8.8	-1	-0.8499	-0.8499	-0.8500	-0.8500	-0.8501	-0.8503	-0.8565	-0.9897	-1.6454	-4.0775
9.0	-1	-0.9239	-0.9239	-0.9239	-0.9239	-0.9240	-0.9243	-0.9275	-0.9860	-1.4644	-3.1504

Opacity c041 for composition : H=0.000, He=0.990, Z=0.010

Log Opacity (cm2/gm)

Log T \ Log Rho I	I	I+1	I+2	I+3	I+4	I+5	I+6	I+7	I+8	I+9
3.3 -12	-4.3435	-2.3126	-4.3552	-4.3529	-4.2748	-3.8510	-3.0150	-2.0885	-1.0788	0.3158
3.4 -12	-4.2756	-4.3030	-4.2855	-4.2698	-4.0139	-3.3958	-2.4440	-1.5227	-0.5026	0.9563
3.5 -12	-4.1827	-4.2130	-4.1804	-4.1040	-3.7365	-3.0500	0.2788	-1.1981	-0.2572	1.0203
3.6 -11	-4.0948	-4.0625	-3.8849	-3.3333	-2.5412	-1.6512	-0.7929	0.0061	1.0041	1.8121
3.7 -11	-3.7559	-3.8717	-3.7222	-3.1725	-2.2769	-1.3511	-0.4652	0.2478	0.9494	1.5412
3.8 -11	-3.3848	-3.5535	-3.3846	-2.8274	-2.0481	-1.2202	-0.2925	0.3287	0.8788	1.4149
3.9 -11	-3.2290	-3.2243	-2.9599	-2.4365	-1.6174	-0.7996	0.0100	0.4307	0.8499	1.3621
4.0 -11	-2.2220	-2.4953	-2.4298	-1.5982	-0.9892	0.1919	0.6207	1.0649	1.4499	2.1959
4.1 -10	-1.2828	-1.3101	-0.9357	-0.4746	0.3787	1.0408	1.8625	1.7110	2.2449	3.2553
4.2 -10	-0.8271	-0.4311	0.1096	0.5661	1.1221	1.6926	2.1530	2.1499	2.4705	3.1517
4.3 -10	-0.9082	-0.6085	0.0440	0.7062	1.1312	1.4306	1.9595	2.3320	2.9869	3.1748
4.4 -10	-0.9767	-0.7556	-0.2710	0.5672	1.4756	2.0829	2.5976	3.0455	3.6457	3.5083
4.5 -10	-0.5659	-0.4841	-0.1701	0.4146	1.3643	2.1967	3.0250	3.5970	4.1829	3.4475
4.6 -9	-0.1573	0.4428	0.8862	1.4709	2.1463	3.1277	4.0313	4.4631	4.1315	2.6393
4.7 -9	-0.1327	0.5183	1.3028	1.9821	2.6461	3.1727	4.2055	4.7213	4.8107	2.9655
4.8 -9	-0.4154	0.2807	0.9088	2.0651	2.9075	3.4311	4.2559	4.9307	5.1684	3.5147
4.9 -9	-0.5294	-0.1340	0.4726	1.5714	2.6444	3.6240	4.4980	4.9778	5.1796	3.7602
5.0 -9	-0.4649	-0.4095	0.2787	1.1681	2.2235	3.3694	4.4980	4.9515	3.7738	4.2564
5.2 -8	-0.4391	-0.0584	0.5509	1.6707	2.7812	3.7940	4.3434	4.3099	4.2639	1.9405
5.4 -8	-0.1955	-0.2618	0.1004	0.8325	1.8181	2.8523	3.2882	3.8368	3.9597	2.5796
5.6 -7	0.4650	0.4003	0.2514	0.8362	1.5363	2.5165	3.0761	3.2291	3.3577	0.8005
5.8 -7	0.5708	0.3561	0.1585	0.5885	0.8112	1.5501	2.1525	2.4859	3.0655	1.4076
6.0 -7	0.0608	0.0201	0.0087	0.0924	0.9646	0.8728	1.5905	2.1479	2.5216	2.2868
6.2 -6	-0.3162	-0.2943	-0.2718	0.3722	0.2544	1.0654	1.3949	1.6439	2.2389	0.2122
6.4 -6	-0.5999	-0.5800	-0.5261	-0.4753	-0.2466	0.3689	1.0410	1.4271	2.0012	0.8570
6.6 -5	-0.6771	-0.6685	-0.6609	-0.5581	-0.2966	0.3558	0.9242	1.3885	1.5510	-0.9059
6.8 -5	-0.6972	-0.6933	-0.6902	-0.6794	-0.5947	-0.2400	0.3009	0.7577	1.2871	-0.3679
7.0 -5	-0.7011	-0.7032	-0.7003	-0.7006	-0.6889	-0.5924	-0.2657	0.1872	0.7675	0.5422
7.2 -4	-0.7089	-0.7087	-0.7073	-0.7047	-0.6685	-0.5182	-0.1951	0.2273	0.5577	-1.6012
7.4 -4	-0.7155	-0.7155	-0.7154	-0.7150	-0.7086	-0.6590	-0.4797	-0.1979	0.2247	-0.9249
7.6 -3	-0.7250	-0.7250	-0.7252	-0.7244	-0.7155	-0.6580	-0.4818	-0.1785	-0.2648	-2.7664
7.8 -3	-0.7392	-0.7392	-0.7394	-0.7394	-0.7380	-0.7239	-0.6585	-0.4674	-0.5642	-2.1585
8.0 -3	-0.7601	-0.7601	-0.7602	-0.7603	-0.7602	-0.7568	-0.7397	-0.6864	-0.5553	-1.2159
8.2 -2	-0.7898	-0.7898	-0.7899	-0.7899	-0.7895	-0.7852	-0.7635	-0.7324	-1.0155	-5.3600
8.4 -2	-0.8302	-0.8302	-0.8302	-0.8303	-0.8302	-0.8287	-0.8251	-0.8181	-0.9666	-2.6665
8.6 -1	-0.8822	-0.8822	-0.8823	-0.8823	-0.8823	-0.8819	-0.8845	-0.9620	-1.8088	-4.5561
8.8 -1	-0.9456	-0.9456	-0.9456	-0.9456	-0.9457	-0.9455	-0.9492	-1.0355	-1.8124	-3.8963
9.0 -1	-1.0196	-1.0196	-1.0196	-1.0196	-1.0196	-1.0199	-1.0221	-1.0608	-1.4474	-2.7625

Opacity c402 for composition : H=0.980, He=0.000, Z=0.020

Log Opacity (cms2/gm)

Log Rho / Log T	I	I	I+1	I+2	I+3	I+4	I+5	I+6	I+7	I+8	I+9
3.3	-12	-2.0486	-2.1727	-1.4732	-2.9188	-3.3151	-3.1155	-2.2425	-1.2828	-0.2260	1.5862
3.4	-12	-2.0060	-2.0039	-2.0106	-2.0618	-2.2224	-2.2812	-1.7016	-0.7257	0.3550	2.1148
3.5	-12	-1.9789	-1.9745	-1.9615	-1.9115	-1.7733	-1.5289	-1.1519	-0.3689	0.5685	1.9607
3.6	-11	-1.9406	-1.9227	-1.8274	-1.5377	-1.0090	-0.3276	0.3110	1.0170	1.9426	3.2921
3.7	-11	-1.8570	-1.8393	-1.7384	-1.4232	-0.7590	0.0345	0.8068	1.5725	2.2412	3.4135
3.8	-11	-1.2910	-1.3124	-1.0789	-0.6385	-0.0976	0.4988	1.1747	1.7431	2.4368	3.5156
3.9	-11	-0.0835	0.0076	0.1653	0.4220	0.7538	1.1517	1.6449	2.2539	2.9915	3.9776
4.0	-11	0.0901	0.7414	1.2982	1.5689	1.8102	2.0642	2.4787	2.9077	3.6235	4.5550
4.1	-10	0.4342	1.3438	2.1536	2.6355	2.9081	3.1870	3.6220	4.1378	4.4628	5.0258
4.2	-10	0.0844	0.8792	1.8815	2.8322	3.4476	3.8274	4.1569	4.6516	4.8270	3.2564
4.3	-10	-0.1101	0.4964	1.4625	2.5475	3.5529	4.3366	4.8808	5.0862	5.1825	5.5947
4.4	-10	-0.1686	0.2699	1.1684	2.2431	3.3631	4.5064	5.0711	5.2705	5.5040	5.9575
4.5	-10	-0.1590	0.1909	0.9958	2.0526	3.2029	4.4169	5.1505	5.5209	5.5129	4.2665
4.6	-9	0.2829	0.9110	1.8748	2.9784	4.0466	4.8736	5.4110	5.5347	4.8467	2.1105
4.7	-9	-0.0823	0.8122	1.7050	2.6326	3.5514	4.3503	5.0106	5.3008	4.9171	2.5219
4.8	-9	-0.2202	0.7071	1.4056	2.2411	3.0553	3.8107	4.5119	4.6317	4.8400	2.5525
4.9	-9	-0.1554	0.3313	0.7886	1.6891	2.6434	3.5415	4.0333	4.4968	4.6654	2.8716
5.0	-9	-0.2457	0.0799	0.4117	1.5146	2.2939	2.9895	3.6134	4.1480	4.4924	3.2091
5.2	-8	-0.2768	0.1936	0.8318	1.5820	2.3248	2.9315	3.4079	3.7168	4.2194	1.4761
5.4	-8	-0.0631	0.0222	0.1962	0.9016	1.6624	2.2262	2.7707	3.2306	3.9814	2.3461
5.6	-7	0.6655	0.7621	0.5550	0.8872	1.5904	2.2125	2.6816	3.3427	2.7432	0.4075
5.8	-7	0.8599	0.4996	0.4675	0.6200	1.0051	1.6741	2.2301	2.7257	3.1849	0.8531
6.0	-7	0.3737	0.2866	0.3348	0.3795	0.3602	1.1557	1.8435	2.3036	2.7568	1.5126
6.2	-6	-0.0035	0.0130	-0.0350	0.1080	0.5376	1.4269	1.9222	2.2446	2.3523	-0.2750
6.4	-6	-0.2956	-0.2688	-0.2158	-0.1571	0.0652	0.8031	1.3682	1.6904	2.0900	0.2875
6.6	-5	-0.3819	-0.3734	-0.3565	-0.2316	0.1669	0.7226	1.1231	1.5770	1.6782	-1.5550
6.8	-5	-0.4051	-0.3987	-0.3976	-0.3812	-0.2756	0.1275	0.5470	0.9890	1.3506	-0.9241
7.0	-5	-0.4090	-0.4074	-0.4069	-0.4079	-0.3859	-0.2466	0.0529	0.4566	0.9657	-0.2589
7.2	-4	-0.4152	-0.4148	-0.4139	-0.4067	-0.3651	-0.2076	0.0562	0.4864	0.5325	-2.0546
7.4	-4	-0.4219	-0.4218	-0.4218	-0.4208	-0.4132	-0.3490	-0.2088	0.0652	0.3164	-1.5050
7.6	-3	-0.4315	-0.4314	-0.4315	-0.4305	-0.4205	-0.3684	-0.2220	0.0101	-0.6455	-3.1103
7.8	-3	-0.4457	-0.4457	-0.4457	-0.4456	-0.4446	-0.4325	-0.3790	-0.2601	-0.3576	-2.6964
8.0	-3	-0.4666	-0.4666	-0.4666	-0.4666	-0.4666	-0.4646	-0.4525	-0.4046	-0.4292	-2.0054
8.2	-2	-0.4962	-0.4963	-0.4963	-0.4963	-0.4965	-0.4950	-0.4852	-0.5057	-1.0772	-3.8162
8.4	-2	-0.5366	-0.5367	-0.5367	-0.5367	-0.5369	-0.5371	-0.5386	-0.5871	-0.9350	-3.2216
8.6	-1	-0.5886	-0.5886	-0.5886	-0.5887	-0.5891	-0.5912	-0.6179	-0.8387	-2.2642	-4.8522
8.8	-1	-0.6520	-0.6520	-0.6520	-0.6520	-0.6522	-0.6551	-0.6676	-0.9568	-1.7002	-4.4442
9.0	-1	-0.7260	-0.7260	-0.7260	-0.7260	-0.7261	-0.7268	-0.7359	-0.8646	-1.5079	-3.7026

Opacity C312 for composition : H=0.730, He=0.250, Z=0.020

Log Opacity (cms2/gm)

Log Rho / Log T	I	I	I+1	I+2	I+3	I+4	I+5	I+6	I+7	I+8	I+9
3.3	-12	-2.1699	-2.2726	-2.5661	-2.9806	-3.3354	-2.9775	-2.0451	-1.0597	-0.0611	1.4055
3.4	-12	-2.1326	-2.1304	-2.1344	-2.1712	-2.3000	-2.2948	-1.6450	-0.6573	0.4148	1.9869
3.5	-12	-2.1054	-2.1013	-2.0870	-2.0370	-1.8930	-1.6178	-1.1644	-0.5352	0.6146	1.8919
3.6	-11	-2.0664	-2.0481	-1.9518	-1.6597	-1.1189	-0.4249	0.2489	0.9937	1.8849	4.8583
3.7	-11	-1.9813	-1.9682	-1.8723	-1.5521	-0.8769	-0.0780	0.7061	1.5652	2.1556	3.2271
3.8	-11	-1.3954	-1.4491	-1.2382	-0.6087	-0.2698	0.3374	1.0307	1.9657	2.3180	3.5552
3.9	-11	-0.2322	-0.1320	0.0217	0.2668	0.6011	1.0044	1.5024	2.0856	2.7954	3.6467
4.0	-11	-0.1027	0.5273	1.1224	1.4174	1.6743	1.9430	2.3995	3.0426	3.4267	4.4109
4.1	-10	0.2163	1.1065	1.9379	2.4768	2.7777	3.0907	3.4802	3.9408	4.4427	3.0909
4.2	-10	-0.0597	0.6810	1.6555	2.6317	3.3002	3.7201	4.0312	4.4553	4.9273	3.3819
4.3	-10	-0.2394	0.3331	1.2659	2.3174	3.3059	4.1231	4.5289	4.3851	5.0665	3.7217
4.4	-10	-0.2799	0.1247	0.9872	2.0409	3.1471	4.2552	4.9383	5.1892	5.2102	4.0405
4.5	-10	-0.1970	0.0716	0.8396	1.8735	2.9932	4.1927	4.9874	5.4426	5.3243	4.4605
4.6	-9	0.2255	0.8961	1.7884	2.8435	3.9860	4.8619	5.4605	5.4805	5.0048	2.1651
4.7	-9	-0.1086	0.8410	1.7648	2.6940	3.6848	4.5296	5.2583	4.4185	5.0006	2.3921
4.8	-9	-0.2005	0.6602	1.2553	2.3650	3.3110	4.1744	4.9051	4.6214	4.9672	2.6770
4.9	-9	-0.1643	0.2630	0.8373	1.9706	2.8865	3.8655	4.6177	4.8360	5.0793	2.9879
5.0	-9	-0.2857	0.0446	0.6672	1.5897	2.5305	3.5585	4.3737	4.6776	4.6494	3.3417
5.2	-8	-0.2874	0.2015	0.9851	1.7952	2.7015	3.5796	4.0148	4.0108	4.2236	1.5523
5.4	-8	-0.0675	0.0018	0.2529	0.9480	1.8437	2.4336	3.1067	3.5234	3.9854	2.1557
5.6	-7	0.6606	0.6517	0.5320	1.0440	1.6557	2.3406	2.6786	3.2651	2.8382	0.4796
5.8	-7	0.8445	0.5010	0.4589	0.6649	1.0634	1.7447	2.2690	2.7615	3.2016	0.9018
6.0	-7	0.3559	0.2831	0.3131	0.5765	0.4423	1.1563	1.6551	2.3400	2.7510	1.6203
6.2	-6	-0.0340	-0.0150	-0.0648	0.4172	0.5066	1.4088	1.9162	2.2304	2.3658	-0.1963
6.4	-6	-0.3453	-0.3184	-0.2582	0.0116	0.0356	0.7765	1.3564	1.7100	2.0801	0.3966
6.6	-5	-0.4573	-0.4289	-0.4128	-0.2926	0.0735	0.0955	1.1347	1.5513	1.2675	-1.2885
6.8	-5	-0.4628	-0.4563	-0.4548	-0.4387	-0.3152	0.0854	0.5008	0.9541	1.3497	-0.8137
7.0	-5	-0.4668	-0.4651	-0.4644	-0.4660	-0.4465	-0.2996	0.0145	0.4259	0.9410	-0.1484
7.2	-4	-0.4733	-0.4729	-0.4719	-0.4648	-0.4205	-0.2528	0.0157	0.4508	0.5500	-1.9661
7.4	-4	-0.4800	-0.4800	-0.4799	-0.4793	-0.4711	-0.4050	-0.2554	0.0210	0.3112	-1.4032
7.6	-3	-0.4896	-0.4896	-0.4897	-0.4883	-0.4778	-0.4207	-0.2724	-0.0175	-0.4434	-3.0486
7.8	-3	-0.5038	-0.5038	-0.5039	-0.5058	-0.5028	-0.4898	-0.4550	-0.2978	-0.3395	-2.5665
8.0	-3	-0.5247	-0.5247	-0.5247	-0.5247	-0.5248	-0.5231	-0.5084	-0.4529	-0.4496	-1.8970
8.2	-2	-0.5544	-0.5544	-0.5544	-0.5545	-0.5546	-0.5517	-0.5369	-0.5430	-1.0517	-3.7557
8.4	-2	-0.5948	-0.5948	-0.5948	-0.5949	-0.5950	-0.5940	-0.5947	-0.6279	-0.9443	-3.1129
8.6	-1	-0.6467	-0.6467	-0.6468	-0.6468	-0.6472	-0.6485	-0.6678	-0.8559	-2.0542	-4.7995
8.8	-1	-0.7101	-0.7101	-0.7101	-0.7102	-0.7103	-0.7112	-0.7225	-0.9540	-1.6839	-4.3357
9.0	-1	-0.7842	-0.7842	-0.7842	-0.7842	-0.7843	-0.7843	-0.7906	-0.8941	-1.4932	-3.5891

Opacity c222 for composition : H=0.490, He=0.490, Z=0.020

Log Opacity (cms2/gm)

Log Rho / Log T	I	I	I+1	I+2	I+3	I+4	I+5	I+6	I+7	I+8	I+9
3.3	-12	-2.3358	-2.4133	-2.6721	-3.0680	-3.4119	-3.0739	3.4125	-1.1630	-0.1611	1.2004
3.4	-12	-2.3030	-2.3017	-2.3025	-2.3238	-2.4138	-2.3912	2.9411	-0.7583	0.3033	1.8020
3.5	-12	-2.2755	-2.2722	-2.2568	-2.2062	-2.0554	-1.7555	-1.2622	-0.4339	0.5160	1.7606
3.6	-11	-2.2371	-2.2173	-2.1192	-1.8215	-1.2684	-0.5677	0.1470	0.8840	1.7924	2.8478
3.7	-11	-2.1480	-2.1401	-2.0494	-1.7235	-1.0295	-0.2268	0.5674	1.3706	2.0563	3.0152
3.8	-11	-1.4895	-1.6237	-1.4458	-1.0309	-0.4941	0.1342	0.8518	1.5122	2.3351	3.1175
3.9	-11	-0.4280	-0.3190	-0.1733	0.0660	0.4012	0.8126	1.3212	1.8648	2.5846	3.4917
4.0	-11	-0.3609	0.2277	0.8788	1.2249	1.4884	1.7697	2.2590	2.8628	3.1929	4.0794
4.1	-10	-0.0619	0.7765	1.6561	2.2604	2.6091	2.9623	3.5412	3.7290	4.2964	3.1954
4.2	-10	-0.2295	0.4429	1.3661	2.3452	3.0898	3.5735	3.9258	4.2932	4.3517	3.5466
4.3	-10	-0.3755	0.1367	1.0259	2.0028	2.9866	3.8315	4.4806	4.5522	4.7142	3.8709
4.4	-10	-0.4148	-0.0469	0.7611	1.8012	2.8617	3.9479	4.9573	5.0269	5.0688	4.2106
4.5	-10	-0.3922	-0.0493	0.6464	1.6457	2.7310	3.9448	5.0602	5.2577	5.2072	4.7661
4.6	-9	0.0562	0.7903	1.6273	2.6214	3.8446	4.8521	5.3378	5.4537	4.9982	2.2709
4.7	-9	-0.0216	0.7924	1.7032	2.5934	3.6116	4.6214	5.2049	4.2331	5.0249	2.4910
4.8	-9	-0.2615	0.6022	1.1780	2.5196	3.3430	4.3152	4.9384	4.9305	5.0209	2.5080
4.9	-9	-0.2757	0.1997	0.7475	1.9080	2.9197	3.8646	4.6859	4.9708	5.2197	3.1545
5.0	-9	-0.2629	-0.0156	0.5699	1.5557	2.5605	3.5900	4.4987	4.8533	5.0163	3.4971
5.2	-8	-0.3532	0.1718	0.7973	1.8244	2.7994	3.7276	4.2101	4.1496	4.2434	1.6339
5.4	-8	-0.0654	-0.0425	0.2705	0.9828	1.8951	2.4859	3.2406	3.7912	3.9998	2.2727
5.6	-7	0.6951	0.6711	0.5105	1.0991	1.7056	2.4110	2.9235	3.4521	3.1487	0.5655
5.8	-7	0.8414	0.5414	0.4438	0.8090	1.6675	1.7717	2.3135	2.8334	3.2055	1.0826
6.0	-7	0.3351	0.2638	0.2846	0.3624	1.0685	1.1686	1.8469	2.3484	2.7261	1.7520
6.2	-6	-0.0657	-0.0423	-0.0799	0.4980	0.4755	1.3795	1.9079	2.2060	2.3959	-0.1072
6.4	-6	-0.4000	-0.3701	-0.3059	0.0485	-0.0354	0.6928	1.3361	1.6945	2.0838	0.5228
6.6	-5	-0.4990	-0.4894	-0.4732	-0.3501	-0.0127	0.6460	0.9365	1.3416	1.4270	-1.2035
6.8	-5	-0.5265	-0.5202	-0.5179	-0.5006	-0.3935	0.0344	0.4697	0.9309	1.3635	-0.6924
7.0	-5	-0.5306	-0.5287	-0.5278	-0.5295	-0.5097	-0.3688	-0.0311	0.3875	0.9213	-0.0284
7.2	-4	-0.5375	-0.5371	-0.5359	-0.5296	-0.4859	-0.3064	-0.0106	0.4075	0.5630	-1.9020
7.4	-4	-0.5444	-0.5443	-0.5445	-0.5455	-0.5346	-0.4664	-0.3043	-0.0290	0.3089	-1.2759
7.6	-3	-0.5539	-0.5539	-0.5539	-0.5525	-0.5416	-0.4826	-0.3272	-0.0495	-0.2710	-2.9762
7.8	-3	-0.5681	-0.5681	-0.5681	-0.5680	-0.5668	-0.5545	-0.5100	-0.3664	-0.3401	-2.4694
8.0	-3	-0.5890	-0.5890	-0.5890	-0.5890	-0.5890	-0.5873	-0.5706	-0.5074	-0.4717	-1.7769
8.2	-2	-0.6187	-0.6187	-0.6187	-0.6188	-0.6188	-0.6158	-0.5988	-0.5823	-1.0196	-3.6786
8.4	-2	-0.6591	-0.6591	-0.6591	-0.6591	-0.6592	-0.6588	-0.6571	-0.6758	-0.9479	-2.9926
8.6	-1	-0.7110	-0.7110	-0.7111	-0.7111	-0.7114	-0.7121	-0.7257	-0.8799	-1.8548	-4.7377
8.8	-1	-0.7744	-0.7744	-0.7744	-0.7745	-0.7746	-0.7750	-0.7838	-0.9628	-1.6657	-4.2157
9.0	-1	-0.8485	-0.8485	-0.8485	-0.8485	-0.8485	-0.8490	-0.8531	-0.9337	-1.4785	-3.4510

Opacity c132 for composition : H=0.250, He=0.730, Z=0.020

Log Opacity (cms2/gm)

Log Rho / Log T	I	I	I+1	I+2	I+3	I+4	I+5	I+6	I+7	I+8	I+9
3.3	-12	-2.6172	-1.4515	-2.8599	-3.2165	-0.5216	-3.1924	-2.2682	-1.2971	-0.2903	1.1130
3.4	-12	-2.5891	-1.7833	-2.5855	-2.5890	-2.6142	-2.5395	-1.8493	-0.8880	0.1684	1.5950
3.5	-12	-2.5597	-2.0492	-2.5398	-2.4901	-2.3255	-1.9830	-1.4037	-0.5664	0.3791	1.6154
3.6	-11	-2.2463	-2.4976	-2.3973	-2.0848	-1.5049	-0.7802	-0.0302	0.7266	1.6664	2.0519
3.7	-11	-2.4199	-2.4234	-2.3358	-1.9975	-1.2725	-0.4657	0.3548	1.1622	1.8765	2.7291
3.8	-11	-1.7487	-1.8979	-1.7772	-1.4106	-0.8375	-0.1729	0.5673	1.2652	1.9249	2.8237
3.9	-11	-0.7668	-0.6351	-0.4877	-0.2579	0.0839	0.5155	1.0449	1.5346	2.1848	3.1732
4.0	-11	-0.7561	-0.2342	0.4382	0.8891	1.1839	1.5155	2.0575	2.0899	2.7943	3.7606
4.1	-10	-0.4777	0.2593	1.1677	1.8785	2.3120	2.7369	3.0838	3.3386	4.2445	5.4105
4.2	-10	-0.4568	0.1230	0.9408	1.8872	2.7326	3.3150	3.6269	3.8969	4.7090	5.7595
4.3	-10	-0.5631	-0.1211	0.7156	1.5887	2.4653	3.2992	4.0282	4.2889	5.2748	6.0715
4.4	-10	-0.6001	-0.2729	0.5007	1.4695	2.4797	3.4376	4.4122	4.6655	5.5836	6.5261
4.5	-10	-0.4523	-0.2226	0.4056	1.3277	2.3979	3.5290	4.5673	4.8997	5.7318	6.9188
4.6	-9	-0.0335	0.6757	1.3926	2.3108	3.4222	4.4676	5.0455	5.2318	6.1950	7.3554
4.7	-9	-0.1296	0.7001	1.5489	2.4107	3.3126	4.2012	5.0319	4.6850	4.9698	2.6664
4.8	-9	-0.3264	0.5161	1.0668	2.2524	3.2028	4.0451	4.8103	5.0050	5.3935	2.9962
4.9	-9	-0.3295	0.0997	0.6184	1.8079	2.8203	3.8618	4.6531	5.0351	5.2997	3.3598
5.0	-9	-0.3916	-0.2300	0.4557	1.4280	2.4396	3.6455	4.5334	4.9408	5.1227	3.6560
5.2	-8	-0.3952	0.1539	0.7136	1.8449	2.8530	3.7922	4.3009	4.2497	4.2480	1.7663
5.4	-8	-0.1330	-0.0556	0.2529	0.9833	1.9752	2.5181	3.3040	3.3956	3.9568	2.4140
5.6	-7	0.6901	0.6421	0.4576	1.1334	1.6895	2.4281	2.9704	3.2208	3.3596	0.6657
5.8	-7	0.8356	0.5771	0.4291	0.6960	1.6758	1.7492	2.3205	2.7686	3.1683	1.2256
6.0	-7	0.3061	0.2486	0.2571	0.5476	0.3751	1.1049	1.8297	2.5139	2.6723	1.9618
6.2	-6	-0.0997	-0.0781	-0.0957	0.4905	0.4075	1.3414	1.8758	2.1709	2.4249	0.0349
6.4	-6	-0.4642	-0.4322	-0.3567	-0.2890	-0.0290	0.6448	1.3059	1.6579	2.0708	0.6706
6.6	-5	-0.5705	-0.5598	-0.5455	-0.4077	-0.0811	0.6239	1.0545	1.5121	1.5315	-1.0995
6.8	-5	-0.6008	-0.5948	-0.5916	-0.5776	-0.4650	-0.0062	0.4507	0.8996	1.3612	-0.5464
7.0	-5	-0.6029	-0.6034	-0.6021	-0.6046	-0.5852	-0.4353	-0.0794	0.3624	0.8798	0.2282
7.2	-4	-0.6128	-0.6124	-0.6107	-0.6054	-0.5614	-0.2993	-0.0746	0.3590	0.5748	-1.7651
7.4	-4	-0.6198	-0.6198	-0.6197	-0.6195	-0.6107	-0.5353	-0.3676	-0.0857	0.2940	-1.1135
7.6	-3	-0.6294	-0.6294	-0.6294	-0.6282	-0.6172	-0.5485	-0.3925	-0.0914	-0.2769	-2.6653
7.8	-3	-0.6436	-0.6436	-0.6436	-0.6437	-0.6422	-0.6258	-0.5460	-0.3965	-0.3511	-2.5500
8.0	-3	-0.6645	-0.6645	-0.6645	-0.6645	-0.6645	-0.6600	-0.6353	-0.5733	-0.4994	-1.5283
8.2	-2	-0.6942	-0.6942	-0.6943	-0.6943	-0.6940	-0.6897	-0.6697	-0.6674	-1.0002	-5.5564
8.4	-2	-0.7345	-0.7345	-0.7346	-0.7346	-0.7346	-0.7356	-0.7307	-0.7353	-0.9493	-2.8486
8.6	-1	-0.7865	-0.7865	-0.7865	-0.7866	-0.7867	-0.7868	-0.7942	-0.9115	-1.8338	-4.6597
8.8	-1	-0.8500	-0.8500	-0.8500	-0.8500	-0.8501	-0.8502	-0.8564	-0.9872	-1.6420	-4.0741
9.0	-1	-0.9239	-0.9239	-0.9240	-0.9239	-0.9240	-0.9244	-0.9271	-0.9850	-1.4628	-3.1492

Opacity c042 for composition : H=0.000, He=0.980, Z=0.020

Log Opacity (cms2/gm)

Log Rho / Log T	I	I	I+1	I+2	I+3	I+4	I+5	I+6	I+7	I+8	I+9
3.3	-12	-4.2630	-4.2715	-4.2825	-4.2793	-4.1591	-3.6192	-2.7279	-1.7924	-0.7809	0.6113
3.4	-12	-4.1772	-4.2137	-4.1941	-4.1751	-3.8443	-3.1455	0.9835	-1.2328	-0.2091	1.2567
3.5	-12	-4.0489	-4.0832	-4.0340	-3.9750	-3.5502	-2.7986	0.5749	-0.9267	0.0273	1.3160
3.6	-11	-3.9379	-3.9031	-3.7055	-3.1007	-2.2772	-1.4125	-0.5417	0.2736	1.2883	2.1147
3.7	-11	-3.6174	-3.6939	-3.5294	-2.9086	-1.9857	-1.0913	-0.2060	0.5058	1.2201	1.6124
3.8	-11	-3.2437	-3.3247	-3.1265	-2.5960	-1.8175	-0.9667	-0.0119	0.5904	1.1449	1.6910
3.9	-11	-2.9920	-2.9493	-2.6911	-2.1911	-1.3521	-0.5668	0.2348	0.6836	1.1375	1.6691
4.0	-11	-2.1883	-2.4014	-2.2376	-1.3357	-0.6975	0.4678	1.0938	2.2133	1.5535	2.0980
4.1	-10	-1.2793	-1.3004	-0.8719	-0.3817	0.5756	1.2419	2.1424	1.6476	2.2374	3.2767
4.2	-10	-0.8260	-0.4287	0.1124	0.5728	1.1665	1.7622	2.2862	2.2655	2.5230	3.2571
4.3	-10	-0.9054	-0.6056	0.0574	0.7139	1.1498	1.4684	2.0543	2.4195	3.0800	3.2879
4.4	-10	-0.9084	-0.7465	-0.2525	0.5888	1.4926	2.1041	2.6521	3.0910	3.6894	3.5459
4.5	-10	-0.5292	-0.4741	-0.1159	0.4586	1.4028	2.2264	3.0672	3.6352	4.2098	3.5068
4.6	-9	-0.1400	0.4843	0.9141	1.5151	2.2165	3.1800	4.1685	4.4584	3.7582	2.6430
4.7	-9	-0.0617	0.5576	1.3188	2.0023	2.7295	3.2827	4.2294	4.7274	4.8137	2.9702
4.8	-9	-0.3612	0.3970	0.9475	2.1012	2.9472	3.4952	4.2835	4.9346	5.1674	3.3187
4.9	-9	-0.4712	-0.0879	0.5743	1.6766	2.6851	3.6460	4.4720	4.9919	5.2854	3.7660
5.0	-9	-0.3771	-0.3866	0.3591	1.6557	2.2664	3.4011	4.5006	4.9471	3.7821	4.2563
5.2	-8	-0.3671	0.0346	0.5836	1.7334	2.8261	3.8055	4.3466	4.3101	4.2649	1.9442
5.4	-8	-0.1609	-0.1450	0.2053	0.9308	1.9378	2.8835	3.8211	3.8473	3.9656	2.5851
5.6	-7	0.7427	0.6662	0.4281	0.9856	1.6771	2.4063	3.1090	3.2544	3.3600	0.6042
5.8	-7	0.8492	0.6271	0.4115	0.6016	0.9836	1.7004	2.2778	2.7607	3.0817	1.4116
6.0	-7	0.2839	0.2480	0.2190	0.3123	1.0258	1.0467	1.7486	2.1711	2.1865	2.2503
6.2	-6	-0.1446	-0.1188	-0.1122	0.4254	0.4001	1.2651	1.8447	2.1147	2.4517	0.2175
6.4	-6	-0.5439	-0.5096	-0.4206	-0.3445	-0.0902	0.5768	1.2646	1.6157	2.0571	0.8624
6.6	-5	-0.6598	-0.6486	-0.6370	-0.4886	-0.1650	0.5721	1.1408	1.4772	1.5749	-0.9595
6.8	-5	-0.6922	-0.6891	-0.6847	-0.6713	-0.5564	-0.1044	0.5038	0.8693	1.3361	-0.3624
7.0	-5	-0.6970	-0.6979	-0.6959	-0.6987	-0.6789	-0.5250	-0.1453	0.2930	0.8168	0.5520
7.2	-4	-0.7084	-0.7079	-0.7062	-0.7019	-0.6534	-0.4699	-0.3104	0.1341	0.5409	-1.5950
7.4	-4	-0.7155	-0.7154	-0.7153	-0.7147	-0.7057	-0.6354	-0.4067	-0.1363	0.2622	-0.9202
7.6	-3	-0.7250	-0.7250	-0.7252	-0.7240	-0.7159	-0.6385	-0.4535	-0.1502	-0.2554	-2.7598
7.8	-3	-0.7392	-0.7392	-0.7393	-0.7394	-0.7377	-0.7201	-0.6444	-0.4800	-0.3474	-2.1556
8.0	-3	-0.7602	-0.7602	-0.7602	-0.7603	-0.7602	-0.7556	-0.7365	-0.6585	-0.5414	-1.2119
8.2	-2	-0.7898	-0.7899	-0.7899	-0.7900	-0.7895	-0.7847	-0.7661	-0.7342	-1.0117	-3.3547
8.4	-2	-0.8302	-0.8302	-0.8302	-0.8303	-0.8302	-0.8273	-0.8258	-0.8192	-0.9642	-2.6635
8.6	-1	-0.8823	-0.8823	-0.8823	-0.8823	-0.8824	-0.8816	-0.8830	-0.9587	-1.8079	-4.3505
8.8	-1	-0.9456	-0.9456	-0.9456	-0.9456	-0.9457	-0.9451	-0.9486	-1.0333	-1.6104	-3.8928
9.0	-1	-1.0196	-1.0196	-1.0196	-1.0196	-1.0196	-1.0199	-1.0220	-1.0599	-1.4455	-2.7617

Opacity c404 for composition : H=0.960, He=0.000, Z=0.040

Log Opacity (cms2/gm)

Log Rho / Log T	I	I	I+1	I+2	I+3	I+4	I+5	I+6	I+7	I+8	I+9
3.3	-12	-2.0562	-2.1784	-1.4667	-2.9149	-3.2530	-2.8654	-1.9511	-0.9903	0.0657	1.8704
3.4	-12	-2.0136	-2.0102	-2.0148	-2.0546	-2.1804	-2.1271	-1.4270	-0.4377	0.6458	2.4056
3.5	-12	-1.9858	-1.9791	-1.9587	-1.8883	-1.7087	-1.4276	-0.9171	-0.1052	0.8665	2.2491
3.6	-11	-1.9441	-1.9131	-1.7760	-1.4048	-0.7989	-0.1250	0.5365	1.2509	2.1929	3.4681
3.7	-11	-1.8612	-1.8387	-1.7056	-1.2791	-0.5208	0.2607	1.0442	1.7946	2.4585	3.5942
3.8	-11	-1.2946	-1.3193	-1.0806	-0.6183	-0.0596	0.5645	1.3357	1.9214	2.6118	3.6547
3.9	-11	-0.0926	0.0019	0.1587	0.4128	0.7527	1.1577	1.6600	2.2814	3.0207	3.9918
4.0	-11	0.0799	0.7247	1.2874	1.5598	1.8089	2.0705	2.5335	2.9104	3.6294	4.5756
4.1	-10	0.4211	1.3266	2.1323	2.6301	2.9091	3.1972	3.6858	4.1389	4.4686	3.0313
4.2	-10	0.0750	0.8655	1.8684	2.8202	3.4456	3.8309	4.1780	4.6550	4.8265	3.2494
4.3	-10	-0.1181	0.4909	1.4544	2.5370	3.5285	4.3526	4.6671	5.0884	5.1643	3.6144
4.4	-10	-0.1687	0.2677	1.1614	2.2363	3.3605	4.5025	5.0730	5.2756	5.4979	3.9468
4.5	-10	-0.1288	0.1781	0.9923	2.0563	3.1767	4.4068	5.1458	5.5171	5.5054	4.2795
4.6	-9	0.3604	0.9413	1.8781	2.9777	4.0447	4.8699	5.4048	5.5244	4.6762	2.1176
4.7	-9	-0.0597	0.9038	1.7866	2.6672	3.5981	4.3682	5.0119	5.2955	4.9179	2.3288
4.8	-9	-0.1603	0.8242	1.5244	2.3305	3.1641	3.8735	4.5386	4.6417	4.8292	2.5034
4.9	-9	-0.1506	0.4350	0.8731	2.0259	2.7862	3.4657	4.1013	4.5149	4.7491	2.8829
5.0	-9	-0.1868	0.2014	0.4879	1.6717	2.4570	3.1273	3.7237	4.1820	4.5253	3.2197
5.2	-8	-0.2408	0.3443	1.0184	1.7581	2.5436	3.1256	3.5814	3.8455	4.0345	1.4868
5.4	-8	0.0898	0.1672	0.3503	1.0594	1.8776	2.4556	2.9521	3.3180	3.9897	2.0593
5.6	-7	0.9415	1.0418	0.7493	1.0579	1.8337	2.4142	2.8967	3.1755	2.7433	0.4188
5.8	-7	1.1179	0.7785	0.7239	0.9144	1.2212	1.9225	2.4279	2.8358	3.1982	0.8868
6.0	-7	0.5972	0.5088	0.5491	0.6258	0.6194	1.3806	2.0676	2.4902	2.8176	1.5282
6.2	-6	0.1725	0.1875	0.1241	0.3150	0.7434	1.0619	2.1620	2.5615	2.3766	-0.2573
6.4	-6	-0.2357	-0.1904	-0.1086	-0.0214	0.2324	1.0403	1.4477	1.6949	2.0359	0.3044
6.6	-5	-0.3680	-0.3566	-0.3267	-0.1470	0.3644	0.9606	1.1615	1.5207	1.0932	-1.5406
6.8	-5	-0.4058	-0.4026	-0.3958	-0.3727	-0.2062	0.3128	0.7505	1.1179	1.4063	-0.9047
7.0	-5	-0.4106	-0.4077	-0.4071	-0.4091	-0.3789	-0.1754	0.1745	0.4189	0.9048	-0.2428
7.2	-4	-0.4190	-0.4182	-0.4172	-0.4056	-0.3437	-0.1194	0.1684	0.5605	0.5628	-2.0391
7.4	-4	-0.4262	-0.4261	-0.4260	-0.4247	-0.4126	-0.3109	-0.1371	0.1264	0.3648	-1.4896
7.6	-3	-0.4358	-0.4358	-0.4359	-0.4342	-0.4184	-0.3453	-0.1863	0.0515	-0.6218	-3.0974
7.8	-3	-0.4501	-0.4501	-0.4501	-0.4500	-0.4482	-0.4293	-0.3665	-0.2441	-0.5336	-2.6792
8.0	-3	-0.4710	-0.4710	-0.4710	-0.4710	-0.4709	-0.4675	-0.4515	-0.3947	-0.4095	-1.9905
8.2	-2	-0.5007	-0.5007	-0.5007	-0.5007	-0.5007	-0.4979	-0.4841	-0.4932	-1.0726	-3.8036
8.4	-2	-0.5411	-0.5411	-0.5411	-0.5411	-0.5412	-0.5393	-0.5411	-0.5839	-0.9308	-3.2077
8.6	-1	-0.5930	-0.5930	-0.5930	-0.5931	-0.5935	-0.5950	-0.6195	-0.8355	-2.2649	-4.8423
8.8	-1	-0.6564	-0.6564	-0.6564	-0.6564	-0.6566	-0.6572	-0.6710	-0.9501	-1.6978	-4.4295
9.0	-1	-0.7304	-0.7304	-0.7304	-0.7304	-0.7305	-0.7312	-0.7380	-0.8639	-1.5048	-3.6908

Opacity c314 for composition : H=0.710, He=0.250, Z=0.040

Log Opacity (cms2/gm)

Log Rho / Log T	I	I	I+1	I+2	I+3	I+4	I+5	I+6	I+7	I+8	I+9
3.3	-12	-2.1799	-2.2803	-2.5698	-2.9754	-3.2518	-2.7135	-1.7555	-0.7692	0.2311	1.6868
3.4	-12	-2.1426	-2.1393	-2.1409	-2.1661	-2.2565	-2.1211	-1.3675	-0.3690	0.6998	2.2745
3.5	-12	-2.1139	-2.1077	-2.0865	-2.0160	-1.8281	-1.5075	-0.9210	-0.0693	0.6953	2.1777
3.6	-11	-2.0725	-2.0410	-1.9028	-1.5259	-0.9133	-0.2214	0.4762	1.2458	2.1375	3.2882
3.7	-11	-1.9870	-1.9690	-1.8376	-1.4045	-0.6371	0.1516	0.9442	1.7282	2.3717	3.4441
3.8	-11	-1.4007	-1.4567	-1.2410	-0.7949	-0.2250	1.8735	1.2067	1.9106	2.5108	3.4979
3.9	-11	-0.2445	-0.1424	0.0106	0.2577	0.5972	1.0098	1.5202	2.1183	2.8358	3.7959
4.0	-11	-0.1185	0.5083	1.1078	1.4059	1.6748	1.9472	2.4454	3.1859	3.4631	4.3758
4.1	-10	0.2005	1.0782	1.9225	2.4671	2.7731	3.1068	3.6514	3.9427	4.3399	3.0999
4.2	-10	-0.0725	0.6647	1.6359	2.6103	3.2904	3.7242	4.3660	4.4667	4.8120	3.3946
4.3	-10	-0.2420	0.3215	1.2523	2.2883	3.2938	4.1186	4.5345	4.6232	5.1750	3.7408
4.4	-10	-0.2790	0.1176	0.9710	2.0296	3.1377	4.2408	4.9115	5.2068	5.3612	4.0664
4.5	-10	-0.3102	0.0843	0.8361	1.8748	2.9843	4.1825	5.0019	5.4362	5.3653	4.4969
4.6	-9	0.3045	0.9418	1.7887	2.6396	3.9699	4.8583	5.4387	5.3803	5.0020	2.1927
4.7	-9	-0.0844	0.9097	1.8011	2.7053	3.6964	4.5233	5.2522	4.5565	5.0011	2.5989
4.8	-9	-0.1611	0.7734	1.2902	2.4015	3.3460	4.1768	4.9057	4.8303	4.9685	2.6909
4.9	-9	-0.1303	0.3752	0.9075	2.0868	2.9486	3.8815	4.6251	4.8427	5.0819	2.9999
5.0	-9	-0.2153	0.1652	0.7553	1.6723	2.6047	3.5940	4.3671	4.6825	4.8953	3.3515
5.2	-8	-0.2575	0.3298	1.1053	1.8878	2.8056	3.6280	4.0356	4.0286	4.2251	1.5028
5.4	-8	0.0632	0.1577	0.3885	1.0752	2.0192	2.6040	3.2065	3.5738	3.9956	2.1664
5.6	-7	0.9460	-0.9000	0.7283	1.2100	1.8652	2.5254	2.9965	3.4453	2.9598	0.4922
5.8	-7	1.1257	0.7720	0.7230	0.9012	1.2752	1.9488	2.4146	2.8119	2.9746	0.9783
6.0	-7	0.5857	0.5040	0.5516	0.6153	0.6604	1.5740	2.0671	2.5151	2.8122	1.0452
6.2	-6	0.1479	0.0072	0.0908	0.5181	0.7075	1.6361	1.9624	2.0727	2.3247	-0.1792
6.4	-6	-0.2827	-0.2383	-0.1447	0.1052	0.2088	0.9830	1.6146	1.9137	2.1582	0.4171
6.6	-5	-0.4223	-0.4110	-0.3818	-0.1869	0.2491	0.9401	1.3604	1.6654	1.2963	-1.2724
6.8	-5	-0.4638	-0.4530	-0.4535	-0.4302	-0.2654	0.2657	0.7116	1.0885	1.4152	-0.7935
7.0	-5	-0.4688	-0.4655	-0.4647	-0.4675	-0.4390	-0.2165	0.1562	0.5626	1.0177	-0.1503
7.2	-4	-0.4776	-0.4769	-0.4757	-0.4609	-0.4030	-0.1718	-0.0352	0.3836	0.5557	-1.9690
7.4	-4	-0.4850	-0.4849	-0.4848	-0.4837	-0.4711	-0.3677	-0.1818	0.0865	0.3648	-1.3835
7.6	-3	-0.4946	-0.4946	-0.4947	-0.4927	-0.4764	-0.5973	-0.2345	0.0251	-0.4177	-3.0559
7.8	-3	-0.5089	-0.5089	-0.5089	-0.5087	-0.5070	-0.4682	-0.4205	-0.2755	-0.5165	-2.5701
8.0	-3	-0.5298	-0.5298	-0.5298	-0.5298	-0.5297	-0.5255	-0.5080	-0.4456	-0.4293	-1.8852
8.2	-2	-0.5595	-0.5595	-0.5595	-0.5595	-0.5594	-0.5558	-0.5383	-0.5298	-1.0431	-3.7412
8.4	-2	-0.5998	-0.5999	-0.5999	-0.5999	-0.6000	-0.5991	-0.5980	-0.6252	-0.9394	-3.0977
8.6	-1	-0.6518	-0.6518	-0.6518	-0.6519	-0.6522	-0.6528	-0.6702	-0.8551	-2.0333	-4.7880
8.8	-1	-0.7152	-0.7152	-0.7152	-0.7152	-0.7154	-0.7162	-0.7265	-0.9491	-1.6811	-4.3199
9.0	-1	-0.7892	-0.7892	-0.7892	-0.7892	-0.7893	-0.7899	-0.7954	-0.8943	-1.4896	-3.5761

Opacity c224 for composition : H=0.480, He=0.480, Z=0.040

Log Opacity (cms2/gm)

Log T \ Log Rho	I	I	I+1	I+2	I+3	I+4	I+5	I+6	I+7	I+8	I+9
3.3	-12	-2.3422	-2.4182	-2.6734	-3.0599	-3.3268	-2.8116	3.7084	-0.8698	0.1322	1.4894
3.4	-12	-2.3091	-2.3069	-2.3052	-2.3155	-2.3663	-2.2173	-1.4555	-0.4681	0.5957	2.0922
3.5	-12	-2.2799	-2.2747	-2.2511	-2.1812	-1.9838	-1.6382	-1.0166	-0.1667	0.7990	2.0734
3.6	-11	-2.2379	-2.2047	-2.0648	-1.6827	-1.0623	-0.5575	0.3645	1.1430	2.1178	2.9889
3.7	-11	-2.1479	-2.1351	-2.0067	-1.5618	-0.7859	0.0060	0.8105	1.5974	2.3077	3.1961
3.8	-11	-1.4744	-1.6250	-1.4420	-1.0052	-0.4325	0.2604	1.0489	1.7214	2.3705	3.2658
3.9	-11	-0.4346	-0.3264	-0.1777	0.0685	0.4037	0.8241	1.3482	1.9167	2.6222	3.5526
4.0	-11	-0.3699	0.2167	0.8673	1.2230	1.4889	1.7840	2.3214	3.0226	3.2070	4.1290
4.1	-10	-0.0710	0.7624	1.6488	2.2534	2.6066	2.9772	3.4195	3.7391	4.3105	5.2072
4.2	-10	-0.2388	0.4310	1.3533	2.3335	3.0881	3.5815	3.9468	4.2771	4.3643	5.5590
4.3	-10	-0.3747	0.1339	1.0175	1.9928	2.9810	3.7840	4.4645	4.5729	4.7174	5.6784
4.4	-10	-0.4135	-0.0470	0.7561	1.7908	2.8543	3.9394	4.9574	5.0207	5.0256	4.2200
4.5	-10	-0.3485	-0.0301	0.6553	1.6476	2.7260	3.9398	5.0451	5.2564	5.1981	4.2061
4.6	-9	0.0834	0.8405	1.6326	2.6292	3.8377	4.8416	5.3525	5.4496	4.9979	2.2762
4.7	-9	0.0039	0.8484	1.7338	2.6019	3.6304	4.6072	5.1967	4.3150	5.0256	2.5017
4.8	-9	-0.2128	0.6982	1.1927	2.3559	3.3767	4.3063	4.9403	4.9342	5.0230	2.8187
4.9	-9	-0.2279	0.3149	0.8083	2.0376	2.9730	5.6840	4.6660	4.9702	5.2164	3.1428
5.0	-9	-0.2116	0.1195	0.6355	1.6491	2.6221	3.6173	4.5016	4.8514	5.0157	3.5095
5.2	-8	-0.3135	0.2947	0.9650	1.9357	2.8751	3.7601	4.2161	4.1501	4.1975	1.6409
5.4	-8	0.0837	0.1073	0.3982	1.0985	2.0505	2.6017	3.3126	3.8078	4.0089	2.2638
5.6	-7	0.9790	0.9210	0.7113	1.1805	1.9072	2.5617	3.0170	3.2395	3.1647	0.5759
5.8	-7	1.1217	0.8186	0.7108	0.9903	1.7560	1.9525	2.4779	2.9285	3.2229	1.0957
6.0	-7	0.5690	0.4967	0.5144	0.6044	1.1499	1.3531	2.0565	2.5212	2.7951	1.7659
6.2	-6	0.1265	0.1530	0.0896	0.5761	0.6657	1.5993	2.1355	2.3475	2.4238	-0.0901
6.4	-6	-0.3326	-0.2830	-0.1851	0.1295	0.1416	0.9310	1.5655	1.6862	1.9803	0.5558
6.6	-5	-0.4805	-0.4677	-0.4382	-0.2307	0.1770	0.9161	1.5150	1.6479	1.4885	-1.1908
6.8	-5	-0.5250	-0.5174	-0.5138	-0.4890	-0.3358	0.2147	0.6801	1.0719	1.4214	-0.6763
7.0	-5	-0.5301	-0.5266	-0.5252	-0.5301	-0.5008	-0.2903	0.1007	0.5383	0.8356	-0.0124
7.2	-4	-0.5397	-0.5389	-0.5375	-0.5283	-0.4632	-0.2127	0.1176	0.4901	0.5904	-1.8649
7.4	-4	-0.5472	-0.5471	-0.5470	-0.5460	-0.5323	-0.4273	-0.2246	0.0457	0.3600	-1.2561
7.6	-3	-0.5568	-0.5568	-0.5568	-0.5549	-0.5382	-0.4569	-0.2866	-0.0061	-0.2572	-2.9627
7.8	-3	-0.5710	-0.5711	-0.5711	-0.5709	-0.5691	-0.5491	-0.4775	-0.3156	-0.3058	-2.4550
8.0	-3	-0.5919	-0.5919	-0.5919	-0.5920	-0.5919	-0.5869	-0.5725	-0.5134	-0.4661	-1.7625
8.2	-2	-0.6217	-0.6217	-0.6217	-0.6218	-0.6214	-0.6171	-0.5960	-0.5707	-1.0110	-3.6651
8.4	-2	-0.6620	-0.6620	-0.6620	-0.6621	-0.6621	-0.6608	-0.6580	-0.6718	-0.9412	-2.9815
8.6	-1	-0.7140	-0.7140	-0.7140	-0.7140	-0.7142	-0.7142	-0.7261	-0.8762	-1.8530	-4.7271
8.8	-1	-0.7774	-0.7774	-0.7774	-0.7774	-0.7775	-0.7774	-0.7859	-0.9585	-1.6630	-4.2057
9.0	-1	-0.8514	-0.8514	-0.8514	-0.8514	-0.8515	-0.8519	-0.8554	-0.9337	-1.4750	-3.4565

Opacity c134 for composition : H=0.250, He=0.710, Z=0.040

Log Opacity (cms2/gm)

Log Rho / Log T	I	I	I+1	I+2	I+3	I+4	I+5	I+6	I+7	I+8	I+9
3.3	-12	-2.6131	-1.1997	-2.8535	-3.2006	-0.2251	-2.9299	-1.9734	-1.0003	0.0133	1.2996
3.4	-12	-2.5839	-1.5882	-2.5770	-2.5703	-2.5567	-2.3575	-1.5658	-0.5949	0.4650	1.8920
3.5	-12	-2.5509	-1.9220	-2.5231	-2.4523	-2.2425	-1.8448	-1.1508	-0.2951	0.6660	1.9078
3.6	-11	-2.4306	-2.4714	-2.3309	-1.9304	-1.2916	-0.5636	0.1961	0.9951	1.9461	2.7350
3.7	-11	-2.4067	-2.4023	-2.2746	-1.8122	-1.0155	-0.2353	0.6070	1.3965	2.1095	2.9255
3.8	-11	-1.7417	-1.8865	-1.7564	-1.3352	-0.7438	-0.0100	0.6142	1.4943	2.1528	3.0213
3.9	-11	-0.7628	-0.6310	-0.4823	-0.2525	0.1010	0.5469	1.0994	1.6247	2.2935	3.2712
4.0	-11	-0.7500	-0.2283	0.4511	0.9053	1.2018	1.5509	2.1432	2.8812	2.8522	3.6516
4.1	-10	-0.4726	0.2646	1.1741	1.8842	2.3205	2.7659	3.1805	3.3755	4.2350	3.4165
4.2	-10	-0.4536	0.1223	0.9400	1.8927	2.7411	3.3309	3.6084	3.9335	4.6669	5.7442
4.3	-10	-0.5631	-0.1146	0.7223	1.5910	2.4774	3.3208	4.0582	4.3272	5.2155	4.0775
4.4	-10	-0.5928	-0.2658	0.5026	1.4756	2.4906	3.4541	4.4335	4.6964	5.5953	4.5392
4.5	-10	-0.4019	-0.1710	0.4233	1.3413	2.4081	3.5352	4.5766	4.9163	5.2474	4.9206
4.6	-9	-0.0237	0.7361	1.4176	2.5396	3.4426	4.4761	5.0359	5.2287	4.9546	2.3641
4.7	-9	-0.2170	0.7467	1.5685	2.4236	3.3551	4.2172	5.0085	4.6944	4.9953	2.6716
4.8	-9	-0.2784	0.6337	1.1019	2.2910	3.2546	4.0683	4.8137	5.0057	5.3916	3.0026
4.9	-9	-0.2619	0.2343	0.7791	1.9340	2.8774	3.8618	4.6568	5.0326	5.2943	3.3462
5.0	-9	-0.3172	-0.2028	0.5924	1.5353	2.4981	3.6703	4.5343	4.9369	5.1179	3.8447
5.2	-8	-0.3443	0.2842	0.7617	1.9191	2.9234	3.8080	4.3108	4.2556	4.2511	1.7724
5.4	-8	0.0065	0.0970	0.3750	1.0913	2.1094	2.6723	3.3639	3.9028	3.9678	2.4200
5.6	-7	0.9784	0.9259	0.6587	1.2804	1.8811	2.5669	3.0528	3.2478	3.3626	0.6725
5.8	-7	1.1198	0.8513	0.7037	0.9134	1.7551	1.9386	2.4772	2.6692	3.1562	1.2351
6.0	-7	0.5438	0.4920	0.4889	0.5953	0.5917	1.5025	2.0552	2.4004	2.7441	1.9704
6.2	-6	0.1016	0.1258	0.0868	0.5664	0.6022	1.5664	2.1024	2.3183	2.4525	0.0452
6.4	-6	-0.3914	-0.3383	-0.2263	-0.1287	0.1681	0.6762	1.5456	1.6652	1.9540	0.6777
6.6	-5	-0.5468	-0.5331	-0.5068	-0.3065	0.0939	0.6717	1.2879	1.6312	1.5546	-1.0860
6.8	-5	-0.5956	-0.5885	-0.5834	-0.5646	-0.4064	0.1803	0.6468	1.0470	1.4269	-0.5379
7.0	-5	-0.5965	-0.6002	-0.5957	-0.6018	-0.5732	-0.3746	0.0610	0.3090	0.7851	0.2352
7.2	-4	-0.6120	-0.6112	-0.6089	-0.6008	-0.5382	-0.1644	0.0552	0.4374	0.6197	-1.7536
7.4	-4	-0.6198	-0.6197	-0.6195	-0.6186	-0.6055	-0.4903	-0.2587	-0.0069	0.3468	-1.1043
7.6	-3	-0.6294	-0.6294	-0.6294	-0.6276	-0.6115	-0.5167	-0.3462	-0.0653	-0.2593	-2.6741
7.8	-3	-0.6436	-0.6436	-0.6436	-0.6436	-0.6416	-0.6184	-0.5448	-0.3676	-0.3933	-2.3210
8.0	-3	-0.6645	-0.6645	-0.6645	-0.6646	-0.6644	-0.6584	-0.6372	-0.5589	-0.4754	-1.5240
8.2	-2	-0.6942	-0.6942	-0.6945	-0.6943	-0.6939	-0.6859	-0.6644	-0.6535	-0.5915	-3.5263
8.4	-2	-0.7346	-0.7346	-0.7346	-0.7347	-0.7346	-0.7309	-0.7289	-0.7286	-0.9406	-2.8428
8.6	-1	-0.7866	-0.7866	-0.7866	-0.7866	-0.7867	-0.7857	-0.7920	-0.9058	-1.0326	-4.6307
8.8	-1	-0.8500	-0.8500	-0.8500	-0.8500	-0.8501	-0.8496	-0.8550	-0.9825	-1.6394	-4.0675
9.0	-1	-0.9240	-0.9240	-0.9240	-0.9240	-0.9240	-0.9244	-0.9266	-0.9833	-1.4597	-3.1469

Opacity c044 for composition : H=0.000, He=0.960, Z=0.040

Log Opacity (cms2/gm)

Log T \ Log Rho I	I	I+1	I+2	I+3	I+4	I+5	I+6	I+7	I+8	I+9
3.3 -12	-4.1370	-4.1495	-4.1664	-4.1652	-3.9971	-3.3627	-2.4384	-1.4984	-0.4866	0.9054
3.4 -12	-4.0347	-4.0786	-4.0572	-4.0290	-3.6447	-2.6832	1.2779	-0.9445	0.0846	1.5508
3.5 -12	-3.8632	-3.9065	-3.8689	-3.8127	-3.3416	-2.5475	0.8604	-0.6560	0.3101	1.6103
3.6 -11	-3.7373	-3.6865	-3.5022	-2.8569	-2.0382	-1.1695	-0.2964	0.5474	1.5800	2.4990
3.7 -11	-3.3992	-3.4705	-3.3052	-2.6303	-1.7166	-0.8605	0.0532	0.7582	1.4905	2.1205
3.8 -11	-3.0037	-3.0900	-2.9218	-2.3683	-1.5742	-0.6947	0.2701	0.8497	1.4179	1.9924
3.9 -11	-2.7236	-2.6648	-2.5145	-1.9440	-1.1405	-0.3332	0.4692	0.9476	1.4487	1.9576
4.0 -11	-2.1268	-2.2583	-2.0395	-1.0530	-0.4759	0.7414	1.5567	2.5106	1.9999	2.7033
4.1 -10	-1.2742	-1.2801	-0.7854	-0.2338	0.8246	1.4908	2.4141	2.1179	2.5040	3.4460
4.2 -10	-0.8262	-0.4328	0.1150	0.5929	1.2346	1.6735	2.4908	2.4963	2.7603	3.4679
4.3 -10	-0.9027	-0.6009	0.0725	0.7241	1.1780	1.5251	2.2550	2.5761	3.5259	3.5569
4.4 -10	-0.8951	-0.7278	-0.2288	0.6206	1.5084	2.1416	2.7176	3.1428	3.7579	3.6373
4.5 -10	-0.4629	-0.4636	-0.0802	0.5253	1.4567	2.2542	3.1075	3.6781	4.2498	3.5967
4.6 -9	-0.1175	0.5435	0.9602	1.5686	2.3026	3.2345	4.1946	4.4697	3.8618	2.6502
4.7 -9	0.0126	0.5993	1.3300	2.0292	2.8210	3.4400	4.2681	4.7373	4.8313	2.9796
4.8 -9	-0.2815	0.5086	1.0029	2.1603	3.0038	3.5765	4.3234	4.9401	5.1642	3.3266
4.9 -9	-0.3871	0.0218	0.7147	1.7956	2.7346	3.6755	4.5142	4.9811	5.1673	3.7763
5.0 -9	-0.2418	-0.3554	0.4595	1.5675	2.3272	3.4411	4.5030	4.9491	3.8052	4.2560
5.2 -8	-0.2771	0.1716	0.6228	1.8145	2.8904	3.8214	4.3525	4.3108	4.2669	1.9515
5.4 -8	-0.0177	-0.0037	0.3299	1.0367	2.0580	2.9324	3.5758	3.8623	3.9781	2.5901
5.6 -7	1.0293	0.9419	0.6272	1.1492	2.2764	2.5360	3.1025	3.2954	3.3640	0.8112
5.8 -7	1.1364	0.9108	0.6852	0.8450	1.1745	1.8608	2.4106	2.6454	2.7477	1.4182
6.0 -7	0.5295	0.4999	0.4570	0.5626	1.0988	1.2427	1.9761	2.4680	2.6667	2.3017
6.2 -6	0.0673	0.0956	0.0868	0.5063	0.5716	1.4868	2.0667	2.2764	2.4848	0.2273
6.4 -6	-0.4677	-0.4100	-0.2798	-0.1725	0.1019	0.8168	1.5282	1.8359	2.1436	0.6715
6.6 -5	-0.6332	-0.6185	-0.5977	-0.5825	0.0115	0.8169	1.3918	1.6081	1.6025	-0.9474
6.8 -5	-0.6834	-0.6819	-0.6754	-0.6571	-0.4936	0.0911	0.7652	0.7727	1.2398	-0.3521
7.0 -5	-0.6896	-0.6912	-0.6882	-0.6956	-0.6665	-0.4587	0.0042	0.2597	0.7079	0.5527
7.2 -4	-0.7074	-0.7065	-0.7041	-0.6972	-0.6293	-0.3495	0.0270	0.3793	0.6350	-1.5854
7.4 -4	-0.7154	-0.7153	-0.7151	-0.7140	-0.7004	-0.5955	-0.2959	-0.0356	0.3188	-0.9110
7.6 -3	-0.7250	-0.7250	-0.7252	-0.7254	-0.7072	-0.6047	-0.3499	-0.1014	-0.2321	-2.7471
7.8 -3	-0.7393	-0.7393	-0.7393	-0.7394	-0.7371	-0.7130	-0.6187	-0.4399	-0.3161	-2.1448
8.0 -3	-0.7602	-0.7602	-0.7602	-0.7604	-0.7601	-0.7552	-0.7292	-0.6520	-0.5162	-1.2044
8.2 -2	-0.7899	-0.7899	-0.7900	-0.7900	-0.7894	-0.7810	-0.7550	-0.7106	-0.9997	-3.3444
8.4 -2	-0.8303	-0.8303	-0.8303	-0.8303	-0.8303	-0.8244	-0.8222	-0.8083	-0.9512	-2.0577
8.6 -1	-0.8823	-0.8823	-0.8823	-0.8823	-0.8824	-0.8804	-0.8805	-0.9523	-1.8061	-4.5598
8.8 -1	-0.9457	-0.9457	-0.9457	-0.9457	-0.9458	-0.9444	-0.9476	-1.0290	-1.6066	-3.8880
9.0 -1	-1.0197	-1.0197	-1.0197	-1.0197	-1.0197	-1.0199	-1.0207	-1.0586	-1.4417	-2.7601

Opacity 6004 for composition : H=0.000, He=0.000, C=1.000

Log Opacity (cms2/gm)

Log Rho / Log T	I	I	I+1	I+2	I+3	I+4	I+5	I+6	I+7	I+8	I+9
3.3	-12	-3.3453	-3.8935	-4.3082	-4.6004	-7.7776	-7.8220	-7.6959	-7.1700	-6.4279	-5.0537
3.4	-12	-2.7606	-2.9027	-2.9542	-3.2390	-3.6856	-4.2126	-4.8059	-6.8309	-6.2009	-5.0303
3.5	-12	-2.6343	-2.7769	-2.7426	-2.7549	-2.8264	-3.0403	-3.4355	-3.9369	-4.4928	-4.9373
3.6	-11	-2.6384	-2.6202	-2.6355	-2.6754	-2.7243	-2.7636	-2.8832	-3.0294	-3.0224	-2.5836
3.7	-11	-2.2050	-2.3685	-2.4608	-2.4803	-2.4098	-2.1045	-1.5887	-1.0329	-0.9300	-0.8600
3.8	-11	-1.5991	-1.8261	-2.2096	-2.6218	-2.9310	-2.9313	-2.5365	-1.9845	-1.3184	-0.2474
3.9	-11	-1.2872	-1.3133	-1.5936	-1.8005	-2.0317	-1.1316	-0.5695	0.0451	0.7966	2.0872
4.0	-11	-1.2232	-1.1410	-0.7369	-0.9417	-0.7585	0.2035	0.6919	1.9936	2.3587	2.5564
4.1	-10	-1.1740	-0.8572	-0.7970	-0.3061	1.0133	1.5163	2.8174	3.3282	3.6646	3.1772
4.2	-10	-1.0992	-1.0470	-0.7873	-0.2007	1.1985	1.9120	3.1408	3.6775	4.2639	3.7184
4.3	-10	-0.9772	-0.9662	-0.7662	-0.1299	0.9504	1.8954	3.1783	4.1782	4.6395	3.9990
4.4	-10	-0.8675	-0.7186	-0.4737	0.1773	0.9527	1.8007	3.2488	4.4186	4.8277	4.1629
4.5	-10	0.3716	-0.1971	-0.0933	0.0440	1.4423	2.3393	3.1316	4.3788	4.1346	4.2793
4.6	-9	0.6974	0.8983	0.0211	1.7566	2.7405	3.5915	4.3204	4.6950	4.3614	3.0452
4.7	-9	1.1133	0.6258	0.5574	2.0739	2.0819	3.7263	4.2229	4.5365	4.3568	3.3752
4.8	-9	0.5080	-0.5020	0.7378	2.3283	3.0819	3.5690	4.2606	4.5586	4.5440	3.3356
4.9	-9	-0.8559	-0.8261	-0.7846	1.2533	2.3201	3.7430	4.2113	4.5133	4.4551	4.1854
5.0	-9	-0.8239	-0.7998	-0.7526	-0.5211	1.0773	3.1930	3.8884	4.3889	3.7159	4.2616
5.2	-8	-0.7851	-0.7353	-0.7167	-0.2729	0.9261	2.6441	3.6911	3.9484	4.1541	2.3003
5.4	-8	-0.7357	-0.7006	-0.6658	-0.5110	-0.0221	0.0154	1.6755	3.6544	4.0595	1.6089
5.6	-7	2.7453	-0.6274	-0.2649	0.1243	0.6089	1.3531	2.6934	3.6534	3.4531	0.9566
5.8	-7	1.8642	-0.6939	-0.6663	-0.5715	0.8312	1.6199	2.6696	3.5546	3.4384	1.6495
6.0	-7	0.7662	-0.6974	-0.6664	-0.6523	-0.3711	0.7428	2.7319	3.4726	3.5735	2.4611
6.2	-6	-0.0046	-0.6950	-0.6658	-0.5561	-0.5772	0.7265	2.7694	2.9634	2.7324	0.3959
6.4	-6	-0.4667	-0.6977	-0.6927	-0.6748	-0.5665	-0.3991	1.0845	2.3686	2.5151	1.0201
6.6	-5	-0.6348	-0.6971	-0.6919	-0.6615	-0.6019	0.1050	1.1935	1.9224	1.8120	-0.7654
6.8	-5	-0.6893	-0.6983	-0.6970	-0.6772	-0.6719	-0.3060	0.3574	1.1646	1.8779	-0.1824
7.0	-5	-0.7036	-0.7031	-0.7017	-0.6947	-0.6916	-0.5492	-0.1456	0.5371	1.4576	0.6874
7.2	-4	-0.7094	-0.7093	-0.7084	-0.6984	-0.6676	-0.4560	0.0018	0.7935	0.9371	-1.4036
7.4	-4	-0.7157	-0.7157	-0.7157	-0.7121	-0.7079	-0.6231	-0.3747	0.1799	0.7303	-0.7002
7.6	-3	-0.7252	-0.7252	-0.7247	-0.7236	-0.6978	-0.5904	-0.2765	0.2487	-0.0369	-2.5515
7.8	-3	-0.7394	-0.7394	-0.7393	-0.7392	-0.7330	-0.6954	-0.5530	-0.2054	-0.0064	-1.9970
8.0	-3	-0.7603	-0.7603	-0.7603	-0.7602	-0.7590	-0.7466	-0.6957	-0.5155	-0.2402	-1.1054
8.2	-2	-0.7900	-0.7900	-0.7900	-0.7898	-0.7874	-0.7717	-0.6985	-0.5359	-0.6507	-3.1697
8.4	-2	-0.8304	-0.8304	-0.8304	-0.8304	-0.8298	-0.8261	-0.8026	-0.7233	-0.7957	-2.5475
8.6	-1	-0.8823	-0.8823	-0.8823	-0.8823	-0.8815	-0.8756	-0.8470	-0.8505	-1.7781	-4.3542
8.8	-1	-0.9457	-0.9457	-0.9457	-0.9457	-0.9455	-0.9444	-0.9369	-0.9604	-1.5309	-3.7551
9.0	-1	-1.0197	-1.0197	-1.0197	-1.0197	-1.0197	-1.0196	-1.0183	-1.0300	-1.3654	-2.7524

Opacity 6013 for composition : H=0.000, He=0.250, C=0.750

Log Opacity (cms2/gm)

Log Rho / Log T	I	I	I+1	I+2	I+3	I+4	I+5	I+6	I+7	I+8	I+9
3.3	-12	-3.4306	-3.9275	-4.2877	-4.6432	-4.8699	-4.9582	-4.9573	-4.9505	-4.8977	-4.4827
3.4	-12	-2.9929	-3.0202	-3.0506	-3.3144	-3.7377	-4.2128	-4.5588	-4.8775	-4.8380	-4.5294
3.5	-12	-2.7781	-2.8976	-2.8621	-2.8793	-2.9442	-3.1324	-3.4997	-3.9554	-4.2451	-4.3663
3.6	-11	-2.7559	-2.7401	-2.7595	-2.7972	-2.8357	-2.8367	-2.8202	-2.6401	-2.3364	-1.8497
3.7	-11	-2.2957	-2.4699	-2.5592	-2.5419	-2.3815	-1.9967	-1.4522	-0.8358	-0.9223	-0.4943
3.8	-11	-1.4723	-1.8950	-2.1642	-2.0982	-1.6623	-1.1216	-0.5380	0.1222	-0.0807	0.4019
3.9	-11	-1.4136	-1.4258	-1.3442	-1.2489	-0.7023	-0.0318	0.5564	1.2022	1.1983	2.1151
4.0	-11	-1.3495	-1.3012	-0.8898	-0.4799	0.0092	0.8907	1.4155	2.2261	2.4130	3.3051
4.1	-10	-1.2084	-0.9248	-0.4575	0.3822	1.5717	2.1950	3.0176	3.2489	3.7966	3.3347
4.2	-10	-1.0153	-0.7048	-0.1815	0.5495	1.6665	2.5863	3.4955	3.6569	4.2447	4.1907
4.3	-10	-0.9507	-0.7942	-0.3430	0.3503	1.1986	1.9666	3.0286	3.8600	4.5297	4.3021
4.4	-10	-0.5836	-0.6189	-0.1765	0.4519	1.2668	2.1997	3.1649	4.1573	4.7924	4.2506
4.5	-10	0.4592	0.1804	0.3971	0.9008	1.6541	1.7665	3.3182	4.3148	3.9982	4.3525
4.6	-9	0.3915	1.5365	0.7280	1.9852	2.6041	3.1927	4.4130	5.1207	4.3991	2.9127
4.7	-9	0.8769	1.1643	1.0499	2.5254	2.7755	3.4135	4.4307	4.8565	4.8179	3.2918
4.8	-9	0.4479	1.2628	1.4279	2.8501	3.3661	3.8560	4.4591	4.8663	4.9468	3.6058
4.9	-9	-0.7672	-0.4788	0.8453	2.7350	2.8558	4.0000	4.4834	4.8191	4.8931	4.2208
5.0	-9	-0.7587	-0.6773	-0.4120	1.5016	2.4537	3.7466	4.5776	4.7255	4.8356	4.6963
5.2	-8	-0.7284	-0.5443	-0.0577	0.9279	2.0503	3.4385	4.1228	4.1919	4.2077	2.1866
5.4	-8	-0.7226	-0.6805	-0.4948	0.0381	0.8939	2.0985	3.1666	3.7644	2.0597	2.8670
5.6	-7	2.6327	2.6377	0.0919	0.4253	1.5495	1.9557	3.0401	3.5012	3.4158	0.9652
5.8	-7	1.7415	1.7928	1.9251	2.0993	1.9862	1.6551	2.7537	3.4984	3.3585	1.5553
6.0	-7	0.6594	0.7232	0.8210	1.0263	1.4142	1.5017	2.9236	3.4845	3.5031	2.5048
6.2	-6	-0.0749	-0.0265	0.0676	0.4517	0.4237	1.7247	2.6037	2.9848	2.7312	0.3605
6.4	-6	-0.4977	-0.4800	-0.4403	-0.3432	0.0157	0.2460	1.6573	2.4299	2.3150	0.9564
6.6	-5	-0.6454	-0.6354	-0.6157	-0.4976	-0.2585	0.0245	1.5742	2.0127	1.7832	-0.0002
6.8	-5	-0.6918	-0.6900	-0.6948	-0.6450	-0.5200	0.0452	0.7164	1.3565	1.8115	-0.2179
7.0	-5	-0.7040	-0.7056	-0.7025	-0.6963	-0.6760	-0.4326	0.0234	0.6484	1.3634	0.6648
7.2	-4	-0.7094	-0.7093	-0.7074	-0.7007	-0.6469	-0.4066	0.0459	0.7024	0.8679	-1.4566
7.4	-4	-0.7157	-0.7157	-0.7157	-0.7128	-0.7049	-0.6157	-0.3699	0.1077	0.6523	-0.7929
7.6	-3	-0.7251	-0.7251	-0.7248	-0.7239	-0.6963	-0.5962	-0.5240	0.1758	-0.2711	-2.5693
7.8	-3	-0.7393	-0.7393	-0.7393	-0.7393	-0.7332	-0.6999	-0.5765	-0.2573	-0.0635	-2.0251
8.0	-3	-0.7602	-0.7602	-0.7602	-0.7601	-0.7593	-0.7505	-0.7054	-0.5453	-0.2961	-1.1185
8.2	-2	-0.7900	-0.7900	-0.7900	-0.7899	-0.7881	-0.7750	-0.7121	-0.5737	-0.8796	-3.2061
8.4	-2	-0.8303	-0.8304	-0.8304	-0.8304	-0.8301	-0.8270	-0.8077	-0.7426	-0.8271	-2.5703
8.6	-1	-0.8823	-0.8823	-0.8823	-0.8823	-0.8817	-0.8771	-0.8551	-0.8730	-1.7764	-4.3937
8.8	-1	-0.9457	-0.9457	-0.9457	-0.9457	-0.9456	-0.9448	-0.9397	-0.9754	-1.5476	-3.7853
9.0	-1	-1.0196	-1.0196	-1.0196	-1.0196	-1.0196	-1.0196	-1.0195	-1.0372	-1.3824	-2.7375

Opacity 6022 for composition : H=0.000, He=0.500, C=0.500

Log Opacity (cms2/gm)

Log Rho / Log T	I	I	I+1	I+2	I+3	I+4	I+5	I+6	I+7	I+8	I+9
3.3	-12	-3.5437	-3.9748	-4.2805	-4.5372	-4.6640	-4.7046	-4.7037	-4.6975	-4.6495	-4.2843
3.4	-12	-3.0943	-3.1831	-3.1933	-3.4209	-3.8085	-4.2222	-4.4760	-4.6494	-4.6149	-4.3565
3.5	-12	-2.9714	-3.0663	-3.0307	-3.0513	-3.1085	-3.2623	-3.5880	-3.9880	-4.1747	-4.2019
3.6	-11	-2.9197	-2.9088	-2.9316	-2.9658	-2.9903	-2.9489	-2.8115	-2.4743	-2.6417	-1.5482
3.7	-11	-2.4219	-2.6111	-2.6980	-2.6640	-2.4079	-1.9729	-1.4091	-0.7538	-0.8497	-0.2064
3.8	-11	-1.6478	-2.0015	-2.1732	-1.9507	-1.4609	-0.9103	-0.5204	0.3511	0.1552	0.8445
3.9	-11	-1.5894	-1.5891	-1.4224	-1.1149	-0.5138	0.1359	0.7317	1.3898	1.2814	2.0698
4.0	-11	-1.5201	-1.4690	-1.2817	-0.4958	0.1600	1.0075	1.5566	2.3157	2.3470	2.6695
4.1	-10	-1.2408	-1.1332	-0.4462	0.4279	1.5454	2.2254	3.0541	3.1400	3.1892	3.7175
4.2	-10	-0.9441	-0.6321	-0.0232	0.6896	1.6725	2.6153	3.5037	3.6070	4.0966	3.9964
4.3	-10	-0.9302	-0.7163	-0.1554	0.5415	1.2246	1.3698	2.8958	3.6486	4.3551	4.1662
4.4	-10	-0.6452	-0.6376	-0.1501	0.5462	1.2557	2.2185	3.0185	3.9485	4.5997	4.1117
4.5	-10	0.4370	0.1104	0.4022	0.8503	1.6246	2.0416	3.2995	4.1419	4.8702	4.0652
4.6	-9	0.6562	1.3765	0.8175	1.9224	2.7289	3.2999	4.5572	5.0533	4.4708	2.8047
4.7	-9	0.6263	1.0925	1.2122	2.4278	2.7345	3.4230	4.4180	4.8399	4.7790	3.1556
4.8	-9	0.3543	1.1263	1.1385	2.7659	3.3083	3.8353	4.4610	4.9376	5.0537	3.4757
4.9	-9	-0.7132	-0.2543	0.8496	2.6692	3.2566	3.9783	4.5223	4.9197	5.0957	4.0586
5.0	-9	-0.7099	-0.5997	-0.2561	1.4975	2.4953	3.7397	4.4602	4.8350	4.0011	4.2659
5.2	-8	-0.6786	-0.4255	0.1722	1.2093	2.4072	3.5245	4.2237	4.2660	4.2626	2.0904
5.4	-8	-0.7094	-0.6515	-0.3828	0.2401	1.1289	2.4544	3.2459	3.8309	2.6169	2.7322
5.6	-7	2.4742	2.4576	0.0146	0.4276	1.1256	2.1179	3.1459	3.4901	3.3670	0.9079
5.8	-7	1.5703	1.6328	1.7520	1.9252	1.9165	1.8084	2.7094	3.4165	3.2962	1.5249
6.0	-7	0.5152	0.5756	0.6679	0.8657	1.3107	1.4099	2.7916	3.3528	3.2057	2.4569
6.2	-6	-0.1655	-0.1225	-0.0379	0.4001	0.3250	1.6182	2.7026	2.8693	2.6720	0.5218
6.4	-6	-0.5355	-0.5204	-0.4874	-0.4088	-0.1123	0.2657	1.6954	2.2749	2.4420	0.9538
6.6	-5	-0.6579	-0.6499	-0.6362	-0.5377	-0.3710	0.0749	1.4181	1.6807	1.7464	-0.8426
6.8	-5	-0.6946	-0.6932	-0.6967	-0.6585	-0.5566	-0.0121	0.5778	1.2017	1.7204	-0.2562
7.0	-5	-0.7044	-0.7042	-0.7033	-0.6986	-0.6832	-0.4583	-0.0725	0.5267	1.2369	0.6550
7.2	-4	-0.7094	-0.7094	-0.7082	-0.7032	-0.6575	-0.4565	-0.0434	0.5860	0.8211	-1.4809
7.4	-4	-0.7156	-0.7156	-0.7156	-0.7156	-0.7066	-0.6334	-0.4207	0.0169	0.5551	-0.6297
7.6	-3	-0.7251	-0.7251	-0.7249	-0.7242	-0.7042	-0.6168	-0.5781	0.0804	-0.1131	-2.6361
7.8	-3	-0.7393	-0.7393	-0.7393	-0.7393	-0.7348	-0.7080	-0.6031	-0.5190	-0.1355	-2.3812
8.0	-3	-0.7601	-0.7602	-0.7602	-0.7602	-0.7596	-0.7527	-0.7165	-0.5796	-0.3657	-1.1450
8.2	-2	-0.7899	-0.7899	-0.7899	-0.7898	-0.7885	-0.7785	-0.7274	-0.6178	-0.9166	-3.2494
8.4	-2	-0.8303	-0.8303	-0.8303	-0.8304	-0.8302	-0.8280	-0.8132	-0.7646	-0.8673	-2.5996
8.6	-1	-0.8823	-0.8823	-0.8823	-0.8823	-0.8819	-0.8786	-0.8639	-0.8995	-1.7870	-4.4594
8.8	-1	-0.9456	-0.9456	-0.9457	-0.9457	-0.9456	-0.9452	-0.9427	-0.9928	-1.5683	-3.8189
9.0	-1	-1.0196	-1.0196	-1.0196	-1.0196	-1.0196	-1.0197	-1.0203	-1.0441	-1.4029	-2.7456

Opacity 6031 for composition : H=0.000, He=0.750, C=0.250

Log Opacity (cms2/gm)

Log Rho / Log T	I	I	I+1	I+2	I+3	I+4	I+5	I+6	I+7	I+8	I+9
3.3	-12	-3.7216	-4.0595	-4.2943	-4.4625	-4.5322	-4.5523	-4.5514	-4.5455	-4.4998	-4.1594
3.4	-12	-3.3926	-3.4533	-3.4436	-3.6060	-3.9250	-4.2310	-4.4200	-4.5141	-4.4822	-4.2506
3.5	-12	-3.2763	-3.3467	-3.3136	-3.3357	-3.3825	-3.4895	-3.7400	-4.0519	-4.1473	-4.1175
3.6	-11	-3.1931	-3.1906	-3.2154	-3.2420	-3.2447	-3.1609	-2.8795	-2.4260	-2.5653	-1.3607
3.7	-11	-2.6423	-2.8454	-2.9283	-2.8364	-2.5147	-2.0366	-1.4545	-0.7813	-0.8453	-0.0724
3.8	-11	-1.9470	-2.2051	-2.2722	-1.9547	-1.4374	-0.8836	-0.2867	0.3947	0.2060	0.9275
3.9	-11	-1.8867	-1.8757	-1.6424	-1.1739	-0.5089	0.1312	0.7584	1.4215	1.2348	1.9208
4.0	-11	-1.7863	-1.7490	-1.4894	-0.7162	0.1704	0.9056	1.5327	2.2965	2.1916	2.5113
4.1	-10	-1.2702	-1.2126	-0.5870	0.2654	1.3214	2.1513	3.0072	2.9476	3.0130	3.6024
4.2	-10	-0.8837	-0.5100	0.0695	0.6470	1.5098	2.4478	3.4560	3.5836	3.4436	3.7589
4.3	-10	-0.9137	-0.6538	-0.0365	0.6499	1.2125	1.6677	2.4781	3.2876	4.0761	3.6995
4.4	-10	-0.7310	-0.7260	-0.1759	0.5936	1.3986	2.2005	2.8538	3.5619	4.2763	3.9080
4.5	-10	0.3201	-0.4271	0.2511	0.7272	1.5774	2.1590	3.2367	3.9441	4.6114	3.8646
4.6	-9	0.4925	1.1843	1.2504	1.8132	2.5990	3.2918	4.2454	4.7902	4.3768	2.7091
4.7	-9	0.4014	0.9651	1.3079	2.2861	2.6648	3.3418	4.3582	4.8001	4.5067	3.0459
4.8	-9	0.1747	0.8805	1.1248	2.0175	3.1891	3.7122	4.4177	4.9499	5.1419	3.5825
4.9	-9	-0.6649	-0.1816	0.7958	2.4639	3.1566	3.5775	4.5195	4.9710	5.2071	3.8014
5.0	-9	-0.6669	-0.5354	-0.1134	1.4056	2.4743	3.6868	4.5053	4.9096	3.9079	4.2556
5.2	-8	-0.6539	-0.3366	0.3345	1.5841	2.6080	3.6822	4.2887	4.3032	4.2567	2.0082
5.4	-8	-0.6970	-0.6195	-0.2994	0.3893	1.3014	2.6501	3.2456	3.8720	4.0072	2.6452
5.6	-7	2.2035	2.1365	-0.0982	0.4176	1.2165	2.2429	3.2257	3.4355	3.3692	0.6551
5.8	-7	1.2818	1.3402	1.4578	1.6266	1.8136	1.7845	2.6418	3.2611	3.2330	1.4680
6.0	-7	0.2867	0.3391	0.4224	0.5984	1.1554	1.1748	2.5732	3.1205	3.0643	2.3055
6.2	-6	-0.2984	-0.2641	-0.1934	0.3418	0.1995	1.4125	2.4261	2.6621	2.5905	0.2741
6.4	-6	-0.5868	-0.5754	-0.5516	-0.4982	-0.3602	0.1359	1.4210	2.0146	2.2765	0.9119
6.6	-5	-0.6736	-0.6681	-0.6611	-0.5865	-0.4159	0.4437	1.1609	1.6808	1.6869	-0.8963
6.8	-5	-0.6980	-0.6971	-0.6992	-0.6744	-0.5983	-0.1743	0.5647	1.0008	1.5772	-0.3074
7.0	-5	-0.7048	-0.7047	-0.7042	-0.7009	-0.6870	-0.5238	-0.2068	0.3517	1.0578	0.6016
7.2	-4	-0.7094	-0.7094	-0.7088	-0.7060	-0.6719	-0.5202	-0.1642	0.4253	0.7253	-1.5556
7.4	-4	-0.7156	-0.7156	-0.7156	-0.7145	-0.7087	-0.6570	-0.4655	-0.0975	0.4163	-0.6755
7.6	-3	-0.7250	-0.7250	-0.7250	-0.7245	-0.7106	-0.6456	-0.4454	-0.0311	-0.1769	-2.6947
7.8	-3	-0.7392	-0.7392	-0.7393	-0.7394	-0.7364	-0.7171	-0.6548	-0.3964	-0.2323	-2.1065
8.0	-3	-0.7601	-0.7601	-0.7602	-0.7602	-0.7599	-0.7552	-0.7285	-0.6209	-0.4492	-1.1774
8.2	-2	-0.7898	-0.7898	-0.7899	-0.7899	-0.7890	-0.7824	-0.7451	-0.6709	-0.9615	-3.5010
8.4	-2	-0.8303	-0.8303	-0.8303	-0.8303	-0.8302	-0.8290	-0.8195	-0.7901	-0.9143	-2.6521
8.6	-1	-0.8822	-0.8822	-0.8823	-0.8823	-0.8821	-0.8805	-0.8739	-0.9296	-1.7979	-4.4956
8.8	-1	-0.9456	-0.9456	-0.9456	-0.9456	-0.9456	-0.9456	-0.9460	-1.0129	-1.5902	-3.6564
9.0	-1	-1.0196	-1.0196	-1.0196	-1.0196	-1.0196	-1.0198	-1.0212	-1.0520	-1.4249	-2.7543

Opacity 8004 for composition : H=0.000, He=0.000, O=1.000

Log Opacity (cms2/gm)

Log Rho / Log T	I	I	I+1	I+2	I+3	I+4	I+5	I+6	I+7	I+8	I+9
3.3	-12	-3.6539	-3.7198	-4.0068	-4.3412	-4.8271	-5.2767	-6.0226	-7.4472	-6.7040	-5.3291
3.4	-12	-3.5383	-3.5521	-3.6011	-3.5745	-3.7125	-4.0433	-4.5132	-5.1666	-6.4820	-5.3071
3.5	-12	-3.4408	-3.4589	-3.4968	-3.4661	-3.4957	-3.5522	-3.6887	-4.0291	-4.4079	-5.2299
3.6	-11	-3.3290	-3.3699	-3.3507	-3.3860	-3.4360	-3.4914	-3.5647	-3.7688	-3.9665	-3.1241
3.7	-11	-3.0912	-3.1923	-3.2067	-3.2547	-3.3106	-3.3221	-3.2586	-2.9674	-2.8662	-2.1125
3.8	-11	-2.2800	-2.6404	-2.8646	-3.0188	-2.9719	-2.7337	-2.2406	-1.6233	-0.2501	-0.9945
3.9	-11	-1.3776	-1.7952	-2.1021	-2.3338	-2.1868	-1.6966	-1.1116	-0.4711	0.2722	0.0076
4.0	-11	-1.3139	-1.2542	-1.2485	-1.5350	-0.4981	-0.6146	0.1693	0.5568	1.2055	0.7406
4.1	-10	-1.2859	-1.2584	-1.1865	0.4498	-1.6680	0.5840	-0.6596	0.4657	0.6747	1.7251
4.2	-10	-1.2253	-1.2000	-1.2289	0.2411	-0.8400	1.3591	1.4680	1.7659	2.0864	2.4563
4.3	-10	-1.1668	-0.9488	-1.1392	0.1383	-0.7604	1.9392	0.7305	2.8269	3.2905	2.9552
4.4	-10	-1.0989	-1.0120	-0.9792	-0.6581	-0.1480	1.8686	2.0631	3.2870	3.8650	3.4000
4.5	-10	-1.0512	-0.9413	-0.7639	-0.4580	0.3081	1.8997	2.2183	3.7466	3.9105	3.9211
4.6	-9	-0.6860	-0.8097	-0.3234	0.5268	1.9099	2.4196	3.6051	4.5135	4.1998	3.0995
4.7	-9	-0.6521	-0.9070	-0.4267	0.5872	1.8387	2.7302	3.8523	4.4493	4.2305	3.3597
4.8	-9	0.3454	-0.5788	-0.3125	0.3256	1.4602	2.6443	3.6077	4.4978	4.4604	3.7953
4.9	-9	0.3882	-0.2724	0.7761	1.0444	1.5162	2.6066	3.7056	4.5121	4.5102	3.9976
5.0	-9	0.5185	-0.3767	1.4346	1.4287	2.2141	2.6568	3.6626	4.4642	3.8670	4.1295
5.2	-8	0.0092	-0.7731	0.0557	2.0917	3.0111	3.6848	4.2716	3.9458	4.1794	2.3770
5.4	-8	-0.7749	-0.7392	-0.7153	-0.5303	-0.0478	2.8665	3.5236	4.0115	4.2015	3.2206
5.6	-7	-0.7447	-0.7032	-0.6261	-0.5220	0.5421	2.0443	3.4662	3.5526	3.5790	1.0863
5.8	-7	2.5260	-0.6918	-0.6221	-0.4231	0.1472	0.2771	2.0762	3.2502	3.5122	1.7077
6.0	-7	1.7503	-0.6967	-0.6819	-0.6424	-0.1080	0.6240	1.6294	2.7905	3.6432	2.5444
6.2	-6	0.7559	-0.6938	-0.6725	-0.6147	-0.3500	1.6505	2.7992	2.7473	2.7962	0.4544
6.4	-6	-0.0763	-0.6969	-0.6904	-0.6693	-0.5235	-0.5069	2.2943	2.6571	2.7686	1.1027
6.6	-5	-0.4805	-0.6962	-0.6867	-0.6096	-0.5461	0.1099	2.5127	2.5289	1.8604	-0.7196
6.8	-5	-0.6484	-0.6978	-0.6950	-0.6784	-0.6567	-0.3264	0.4601	1.5663	1.9232	-0.1576
7.0	-5	-0.6945	-0.6928	-0.6896	-0.6825	-0.6776	-0.5731	-0.0565	0.6963	1.5455	0.7180
7.2	-4	-0.7073	-0.7068	-0.7085	-0.6850	-0.6745	-0.4040	0.1208	0.9516	1.0260	-1.3513
7.4	-4	-0.7152	-0.7152	-0.7154	-0.7095	-0.7050	-0.6022	-0.3026	0.2933	0.9057	-0.7154
7.6	-3	-0.7247	-0.7247	-0.7245	-0.7222	-0.6917	-0.5531	-0.1673	0.4249	0.0120	-2.4960
7.8	-3	-0.7390	-0.7390	-0.7390	-0.7386	-0.7301	-0.6600	-0.5026	-0.0803	0.0955	-1.9511
8.0	-3	-0.7599	-0.7599	-0.7599	-0.7597	-0.7581	-0.7453	-0.6724	-0.4455	-0.1293	-1.0691
8.2	-2	-0.7896	-0.7896	-0.7896	-0.7893	-0.7857	-0.7673	-0.6666	-0.4586	-0.7965	-3.1161
8.4	-2	-0.8299	-0.8299	-0.8300	-0.8300	-0.8292	-0.8260	-0.7908	-0.6822	-0.7261	-2.5080
8.6	-1	-0.8819	-0.8819	-0.8819	-0.8818	-0.8809	-0.8717	-0.8295	-0.8033	-1.7619	-4.2956
8.8	-1	-0.9453	-0.9453	-0.9453	-0.9453	-0.9452	-0.9451	-0.9306	-0.9317	-1.4969	-3.7092
9.0	-1	-1.0195	-1.0193	-1.0193	-1.0193	-1.0193	-1.0190	-1.0160	-1.0177	-1.3323	-2.7200

Opacity 8031 for composition : H=0.000, He=0.750, O=0.250

Log Opacity (cms2/gm)

Log T \ Log Rho I	I	I+1	I+2	I+3	I+4	I+5	I+6	I+7	I+8	I+9
3.3 -12	-4.0066	-4.1282	-4.1764	-4.5274	-4.4643	-4.5301	-4.5585	-4.5526	-4.5075	-4.1743
3.4 -12	-3.9199	-4.0538	-4.0221	-4.0162	-4.0638	-4.2034	-4.3827	-4.4731	-4.4967	-4.2754
3.5 -12	-3.8213	-3.9742	-3.9497	-3.9477	-3.9755	-4.0104	-4.0613	-4.1795	-4.3299	-4.2774
3.6 -11	-3.8570	-3.8436	-3.8483	-3.8814	-3.9177	-3.9356	-3.8951	-3.7135	-3.7264	-2.6574
3.7 -11	-3.5732	-3.6672	-3.7103	-3.6790	-3.5769	-3.2891	-2.7950	-2.1440	-2.2254	-1.3101
3.8 -11	-2.6486	-2.9739	-3.1231	-2.9222	-2.4834	-1.9527	-1.3671	-0.6983	-0.8715	-0.1757
3.9 -11	-1.9800	-1.9835	-2.2134	-1.8579	-1.3317	-0.7727	-0.1842	0.4856	0.2201	0.7146
4.0 -11	-1.8654	-1.8760	-1.4786	-0.9591	-0.3124	0.1958	0.7616	1.4572	1.1364	1.6914
4.1 -10	-1.3078	-1.1757	-0.7324	0.2930	0.8271	1.5172	2.2431	1.8482	2.0743	2.9374
4.2 -10	-0.9171	-0.5162	0.0024	0.6200	1.3089	2.1130	2.8730	2.4910	2.6508	3.2260
4.3 -10	-0.9750	-0.7120	-0.0871	0.6196	1.0316	1.3322	1.9860	2.6063	3.3177	3.7090
4.4 -10	-0.9663	-0.8201	-0.3645	0.4793	1.3671	1.9713	2.5527	3.1521	3.7653	3.9957
4.5 -10	-0.6723	-0.5182	-0.2165	0.5725	1.2317	2.1122	2.9550	3.6604	4.2138	3.9707
4.6 -9	-0.2713	0.3301	0.8151	1.3821	2.0611	3.0598	4.0207	4.6694	4.5310	2.7290
4.7 -9	-0.4267	0.2332	1.1737	1.9090	2.4461	3.1405	4.2000	4.7436	4.8575	3.0675
4.8 -9	-0.0467	0.1973	0.7634	1.9403	2.8090	3.3740	4.2926	4.9236	5.1554	3.5951
4.9 -9	0.0736	0.4141	0.7980	1.5191	2.5781	3.5500	4.4006	4.9560	5.2154	3.9158
5.0 -9	0.1512	-0.2646	0.8577	1.6545	2.3559	3.4077	4.4261	4.9088	3.9575	4.2577
5.2 -8	-0.1443	0.8415	0.8413	2.2616	3.2115	3.8338	4.3793	4.3254	4.3077	2.0201
5.4 -8	-0.7069	-0.6317	-0.3108	0.9116	2.4400	2.6460	3.5522	3.9770	2.7699	2.0551
5.6 -7	-0.6984	-0.6310	-0.3601	0.2341	1.2926	2.6240	3.3079	3.4731	3.3918	0.8700
5.8 -7	1.9887	1.7475	-0.5399	-0.1473	1.3290	1.1674	2.4505	2.9877	3.1912	1.4842
6.0 -7	1.1845	1.2468	1.3504	1.4150	1.0838	0.6899	1.7039	2.6607	2.7581	2.3777
6.2 -6	0.2775	0.3324	0.4740	0.8587	0.9709	1.7905	2.4556	2.4997	2.6426	0.2960
6.4 -6	-0.3467	-0.3178	-0.2602	-0.1461	0.2043	0.8698	2.1220	2.3542	2.5067	0.9507
6.6 -5	-0.5955	-0.5768	-0.5529	-0.3793	-0.2307	1.0662	2.1537	2.0347	1.7048	-0.6705
6.8 -5	-0.6808	-0.6767	-0.6682	-0.6303	-0.5618	0.0685	1.3755	1.5771	1.6166	-0.2857
7.0 -5	-0.7016	-0.7009	-0.6996	-0.6962	-0.6582	-0.4117	0.1259	0.6571	1.1238	0.6240
7.2 -4	-0.7088	-0.7086	-0.7090	-0.7027	-0.6368	-0.3925	0.0151	0.4992	0.8012	-1.5065
7.4 -4	-0.7155	-0.7155	-0.7155	-0.7157	-0.7063	-0.6191	-0.4045	-0.0107	0.5329	-0.8520
7.6 -3	-0.7249	-0.7249	-0.7250	-0.7241	-0.7030	-0.6163	-0.3932	0.0683	-0.1349	-2.6654
7.8 -3	-0.7391	-0.7391	-0.7392	-0.7392	-0.7353	-0.7083	-0.6142	-0.3347	-0.1684	-2.0844
8.0 -3	-0.7600	-0.7600	-0.7601	-0.7601	-0.7595	-0.7530	-0.7204	-0.5905	-0.3922	-1.1597
8.2 -2	-0.7897	-0.7897	-0.7898	-0.7897	-0.7885	-0.7799	-0.7551	-0.6361	-0.9353	-3.2755
8.4 -2	-0.8302	-0.8302	-0.8302	-0.8302	-0.8300	-0.8284	-0.8154	-0.7736	-0.6868	-2.6164
8.6 -1	-0.8821	-0.8821	-0.8822	-0.8821	-0.8820	-0.8794	-0.8676	-0.9118	-1.7927	-4.4667
8.8 -1	-0.9455	-0.9455	-0.9455	-0.9455	-0.9455	-0.9453	-0.9439	-1.0016	-1.5791	-3.6361
9.0 -1	-1.0195	-1.0195	-1.0195	-1.0195	-1.0195	-1.0196	-1.0206	-1.0477	-1.4138	-2.7507

Opacity 8022 for composition : H=0.000, He=0.500, O=0.500

Log Opacity (cms2/gm)

Log Rho / Log T	I	I	I+1	I+2	I+3	I+4	I+5	I+6	I+7	I+8	I+9
3.3	-12	-3.7918	-3.9574	-4.0773	-4.3140	-4.5517	-4.6614	-4.7198	-4.7137	-4.6672	-4.3184
3.4	-12	-3.6878	-3.8492	-3.8220	-3.8121	-3.8949	-4.1251	-4.4093	-4.5706	-4.6442	-4.4053
3.5	-12	-3.5757	-3.7508	-3.7339	-3.7252	-3.7579	-3.8057	-3.8891	-4.1167	-4.3399	-4.4220
3.6	-11	-3.6228	-3.6177	-3.6170	-3.6553	-3.7003	-3.7357	-3.7410	-3.6758	-3.7515	-2.7539
3.7	-11	-3.3546	-3.4388	-3.4673	-3.4818	-3.4381	-3.2343	-2.7937	-2.1682	-2.1810	-1.4506
3.8	-11	-2.4672	-2.8071	-2.9750	-2.8678	-2.4771	-1.9650	-1.3885	-0.7255	-0.6760	-0.0634
3.9	-11	-1.6818	-1.9949	-2.0997	-1.8401	-1.3433	-0.7900	-0.2045	0.4527	0.3291	1.2606
4.0	-11	-1.6102	-1.5952	-1.1503	-1.0020	-0.2072	0.1996	0.7670	1.4184	1.1327	1.4546
4.1	-10	-1.3062	-1.0673	-0.6184	0.5513	0.8864	1.5150	2.1911	1.8162	2.0315	2.9050
4.2	-10	-1.0038	-0.6301	-0.1309	0.6584	1.4023	2.0021	2.8265	2.5013	2.6537	3.1776
4.3	-10	-1.0336	-0.8276	-0.2535	0.5045	0.9061	1.2821	1.8582	2.7590	3.4397	3.5352
4.4	-10	-1.0010	-0.8813	-0.4699	0.3865	1.2409	1.9922	2.5332	3.2471	3.8215	3.8566
4.5	-10	-0.7485	-0.5805	-0.2696	0.2024	1.1135	2.0999	2.8232	3.6930	4.2254	4.1477
4.6	-9	-0.3862	0.2103	0.7215	1.2646	2.1064	2.9450	3.9780	4.5954	4.5079	2.8397
4.7	-9	-0.4945	0.0691	1.0102	1.7854	2.4683	3.1330	4.1420	4.7384	4.7955	3.1656
4.8	-9	0.0160	0.2952	0.6811	1.7754	2.6910	3.3200	4.2230	4.8760	5.0395	3.5182
4.9	-9	0.6630	-0.2343	1.0008	1.5776	2.4794	3.4127	4.3154	4.9015	5.1127	4.1607
5.0	-9	0.3703	-0.1627	1.2946	1.8191	2.3797	3.3449	4.3089	4.9279	4.9907	4.3208
5.2	-8	-0.0398	1.0414	1.0965	2.4451	3.3010	3.8977	4.3612	4.3611	4.4144	2.1170
5.4	-8	-0.7286	-0.6750	-0.4090	0.7074	2.5842	2.9393	3.6952	4.1265	2.7062	2.7623
5.6	-7	-0.7131	-0.6634	-0.4348	0.1314	1.7298	2.4352	3.4506	3.5821	3.4526	0.9341
5.8	-7	2.2575	1.8317	-0.4452	-0.1722	1.1351	1.0144	2.6305	3.1530	3.3416	1.5549
6.0	-7	1.4661	1.5240	1.6429	1.7107	1.1616	0.6262	1.7974	2.6560	2.4121	2.4447
6.2	-6	0.5055	0.5679	0.7313	1.0818	0.6964	1.9864	2.6459	2.6415	2.7154	0.6509
6.4	-6	-0.2251	-0.1879	-0.1144	0.0385	0.4444	0.9046	2.4251	2.1891	2.4668	0.9803
6.6	-5	-0.5466	-0.5180	-0.4780	-0.2532	-0.1752	1.2981	2.4286	2.2784	1.7751	-0.8072
6.8	-5	-0.6678	-0.6572	-0.6488	-0.5847	-0.5266	0.2384	1.8150	1.4275	1.5607	-0.2244
7.0	-5	-0.6989	-0.6979	-0.6958	-0.6920	-0.6336	-0.3118	0.3495	0.8968	1.3195	0.6644
7.2	-4	-0.7083	-0.7080	-0.7088	-0.6955	-0.6354	-0.2650	0.2003	0.7306	0.9086	-1.4415
7.4	-4	-0.7154	-0.7154	-0.7155	-0.7122	-0.7023	-0.5636	-0.2907	0.1533	0.7041	-0.7975
7.6	-3	-0.7249	-0.7249	-0.7248	-0.7234	-0.6909	-0.5545	-0.3166	0.2250	-0.0675	-2.5937
7.8	-3	-0.7391	-0.7391	-0.7391	-0.7390	-0.7326	-0.6694	-0.5564	-0.2272	-0.0503	-2.0271
8.0	-3	-0.7599	-0.7599	-0.7600	-0.7599	-0.7589	-0.7152	-0.6647	-0.5317	-0.2803	-1.1189
8.2	-2	-0.7897	-0.7897	-0.7897	-0.7896	-0.7875	-0.7231	-0.7075	-0.5657	-0.4772	-3.2100
8.4	-2	-0.8301	-0.8301	-0.8301	-0.8302	-0.8298	-0.7559	-0.8065	-0.7376	-0.8253	-2.5754
8.6	-1	-0.8821	-0.8821	-0.8821	-0.8820	-0.8816	-0.8766	-0.8531	-0.8696	-1.7774	-4.3973
8.8	-1	-0.9454	-0.9454	-0.9454	-0.9455	-0.9454	-0.9445	-0.9390	-0.9743	-1.5485	-3.7864
9.0	-1	-1.0194	-1.0194	-1.0194	-1.0194	-1.0194	-1.0194	-1.0188	-1.0355	-1.3830	-2.7391

Opacity 8013 for composition : H=0.000, He=0.250, O=0.750

Log Opacity (cms2/gm)

Log Rho / Log T	I	I	I+1	I+2	I+3	I+4	I+5	I+6	I+7	I+8	I+9
3.3	-12	-3.6686	-3.8332	-4.0243	-4.3211	-4.6638	-4.8611	-4.9884	-4.9819	-4.9322	-4.5489
3.4	-12	-3.5572	-3.6859	-3.6923	-3.6757	-3.7942	-4.0782	-4.4544	-4.7117	-4.8888	-4.6109
3.5	-12	-3.4564	-3.5926	-3.5956	-3.5769	-3.6101	-3.6621	-3.7756	-4.0663	-4.3679	-4.6051
3.6	-11	-3.4624	-3.4735	-3.4648	-3.5033	-3.5519	-3.5967	-3.6407	-3.7049	-3.8338	-2.9052
3.7	-11	-3.2088	-3.2948	-3.3179	-3.3526	-3.3601	-3.2404	-2.9186	-2.3558	-2.4356	-1.7605
3.8	-11	-2.3602	-2.7086	-2.9046	-2.9030	-2.6015	-2.1329	-1.5085	-0.9202	-1.0257	-0.4918
3.9	-11	-1.5063	-1.8738	-2.0801	-1.9622	-1.5152	-0.9688	-0.3879	0.2567	0.1021	0.5118
4.0	-11	-1.4420	-1.4242	-0.9661	-1.1435	-0.2367	0.1224	0.7298	1.2304	1.0306	1.2897
4.1	-10	-1.2989	-0.9857	-0.6878	0.4364	0.7390	1.5846	1.9805	1.9112	1.8078	2.7449
4.2	-10	-1.1054	-0.8401	-0.3539	0.6362	1.2978	2.0595	2.6404	2.3620	2.4983	3.1253
4.3	-10	-1.0956	-0.9686	-0.5057	0.5455	0.6512	1.7965	2.1837	2.8395	3.4415	3.4505
4.4	-10	-1.0469	-0.9535	-0.6263	0.0775	0.9226	1.9510	2.4369	3.2523	3.8326	3.8159
4.5	-10	-0.8482	-0.6987	-0.3524	0.0690	0.8814	2.0448	2.8731	3.7060	4.0001	4.1105
4.6	-9	-0.5290	0.0259	0.5266	1.1329	2.0970	2.8048	3.9237	4.1766	4.4366	2.9690
4.7	-9	-0.5201	-0.1467	0.7398	1.5806	2.4137	3.0730	4.0512	4.7023	4.7499	3.5141
4.8	-9	0.4451	0.3253	0.5687	1.4515	2.4138	3.2215	4.1246	4.8090	4.9562	3.7471
4.9	-9	0.3190	-0.2788	1.0971	1.5896	2.3201	3.2302	4.1467	4.7806	4.9360	4.2186
5.0	-9	0.4060	-0.1547	1.1952	1.9824	2.4041	3.2215	4.1344	4.7217	4.1350	4.3026
5.2	-8	-0.0018	1.1370	0.9500	2.5349	3.3407	3.6222	4.3685	4.3363	4.1379	2.2724
5.4	-8	-0.7513	-0.7225	-0.5372	-0.0051	2.6698	2.9070	3.7610	4.0676	2.1621	3.0503
5.6	-7	-0.7278	-0.6986	-0.5159	0.0001	1.4413	2.4275	3.5197	3.6073	3.5075	1.0052
5.8	-7	2.4184	2.1053	-0.3890	-0.2044	0.8605	0.8298	2.7697	3.2575	3.4646	1.6260
6.0	-7	1.6328	1.6979	1.8158	1.8908	1.3142	0.5415	1.8565	2.9574	3.0569	2.5462
6.2	-6	0.6495	0.7149	0.8902	1.2326	0.8263	2.1181	2.7815	2.7359	2.7760	0.5957
6.4	-6	-0.1416	-0.1014	-0.0175	0.1606	0.5964	1.0963	2.5041	2.6913	2.7823	1.0463
6.6	-5	-0.5105	-0.4797	-0.4299	-0.1679	-0.0458	1.4751	2.6044	2.4259	1.8053	-0.7605
6.8	-5	-0.6574	-0.6498	-0.6333	-0.5788	-0.5026	0.3371	1.6575	1.7918	1.8562	-0.1763
7.0	-5	-0.6966	-0.6952	-0.6925	-0.6873	-0.6138	-0.3328	0.5030	1.0417	1.4489	0.6956
7.2	-4	-0.7078	-0.7074	-0.7085	-0.6904	-0.6202	-0.1828	0.3111	0.8110	0.9757	-1.3898
7.4	-4	-0.7153	-0.7152	-0.7154	-0.7108	-0.6932	-0.5374	-0.2305	0.2449	0.6190	-0.7555
7.6	-3	-0.7248	-0.7248	-0.7247	-0.7228	-0.6802	-0.5373	-0.2484	0.5370	-0.0226	-2.5399
7.8	-3	-0.7390	-0.7390	-0.7390	-0.7387	-0.7303	-0.6800	-0.5336	-0.1462	0.0320	-1.9817
8.0	-3	-0.7599	-0.7599	-0.7599	-0.7598	-0.7584	-0.7449	-0.6863	-0.4850	-0.1965	-1.0875
8.2	-2	-0.7897	-0.7897	-0.7897	-0.7895	-0.7866	-0.7690	-0.6656	-0.5065	-0.8320	-1.1582
8.4	-2	-0.8300	-0.8300	-0.8301	-0.8301	-0.8296	-0.8255	-0.7982	-0.7078	-0.7711	-2.5565
8.6	-1	-0.8820	-0.8820	-0.8820	-0.8819	-0.8810	-0.8741	-0.8406	-0.8338	-1.7632	-4.3465
8.8	-1	-0.9453	-0.9453	-0.9454	-0.9454	-0.9452	-0.9438	-0.9346	-0.9514	-1.5206	-3.7462
9.0	-1	-1.0193	-1.0193	-1.0193	-1.0193	-1.0193	-1.0192	-1.0181	-1.0280	-1.3561	-2.7282